The University Of Sheffield.

The control of inflammation in airway epithelial cells

Claudia Correia De Paiva

Academic Unit of Respiratory Medicine

Department of Infection, Immunity & Cardiovascular Disease

University of Sheffield

Thesis submitted for the degree of Doctor of Philosophy

January 2016

ABSTRACT

COPD is a severe chronic and complex airway disease that represents a major financial burden on the healthcare and economic system. Environmental risk factors such as cigarette smoke have been associated with the predisposition to COPD. Other factors such as exposure to viral pathogens can exacerbate airway inflammation and tissue destruction generated by recruited neutrophils, culminating in altered epithelial cell responses in COPD. This thesis investigated the physiological role of Pellino-1, an E3-ubiquitin ligase, and its regulation in human primary bronchial epithelial cells (HBEpCs) in response to viral infection.

The viral mimic poly(I:C) increased Pellino-1 protein and gene expression in HBEpCs. In addition, Pellino-1 gene expression was significantly increased by RV-16 and RV-1B infection in primary bronchial epithelial cells from COPD patients. Pellino-1 knockdown in HBEpCs led to a reduction in NF-κB regulated cytokines CXCL8, IL-1α and β gene expression and release of CXCL8 in response to poly(I:C) while having no measurable effect on IFNβ mRNA expression.

Furthermore, the transient knockdown of Pellino-1 resulted in the decrease in IKKα/β phosphorylation. The role for Pellino-1 in the non-canonical NF-κB pathway was also investigated and while Pellino-1 knockdown did not alter the expression of the non-canonical NF-κB precursor protein NFKB1 following poly(I:C) stimulation, NFKB2 protein expression was suppressed. In contrast to Pellino-1 knockdown, the transient knockdown of NFKB2 resulted in significant increase in CXCL8 mRNA and protein expression and in turn did not regulate Pellino-1 mRNA expression to poly(I:C). These data suggest that following viral infection in airway epithelial cells, TLR3 activation culminates in the up-regulation of Pellino-1 leading to an increase in NFKB2 expression, resulting in the suppression of NF-κB specific gene transcription.

In addition to activating non-canonical NF-κB, NFKB1 regulates the activation of ERK signalling via MEK1. Treatment of HBEpCs with MEK1 inhibitors, PD98059 and U0126, resulted in a significant reduction in Pellino-1 protein and gene expression which led to the suggestion of ERK as a potential Pellino-1 regulator.

Proteomics analysis of primary epithelial cells obtained from COPD patient airways further identified a potential novel mechanism of action for Pellino-1 in the NF-κB signalling pathway, wherein it Pellino-1 may inhibit A20's negative regulatory role or its adaptor proteins TNIP1 or TAX1BP. Taken in combination these data support Pellino-1 as a potential target to down-regulate neutrophilic inflammation whilst retaining antiviral immunity by selectively mediating the TLR3 TRIF-dependent NF-κB/MAPK pathway and not TLR3-mediated IRF3 and IFNβ activation.

ACKNOWLEDGEMENTS

Firstly I would like to extend my sincerest gratitude to my supervisors, Professor Ian Sabroe and Dr. Lisa Parker, not only for giving me the opportunity of a lifetime but for their consistent support and guidance. I would also like to thank them for the time they have invested in me and above all for believing in me even when I did not. They have not only helped me develop as a researcher, but above all they have helped me grow into the person I am today.

I would also like to thank all of my past and present colleagues in the Department of Infection, Immunity and Cardiovascular Disease, who were always happy to offer their help and advice. In particular, I would like to say a special thank you to Elizabeth Prestwich as a member of 'team Pellino' not only for her willingness to work jointly with me through some of the harder aspects of the research, but mostly to have survived it with me. Also a massive thank you to Julie Bennett not only for her pioneering work on Pellinos which helped pave the way for my PhD, but above all for becoming one of my greatest friends and still offering her help and expertise even 4 years after having left the department. She has given me some of the best and funniest memories of my time in the department.

I would also like to say a big thank you to Amanda, Louise, Laura, Vicky and Anna who I am also very privileged to call my friends, for their support and encouragement in the form of laughs, coffees and happy memories.

To my husband Richard, who has lived through every single day of this PhD with me, through some of the best and worst moments of my life, I owe you everything. I am thankful for your strength, your pride in me, for always believing in me (despite not possibly having any foundations for such) and above all for never ever failing me.

Thank you to the Paiva clan for their unconditional love. However first and foremost I would like to thank my mom and brother for their permanent support and always reminding me of what I am capable of. Both have shown me what great strength looks like and have taught me to never give up in the face of adversity.

And finally I would like to dedicate this thesis, this part of my life, to my dad. He may no longer be with me, but without him, his spirit and his unwavering confidence in me I would never have accomplished this chapter of my life.

TABLE OF CONTENTS

LIST OF FIGURES

LIST OF TABLES

ABBREVIATIONS

Abs	Antibodies
AcP	Accessory protein
AP-1	Activator protein 1
ASMCs	Airway smooth muscle cells
ATP	Adenosine triphosphate
BAFF-R	B cell–activating factor receptor
BAL	Bronchoalveolar lavage
BALF	Bronchoalveolar lavage fluid
BEAS-2B	Human bronchial epithelial cell line
BEBM	Bronchial epithelial basal media
BEGM	Bronchial epithelial growth media
BMDCs	Bone marrow-derived dendritic cells
BP	Base pair
BPI	Bactericidal permeability-increasing
bZIP	Basic leucine zipper
CARD	Caspase recruitment domain
CCL	CC-chemokine ligand
CCR	CC-chemokine receptor
cDNA	Complementary DNA
cIAP	Cellular inhibitor of apoptosis
COPD	Chronic obstructive pulmonary disease
CSE	Cigarette smoke extract
CXCL8	Interleukin 8
DAMP	Damage associated molecular pattern
DCs	Dendritic cells
DD	Death domain
DMEM	Dulbecco's modified eagle medium
DNA	Deoxyribonucleic acid
dsRNA	Double-stranded RNA
ECL	Enhanced chemiluminescence
ECM	Extracellular matrix
ELISA	Enzyme-linked immunosorbent assay
ER	Endoplasmic reticulum
ERK	Extracellular signal-regulated kinases
FADD	Fas-associated death domain

FAM	6-carboxyfluorescein
FCS	Foetal calf serum
FHA	Forkhead-associated domain
GFP	Green fluorescent protein
GOLD	Global initiative for obstructive lung disease
GRR	Glycine-rich region
HBECs	Human bronchial epithelial cells
HBEpC	Human bronchial epithelial primary cell
HBSS	Hank's buffered salt solution
HEK293	Human embryonic kidney 293 cells
HeLa	Human cervical epithelial cell line
HEPES	4-(2-hydroxyethyl)-1-piperazineethanesulfonic acid
HMGB1	High-mobility group box 1
HRP	Horseradish peroxidase
HSV	Herpes simplex virus
ICAM-1	Intercellular adhesion molecule 1
ICS	Inhaled corticosteroid
IFN	Interferon
Ig	Immunoglobulin
IKK	Iκb kinase
IL-1	Interleukin 1
IL-1R	Interleukin 1 receptor
IL-1RA	Il-1 receptor antagonist
IL-1RAcP	Il-1 receptor accessory protein
IL-6	Interleukin 6
IP-10	Interferon gamma-induced protein 10
IRAK	IL-1R associated kinase
IRF	Interferon regulatory factor
ISG	Interferon-stimulated gene
ISGF3	IFN-stimulated gene factor 3
IκB	Inhibitory κB
JAK	Janus kinase
JNK	C-jun n-terminal kinases
Kd	Dissociation constant
KD	Kinase domain
LDLR	Low-density lipoprotein receptor
LPS	Lipopolysaccharide
LRR	Leucine-rich repeat
LTβR	Lymphotoxin-b receptor

MAPK	Mitogen activated protein kinase
MAVS	Mitochondrial antiviral signaling protein
MCP-1	Monocyte chemoattractant protein 1
MDA5	Melanoma differentiation-associated gene 5
MEFs	Mouse embryonic fibroblasts
MMP	Matrix metalloproteinase
MOI	Multiplicity of infection
MyD88	Myeloid differentiation factor 88
NE	Neutrophil elastase
NEMO	NF-κB-essential modulator
NF-κB	Nuclear factor kappa B
NIK	NF-κb-inducing kinase
NLR	Nod-like receptor
NLS	Nuclear location sequence
NOD	Nucleotide-binding oligomerization domain
OD	Optical density
p.i.	Post-infection
PAMP	Pathogen associated molecular pattern
PBMCs	Peripheral blood mononuclear cells
PCR	Polymerase chain reaction
PE	Phosphatidylethanolamine
PMSF	Phenylmethanesulfonylfluoride
Poly(I:C)	Polyinosinic:polycytidylic acid
PPP	Platelet poor plasma
PRR	Pattern recognition receptor
qPCR	Quantitative PCR
RANK	Receptor activator for NF-κB
RANTES	Regulated upon activation in normal t-cells, expressed and secreted
RHD	Rel homology domain
RIG-I	Retinoic acid-inducible gene-I
RING	Really interesting new gene
RIP1	Receptor-interacting protein 1
RLR	Rig-I-like receptor
RNA	Ribonucleic acid
ROS	Reactive oxygen species
rpm	Repetitions per minute
RSV	Respiratory syncytial virus
RT-PCR	Reverse transcription polymerase chain reaction
RV	Rhinovirus

SAPK	Stress-activated protein kinase
SDS-PAGE	Sodium dodecyl sulfate polyacrylamide gel electrophoresis
Ser	Serine
SeV	Sendai virus
shRNA	Short hairpin RNA
siRNA	Small interfering RNA
ssRNA	Single-stranded RNA
STAT	Signal transducer and activator of transcription
TAB	TAK1 binding protein
TAD	Transactivating domain
TAK1	TGF-β-activated kinase 1
TAMRA	Tetramethylrhodamine
TANK	TRAF-family member associated NF-κB activator
TBK1	TANK binding kinase 1
TEMED	Tetramethylethylenediamine
TGF-β	Transforming growth factor-beta
TIR	TLR/IL-1R
TLR	Toll-like receptor
TNF	Tumour necrosis factor
TNFAIP3	Tumor necrosis factor, alpha-induced protein 3
TRADD	TNF receptor-associated death domain
TRAF	TNF receptor-associated factor
TRIF	TIR-domain-containing adaptor protein inducing ifn-β
TWEAK	TNF-like weak inducer of apoptosis
UTR	Untranslated region
UV	Ultraviolet light
w/v	Weight/volume ratio
WHO	World health organisation

CHAPTER 1 - INTRODUCTION

1.1 Chronic Obstructive Pulmonary Disease (COPD)

COPD is a complex airway inflammatory disease that involves a multitude of cell types, both inflammatory and structural, in its pathophysiology. The disease is characterized by the obstruction of airflow that is not fully reversible (Pauwels et al., 2001). COPD mainly consists of two conditions of the lung, chronic obstructive bronchitis and emphysema. Whilst obstructive bronchitis causes fibrosis due to inflammation of the bronchioles, leading to an impediment of small airways, emphysema on the other hand, triggers the enlargement of airspaces causing the loss of lung elasticity ultimately resulting in the closure of small airways (Barnes, 2004, 2008b).

The World Health Organisation (WHO) estimated that COPD would become the third most common cause of death and fifth most common cause of disability worldwide by 2020 (Lopez and Murray, 1998). WHO has since predicted that COPD will rise from its current fifth place in the table of most common causes of death, to the fourth by 2030 (Mathers and Loncar, 2006). This highlights the importance of further elucidation of the underlying cellular and molecular mechanisms involved in the pathogenesis of this complex disease.

1.2 Cells involved in COPD

There are many cell types involved in this complex inflammatory disease. These vary from structural cells such as epithelial and endothelial cells to the abnormally high numbers of infiltrating inflammatory cells including monocytes, macrophages and neutrophils.

Human airways are constantly bombarded with foreign and invading pathogens viruses, bacteria and environmental toxins such as cigarette smoke. The respiratory mucociliary epithelium provides a physical barrier, in the form of mucus, wherein beating cilia propel mucus-trapped debris away from the respiratory system (Braiman and Priel, 2008). Epithelial lining fluid surrounding airway epithelial cells also contain a multitude of glycoproteins, proteins and molecules such as lysozymes, lactoferrins and defensins responsible for the

effective neutralising of microbial contaminants (Diamond et al., 2000). In the airways of patients with COPD, epithelial cells show a hyper-proliferative phenotype resulting in squamous metaplasia (Demoly et al., 1994). The underlying processes and growth factors involved in these changes remain unclear. For instance expression of the receptor for advanced glycation end products (RAGE) and its binding partner high-mobility group box 1 (HMGB1), a nuclear protein that is released during inflammation and repair and interacts with pro-inflammatory cytokines are increased in airway epithelium of patients with COPD (Ferhani et al., 2010). However, when these structural cells encounter certain inflammatory stimuli this can lead to the expression of adhesion molecules on endothelial cells, the release of reactive oxygen species, proteolytic enzymes and the synthesis of a variety of cytokines and chemokines including IL-6, TNFα, IL-1β and the neutrophil chemoattractant IL-8/CXCL8 resulting in the recruitment and activation of inflammatory cells as seen in the disease state (Brusselle et al., 2011; Cromwell et al., 1992).

Neutrophils are the most abundant granulocyte in the human circulation (Bainton et al., 1971). These short-lived polymorphonuclear cells are among the first recruited immune cells to a site of injury or infection. Neutrophils limit infection by engulfing pathogens into the phagosome wherein noxious agents such as reactive oxygen species and hydrolytic enzymes are released through the activity of the NADPH oxidase, or respiratory burst (Leto and Geiszt, 2006). Intracellular granulocytes then release potent antimicrobial peptides and proteolytic enzymes into the phagosome such as cathepsin G, defensins, protinase-3 and bactericidal permeability-increasing (BPI) protein resulting in the effective killing and digestion of microorganisms (Borregaard et al., 2007). These cells also release matrix metalloproteinases (MMP)-8 and MMP-9 as well as reactive oxygen species (ROS), which may contribute to alveolar wall destruction (emphysema) seen in COPD pathogenesis (Barnes, 2004; Nadel, 2000). Neutrophils also contribute to the recruitment of other immune cells through the release of chemokines and ultimately assist in mounting an adaptive immune response (Parker et al., 2005). Normally, neutrophils undergo spontaneous apoptotic cell death within a day of entering circulation, however in the presence of infection or inflammation, their life span can be prolonged by several days to aid in pathogen clearance through the actions of cytokines such as granulocyte-macrophage colony stimulating factor (GM-CSF) and granulocyte colony stimulating factor (G-CSF) (Mantovani et al., 2011). Like many other types of inflammatory cells, increased numbers of neutrophils are found in COPD patient airways and their numbers in turn correlate with decreased lung function (Lacoste et al., 1993; Stanescu et al., 1996).

In contrast to neutrophils, macrophages are long-lived immune cells that can reside in tissues providing homeostasis through the removal of circulating old red blood cells, necrotic tissue and toxic agents (Gordon and Taylor, 2005). Macrophages mature from circulating monocytes produced in the bone marrow. In the airway, alveolar macrophages migrate into the interstitium and alveoli and can also be found within the epithelial lining fluid serving as sentinel cells for the immune response against inhaled pathogens and toxins. Alveolar macrophages are one of the main types of inflammatory cells involved in COPD. They produce a plethora of proteases including MMP-2, MMP-9, MMP-12, cathepsins K, L and S associated with the activation of inflammatory mediators and onset of emphysema (Di Stefano et al., 1998; Tetley, 2002). In addition, alveolar macrophages are involved in the increased production of proinflammatory cytokines such as IL-1β, IL-6, IP-10 and TNFα. Macrophages collected from COPD patient sputum show increased NF-κB activation, which is further enhanced during exacerbations (Caramori et al., 2003). Bronchoalveolar lavage (BAL) fluid, sputum and lung parenchyma analysis of COPD patients showed a 5- to 10-fold increase in numbers of macrophages in the airways when compared to healthy controls (Retamales et al., 2001; Tetley, 2002). The increase in numbers of sequestered macrophages suggests a pivotal role for macrophages in disease progression. In support of this, a direct correlation exists between macrophage numbers in alveolar walls and the severity of emphysema experience by COPD patients (Ohnishi et al., 1998).

This increase in macrophage numbers occurs following the recruitment of monocytes from the circulation in response to the production of CCL2 also known as monocyte chemoattractant protein (MCP)-1 (de Boer et al., 2000). Human monocytes can be sub-categorised on the basis of their chemokine receptor expression and specific identifying surface molecules, namely CD14 and CD16 expression (Geissmann et al., 2003; Ziegler-Heitbrock, 2007). Classical or $CD14^{++}CD16^{-}$ monocytes are the most prevalent monocyte subset in the human blood and express high surface levels of CC-chemokine receptor 2 (CCR2) but low levels of CX3C-chemokine receptor 1 (CX3CR1) (Ziegler-Heitbrock et al., 2010). In contrast, $CD16^{+}$ monocytes population can be further sub-divided by the non-classical or $CD14^{+}CD16^{++}$ monocytes and the intermediate or $CD14^{++}CD16^{+}$ monocytes and consist of high surface levels of C X3CR1 but low levels of CCR2 (Belge et al., 2002; Grage-Griebenow et al., 2001; Ziegler-Heitbrock et al., 2010).

In an inflammatory disease state the balance between recruited monocytes and resident macrophages is shifted and results in monocytes outnumbering macrophages (Maus et al.,

2006). Whilst monocytes are believed to be more pro-inflammatory than macrophages in that they produce higher levels of pro-inflammatory cytokines such as IL-1β, they however display less phagocytic capabilities than resident macrophages (Netea et al., 2009).

Small airway biopsies from COPD patients present with a surge of leukocyte infiltration consisting of monocytes and neutrophils. These changes coupled with fibrosis-induced airway remodelling cause the progressive and irreversible narrowing of the airway that are the hallmarks of COPD (Hogg et al., 2004).

Fibrosis of the small airways in COPD patients is often a result of uncontrolled proliferation of fibroblasts. Fibroblasts are structural cells closely apposed to the epithelium or endothelium with an essential role in tissue repair and injury responses through the production and homeostasis of extracellular matrix (ECM) proteins (reviewed in (Araya and Nishimura, 2010)). Furthermore, fibroblasts contribute to tissue architecture and matrix turnover rates through MMPs and their inhibitors, tissue inhibitor of metalloprotinases (TIMPs) generation. The production of essential ECM such as fibronectin, decorin, perlecan and versican is disregulated in COPD patients contributing to the fibrotic phenotype associated with the disease (Hallgren et al., 2010; Noordhoek et al., 2005). Evidence also supports a role for fibroblasts in inflammatory response through the secretion of several cytokines in addition to direct interaction with inflammatory cells (reviewed in (Buckley et al., 2001)).

The complex communication between these structural and inflammatory cells result in the release of lipid mediators, reactive oxygen species, peptide mediators, chemokines and cytokines capable of ultimately destroying the lung tissue and leading to the pathogenesis of the disease (Barnes, 2004; Shapiro, 1999). Research into the mechanisms behind this communication will be invaluable in developing a better understanding of COPD and lead to the discovery of new treatments.

1.2.1 Cytokines

Cytokines are small non-structural intercellular signalling proteins ranging from 8-30 kDa in mass. Cytokines have roles in most biological processes including immunity and inflammation and can act across a spectrum of distances to include autocrine, paracrine and endocrine

ranges (Cannon, 2000). The family of cytokines encompasses interleukins, chemokines, interferons, mesenchymal growth factors, tumour necrosis factors and adipokines (Dinarello, 2007).

Abnormalities in cytokine production, their receptors or their signalling pathways can result in the evolution of a wide variety of diseases such as COPD and asthma. Cytokines play a key role in orchestrating the chronic inflammation of COPD through the recruitment, activation, and increased survival of multiple inflammatory cells in the respiratory tract with over 50 cytokines identified in COPD (Barnes, 2008a) (**see section 1.2.1**). The cytokines that are frequently referred to throughout this thesis, due to their predominant roles in inflammation and viral infection, are individually described below.

1.2.1.1 Interleukin-1 (IL-1)

The IL-1 family is composed of 11 members including agonistic and antagonistic molecules and receptors (Reviewed by (Dinarello, 1996, 2011)). This section focuses on the originally identified agonistic members, IL-1α and IL-1β, and the physiological inhibitor of IL-1 termed IL-1 receptor antagonist (IL-1Ra).

Multiple cell types produce and secrete IL-1α, IL-1β, and IL-1Ra upon inflammatory activation, IL-1 is also a classic NF-κB target (**see section 1.6.1.1**). IL-1α and IL-1β are synthesized as precursors of 31 kDa followed by protease cleavage to their active 17 kDa forms.

IL-1α is a ubiquitously expressed intracellular protein rarely secreted by living cells with its release often associated with necrotic death. Under normal cellular conditions, IL-1α precursor is sequestered in the cytoplasm by IL-1 receptor type 2 (IL-1R2) preventing it from protease cleavage and IL-1 receptor type 1 (IL-R1) activation (Di Paolo and Shayakhmetov, 2013; Zheng et al., 2013). However, following inflammatory activation, IL-1R2 is cleaved by caspase-1, freeing IL-1α precursor to be cleaved by calpain, a calcium-dependent non-lysosomal cysteine protease, generating its 17 kDa mature form which can be secreted from cells (Zheng et al., 2013).

IL-1β is released in response to injury or inflammatory signals. It is largely produced by immune cells including monocytes, macrophages, dendritic cells, B cells and NK cells although

epithelial and endothelial cells have also been implicated in IL-1β production (Cannon, 2000). IL-1β precursor is biologically inactive and requires cleavage by the cysteine protease IL-1β-converting enzyme (caspase-1) in the cytoplasm on the inflammasome platform (Dinarello, 2009). Alternatively, the IL-1β precursor can also be cleaved at distinct sites into its secreted biologically active form by neutrophil proteases including caspase-8, cathepsin G (CG), neutrophil elastase (NE), and proteinase 3 (PR3) as well as mast cell proteases granzyme and chymase (Hazuda et al., 1990; Irmler et al., 1995; Maelfait et al., 2008; Mizutani et al., 1991).

An extensive list of agonists are involved in IL-1β secretion, including bacterial and viral pathogens through TLR signalling. IL-1 also induces its own production in monocytes (Dinarello et al., 1987). IL-1β is also a potent pyrogen (Murakami et al., 1990) and is involved in recruiting circulating leukocytes to inflamed tissue as well as stimulating neutrophilia.

In order to transduce a signal both extracellular IL-1α, active or precursor form, and mature IL-1β activate the membrane bound receptor IL-1R1. This leads to recruitment of IL-1 receptor accessory protein (IL-1RAcP). The TIR domains formed from the heterodimerisation of the receptor and accessory protein results in MyD88 recruitment. This leads to the activation of IRAKs, which leads to the subsequent interaction with TRAF6. Following a sequence of both phosphorylation and ubiquitination events, NF-κB and the JNK and p38 MAPK pathways are activated leading to the expression of IL-1 target genes such as IL-6, TNFα, IL-8/CXCL8, MCP-1, COX-2, IκBα, IL-1α and IL-1β through transcriptional and post-transcriptional mechanisms (Dinarello, 2009).

IL-1Ra is a receptor antagonist consisting of two structural variants, one a secretory molecule, the other an intracellular molecule with three isoforms (icILIRa1, 2 and 3) (Akdis et al., 2011; Arend and Guthridge, 2000). IL-1Ra's role is to counter the effects of IL-1 function and neutralise the proinflammatory function of IL-1β by competing for IL-1R1 cell surface receptors and preventing their intracellular responses by preventing recruitment of IL-1RAcP (Akdis et al., 2011; Arend, 1993). Following viral infection, AMs and PBMCs from patients with COPD show release of IL-1β while the release of IL-1RA was diminished resulting in a significantly higher IL-1β/IL-1RA ratio when compared to healthy controls (Rupp et al., 2003).

1.2.1.2 Interleukin-8 (IL-8) or CXCL8

IL-8, also known as CXCL8, is a member of the CXC chemokine family. IL-8/CXCL8 is expressed in response to inflammatory stimuli and is a classic NF-κB/MAPK target (**see section 1.6.1.1**). High levels of IL-8/CXCL8 are often observed in association with chronic and acute inflammatory conditions such as COPD and correlate with tissue neutrophil infiltration (**see section 1.2**).

IL-8/CXCL8 is a potent neutrophil chemotactic factor and activator secreted by a number of cell types including monocytes, macrophages, neutrophils, fibroblasts, endothelial and epithelial cells. IL-8/CXCL8 cDNA is transcribed as a 99-amino acid precursor protein, which can be cleaved to yield predominantly 77- or 72-amino acid mature proteins, which can undergo further processing resulting in truncation analogues of different sizes (77-, 72-, 71-, 70- and 69-residue proteins) (Matsushima et al., 1988; Mukaida, 2003). Fibroblasts and endothelial cells predominantly produce the 77-amino acid variant of IL-8/CXCL8 whilst leukocytes release 72- and 69- amino acid forms. While all forms of IL-8/CXCL8 have neutrophil chemoattractant activities, 77- amino acid variant appears to be essential for neutrophil adhesion to endothelial cells before transmigration (Huber et al., 1991; Mukaida, 2003; Murphy and Tiffany, 1991).

The effects of IL-8/CXCL8 are mediated through the receptors CXCR1 and CXCR2, which are present on a variety of cell types including non-haematopoeitic cells such as epithelial cells, however they are predominantly present on myeloid lineage cells such as monocytes and mature polymorphonuclear cells (Holmes et al., 1991; Stillie et al., 2009). IL-8/CXCL8 signalling through CXCR1 and CXCR2 is responsible for neutrophil antimicrobial activity including chemotaxis (predominantly through CXCR1), degranulation and oxidative burst (Hammond et al., 1995; Stillie et al., 2009).

1.2.1.3 Interferon (IFN)

IFNs are a group of secreted cytokines that act as antiviral agents extensively studied for their crucial role in immunity. IFNs are multi-functional cytokines that bridge innate and adaptive immunity and play important roles in the host response to pathogens, immunomodulation and haematopoietic development (Mamane et al., 1999). IFNs have been categorized into three groups based on amino acid sequence and receptor recognition, known as Type I, II and III (Reviewed by (Randall and Goodbourn, 2008)).

Type I IFNs comprise of a large group of genes including IFN-α/β and other less well defined members such as IFNω –ε –τ -δ and –κ. IFNα, composed of 13 subfamily genes, and a single IFNβ, all of which are located in one locus on the same chromosome and are induced directly in response to viral infection (Taniguchi et al., 1980; van Boxel-Dezaire et al., 2006; Weissmann and Weber, 1986). A mutation in the type I IFN receptor gene of mice results in elimination of antiviral responses highlighting the essential role of IFNα and IFNβ in viral defence (Hwang et al., 1995). pDCs are the main Type I IFNs producing cells, however they can be released by most cells. IFNα and IFNβ can regulate their own production and have two main forms of action, either by direct inhibition of viral replication by blocking viral entry into the cell, cleavage of RNA, or prevention of viral translation, or indirectly through the initiation of innate and adaptive immune responses (Jacobs and Langland, 1996; Sen, 2001). Virally infected host cells lead to the induction of type I IFNs, which require the assembly of complexes known as enhanceosomes, composed of transcription factors such as NF-κB, AP-1, IRF-3 and IRF-7 that recruit transcriptional machinery to the IFNβ promoter region (Honda et al., 2006; Maniatis et al., 1998).

Type II IFN has a single member known as IFN-γ and is a TH1 cytokine inducible by activated immune cells such as T cells and natural killer (NK) cells, rather than in direct response to viral infection and will therefore not be reviewed in this section (Schreiber and Farrar, 1993).

The most recently discovered of the IFNs are the type III IFNs or IFN-λ. Their production occurs in a wide range of cell types including epithelial, lymphoid and myeloid cells. There are three isoforms of IFN-λ, IFNλ1 –λ2 and –λ3 and unlike type I IFNs, IFN-λ displays an IFN-inducible nature, allowing ISGF3 and IRF-1 to regulate its induction (Ank et al., 2006). In addition, IFN type III family present with IRF and NF-κB binding sites at their promoters. IFNλ1 is regulated similarly to IFNβ through virus activated IRF3 and NF-κB, whilst IFNλ2 and IFNλ3 are regulated by IRF7 and thus resemble IFNα (Onoguchi et al., 2007).

The initiation of the transcription of IFN genes is in most part mediated by multiple transcription factors known as interferon regulatory factors (IRFs) post TLR/RLR signalling (**see section 1.4.1 and 1.4.2**). This leads to first phase of IFN production that in turn activates Janus kinase (JAK)- signal transducer and activator of transcription (STAT) and MAPK signalling pathway resulting in further IFN production (Darnell et al., 1994).

1.2.1.4 Regulated on activation, normal T cell expressed and secreted (RANTES) or CCL5

RANTES, also known as CCL5, is a 7.8 kDa member of the CC chemokine family with a pro-inflammatory role in chronic inflammation. RANTES/CCL5 is an IFN inducible gene secreted upon viral infection by cell types including endothelial cells, smooth muscle cells, epithelial cells, macrophages and platelet-activated T cells. RANTES/CCL5 causes the selective adhesion and transmigration of human blood monocytes, CD4+, and CD45R0+ positive T lymphocytes in endothelial-free system and CD4+ and CD8+ T lymphocytes in transendothelial assays (Roth et al., 1995; Schall et al., 1990). RANTES/CCL5 also induces NK cell migration and activation and eosinophil activation (Rot et al., 1992; Taub et al., 1995). The effects of RANTES/CCL5 are mediated through the receptors CCR1, CCR3 and CCR5 (Combadiere et al., 1996; Daugherty et al., 1996; Gao et al., 1993).

1.3 Exacerbations of COPD

The clinical course of COPD is interspersed by acute exacerbations. Exacerbations of COPD have been characterised as an acute increase in respiratory symptoms that are beyond normal daily variations (Vestbo et al., 2013). Symptoms of exacerbations include dyspnoea, cough and increase in sputum volume or purulence and may result in the administration of additional treatments such as steroids or systemic antimicrobials (Kurai et al., 2013). There is a direct correlation between the frequency of exacerbations and accelerated decline in lung function (Patel et al., 2002; Seemungal et al., 1998). Acute exacerbations of COPD severely affect the state of health of patients. A distinct subgroup of patients termed 'frequent exacerbators' have also been recognized as being particularly susceptible to exacerbations (Wedzicha et al., 2013). The severity and rapidly escalating frequency of exacerbations leads to significant increasing burdens on healthcare costs as well as patient quality of life (Seemungal et al., 1998).

Many triggers of acute exacerbations of COPD have been reported, with bacterial or viral respiratory infections of the airway, or indeed co-infection with both pathogens, identified as the predominant cause of acute exacerbations (Caramori et al., 2006; Celli and Barnes, 2007). Bacteria such as *Streptococcus pneumoniae, Haemophilus influenzae*, *Moraxella catarrhalis,*

and *Pseudomonas aeruginosa* and viruses such as human rhinovirus (RV), respiratory syncytial virus (RSV), influenza virus, human metapneumovirus (HMPV) and coronavirus are commonly detected during exacerbations (Sapey and Stockley, 2006; Sethi and Murphy, 2008).

Interestingly, while respiratory virus-induced exacerbations appear similar at the various stages of disease progression, bacteria-induced exacerbations increase with the severity of the disease or decrease in lung function (Dimopoulos et al., 2012). Studies have determined that up to 50% of COPD patients harbour bacteria in their lower respiratory tracts (Zalacain et al., 1999). Respiratory viruses have also been identified as the cause of up to 57% of COPD exacerbations, with RV accounting for up to 26.6%, RSV up to 40.5% and influenza virus up to 22.4% (Beckham et al., 2005; Dimopoulos et al., 2012; Hutchinson et al., 2007; Kherad and Rutschmann, 2010; Ko et al., 2007; Kurai et al., 2013; McManus et al., 2008; Papi et al., 2006; Perotin et al., 2013; Seemungal et al., 2001; Tan et al., 2003).

Co-infection with RV and bacterial pathogens can lead to an even more pronounced functional impairment of the airway resulting in a rise in severity and frequency of exacerbations (Wilkinson et al., 2006). It has been suggested that respiratory virus-induced exacerbations result in a worse prognosis with larger lung function decline and recovery than non-viral exacerbations (Bafadhel et al., 2011; Seemungal et al., 2001). These exacerbations can in turn result in secondary bacterial infections culminating in severe respiratory symptoms (Wilkinson et al 2006b; Harper et al., 2009; Mallia et al., 2012).

1.3.1 Cigarette smoke

Cigarette smoking or active exposure to cigarette smoke is the predominant causative factor in the development of COPD and contributes to increased incidence of pulmonary diseases such as asthma, allergic rhinitis and cancer (Reviewed by (Thorley and Tetley, 2007)). In the United States cigarette smoking accounts for over 80% of COPD cases (Sethi and Rochester, 2000). In 2008, the WHO estimated that 5.4 million premature deaths worldwide could be attributed to cigarette smoking.

Cigarette smoke is a complex and reactive mixture composed of over 5000 chemicals some of which are highly toxic and carcinogenic (Borgerding and Klus, 2005). Cigarette smoke components can be split into the gaseous phase and the particulate phase. The gaseous

components of cigarette smoke include oxygen, nitrogen, carbon dioxide, acetaldehyde, methane, hydrogen cyanide, nitric acid and ammonia to name a few of the most studied components (Borgerding and Klus, 2005). The particulate components include carboxylic acids, phenols, nicotine, terpenoids, paraffin waxes and tobacco-specific nitrosamines.

Long term exposure to cigarette smoke can result in epithelial cell changes associated with the development of bronchitis (Vestbo and Hogg, 2006). It can lead to goblet cell and submucosal gland hypertrophy linked with the loss of ciliated epithelial cell function resulting in decreased mucociliary clearance and mucus plug formation in the large airways (Jeffery, 1998). Increased goblet cell numbers can also be found in the small airways and bronchioles (Cosio et al., 1980).

1.3.2 Rhinovirus

Human RVs are the predominant cause of the common cold and are a major cause of asthma and COPD acute exacerbations (Johnston, 2005). Human RVs are members of the *Picornaviridae* viral family and are non-enveloped viruses with an icosahedral protein capsid encasing a single-stranded, positive-sense RNA genome (Rossmann and Palmenberg, 1988). RVs are small viruses around 30nm in diameter containing a genome of approximately 7.2 kb composed of a 5' untranslated region (UTR), an open reading frame coding for caspid proteins VP1-4 and several non-structural proteins, and a 3'UTR and poly A tail (Huang et al., 2009; Johnston et al., 1993). RVs are an extremely effective pathogen due to their small genomes, fast replication cycles and high RNA mutation frequency wherein up to 10^{-3} errors per nucleotide are inserted per replication cycle (Drake, 1999).

Over 100 serotypes of RV haven been discovered to date and these can be sub-divided into three distinct genetic clades, HRV-A, HRV-B and HRV-C (Cox and Le Souef, 2014; Ledford et al., 2004). Human RVs can also be sub-divided based on their receptor specificity; the majority of RVs enter host cells through the use of either intercellular adhesion molecule-1 (ICAM-1) termed the 'major group' (these include strains belonging to both HRV-A and HRV-B). A smaller population of RV strains gain host entry through the low-density lipoprotein receptor (LDLR) termed the 'minor group' (HRV-A strains only) (Greve et al., 1989; Marlovits et al., 1998). However a very small group of human RVs use heparin sulphate proteoglycans instead of ICAM-1 and LDLR to adhere onto cell surfaces (Vlasak et al., 2005). Once RV bind their respective receptors, they are taken up into endosomes wherein low pH results in

conformational changes of the capsid leading to viral RNA release into the cytoplasm (Nurani et al., 2003). The receptors used by the third group of more recently identified HRV-C strains, remains unknown (Cox and Le Souef, 2014).

RV can gain entry into the respiratory tract through the nose or lacrimal duct in the eyes before commencing infection in the nasopharynx. Upon cell entry, RV inhibits host cell protein synthesis through the cleavage of CAP-binding complex by viral protease 2a before it undergoes RNA translation through the binding of host ribosomes (Belsham and Sonenberg, 1996). Within 6 hours a single infection can result in the release of 100,000 mature virions into the surrounding airway epithelia following viral-induced cell lysis (Belsham and Sonenberg, 1996).

RVs are capable of infecting ciliated epithelial cells in the upper respiratory tract, however increasing evidence suggests RVs can also replicate in the lower respiratory tract (Kirchberger et al., 2007). Under normal respiratory conditions, human RVs only infect and replicate in a small proportion of epithelial cells (approximately 10%) with little cytopathic effect (Heikkinen and Jarvinen, 2003). However, RV infection is accompanied by a release of inflammatory mediators including cytokines such as IL-1β, IL-8/CXCL8, TNFα, IL-6 and IL-11, as well as chemokines including RANTES/CCL5, MCP-1 and IP-10 (Kirchberger et al., 2007). Increasing sputum levels of IL-8/CXCL8 and IL-6 directly correlates with the severity of symptoms following RV infection (Turner et al., 1998; Zhu et al., 1996). COPD patients experimentally infected with RV present with increased viral load, which is consistent with increased sputum neutrophils and IL-8/CXCL8 levels (Mallia et al., 2011). As a result of inflammatory mediator production, RV infection leads to the initiation and amplification of host inflammatory response through the proliferation, chemotaxis and activation of innate immune cells.

In healthy individuals RV infections are generally contained within the upper airways with little evidence of lower respiratory tract involvement (Message et al., 2008). However people with COPD, it has been reported that RV infection is more severe and shows prolonged lower respiratory symptoms including airway obstruction and increased numbers of neutrophils when compared to healthy controls (Mallia et al., 2011). RVs have also been associated with the attenuation of anti-bacterial innate immune responses in COPD. RV infection results in increased neutrophil elastase production and the consequent reduction in antimicrobial peptides, such as elafin and secretory leukoprotease inhibitor, lead to the predisposition to

secondary bacterial infection often seen in COPD patient airways (Mallia et al., 2012). RV can also interfere with epithelial cell barrier function allowing bacterial translocation across the epithelium (Sajjan et al., 2008).

Exacerbation prone COPD patients present with lower serum levels of rhinovirus-specific antibody, anti-VP1 IgG_1, and IL-21 than stable COPD patients (Yerkovich et al., 2012). COPD patients experimentally infected with RV also show reduced IFN induction (Mallia et al., 2011). In addition, COPD patient airway epithelial cells have been shown to be more susceptible to RV infection in vitro (Schneider et al., 2010). These data suggest COPD patients may have impaired host responses to RV.

1.4 Pattern recognition receptors (PRRs) and Innate Immunity

The innate immune system is the first form of host defence against the invasion of pathogenic microorganisms. Innate immunity was once thought to be a non-specific mechanism for recognising microbial components, subsequently leading to a more specific adaptive immunity. However the emergence of a wide variety of germline-encoded pattern recognition receptors (PRRs) has since bestowed specificity to innate immunity. Host-pathogen interactions are initiated by the recognition of either endogenous danger signals such as IL-1, or through the recognition of pathogen components termed pathogen-associated molecular patterns (PAMPs) (Janeway and Medzhitov, 2002). In addition, PRRs can also detect molecules released from damaged tissue or necrotic cells known as damage-associated molecular patterns (DAMPs) to promote an inflammatory response (Jiang et al., 2005). The innate immune response comprises the effective sensing of PAMPs by PRRs followed by a rapid induction of complex signalling pathways that culminate in the induction of inflammatory responses regulated by a plethora of cytokines and chemokines to facilitate the elimination of the invading pathogen.

To date, several classes of PRR have been identified, of these receptors, the transmembrane and endosomal bound toll-like receptors (TLRs) are the most extensively studied (Reviewed by (O'Neill et al., 2013)). The discovery of TLR3 gene-disrupted mice with preserved anti-viral signalling to specific viral agonists led to the surfacing identification of additional PRRs (Takeda and Akira, 2004). Since, PRR such as retinoic acid-inducible gene-I (RIG-I) like receptors (RLRs) (Reviewed by (Loo and Gale, 2011)), nucleotide-binding oligomerization domain (NOD)- like

receptors (NLRs) (Reviewed by (Chen et al., 2009)) and the recently identified cytosolic DNA receptors (CDRs) have been identified (Kato et al., 2011; Keating et al., 2011) (Reviewed by (Paludan and Bowie, 2013)).

Each set of receptors has distinct expression patterns and activate specific signalling pathways, which can lead to targeted anti-pathogen responses. However, similarities in structure and cross talk between these receptors, and overlap in signalling pathways have been documented. The following sections will summarise TLR and RLR signalling due to their relevance to this thesis.

1.4.1 Toll-like Receptors (TLRs)

Toll protein was originally discovered in *Drosophila melanogaster* involved in establishment of dorsoventral polarity during embryogenesis (Hashimoto et al., 1988). Their important role in innate defence was first observed when mutation of the Toll gene was found to render adult flies susceptible to fungal infections (Lemaitre et al., 1996). The cloning and characterisation of the human homologues of Toll led to widespread interest in this family of proteins (Medzhitov et al., 1997). Subsequently, ten highly conserved homologues were identified in humans and designated as toll-like receptors, each recognising specific PAMPs (**detailed in Table 1.1**).

TLRs are type I transmembrane receptors characterised by an ectodomain consisting of leucine-rich repeats (LRR) containing the consensus sequence $L(X_2)LXL(X_2)NXL(X_2)L(X_7)L(X_2)$, essential for the recognition of specific ligands (Bowie and O'Neill, 2000; Kobe and Deisenhofer, 1994). The cytoplasmic domain of TLRs contains an IL-1R homologue termed the Toll/IL-1R (TIR) domain because of the sequence similarity between IL-1R1 and the Drosophila melanogaster protein Toll (Gay and Keith, 1991), which consists of a 200 amino acid domain arranged into three highly conserved regions, termed box1, box2 and box3. Box1 and box2 are involved in protein-protein interactions whilst box3 is mostly involved in the localisation of the receptor through its interactions with the cytoskeleton (Slack et al., 2000). The TIR domain in turn recruits various TIR-containing adaptor proteins to activate the transmission of downstream signalling (Akira et al., 2006; Bowie and O'Neill, 2000).

TLRs can be broadly categorized into two subgroups based on their cellular localisation. TLR1, TLR2, TLR4, TLR5, TLR6 and TLR10 are located on the plasma membrane of cells and can be

subdivided based on their related agonists; TLR1, TLR2 and TLR6 recognise lipids. TLR2 can form dimer complexes with TLR1 and TLR6 and respond to major components of Gram-positive bacteria cell wall such as lipopeptides and lipoteichoic acids (LTA) (Knapp et al., 2004). This combinational pattern of TLR heterodimerisation enhances the diversity of PAMP recognition by TLRs.

Some TLRs can detect multiple structurally unrelated ligands. For example, TLR4, the first human TLR to be reported, acts as a homodimer eliciting a response to a broad range of agonists including the fusion protein of RSV, fibronectin and heat shock proteins amongst others (Akira et al., 2006). TLR4 is also critical in mediating responses to components of Gram-negative bacteria outer-membrane known as lipopolysaccharide (LPS) (Hoshino et al., 1999). In this particular instance, TLR4 requires functional interacting partners such as myeloid differentiation protein-2 (MD-2) and CD14 to elicit NF-κB activation resulting in the production of pro-inflammatory cytokines (**see section 1.6.1**). Flagellins, found in both Gram-positive and Gram-negative bacteria, are identified exclusively by TLR5 (Zhang et al., 2005). The agonist for TLR10 still remains to be identified, however studies suggest it may act by dimerisation with TLR1 and TLR2 (Hasan et al., 2005).

TLR3, TLR7, TLR8 and TLR9 are located intracellularly on endoplasmic reticulum (ER), lysosomes and endosomes where they predominantly detect viral nucleic acids. TLR3 recognises viral genomic double-stranded RNA (dsRNA) or viral replication intermediates released in endolysosomal compartments (Akira et al., 2006; Alexopoulou et al., 2001). TLR3 is also activated by endogenous dsRNA released from dying cells (Kariko et al., 2004). In addition, the stable synthetic dsRNA analogue Polyinosinic:polycytidylic acid [poly(I:C)], is also frequently used as a TLR3 agonist to mimic viral infection.

TLR7 and TLR8 recognise viral ssRNA. Both TLR7 and TLR8 are structurally homologous but are primarily presented in different cell types. TLR7 is mainly expressed in plasmacytoid dendritic cells (pDCs) and B cells whilst TLR8 is located in myeloid dendritic cells (mDCs) and monocytes (Lund et al., 2004; Triantafilou et al., 2005; Yoneyama and Fujita, 2010). In contrast, TLR9 recognises nonmethylated CpG motifs found predominantly in pathogenic DNA (Chuang et al., 2002).

TLRs are expressed on various cell types including immune cells (monocytes, macrophages, dendritic cells) and non-immune cells (epithelial cells and fibroblasts). Their expression and regulation is both cell type and stimulus dependent which adds to the complexity of their characterisation and function. TLR signalling is a tightly regulated process wherein even the slightest mutation or disruption can result in impaired immune responses and disease onset. For instance, two naturally occurring intronic single nucleotide polymorphisms (SNP) TLR2 rs1898830 and rs11938228 were associated with a lower level of forced expiratory volume in 1 second (FEV_1) and higher numbers of inflammatory cells present in sputum from COPD patients suggesting a role in the severity and progression of COPD (Budulac et al., 2012).

TLR	Localisation	Ligand	Adaptor Protein
TLR 1	Cell membrane	Triacyl lipopeptide	MyD88
TLR 2	Cell membrane	Bacterial Lipoproteins	MyD88
		Porin (Influenza)	
		Haemagglutinin (Measles)	
		Zymosan (Fungi)	
TLR 3	Intracellular	dsRNA	TRIF/TRAM
TLR 4	Cell membrane	LPS	MyD88/TIRAP
		F protein (RSV)	TRIF/TRAM
		Env (MMTV)	
TLR 5	Cell membrane	Flagellin	MyD88
TLR 6	Cell membrane	Diacyl lipopeptide	MyD88
TLR 7	Intracellular	ssRNA	MyD88
		Imiquimod	
TLR 8	Intracellular	ssRNA	MyD88
		Resiquimod	
TLR 9	Intracellular	CpG DNA	MyD88
TLR 10	Cell membrane	Unknown	Unknown

Table 1.1 TLRs, their ligands and adaptor proteins

Table listing the mammalian TLRs, their cellular localisation, their main agonists and adaptor proteins.

1.4.2 RIG-I-like receptors (RLRs)

The preserved immune response in TLR3 knockout mice to poly(I:C) and viral infection led to the discovery of two new receptors, retinoic acid inducible gene-I (RIG-I) and melonoma differentiation-associated gene 5 (MDA5), involved in cytoplasmic viral RNA detection (Yoneyama et al., 2004) (see **Figure 1.1**). These receptors are capable of recognising the genomic content of dsRNA viruses as well as ssRNA viruses via their intermediate dsRNA-state seen during viral replication as well as host self RNA in the cytoplasm (Takeuchi and Akira, 2009; Yoneyama and Fujita, 2008). Specifically, RIG-I recognises blunt-ended dsRNA with a 5′-triphosphate cap while MDA5 binds dsRNA greater than 1kb in size (Berke et al., 2013). A third RLR, laboratory of genetics and physiology 2 (LGP2), has been shown to have an inhibitory affect on RIG-I signalling, as it has greater affinity for dsRNA then RIG-I. LGP2 structurally lacks caspase recruitment domain (CARD) copies (Akira et al., 2006; Tanner and Linder, 2001; Yoneyama and Fujita, 2007). It has been postulated that LPG2 cooperates with MDA5 in the recognition of dsRNA, however the precise mechanisms behind LPG2 signalling are still not completely understood (Komuro and Horvath, 2006; Yoneyama and Fujita, 2010).

Structurally, both RIG-I and MDA5 contain two copies of CARD, required for downstream signalling, and a DExD/H box RNA helicase domain, with the ability to intrinsically unwind dsRNA (Tanner and Linder, 2001). The CARD domains transduce signals that lead to the activation of IRF-3 and NF-κB whilst the RNA helicase domain can bind viral RNA directly in an ATP-dependent manner (Saito et al., 2007; Yoneyama et al., 2004). RIG-I recognises members of the Paramyxoviridae, Rhabdoviridae, and Orthomyxoviridae virus genera, whilst MDA5 has been linked to members of the Picornaviridae (Kato et al., 2006; Loo and Gale, 2011). In contrast, both RIG-I and MDA5 can detect a subset of viruses which include Dengue virus, West Nile virus and reovirus (Fredericksen et al., 2008; Loo et al., 2008).

RIG-I and MDA-5 both interact with Interferon beta promoter stimulator-1 (IPS-1), which is also known as mitochondrial antiviral signalling protein (MAVS), virus-induced signalling adaptor (VISA) or CARD adaptor inducing interferon-β (Cardif). IPS-1 is a CARD containing mitochondrial adaptor molecule that links RIG-I and MDA5 with downstream signalling molecules (Kawai et al., 2005; Meylan et al., 2005; Seth et al., 2005; Xu et al., 2005). The RIG-I or MDA5 and IPS-1 complex recruits several signalling molecules, including TRAF3/6, TNF receptor associated death domain (TRADD), RIP1, caspase-8/10 and Fas-associated death

domain (FADD). These signalling molecules set in motion the activation of IKKα/IKKβ and TBK1/IKKi complexes resulting in NF-κB, and IRF-3 and IRF-7 activation and translocation into the nucleus that ultimately leads to the induction of proinflammatory cytokine and type I IFN genes (Takeuchi and Akira, 2010; Yoneyama and Fujita, 2010).

1.5 TLR signalling

TLR signalling can be divided into a further two categories based on the distinct signalling pathways which lead to the production of a plethora of proinflammatory cytokines and type I interferons (IFNs). The distinction is made based on the TIR-domain-containing adaptor molecules that bind to the TLR-cytoplasmic domain, Myeloid differentiation primary response gene 88 (MyD88) and TIR-domain containing adaptor protein inducing IFN (TRIF).

1.5.1 MyD88-dependent signalling

MyD88 is a pivotal adaptor protein utilized by all TLRs with the exception of TLR3 (**Figure 1.1 and 1.2**). It was identified because of shared homology to the TIR domain (Hultmark, 1994). A further TIR domain-containing adaptor protein was identified as a bridging adaptor for MyD88-dependent signalling through TLR2 and TLR4 activation known as MyD88 adaptor like (MAL) or TIR domain containing adaptor protein (TIRAP) (Fitzgerald et al., 2001; Horng et al., 2002).

MyD88 is recruited to the cytoplasmic TIR domain of the TLR receptor after ligand stimulation and interacts with IL-1R-associated kinase (IRAK)-4 through its cytosolic death domain contained within the N-terminus of MyD88. The death domain mediates protein-protein interactions giving MyD88 its adaptor molecule properties.

The MyD88/IRAK-4 complex then results in the recruitment and phosphorylation of IRAK-1 and IRAK-2, which sequentially activates TNF receptor-associated factor (TRAF)-6 (Kawagoe et al., 2008). TRAF6 is an E3 ubiquitin ligase that catalyzes the formation of lysine 63-linked ubiquitin chain through the interaction with E2 ubiquitin-conjugating enzymes Ubc12 and Uev1A (Xia et al., 2009) (**see section 1.7.2**). This results in the activation of the complex known as TGF-β-activated kinase (TAK)-1/TAK1 binding protein (TAB) -1, -2 and 3. TAK-1 activates the IκB kinase

(IKK) complex comprised of two catalytic subunits IKK-α and IKK-β and a non-catalytic regulatory subunit NF-κB essential modulator (NEMO) resulting in IκBα ubiquitination and degradation (Muzio et al., 2000). This classical pathway otherwise known as canonical NF-κB signalling results the freeing of the nuclear localisation domain of NF-κB allowing its translocation to the nucleus to act as a pro-inflammatory gene transcription factor (**see section 1.6.1**) (Baeuerle and Baltimore, 1996) (Karin and Ben-Neriah, 2000).

The activation of TAK1 also activates the parallel mitogen activated protein kinase (MAPK) signalling pathway resulting in the activation or the transcription factor AP-1 (Ropert et al., 2001) (**see section 1.6.3**). These pathways lead to the transcription of numerous proinflammatory genes, including IL-1, TNFα, IL-8/CXCL8 and IL-6. (Brown et al., 2010; Cao et al., 1996; Kawai et al., 2001; Takeuchi and Akira, 2001).

1.5.2 MyD88-independent signalling

As noted above, TLR3 signals via TRIF (**Figure 1.2**), an adapter protein that was first discovered following the stimulation of MyD88-deficient mice with LPS wherein the mice showed late phase activation of NF-κB (**see section 1.6.1**) and MAPKs (**see section 1.6.3**) associated with the activation of type I IFNs (**see section 1.2.1.3**) (Kawai et al., 1999; Kawai et al., 2001). In contrast, the knockdown of TRIF resulted in early phase NF-κB signalling but a reduced pro-inflammatory cytokine and type I IFN production in mice (Hoebe et al., 2003; Yamamoto et al., 2003).

TRIF is selectively recruited by TLR3 and TLR4, however TLR4 requires a further bridging adaptor protein TRIF related adaptor molecule (TRAM) (Yamamoto et al., 2003). The activation of TRIF post ligand stimulation leads to the recruitment of TRAF3. Activated TRAF3 is involved in the nuclear translocation of IFN regulatory factor (IRF)-3 and IRF7 by activating a complex known as TRAF-family member associated NF-κB activator (TANK)-binding kinase (TBK)-1/IKKi. IRF3 and IRF7 form homo- or heterodimers post phosphorylation and bind to the IFN-stimulated response element (ISRE) leading to the expression of IFN-inducible genes. This process results in the induction of type I (IFN α, β) and type III (IFNλ) genes. TRIF can also recruit and activate TRAF6, which leads to the interaction with receptor interacting protein (RIP)-1, resulting in canonical NF-κB activation and cytokine production (Akira et al., 2006; Brown et al., 2010; Honda et al., 2005).

TLR4 activates both MyD88-dependent pathway and TRIF-dependent pathway. It has been shown that TLR4 activation occurs at the plasma membrane whereby MyD88 and bridging adaptor, TIRAP, activate NF-κB gene transcription as described above, which leads to the translocation of TLR4 into the endosome or lysosome to recruit TRAM. The subcellular localisation of TRAM is essential for efficient signal transduction and is controlled by myristoylation and phosphorylation resulting in activation of IRF gene transcription (Kenny and O'Neill, 2008; Tanimura et al., 2008).

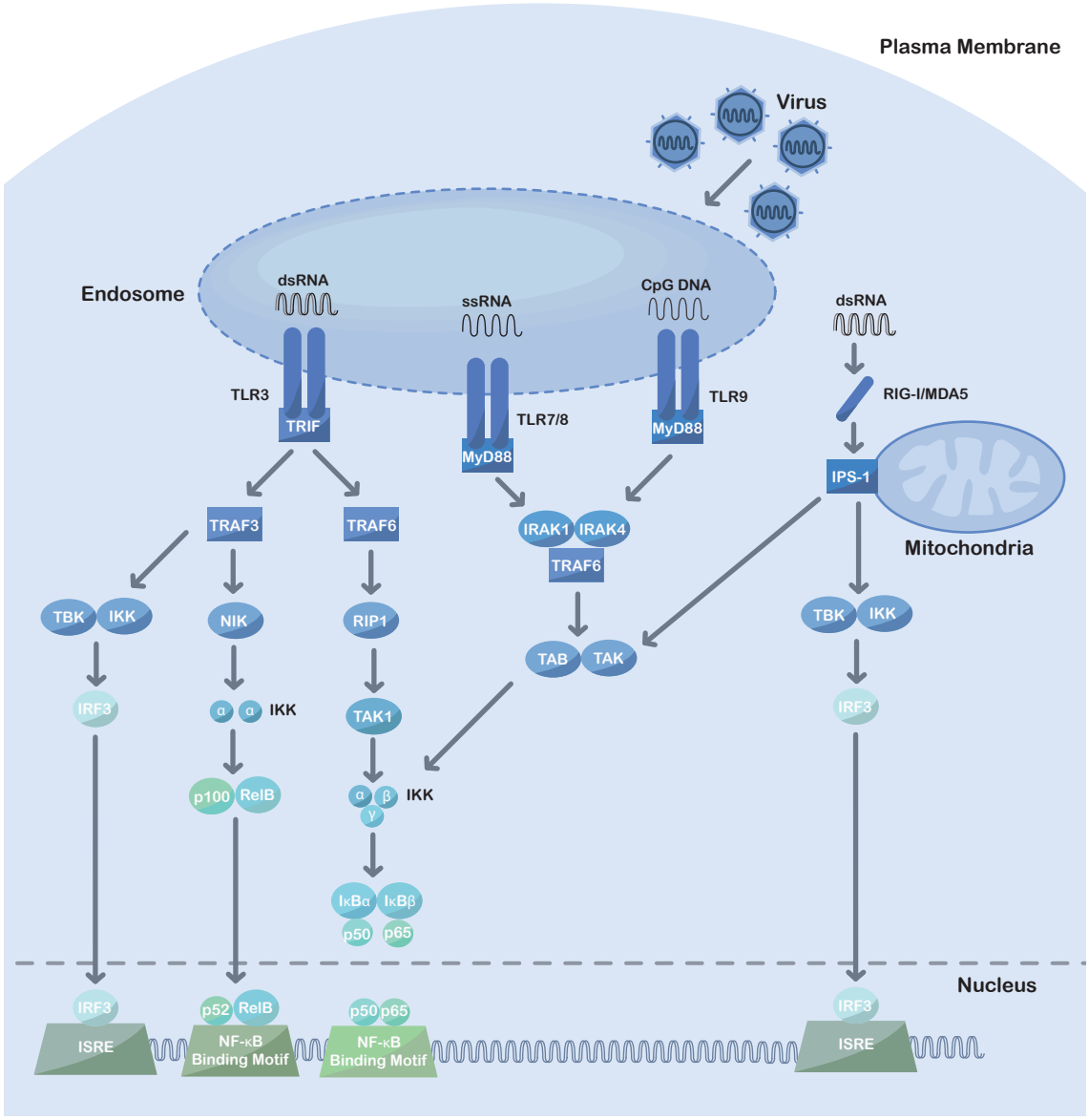

Figure 1.1 Mechanisms of Viral Detection

TLR3 and RIG-I/MDA5 recognise cytoplasmic viral dsRNA and recruit TRIF, leading to the activation of NF-κB via TRAF6 and RIP1 and the phosphorylation of IRF3 via the TBK/IKKi complex. RIG-I/MDA5 requires the mitochondria-bound adaptor molecule, IPS-1, to achieve this activation. This results in the induction of type I IFNs and proinflammatory cytokines.

TLR7/8 and TLR9 recognise cytoplasmic viral ssRNA and CpG DNA respectively. MyD88 is recruited to the cytoplasmic TIR domain of the receptors after ligand stimulation and interacts

with IRAK-4, IRAK-1, TRAF3 and TRAF6. This interaction leads to the phosphorylation and subsequent nuclear translocation of IRF-7 resulting in type I IFN production.

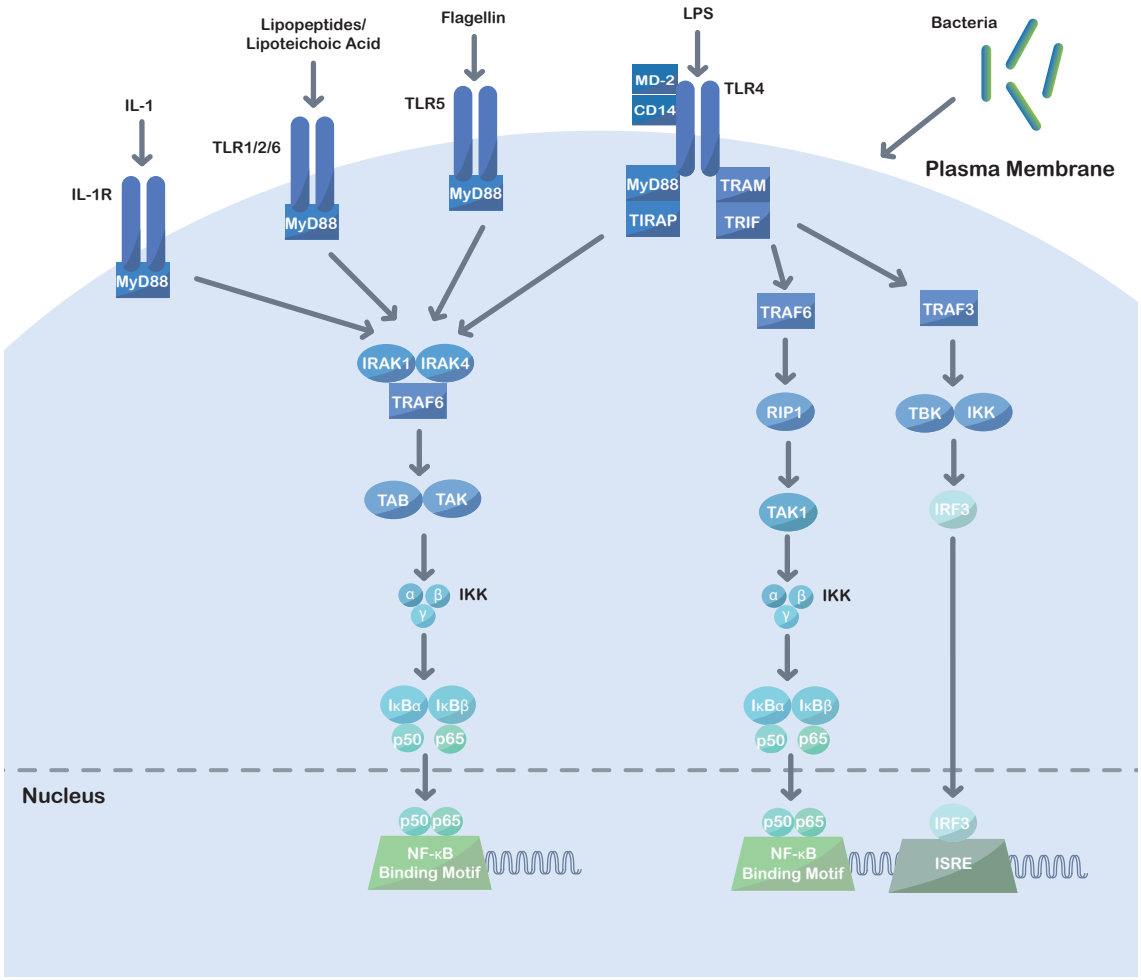

Figure 1.2 Mechanisms of Bacterial Detection

TLRs and IL-1R share common signaling pathways. TLR2, TLR4 and TLR5 recognise lipoproteins, LPS and flagellins respectively whilst IL-1R recognises IL-1 family members. Once ligand/receptor interaction occurs, MyD88 is recruited to the receptor. TLR4 requires an additional bridging molecule TIRAP to subsequently form a complex with IRAK-4, IRAK-1 and TRAF6. This results in the activation of TAK1/TAB, which is ultimately responsible for the activation of NF-κB signaling through the IKK complex and MAPK respectively leading to induction of proinflammatory cytokine.

TLR4 also triggers the TRIF-dependent pathway via the adaptor molecule TRAM. This leads to the activation of NF-κB and IRF-3 and IRF-7 phosphorylation, resulting in the expression of IFN-induced genes by binding to ISRE producing type I IFN and proinflammatory cytokines.

1.6 PRR-induced transcription factors

1.6.1 NF-κB

The NF-κB family regulates multiple biological processes including immunity, inflammation, cell survival, growth and differentiation (Hayden and Ghosh, 2008). In mammals, the NF-κB family of transcription factors is comprised of five members: RelA (p65), RelB, c-Rel, p105 (NFKB1) and p100 (NFKB2). These NF-κB proteins can be characterised by their shared conserved 300-amino acid Rel homology domain (RHD), which is responsible for homo- or heterodimerisation, IκB interaction and encompasses DNA-binding motifs and a nuclear localisation sequence (NLS) (Hayden and Ghosh, 2004).

1.6.1.1 Canonical NF-κB signalling

NF-κB activation is signal dependent and can be regulated by a number of extracellular stimuli including viral or bacterial pathogens, cytokines, oxidative stress and injury (Sun, 2011). In unstimulated cells, NF-κB is sequestered in the cytoplasm through its interaction with IκB inhibitory proteins. Seven members of the mammalian IκB family have been identified and are characterised by their inhibitory role through their binding of ankyrin-like repeats to the RHD resulting in the masking of the nuclear localisation signal (Hatada et al., 1992). IκBα, IκBβ and IκBε have been associated with mammalian NF-κB due to the N-terminal regulatory regions necessary for stimulus-induced degradation (Arenzana-Seisdedos et al., 1997).

Following extracellular stimulation IκBs undergo degradation regulated by the IKK complex (Karin and Ben-Neriah, 2000). The serine kinases IKKα and IKKβ contain N-terminal kinase domains, a C-terminus helix-loop-helix motif and leucine-zipper domain within their structure (Mercurio et al., 1997). In canonical NF-κB signaling, IKKβ mediates the phosphorylation of IκBα and IκBβ at two N-terminal serine residues (Ser-32 & Ser-36 and Ser-19 & Ser-23 respectively) leading to Lys-48 linked polyubiquitination (**see section 1.7.2**) and subsequent protein degradation releasing NF-κB dimers for nuclear translocation (Lee et al., 1997; Mercurio et al., 1997; Napetschnig and Wu, 2013) (**Figure 1.3**). Interestingly, whilst IKKβ and NEMO are indispensable for canonical-NF-κB gene transcription, the role of IKKα remains poorly understood (Gray et al., 2014), although in macrophages, IKKα has been described as a

negative regulator of activation and inflammation through the accelerated removal of RelA and c-Rel from the NF-κB gene promoter (Lawrence et al., 2005).

1.6.1.2 Non-canonical NF-κB signalling

Whilst canonical NF-κB activation relies on the inducible degradation of IκBs to release NF-κB dimeric complexes, non-canonical NF-κB relies on the inducible proteolytic processing of the precursors p105 (NFKB1) or p100 (NFKB2) by the proteasome to produce their active subunits p50 and p52 respectively (Betts and Nabel, 1996; Fan and Maniatis, 1991). Structurally, p105 and p100 contain C-terminus ankyrin repeat-containing domains (ARD) giving them similar inhibitory characteristics to IκBs and constricting their inactive forms to the cytoplasm. Once processed, the active p50 and p52 do not contain transactivation domains (TAD) essential for targeting gene transcription. p50 and p52 therefore require dimerization with TAD-containing RelA, RelB or c-Rel to activate NF-κB gene transcription. The formation of p52 and p50 homodimers are associated with negative regulation of NF-κB through the association with histone deacetylase-1 (HDAC-1) resulting in inhibition of gene transcription (Zhong et al., 2002).

p105 is constitutively processed into its active fragment p50 through the partial proteolysis by the 26S proteasome. In addition to containing a RHD required for homo- (p50/p50) and heterodimerisation (p50/p65), p105 also presents with a glycine-rich region (GRR) responsible for preventing its complete degradation by the 26S proteasome and stabilising the active p50 protein (Lin et al., 1998).

In addition to regulating NF-κB signalling, p105 has also been associated with other signalling pathways involved in the regulation of cell signalling. For instance, p105 can bind Caspase-8-related protein (Casper)/ Cellular FLICE-like inhibitory protein (c-flip), a protein involved in the regulation of caspase-8 induced apoptosis. This interaction is mediated through IκBγ and halts p105 proteasomal processing resulting in the inhibition of NF-κB activation and increase in Casper/c-flip induced apoptosis (Li et al., 2003). p105 also plays a role in the regulation of MAPK signalling by forming a complex with the otherwise unstable Tpl2 (MEK kinase). The p105/Tpl2 complex inhibits MAPK signalling in unstimulated cells whilst maintaining a cellular reservoir of Tpl2 required for effective activation of MAPK signalling in response to LPS (Pereira and Oakley, 2008).

Contrary to p105 constitutive processing, p100 is a tightly regulated process dependent on inducible phosphorylation and ubiquitination (Xiao et al., 2001). The activation of specific TNF-family receptors has been identified as the trigger for the processing of p100, including lymphotoxin-b receptor (LTβR), B cell–activating factor receptor (BAFF-R), CD40 and receptor activator for NF-κB (RANK) (Coope et al., 2002; Dejardin et al., 2002; Kayagaki et al., 2002). In addition, TNF-induced cytokine TNF-like weak inducer of apoptosis (TWEAK) and the bacterial PAMP, LPS, have also been associated with instigating p100 processing (Mordmuller et al., 2003; Saitoh et al., 2003).

The activation of p100 signalling is dependent on the catalytic properties of NF-κB-inducing kinase (NIK). In unstimulated cells, NIK undergoes constant rapid synthesising and degradation through the interaction with a TRAF-cIAP E3 complex consisting of TRAF2, TRAF3, cellular inhibitor of apoptosis 1 (cIAP1) and cIAP2 complex (Sun, 2010). Upon extracellular stimulation NIK is released from this complex and in turn recruits and activates IKKα (but not IKKβ or NEMO) resulting in the formation of a p100 complex through the NIK-induced phosphorylation of two serine residues (ser-866 and ser-870) in the C-terminus NIK-responsive domain of p100 (Fong and Sun, 2002; Xiao et al., 2004). Consequently, specific p100 serine residues (ser-99, ser-108, ser-115, ser-123, and ser-872) are phosphorylated by IKKα resulting in the ubiquitination of p100 and processing into p52 (Xiao et al., 2004). Whilst p100 serves as a precursor to p52, p100 also acts as a cytoplasmic inhibitor much like IκB proteins and inhibits RelB nuclear translocation and NF-κB gene transcription (Heusch et al., 1999; Solan et al., 2002).

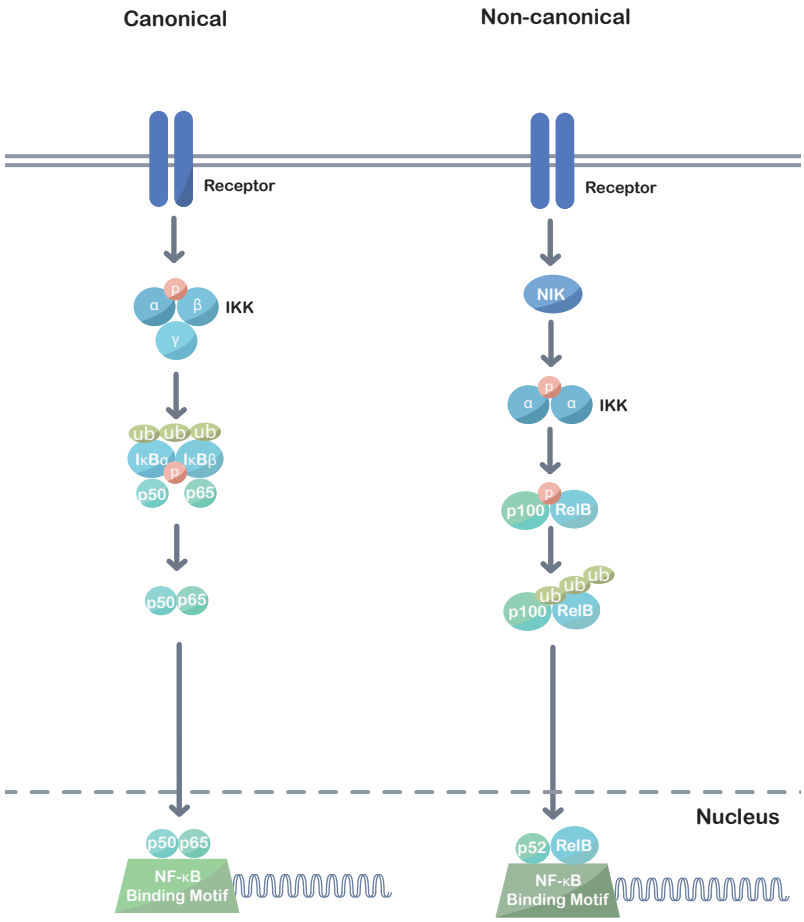

Figure 1.3: Canonical and Non-canonical NF-κB signalling pathway

Following receptor activation, the canonical NF-κB pathway activates the IKKβ subunit of the IKK complex. IKKβ then phosphorylates classical IκB proteins bound to NF-κB dimers such as p50-p65 resulting in IκB ubiquitination and proteasome-induced degradation releasing NF-κB to translocate to the nucleus where it activates target genes.

Non-canonical NF-κB signalling pathway requires NIK activation followed by phosphorylation of two IKKα subunits. The activated IKKα complex leads to the phosphorylation of the IκB domain of p100 subunit releasing the active p52 component. The active p52 dimerises with RelB and subsequently enters the nucleus to bind specific DNA sequences.

1.6.2 Interferon Regulatory Factors (IRFs)

The IRF family comprises of nine transcription factors known as IRF-1, IRF-2, IRF-3, IRF-4 (otherwise known as ICSAT or PIP), IRF-5, IRF-6, IRF-7, IRF-8 (alternately known as ICSBP) and IRF-9. As the name suggests, IRFs are responsible for the transcriptional regulation of IFNs. However, IRFs also play multiple roles in the regulation of innate and adaptive immune responses, including roles in pathogen response, cytokine signalling and cell growth regulation.

All IRFs share homology in their N-terminal DNA binding domain that encompasses five tryptophan residue repeats. The DNA binding domain forms a helix-turn-helix binding motif, which allows the recognition of the IFN-stimulated response element (ISRE), found in promoters of most IFN-inducible genes (Mamane et al., 1999). All IRFs, with the exception of IRF-1 and IRF-2 contain an IRF association domain in their C-terminal region, which accounts for the regulation of homo- and heterodimerisation with family members or other transcription factors (Mamane et al., 1999; Taniguchi et al., 2001). IRF-1, IRF-3, IRF-5 and IRF-7 have been implicated as positive regulators of type I IFN genes.

IRF-3 and IRF-7 share the greatest homology with both playing a role in regulating type I and type III IFN gene expression induced by viruses via the RIG-I/MDA5 signalling pathway. IRF-3 can also be induced via TRIF in TLR3 and TLR4 signalling, whilst IRF-7 is induced via TLR7, TLR8 and TLR9 signalling (Honda et al., 2005; Taniguchi et al., 2001). IRF-3 is constitutively expressed in its inactive form the cytosol of most cells. Upon viral stimulation, IRF-3 undergoes serine phosphorylation followed by homodimerisation or heterodimerisation with IRF-7 (Honda and Taniguchi, 2006). This dimer complex then undergoes nuclear translocation where it forms a holocomplex with the transcriptional co-activators, cyclic-AMP responsive element binding protein (CREB)-binding protein (CBP) and p300, ultimately resulting in type I IFN gene activation (Lin et al., 1998; Sato et al., 1998). The different combinations of IRF-3 and IRF-7 dimer complexes result in altered gene transcription profiles, where IRF3 specifically activates IFN-β genes and IFN-α4 whilst IRF7 results in the activation of both IFN-α and IFN-β gene transcription (Marie et al., 1998; Sato et al., 1998; Sato et al., 2001). Unlike IRF-3, IRF-7 is expressed in small quantities in most cell types unless induced by type I and III IFNs. Type I IFNs elicit the induction of IRF-7 via activation of IFN-stimulated gene factor 3 (ISGF3), a heterotrimeric transcriptional activator consisting of IRF-9, STAT1 and STAT2.

1.6.3 MAPK Signalling

TLR signalling results in the activation of transcription factors such as NF-κB and mitogen-activated protein kinases (MAPKs). MAPKs are a highly conserved family of serine/threonine protein kinases (Arthur and Ley, 2013; Blenis, 1993). MAPK signalling plays a key role in many fundamental cellular processes including induction of cell proliferation, cell growth, differentiation and the inflammatory response. The three best-characterised members of the MAPK family includes the extracellular signal regulated kinase (ERK), C-Jun N-terminal kinase/ stress-activated protein kinase (JNK/SAPK) and p38 MAPK. MAPKs form part of a protein kinase cascade consisting of at least three sequentially activated enzymes. This three-stage protein kinase cascade begins with the phosphorylation of MAPKK by MAPKKK resulting in the activation of p38s, ERK and JNK/SAPKs (Karin, 1996) (**Figure 1.4**).

ERKs were the first mammalian members of the MAPK family to be cloned and characterised (Boulton et al., 1991; Boulton et al., 1990). ERK1/2 are regulated by their upstream MAPKK ligands MAPK/ERK kinase 1 and 2 (MEK1 and MEK2), which in turn are activated by their upstream counterparts MAPKKK, A-Raf, B-Raf and Raf-1. A further two MAPKKKs, Mos and Tpl2 (also known as Cot), have also been identified but function only in restricted cell type and stimulus specific manner (Posada et al., 1993; Waterfield et al., 2003).

The JNK family consists of three isoforms termed JNK1, JNK2 and JNK3. Whilst JNK1 and JNK2 are broadly distributed amongst tissue, JNK3 is mostly localised to neuronal tissues, testis and cardiac myocytes (Bode and Dong, 2007). The MAPKKKs involved in the JNK signalling pathway differ from those of ERK. MEK kinase 1 (MEKK1) functions as MAPKKK in the JNK pathway. MEKK1 then phosphorylates MKK4 at serine and threonine residues consequently leading to JNK phosphorylation and activation.

The p38 MAPKs were originally described as protein kinases activated by LPS following tyrosine phosphorylation (Han et al., 1994). A total of four p38 isoforms have been identified as p38α, p38β, p38γ and p38δ. Similarly to JNK, a plethora of MAPKKKs are involved in p38 activation including MEKK1-3, MLK2/3, TAK1, ASK1, TAO1/2 and Tpl2 (Cuadrado and Nebreda, 2010). The MAPKK MKK6 acts on all p38 isoforms whilst MMK3 selectively phosphorylates p38α, p38γ and p38δ.

AP-1 is a heterodimer composed of sequence-specific transcriptional activators belonging to the basic leucine zipper (bZIP) superfamily of DNA binding proteins such as c-Jun, c-Fos and ATF2 (Karin, 1996; Karin et al., 1997). MAPKs can regulate the activation of activator protein-1 (AP-1) by direct phosphorylation of AP-1 proteins and altering the abundance of individual AP-1 components within a cell (Silvers et al., 2003). ERK, p38 and JNK substrates such as Elk-1 or serum response factor accessory protein (SAP) 1a and 2 increase AP-1 complex component, c-Fos (Pearson et al., 2001). Both p38 and JNK can phosphorylate the transactivating domain of ATF2, while JNK can directly phosphorylate the c-Jun activation domain. In addition, both ERK and p38 phosphorylate MEF2 transcription factors that bind the c-jun promoter (Han et al., 1997). AP-1 activation results in transcription of multiple genes including IL-1, TNF, c-Jun itself and various proteases and cell adhesion molecules such as E selectin (Read et al., 1997).

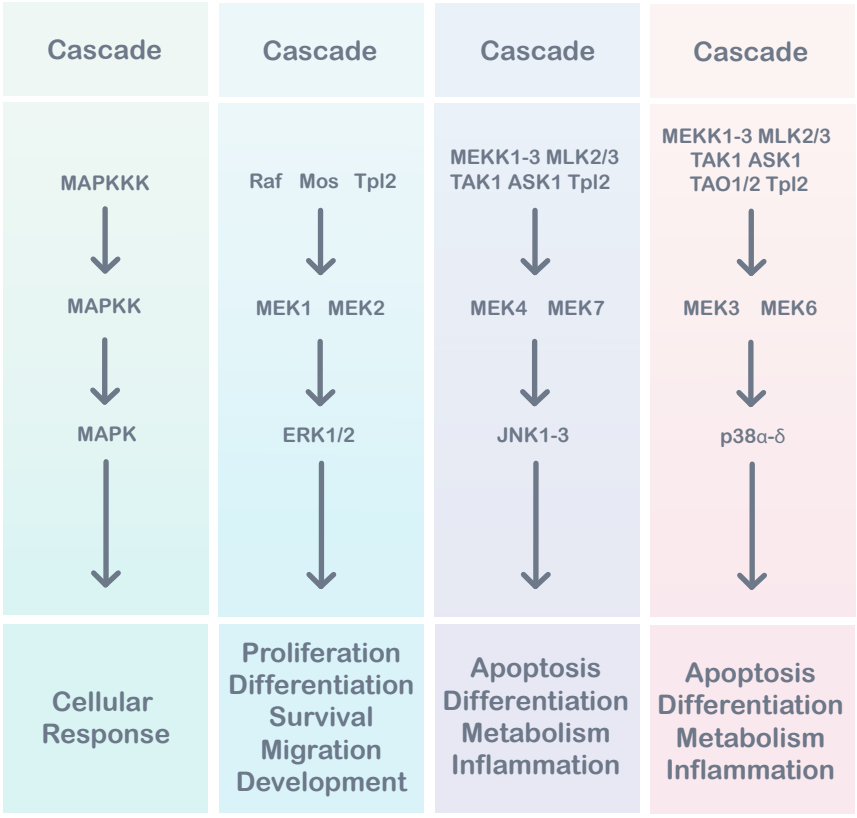

Figure 1.4: MAPK cascades in mammalian cells

MAPK signalling cascade involves the sequential phosphorylation of three kinases: MAP kinase kinase kinase (MAPKKK), MAP kinase kinase (MAPKK) and MAP kinase (MAPK). This figure provides a simple overview of three mammalian MAPK cascades that regulate the activity of ERK, JNK and p38 and their corresponding cellular responses.

1.7 Pellino

Pellino was first characterised in *Drosophila melanogaster* as a binding partner of Pelle, the *Drosophila* counterpart of mammalian IRAK (Grosshans et al., 1999). In *Drosophila melanogaster,* Pellino positively regulates the innate immunity in response to gram-positive bacteria (Haghayeghi et al., 2010). Since its discovery, a role for Pellino in TLR/IL-1 signalling has been identified (Grosshans et al., 1999). In humans the Pellino family is composed of Pellino-1, Pellino-2 and splice variants Pellino-3a and Pellino-3b (Jensen and Whitehead, 2003a; Jiang et al., 2003; Resch et al., 2001; Rich et al., 2000; Yu et al., 2002). These highly conserved Pellino isoforms share approximately 85% homology with each other (Jensen and Whitehead, 2003b). Pellino-1, Pellino-2 and Pellino-3 have all been shown to interact with TLR signalling molecules such as IRAK1, IRAK 4, TRAF6 and TAK1 (Butler et al., 2005; Jensen and Whitehead, 2003a, b; Jiang et al., 2003; Yu et al., 2002). Previous work from my group has identified a role for Pellino-1 in the regulation of human pathogens indicating a potential novel target for the regulation of viral pathogens in airways (Bennett et al., 2012).

1.7.1 Pellino-1

Pellino-1 is a ubiquitously expressed protein, however its levels of expression vary across different organs; In murine tissue Pellino-1 was found to be highly expressed in peripheral blood leukocytes, moderately in lung, liver, placenta, kidney, spleen and brain, with low levels of expression in the small intestine, heart and colon (Jiang et al., 2003).

Pellino-1 was first described in 2003 and associated with TLR/IL-1R signalling. *Jiang et at* identified a role for Pellino-1 in the IL-1-dependent activation of NF-κB signalling and the resulting CXCL-8 production; the group proposed Pellino-1 induces its effects through its IL-1-dependent interaction with the IRAK4/IRAK1/TRAF6 signalling complex (Jiang et al., 2003). Initially Pellino-1 was believed to function solely as a scaffolding protein due to its perceptible lack of enzymatic activity and functional domains. However, in 2006 *Schauvliege et al* determined Pellino-1's biochemical function as an E3-ubiquitin ligase (**see section 1.7.2**). The group identified a novel RING (really interesting new gene)-like motif, CHC2CHC2, in the C-terminal containing a unique Cys-Gly-His triplet sandwiched between two Cys-Pro-X-Cys motifs, which closely resemble the structure of a traditional C3HC4 RING, best known for their

occurrence in RING E3-ubiquitin ligases (Schauvliege et al., 2006). The group further showed that Pellino-1 exerts its activation on NF-κB signalling through polyubiquitination of IRAK-1 via its RING-like domain; whilst Pellino-1 mutants containing mutated cysteine and histidine residues did not induce the polyubiquitination of IRAK1 (Schauvliege et al., 2006, 2007).

Subsequent publications confirmed the role for Pellino-1 as an E3-ubiquitin ligase and identified its ability to catalyse a variety of polyubiquitin chains *in vitro*, depending on the presence of the E2 enzymes available (Butler et al., 2007). Pellino-1 can act with E2 conjugating complex UbcH3 to form Lys48-linked polyubiquitin chains, or interact with UbcH4, UbcH5a or UbcH5b to catalyse the formation of Lys48- and Lys11-linked chains (Ordureau et al., 2008). Pellino-1 can also interact with E2 heterodimer Ubc13-Uev1a to form Lys63-linked polyubiquitin chains associated with IRAK1 ubiquitination (Butler et al., 2007; Ordureau et al., 2008; Xiao et al., 2008).

1.7.2 Ubiquitination

Ubiquitination plays a critical role in regulating a host of crucial cellular functions including the initiation of inflammatory responses through the regulation of signalling molecules (Deng et al., 2000; Pickart, 2001) (Reviewed extensively by (Malynn and Ma, 2010)). The highly conserved process of ubiquitination involves the formation of an isopeptide bond between the C-terminus of the 76-amino acid peptide, ubiquitin, to the ε-amino group of a lysine residue of the target protein. This post-translational modification occurs through the sequential action of three enzymes: E1 ubiquitin-activating enzyme (E1), E2 ubiquitin-conjugating enzyme (E2) and E3 ubiquitin-protein ligase (E3) (**Figure 1.5**). Initially, ubiquitin is activated via the formation of a thioester bond between the C-terminus of ubiquitin and the active site cysteine of the E1 enzyme. The thioester-ubiquitin is then transiently transferred by the E2 enzyme to the E3 ligase where it is covalently attached to its target substrate (Pickart, 2001) (d'Azzo et al., 2005).

Although there are only two isoforms of E1 enzymes encoded in the human genome, there are 37 E2 enzymes known, and over 600 E3 ligases dictating the substrate specificity of the ubiquitination process (Komander, 2009). There are three primary types of E3 ligases distinguished by the presence of a HECT (homologous to E6-AP carboxyl terminus) domain, RING domain and U-box domain (Hatakeyama and Nakayama, 2003). E3 ligases containing a HECT domain catalyse ubiquitination by intermediately binding ubiquitin through the

formation of a thioester bond before transferring to the target substrate. In contrast, E3 ligases containing a RING domain and U-box domain serve as a scaffold that bridges the E2 enzyme's active site directly to the substrate.

Ubiquitin contains seven distinct lysine residues, Lys6, Lys11, Lys27, Lys29, Lys33, Lys48 and Lys63, which can result in further versatility of the reaction. The multiple lysine residues in ubiquitin allow for the addition of further ubiquitin molecules to itself, resulting in ubiquitin polymers. A substrate ubiquitinated with a single ubiquitin molecule on a single lysine residue is termed monoubiquitination; whilst the ubiquitination of multiple ubiquitin chains can form via a process termed polyubiquitination. The nature of the lysine linkages used in individual polyubiquitin chains have great physiological implications. The conjugation of lysine-specific ubiquitin chains to a substrate protein can result in the modulation of a myriad of cellular processes. For instance, the mediation of protein degradation by 26S proteasome occurs through the recognition of Lys48-tagged polyubiquitin chains. Whereas Lys63 polyubiquitin chains are involved in the regulation of gene expression through its effects on protein-protein interactions and activation of kinases and phosphatases (d'Azzo et al., 2005; Liu et al., 2005; Moynagh, 2009).

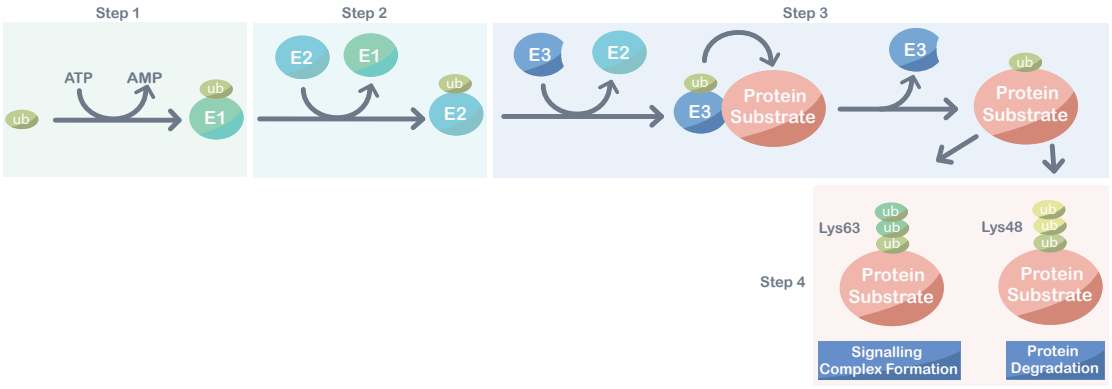

Figure 1.5: Ubiquitination pathway

Ubiquitination is a post-translational modification that occurs in a three step process. Firstly an ATP-dependent thioester bond is formed between the C-terminus of ubiquitin and the active site cysteine of the E1 enzyme (Step 1). The thioester-ubiquitin is then transiently transferred by the E2 enzyme (Step 2) to the E3 ligase where it is covalently attached to its target substrate (Step 3). The multiple lysine residues in ubiquitin allow for the addition of further ubiquitin molecules to itself, resulting in ubiquitin polymers (Step 4). The conjugation of lysine-specific ubiquitin chains to a substrate protein can result in the modulation of a myriad of cellular processes. For instance, Lys48-tagged polyubiquitin result in protein degradation by 26S proteasome, whereas Lys63 polyubiquitin chains are involved in signalling complex formation.

1.7.3 Pellino-1 phosphorylation

In addition, IRAK1 and IRAK4 have the potential to phosphorylate Pellino-1 and in turn enhance Pellino-1's E3-ubiquitin ligase activity culminating in the polyubiquitination of IRAK1 (Ordureau et al., 2008; Schauvliege et al., 2006). Phosphorylation of any of the Pellino-1 activating serine/threonine residues Ser-76, Thr-86, Thr-288 or Ser-293, or a combination of Ser-78, Thr-80 and Ser-82 results in the complete activation of Pellino-1 E3 ubiquitin ligase activity (Smith et al., 2009).

Pellino-1 serves as a substrate for the IRAK1 kinase domain which results in Pellino-1 phosphorylation followed by IRAK1 and IRAK4 Lys63-polyubiquitination (Butler et al., 2007; Schauvliege et al., 2006; Xiao et al., 2008). This process however also promotes IRAK-dependent Pellino-1 degradation via a reciprocal polyubiquitination by a separate unidentified E3 ubiquitin (Butler et al., 2007). This bidirectional signalling between the IRAK and Pellino family may act as a negative feedback loop to sequester TLR/IL-1R signalling.

1.7.4 Pellino-1 sumoylation

Pellino-1 also undergoes a post-translational modification called sumoylation. The process of sumoylation is similar with that of ubiquitination wherein a protein called small ubiquitin-like modifier (SUMO) covalently adheres to lysine residues of target substrates through an analogous enzyme cascade of E1-activating enzyme, E2-conjugating enzymes and E3-ligase enzymes. Pellino 1 undergoes sumoylation to its Lys169, Lys202, Lys266, Lys295, Lys297 and Lys303 regions, which coincide with its ubiquitination sites Lys169, Lys202, and Lys266 (Kim et al., 2011a). This not only suggests a competitive nature between ubiquitination and sumoylation, but also infers a further distinct role for Pellino-1 that has yet to be identified.

1.7.5 Pellino-1 Physiological function

The physiological function of Pellino-1 remains elusive with existing data providing both varying and contradicting results. A role for Pellino-1 was first identified in MyD88-dependent signalling wherein Pellino-1 regulated IL-1 induced NF-κB activation and IL-8/CXCL8 gene expression in the HEK293 cell line (Jiang et al., 2003). Interestingly, this regulation of TLR/IL-1R

signalling by Pellino-1 can be negatively regulated by the anti-inflammatory cytokine, TGF-β1, through its induction of inhibitory Smads (I-Smads), Smad6 and Smad7. I-Smads exert their anti-inflammatory activity by binding Pellino 1 and restricting NF-κB activation by disrupting the formation of Pellino-1/IRAK4/IRAK1/TRAF6 complex (Choi et al., 2006; Lee et al., 2010). Similarly, microRNA-21 (miR-21) has been shown to negatively regulate NF-κB signalling by directly inhibiting Pellino-1 expression during the proliferative phases of liver regeneration. miR-21 exerts its effects on Pellino-1 by binding to the 3' untranslated region (UTR) of its mRNA resulting in reduction of Pellino-1 expression (Marquez et al., 2010).

More recently with the generation of the Pellino1 knockout mouse, it has been suggested that it is involved in TLR3 signalling (Chang et al., 2009). Pellino1 deficient mice develop normally but are resistant to LPS-induced toxic shock and show impaired B-cell proliferation and induction of co-stimulatory molecules CD86 and MHC class II molecules. In contrast to previous studies, Pellino1 deficient MEFs showed preserved IL-1 signalling but had impaired responses to the TLR3 agonist and viral mimic poly(I:C) (Chang et al., 2009). This study also showed that Pellino-1 was capable of binding to and ubiquitinating RIP1 and this was suggested as a potential Pellino-1 target in TLR3 signalling (Chang et al., 2009).

These data indicate Pellino-1 has an important role in mediating TLR/IL-1R signalling. However, with the generation of Pellino-1 knockout mice came the discovery of a role for Pellino-1 in TLR3 and TLR4 signalling (Chang et al., 2009). Pellino-1 knockout mice develop normally but show resistance to LPS- and poly(I:C)-induced sceptic shock and resulted in decreased B-cell proliferation. In addition a role for Pellino-1 in the TRIF-dependent IKK-signalling arm of TLR3 signalling via its interaction with RIP1 and mediation of RIP1 ubiquitination in MEFs taken from the Pellino-1 knockout mouse was identified (Chang et al., 2009). Furthermore and in contrast to previous data, Pellino-1 was found to be dispensable for MyD88-dependent and IL-1R signalling in Pellino-1 deficient MEFs (Chang et al., 2009). Pellino-1 phosphorylation and activation has been shown to be mediated by IKKε and TBK1 axis of TLR3 signalling in murine bone marrow derived macrophages (BMDM) in an IRF-3 dependent manner (Smith et al., 2011). In addition, Pellino-1 knockdown performed on HEK293 cells did not affect IL-1 and LPS-induced IRAK1 Lys63-linked polyubiquitination (Kim et al., 2012). These studies contradict the results obtained from previous studies and also highlight the increasingly complex field of Pellino-1 physiology.

1.8 Hypothesis and Aims

Viral and bacterial infections account for the majority of exacerbations of COPD and can subsequently result in pronounced functional impairment of the airway increasing both the severity of the disease and frequency of exacerbations. In addition, COPD patient airways often chronically harbour bacterial and viral pathogens within their airways despite ongoing inflammation aimed at their resolution (Hurst et al., 2006). Thus, understanding the key regulatory pathways governing pathogen-induced chronic inflammation could provide pivotal information regarding COPD pathogenesis.

Pellino-1, originally identified as a regulator of IL-1 signalling (Jiang et al., 2003), and more recently identified in TLR signalling in response to viral infection (Chang et al., 2009) may play a central role in the regulation of innate immunity. This thesis investigates the regulation of Pellino-1 and its role in viral infection in human bronchial airway epithelial cells.

Therefore, it was hypothesized that:

1. Continuous activation of human bronchial epithelial cells by pathogenic agonists will alter their ongoing inflammatory response.
2. Pellino-1 regulates inflammatory responses to viral pathogens.

The aims of this thesis were:

1. To create an *in vitro* model of chronic airway inflammation using cell lines and primary airway epithelial cells.
2. To understand whether chronic inflammation uses different molecular pathways and presents different targets for treatment of disease.
3. To dissect of the roles of Pellino-1 in regulation of TLR3 signaling in response to viral stimuli.
4. To identify proteins or complexes regulated by Pellino-1 in response to viral stimuli.

CHAPTER 2 - MATERIALS AND METHODS

2.1 Materials

Reagents were purchased from Sigma-Aldrich (Poole, UK) or Invitrogen (Paisley, UK), except where specified. Recombinant human IL-1β was purchased from Peprotech (London, UK). Poly(I:C) was purchased from Invivogen (Toulouse, France) and purified LPS was from Axxora (Nottingham, UK). IL-1Ra was from the National Institute for Biological Standards and Control (Potters Bar, UK). OptiPrep^{TM} density gradient was purchased from Axis shield (Oslo, Norway). MACS LS columns were purchased from Miltenyi Biotec (Bergisch Gladbach, Germany). Cell culture flasks were purchased from Nunc (Thermo Fisher Scientific, Loughborough, UK) and cell culture plates were purchased from Costar (Sigma-Aldrich). All flow cytometry antibodies and isotype controls were from eBioscience (San Diego, USA). The protease inhibitor cocktail III was from Calbiochem (Nottingham, UK), 30% polyacrylamide from Gene Flow (Staffordshire, UK) RT-PCR primers were ordered from Eurogentec (Southampton, UK) unless otherwise stated. Matched ELISA antibody pairs were purchased from R&D Systems (Abingdon, UK).

2.2 Mammalian Cell Culture

2.2.1 BEAS-2B cell line maintenance

The immortalized bronchial epithelial cell line BEAS-2B was purchased from American Type Culture Collection (Manassas, VA, USA) and maintained in RPMI 1640 supplemented with 10% low-endotoxin Foetal Bovine Serum (FBS) purchased from Promocell (Heidelberg, Germany), 100 U/ml penicillin and 100 μg/ml streptomycin.

Cells were seeded at a density of $1x10^6$ cells per T75 cm^2 flask and were passaged when 80-90% confluence was reached (approximately every 3 days). Cell detachment was obtained by gently washing the cell surface layer with 10 ml PBS followed by the addition of 2 ml of non-enzymatic cell-dissociation solution and incubation at 37°C for between 5 to 10 minutes. This reaction was suspended by the addition of a further 8 ml of cell culture media. Cells were

maintained at 37°C and humidified 5% CO_2. Cell culture media was tested monthly for the presence of mycoplasma using EZ-PCR mycoplasma test kit (Geneflow, Staffordshire, UK) according to manufacturer's instructions.

2.2.2 THP-1 cell line maintenance

The human acute monocytic leukemic cell line THP-1 was purchased from ATCC (Manassas, VA, USA) and maintained in RPMI 1640 medium supplemented with 10% low-endotoxin FBS, 100 U/ml penicillin and 100 μg/ml streptomycin 2 mM L-glutamine.

Cells were maintained at $2x10^5$ cells/ml and were passaged when $8x10^5$ cells/ml was reached by the replacement or addition of fresh media. Cells were maintained at 37°C and humidified 5% CO_2. Cell culture media was tested monthly for the presence of mycoplasma using EZ-PCR mycoplasma test kit (Geneflow, Staffordshire, UK) according to manufacturer's instructions

2.2.3 Human bronchial epithelial primary cell (HBEpC) maintenance

Primary human bronchial epithelial cells from healthy volunteers were purchased from PromoCell (Heidelberg, Germany) and maintained in Airway Epithelial Cell Growth (AECG) medium purchased from PromoCell (Heidelberg, Germany) supplemented with bovine pituitary extract (0.05 mg/ml), epidermal growth factor (10 ng/ml), insulin (5 μg/ml), hydrocortisone (0.5 μg/ml), epinephrine (0.5 μg/ml), triiodo-L-thyronine (6.7 ng/ml), transferring (10 μg/ml), retinoic acid (0.1 ng/ml), 100 U/ml penicillin and 100 μg/ml streptomycin.

Cells were seeded at a density of $7.5x10^5$ cells per T75 cm^2 flask and were passaged when 85-95% confluence was reached. Cell detachment was obtained using PromoCell DetachKit according to manufacturer's instruction. Cells were maintained at 37°C and humidified 5% CO_2. Cell culture media was tested monthly for the presence of mycoplasma using EZ-PCR mycoplasma test kit (Geneflow, Staffordshire, UK) according to manufacturer's instructions.

2.3 Peripheral Blood Mononuclear Cell (PBMC) isolation

2.3.1 Cell separation by OptiPrep™ gradient

Peripheral venous blood was taken from consenting healthy volunteers in accordance with a protocol approved by the South Sheffield Local Research Ethics Committee. 4.4 ml of the anticoagulant 3.8 % tri-sodium citrate was added to 35.6 ml of blood and centrifuged at 320 g for 20 minutes. The plasma upper phase was removed and centrifuged at 1000 g for 20 minutes to produce platelet poor plasma (PPP).

The cell rich lower phase from the first centrifugation step was mixed with 6 ml of 6% Dextran T500, then topped up to 50 ml with 0.9% saline and gently inverted to mix. The erythrocytes were then allowed to sediment for 30 minutes. The leukocyte-rich layer was removed and centrifuged at 221 g for 6 minutes. The remaining leukocyte pellet was gently resuspended in 6 ml of Hank's Buffered Salt Solution (HBSS) supplemented with 20% PPP followed by 4 ml of OptiPrep™. After gentle inversion, the cell mixture was overlaid with 10 ml 1.095 g/ml OptiPrep™ (8.036 ml HBSS with 20% PPP and 3 ml OptiPrep™). A further 10 ml of 1.080 g/ml OptiPrep™ (10.435 ml HBSS with 20% PPP and 3 ml OptiPrep™) was overlaid followed by a 10 ml layer of HBSS with 20% PPP. These layers resulted in an OptiPrep™ gradient which was centrifuged at 700 g for 30 minutes without a deceleration break. This led to the separation of three distinct populations of cells (**Figure 2.1**) including a red cell layer located below the 1.095 g/ml OptiPrep™, a polymorphonuclear (PMN) layer located between the 1.095 g/ml and 1.080 g/ml OptiPrep™ layers, and a PBMC layer located between the 1.080 g/ml OptiPrep™ and HBSS with 20% PPP. The PBMCs were harvested using a Pasteur pipette, transferred into a clean tube, resuspended in 10 ml HBSS with 20% PPP and centrifuged at 511 g for 6 minutes. The resulting pellet was resuspended in RPMI 1640 with 10% low endotoxin FBS, 1% penicillin (100 units/ml) and 1% streptomycin (100ug/ml).

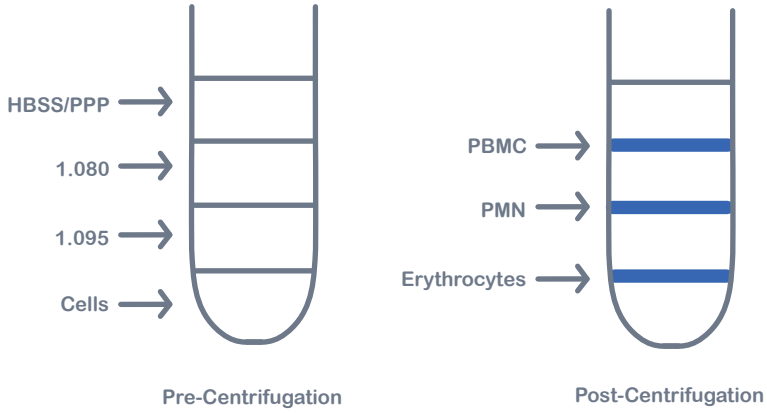

Figure 2.1 The OptiPrep™ gradient demonstrating separation of cell populations

2.4 Negative magnetic selection of monocytes

Monocytes were extracted from the PBMC mixture by negative magnetic selection using the Monocyte Isolation Kit II (Miltenyi Biotec, Audurn, CA, USA) according to manufacturer's protocol. PBMCs prepared in **section 2.2.1** were resuspended in monocyte column buffer at 30 µl per 10 x 10^6. The negative magnetic selection worked by depleting the non-monocytic cells within the mixture, including red cells, T cells, B cells, granulocytes and natural killer cells. These non-monocytic cells were labelled with a biotin-conjugated monoclonal antibody cocktail at 10 µl per 10 x 10^6 (CD3, CD7, CD16, CD19, CD56, CD123 and Glycophorin A) and a secondary labelling anti-biotin monoclonal antibodies conjugated to MicroBeads™ at 20µl per 10 x 10^6. These magnetically labelled cells were then depleted due to their retention on a MACS Column in the magnetic field of a MACS separator allowing the unlabelled monocytes to pass through.

2.4.1 Flow cytometry for monocyte purity

The purified cells obtained by negative selection were resuspended at a density of 2-3 x 10^5 cells in 22.5 µl of PBS, followed by the addition of 2.5 µl of PE-conjugated mouse anti-human CD14 antibody or mouse IgG_1 isotype control antibody and incubated for 20 minutes at 4 °C in the dark. Cells were centrifuged for 3 minutes at 1000 g then fixed with 10% CellFIX before fluorescence analysis using FACSCalibur flow cytometer. All data analysis was performed using FlowJo software (Tree Star Inc., Ashland, OR, USA).

2.5 Enzyme-linked immunosorbent assay (ELISA)

Supernatants from stimulated cells were collected into fresh microcentrifuge tubes then centrifuged at 1000 g for 3 minutes to pellet any cells in suspension. The remaining supernatant was transferred to a fresh microcentrifuge tube and stored at -80 °C until use.

A Maxisorp plate was coated with CXCL8 or RANTES/CCL5 coating antibody at 1.5 µg/ml or 2 µg/ml respectively diluted in coating buffer (see **Appendix**) and incubated overnight at room temperature. The plate was washed with wash buffer (see **Appendix**) 4 times using an ELx50 auto strip washer followed by a 1 hour block with 100 µl/well of 1% ovalbumin in coating buffer. All incubations occurred on an orbital shaker at room temperature. The plate was washed again as above, followed by the addition of 100 µl duplicates of each CXCL8 standard (ranging from 5000 pg/ml to 15.625 pg/ml) or RANTES/CCL5 standard (ranging from 10000 pg/ml- 39pg/ml or samples (diluted in basal media as required to ensure analysis within the linear portions of a log (concentration) / linear (optical density) standard curve) then incubated for 2 hours. The plate was washed and incubated with 100 µl biotinylated CXCL8 antibody (at 40 ng/ml) or biotinylated RANTES/CCL5 antibody (20ng/ml) diluted in wash buffer for 2 hours. After further washing, the plate was incubated in the dark with streptavidin HRP (Horse Radish Peroxidise) (Dako, UK) diluted 1 in 200 in wash buffer and finally washed again before a final incubation with substrate reagent (R&D Systems) prepared according to the manufacturer's instructions) for between 15-20 minutes. The reaction was terminated by the addition of 50 µl of 1 M H_2SO_4. Absorbance was measured on an Opsys MR™ Microplate Reader using Revelation software. The optical density (OD) of the plate was read at 450nm and further analysed using GraphPad Prism® software and plotted using a log/linear standard curve. The detection limit of the CXCL8/ RANTES/CCL5 ELISA was 31.25 pg/ml and 39 pg/ml respectively.

2.6 Reverse transcription PCR (RT-PCR)

2.6.1 RNA isolation from cells

DNA and RNA were isolated from cells using TRI Reagent® (Sigma-Aldrich) according to manufacturer's instruction. Briefly, cells were washed with PBS before the addition of 1 ml of TRI Reagent® per 5-10 million. Cells were incubated for 5 minutes at room temperature to allow for complete lysis. 200 µl of chloroform was added per 1 ml of TRI Reagent® and mixed vigorously for 15 seconds before incubation at room temperature for 10 minutes. Samples were centrifuged at 12,000 g for 15 minutes at 4°C resulting in three distinct phases, an RNA-containing aqueous phase, DNA-containing interphase and protein-containing organic phase. The aqueous phase was transferred into a fresh microcentrifuge tube and precipitated by mixing with 500 µl of isopropanol and incubated for 10 minutes at room temperature. The resulting RNA was then pelleted by centrifugation at 12,000 g for 10 minutes at 4°C. The RNA pellet was then washed with 1 ml of 75 % ethanol and centrifuged at 7500 g for 5 minutes at 4°C. The supernatant was discarded whilst the RNA pellet was air-dried for 5-10 minutes before being resuspended in 20 µl of sterile water.

2.6.2 DNase treatment of purified RNA

Isolated RNA underwent a DNase treatment step using the DNA-free kit from Applied Biosciences according to manufacturer's protocol. Briefly, 0.1 volume of DNase I Buffer and 1 µl rDNase I were added to the RNA and mixed gently before a 20-30 minute incubation at 37°C. 0.1 volume of DNase Inactivation Reagent was then added and incubated for 2 minutes at room temperature with occasional mixing. The RNA sample was centrifuged at 10,000 g for 1.5 minutes. The remaining RNA in suspension was transferred into a fresh microcentrifuge tube and quantified using a NanoDrop™ 1000 spectrometer (NanoDrop Tech. Inc. Wilmington, USA). RNA integrity and purity was measured by optical density ratios at 260/280 nm (with a ratio of 1.8-2) and 260/230 (with a ratio greater than 1.8).

2.6.3 cDNA synthesis

RNA was reverse transcribed to produce cDNA using the High-Capacity cDNA Reverse Transcription Kit (Applied Biosystems) according to manufacturer's protocol. Briefly, RNA was resuspended in sterile water to make a 1 µg/ 20 µl stock, which was mixed with the 2x Reverse Transcription Master Mix to form the components of the cDNA synthesis reaction as shown in

Table 2.1. This mix was then added to RNA reaction vials and the samples run on a Hybaid PCR Express Thermal Cycler (Hybaid Ltd, UK) at 25°C for 10 min followed by a 37°C for 120 minutes and 85°C for 5 minutes. The samples were stored at - 80°C until required.

Component	Volume/ Reaction
10x RT Buffer	4 µl
25x dNTP Mix (100mM)	1.6 µl
10x RT Random primers	4 µl
MultiScribe™ Reverse Transcriptase	2 µl
RNase Inhibitor	2 µl
Nuclease-free water	6.4 µl
Template RNA	20 µl
Total Volume	40 µl

Table 2.1 Components of cDNA synthesis reaction

2.6.4 Reverse transcription polymerase chain reaction (RT-PCR)

Template cDNA was incubated with reagents as described in **Table 2.2**. The resulting mix was then denatured at 94°C for 2 minutes followed by a 30 cycle reaction step consisting of 94°C denaturing step for 30 seconds, an annealing step specific to the primer pairs (55 °C- 68°C; **see Table 2.3**) for 1 minute and a 72°C extension step for 30 seconds. A final extension step at 72 °C for 2 minutes completed the process. The samples were run on Hybaid PCR Express Thermal Cycler then stored at - 20°C until required. Primers sequences are detailed in **Table 2.3**.

Component	Volume / Reaction
5 x Green GoTaq® Flexi Buffer	5 µl
$MgCl_2$ (25mM)	1.5 µl
dNTP Mix (10mM)	1 µl

Forward primer (100uM)	0.7 µl
Reverse primer (100uM)	0.7 µl
GoTaq® DNA Polymerase (5U/ µl)	0.25 µl
Nuclease-free water	13.85 µl
Template cDNA	2 µl
Total Volume	25 µl

Table 2.2 Components of PCR synthesis reaction

2.6.5 Primers for PCR

All PCR primers (**Table 2.3**) used in this project were designed using MacVector software (MacVector Inc., Cary, USA) and specificity checked using NCBI BLAST software. Genomic and mRNA sequences used in the primer design were obtained from NCBI nucleotide database. All primers were resuspended in nuclease-free water and stored at -20°C.

Primer	Sequence (5'-3')	Annealing Temperature
IRF 1 forward	TGGCTGGGACATCAACAAGG	63.3°C
IRF 1 reverse	TTCCTGCTCTGGTCTTTCACCTCC	
IRF 2 forward	GTCATCTCTGGGGCTTAGTAATGG	56.3°C
IRF 2 reverse	CTCAGTGGTCACCTCTACAACTTGG	
IRF 3 forward	CAAGAGGCTCGTGATGGTCAAG	67.6°C
IRF 3 reverse	TGGGTGGCTGTTGGAAATGTG	
IRF 4 forward	ACACACAGCAGTTCTTGTCAGAGC	55.5°C
IRF 4 reverse	CTTGAATAGAGGAATGGCGGATAG	
IRF 5 forward	TTATGCCATCCGCCTGTGTC	63.3°C
IRF 5 reverse	GCCATTCTTCCCCAAAGCAG	
IRF 6 forward	AGCGGTCAAGGGAAAGACAAGC	64.2°C

IRF 6 reverse	TGGTGCCATCATACATCAGGTTG	
IRF 7 forward	TCGTGATGCTGCGGGATAAC	67.6°C
IRF 7 reverse	ATGTGTGTGTGCCAGGAATGG	
IRF 8 forward	TTGGAAACACGCTGGCAAGC	59.4°C
IRF 8 reverse	TCTGGGCTCTTATTCAAAGCACAG	
IRF 9 forward	GGATGTTGCTGAGCCCTACAAG	63.3°C
IRF 9 reverse	AGAACTGTGCTGTCGCTTTGATG	
GAPDH forward	ACTTTGGTATCGTGGAAGGAC	50°C
GAPDH reverse	TGGTCGTTGAGGGCAATG	
Pellino1 forward	CCAAATGGCGATAGAGGAAGG	55°C
Pellino1 reverse	CATAAATCCGTGCTGTAAAGGGAG	

Table 2.3 Primer Sequences

2.6.6 Gel electrophoresis

5 µl of each PCR sample was resolved at 100 V for 45 minutes on a 1 % agarose electrophoresis gel (1 g in 100 ml TAE made up from a 50x TAE stock (see **Appendix**)) with 3.5 µl ethidium bromide alongside the marker HyperLadder I (Bioline) and visualized under UV light using Chemi Genius$_2$ Bio Imaging System (Syngene, Cambridge, UK).

2.7 Quantitative PCR (qPCR)

Quantitative PCR experiments were performed in a total volume of 20µl consisting of 1 µl of cDNA sample (**section 2.6.3**) or standard (**section 2.7.1**), 10 µl of 2x qPCR Mastermix (Eurogentec, Southampton, UK), 1 µl of pre-mixed primer probes and 8 µl of sterile water. Pre-mixed primer probe sets were purchased from either Applied Biosystems (Pellino1, Hs00221035_m1; IRF3, Hs01547283; IL-1α, Hs00174092; IL-1β, Hs01555410 and GAPDH, Hs00182082_m1) or as separate components from Sigma-Aldrich (IFNβ and RV1B – sequences are listed in **Appendix**). Primers purchased from Sigma-Aldrich were diluted in sterile water to

a concentration of 300 nM for forward primers, 900 nM for reverse primers and 175 nM for probes. The 384-well qPCR plate was sealed with an optical lid and centrifuged at 300 g for 2 min. The qPCR reactions were carried out using an ABI 7900 Automated TaqMan^{TM} (Applied Biosystems), with an amplification cycle consisting of 50°C for 2 min, 94°C for 10 min, and 45 cycles of 94°C for 15 sec, 60°C for 15 sec. The fluorescence is detected analysed using SDS software version 2.2.1 (Applied Biosystems) and presented as ratio of target copy number compared to a non-regulated reference gene copy number or as arbitrary units.

2.7.1 qPCR standards and plasmid calculations

Initially the plasmid yield was quantified and its integrity determined using a NanoDrop™ 1000 spectrometer (NanoDrop Tech. Inc. Wilmington, USA). The molecular weight of each plasmid was determined based on the average molecular weight of a base pair, 650 Daltons. The number of moles was then established by dividing the plasmid DNA yield by its molecular weight. The number of molecules per sample were then determined by the multiplying the number of moles (determined by equation 1) by Avogadro's constant (6.02×10^{23}), then divided by the volume of the plasmid (summarised by equation 2).

$$(1) \qquad \text{Moles} = \frac{\text{plasmid DNA yield(g)}}{\text{plasmid molecular weight (Daltons)}}$$

$$(2) \qquad \text{Molecules (copies)/ µl} = \frac{(\text{Moles} \times 6.02 \times 10^{23})}{\text{plasmid volume (ul)}}$$

The optimum standard curve was then set up by running a range of serial dilutions of the stock cDNA or plasmid standards (e.g. 1:2, 1:5 and 1:10) to determine the best range and intervals of Ct values starting from around 10^8 copies per µl.

2.8 Western blot

Following stimulation, BEAS-2B cells or HBEpCs were collected and lysed for protein analysis by western blot. Supernatants were discarded and the remaining adhered cellular monolayers were lysed in phosphatase lysis buffer (see **Appendix**) containing 1 mM PMSF and 1 in 100 diluted protease-inhibitor cocktail (Calbiochem, Merck, Germany) added immediately prior to

use. Following a 2 minute incubation on ice, samples were transferred into Eppendorf tubes and spun by centrifugation at 2000 g for 10 minutes at 4°C to remove insoluble material. The resulting soluble material was then transferred and suspended in hot SDS-PAGE lysis buffer (see **Appendix**) and heated to 95°C for 5 minutes. Lysates were then stored at -80°C until analysis.

The Bio-Rad mini PROTEIN II electrophoresis apparatus (Bio-Rad Laboratories Ltd, UK) was assembled according to manufacturer's instructions prior to each use. The resolving gel (see **Appendix**) containing freshly added TEMED was poured in between two glass plates separated by 0.75 or 1.25 mm spacers. An approximate gap of 2 cm was left at the top of the resolving gel and overlaid with a thin layer of isopropanol to avoid evaporation of the gel during the setting at room temperature. Once set, the isopropanol was poured out and the remaining gel rinsed with distilled water. The stacking gel (see **Appendix**) was then carefully overlaid and a 10 or 15-well comb was carefully inserted to avoid the addition of bubbles. The set gels were then transferred and assembled in the electrophoresis tank according to manufacturer's instructions and covered with SDS-PAGE running buffer (see **Appendix**). The combs were then carefully removed and 15-25 µl of protein lysate were loaded into each well or 5 µl of ColorPlus Prestained Protein Ladder (New England BioLabs, Massachusetts, USA) and electrophoresed at 60 V for 15 minutes through the stacking gel and 200 V (PowerPac 300, Bio-Rad Laboratories Ltd, UK) through the resolving gel.

The proteins from the gel were transferred to a Hyband-c-extra nitrocellulose membrane (0.45 µm pore size; GE HealthcareLife Sciences, UK) by sandwiching the gel and membrane between two pre-soaked pieces of 3 mm filter paper and two fiber sponges encased in a transfer cassette. The transfer cassettes were then assembled into the Trans-Blot electrophoretic transfer cell (Bio-Rad Laboratories Ltd, UK) with the gel facing the black side of the cassette (negative charge) and the membrane facing towards the white side of the cassette (positive charge) to allow the effective transfer of proteins from the gel to the membrane. The tank was then filled with transfer buffer (see **Appendix**) and the addition of an ice pack to prevent overheating during the 70 minute transfer at 100 V. Protein transfer and equal loading was visualized by Ponceau S staining for 30-60 seconds then rinsed with 0.2% PBS-tween before the addition of 5% milk in 0.2% PBS-tween for 1 hour at room temperature on an orbital shaker to block non-specific binding sites.

The nitrocellulose membrane was washed for 5 minutes in PBS before the incubation in primary antibody (see **Table 2.4**) in 5% milk in 0.2% PBS-tween and incubated at 4°C overnight on an orbital shaker. The membrane was then washed 4 times for five minutes in 0.2% PBS-tween to remove any unbound antibody before the addition of the corresponding HRP-conjugated secondary antibody (see **Table 2.4**) diluted in 5% milk in 0.2% PBS-tween for 1 hour at room temperature on an orbital shaker. The membrane was washed 4 times for 5 minutes in 0.2% PBS-tween to remove any unbound antibody before protein detection. Labelled proteins were visualised by using EZ-ECL mixture (EZ-ECL™ Chemiluminescence Detection kit for HRP, Geneflow) for 2 minutes before developing and analysing the membrane using ChemiDoc XRS+ System with Image Lab Software (BioRad Laboratories Ltd, UK).

Membranes were occasionally stripped and re-probed by the removal of bound primary and secondary antibodies. Membranes were soaked in 0.2 M solution of sodium hydroxide for 8-10 minutes before rinsing the blot 4 times in 0.2% PBS-tween. The blots were then blocked in 5% milk in 0.2% PBS-tween before the addition of new antibodies as described above.

Target	Manufacturer	Species	Dilution
Pellino-1	Santa Cruz Biotechnology	Mouse	1:250
NFKB2 (p100/p52)	Cell Signaling Technology	Rabbit	1:500
NFKB1 (p105/p50)	Cell Signaling Technology	Rabbit	1:1000
Phospho p38	Cell Signaling Technology	Rabbit	1:1000
Phospho IKKa/b	Cell Signaling Technology	Rabbit	1:500
Phospho p44/p42	Cell Signaling Technology	Rabbit	1:500
IkBa	Cell Signaling Technology	Rabbit	1:500
RIP-1	BD Biosciences	Mouse	1:1000
Actin	Sigma-Aldrich	Rabbit	1:10000

Table 2.4 Working dilutions of western blotting antibodies

2.9 Transient siRNA knockdown

Transfections were carried out on BEAS-2B cells or HBEpCs cultured to approximately 85% confluence on 12-well plates. Target genes (Pellino-1 (L-013814-01-0005), NFKB2 (L-003918-00-0005), IRF3 (L-006875-00-0005) and RIP1 (L-004445-00-0005), Dharmacon, Thermo Fisher

Scientific) were knocked down using ON-TARGET plus SMARTpool™ (Dharmacon, Thermo Fisher Scientific) and Lipofectamin 2000™ (Invitrogen) as the delivery tool. Non-targeting siRNA was used as a control. A 200 µl solution of 1 µM siRNA was prepared from 20 µM stocks by diluting in Opti-MEM, while in a separate Eppendorf tube containing 2.5 µl of Lipofectamine 2000 was diluted with 97.5 µl of OptiMEM. Both tubes were gently inverted and allowed to equilibrate for 5 minutes in dark at room temperature. Both tubes were then combined to allow the siRNA to complex with the transfection reagent at room temperature for 20 minutes. In the meantime, cells were washed twice with PBS before the addition of 800 µl of either RPMI with 10% FCS containing no antibiotics (for BEAS-2B cells) or serum-free Airway Epithelial Cell Growth (AECG) medium containing no antibiotics (for HBEpCs). 200 µl of the complexed siRNA was then combined with the 800 µl of media in each well to reach a total plating volume of 1,000 µl per well. This was followed by cell incubation for 4 hours at 37°C in 5 % CO_2. Cells were washed once with PBS followed by the addition of 1 ml complete growth media for BEAS-2B cells or complete AECG medium minus the bovine pituitary extract for HBEpCs for 18 hours at 37°C in 5% CO_2 to allow for recovery before stimulation with pro-inflammatory cytokines or protein extraction. Additional mock transfected controls treated only with transfection reagent in OptiMEM were also included. Knockdown efficiency was determined by measuring protein expression of the target genes by western blotting.

2.10 Preparation of cigarette smoke extract (CSE)

Research grade cigarettes 3R4F (Tobacco and Health Research Institute, University of Kentucky, Lexington, KY) were used in this thesis. Cigarette smoke extract was prepared as previously described with some minor modifications (Proud et al., 2012). Mainstream smoke of two unfiltered cigarettes was drawn through 25 ml of basal media with the use of a peristaltic pump for 5 minutes each and regarded as 100%. Particulate matter was extracted through the use of a 0.22 mm filter syringe. CSE was freshly prepared before each use. All exposures in this thesis were done using 10% CSE.

2.11 Rhinoviral infection *in vitro*

Human rhinovirus (RV) stocks were prepared by other members of the research group. Prior to rhinoviral infection of BEAS-2Bs or HBEpCs with RV-1B or RV-16, cells were grown in 12-well

plates until confluency was reached. Cells were rendered quiescent in RPMI 1640 supplemented with 2% FCS and 1% penicillin and 1% streptomycin (for BEAS-2B cells) or unsupplemented AECG (for HBEpCs) for 18 hours at 37°C + 5 % CO_2. Cells were rinsed once with PBS before the addition of 250 µl of the desired concentration (determined by $TCID_{50}$) of RV was administered. An inactivated RV control was also administered to highlight viral replication induced phenotype. The 250 µl control was inactivated under a UV cross linker at 1000 mJ/cm2 for 10 minutes. An additional filtrate control was obtained by centrifuging viral inocula in 0.2 micron filter tubes (Millipore, Cork, Ireland) at 12000 x *g* for 5 min. The virus and respective controls were then incubated at room temperature for 1 hour on an orbital shaker. Virus was then removed and replaced with 1 ml of fresh basal media (RPMI 1640 supplemented with 2% FCS and 1% penicillin and 1% streptomycin (for BEAS-2B cells) or unsupplemented AECG (for HBEpCs) for 24 hours at 37°C + 5 % CO_2.

2.12 Caspase-8 activity

The caspase-8 activity levels were determined using Promega's Caspase-Glo® 8 assay (Wisconsin, USA). HBEpCs were grown in 24-well plates and allowed to reach confluence before undergoing stimulation of interest for 24 hours.

Prior to starting, the Caspase-Glo® 8 reagent was thawed to room temperature. 250 µl of the existing 500 µl of supernatant was removed and discarded per well. 250 µl of the Caspase-Glo® 8 reagent was then added to each sample, including a cell-free control. The contents were then gently mixed on an orbital shaker for 30 seconds followed by a 1 hour incubation at room temperature. This enables the reagent to lyse the cells allowing caspase cleavage of the substrate and generating a luminescent signal produced by the luciferase reaction. The luminescence for each sample was then determined using Opsys MR™ Microplate Reader (Dynex technologies) using Revelation software (Dynex technologies) for analysis.

2.13 Statistical Analysis

Statistical analysis were performed using GraphPad Prism® v6.0. (GraphPad Inc, San Diego, CA, USA). Data are presented as means ± SEM. Data were analysed using the appropriate statistical

test and post-test as stated in the figure legends. A p value of ≤ 0.05 was considered statistically significant.

CHAPTER 3 - RESULTS. ESTABLISHING AN *IN VITRO* CHRONIC MODEL OF INFLAMMATION

COPD is a chronic inflammatory disease that is driven by a multitude of inflammatory mediators derived from activated inflammatory cells, including monocytes and macrophages, as well as structural cells such as epithelial and endothelial cells (**See section 1.2**). Patients suffering from COPD display abnormal infiltration of inflammatory cells in their airways, and the relationship between these cells and their effect on chronic inflammation within the airways is not fully understood.

The epithelial lining in the airway is the first form of defence against invading pathogens or environmental insults. In addition to the formation of tight junctions and mucociliary clearance to form a physical barrier to pathogens and other foreign substances, epithelial cells also produce a plethora of immune cell-recruiting cytokines as part of the innate immune response against invading pathogens (Kulkarni et al., 2010). However, bacterial, viral and environmental agents such as cigarette smoke (the predominant cause of COPD) can alter the epithelial cells' ability to generate an effective innate immune response. As chronic inflammation of COPD is underpinned by airway colonisation and infection, I hypothesised that persistent inflammation would alter epithelial cell innate responses with consequences on the responses to infection.

Cooperative signalling between inflammatory cells and resident tissue cells has been well documented, and the importance of monocytes in mounting an effective immune response to both bacteria and viruses highlighted (Chaudhuri et al., 2010; Morris et al., 2006; Parker et al., 2008; Parker et al., 2007; Stokes et al., 2011; Ward et al., 2009). While these studies provide valuable insight into crucial airway responses to pathogens, they only focus on the immediate acute responses in these systems during the first 24 hours. Therefore the following study sought to create an *in vitro* chronic model of inflammation to enable the exploration of epithelial cell immunity and cellular communication during prolonged pathogen handling.

3.1 Comparison of LPS-induced CXCL8 release in monocytes and $VitD_3$-differentiated THP-1 cells

The effective inflammatory response to bacterial stimuli is mediated in part by cooperative signalling between monocytes and airway tissue cells (Chaudhuri et al., 2010). The proposed model for chronic inflammation therefore involved prolonged low-grade bacterial stimulation of epithelial cells in the presence of inflammation-driving monocytes. However, the duration of the proposed model and the large number of cells required presented a barrier to the use of primary cells. The scale of the model would require the use of large volumes of donor blood to obtain enough cell numbers, while the recurrent nature of the chronic model would require multiple donors, each presenting with donor variability and adding an added layer of complexity to the interpretation of results. Thus the use of a differentiated leukemic monocytic cell line, THP-1, was proposed and further explored in this thesis.

Monocytic cells lines are often used in place of primary cells due to the ease of their acquisition. THP-1 cells are an immortal human acute monocytic leukemic cell line (Tsuchiya et al., 1980) and ideal for use in the chronic model due to their non-adherent properties allowing for ease of removal and replacement *in vitro*. Furthermore, THP-1 cells can be manipulated *in vitro* into varying states of differentiation including a more monocytic phenotype (Parker et al., 2004). The initial aims of this project were two-fold; firstly it was necessary to determine the efficacy of the chosen THP-1 differentiation protocol. Secondly, it was crucial to determine the THP-1 cell density required to mimic primary monocyte responses *in vitro*.

THP-1 cells were differentiated in accordance with established protocols of 100nM of vitamin D_3 ($VitD_3$) (also known as calcitriol, a hormonally active metabolite of vitamin D_3) stimulation for 72 hours before use (Daigneault et al., 2010). The monocytic marker CD14 expression was measured by flow cytometry to establish differentiation efficacy. Undifferentiated THP-1 cells showed no difference in CD14 detected fluorescence intensity in comparison to the IgG_1 isotype control (**Figure 3.1a and Figure 3.1c**). Conversely, $VitD_3$-differentiated THP-1 cells showed an increased CD14 expression confirming acquisition of a marker associated with a monocytic phenotype (**Figure 3.1b and Figure 3.1d**).

$VitD_3$-differentiated THP-1 CXCL8 cytokine production in response to the bacterial cell wall component LPS was then determined by ELISA (**Figure 3.2a**) and compared with primary monocyte responses (**Figure 3.2b**). Varying numbers of both cell types were stimulated with LPS (1 ng/ml- 100 ng/ml) for 24 hours respectively. Responses were quantified by the measure of pro-inflammatory cytokine CXCL8. The CXCL8 release in THP-1 cells was less than that of monocytes. Specifically, 10,000 and 30,000 THP-1 cells stimulated with LPS produced 10 fold less CXCL8 than 10,000 and 30,000 LPS-stimulated monocytes respectively (**Figure 3.2**).

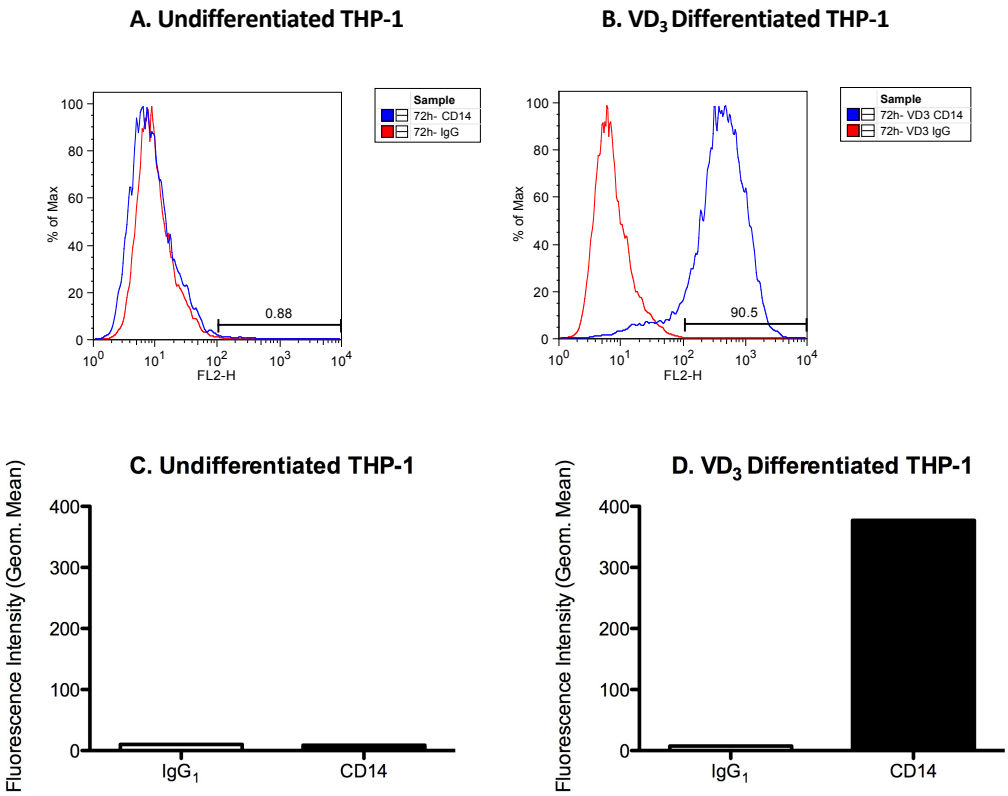

Figure 3.1 Representative flow analysis histograms demonstrating THP-1 CD14 expression following Vitamin D_3 differentiation

THP-1 differentiation was determined by staining with a PE-conjugated mouse anti-human CD14 antibody or mouse IgG_1 isotype control antibody. Fluorescence was measured in the FL-2 channel of a FACSCalibur flow cytometer. Data analysis was performed using FlowJo software. (**A**) Histogram of undifferentiated THP-1 cells, (**B**) Histogram of vitamin D_3 differentiated THP-1 cells, (**C**) Fluorescence intensity of undifferentiated THP-1 cells, (**D**) Fluorescence intensity of vitamin D_3 differentiated THP-1 cells. n=1

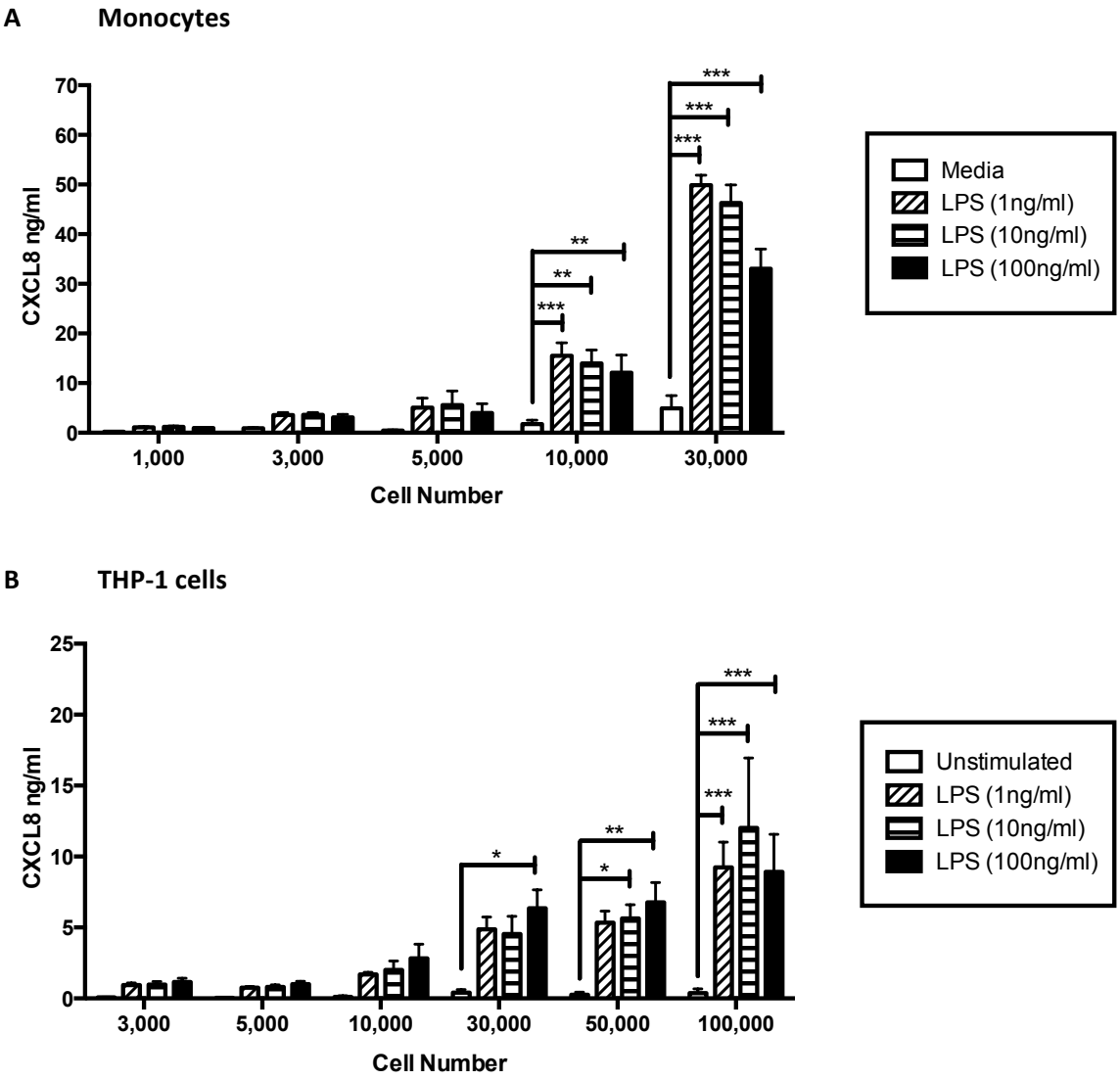

Figure 3.2 Comparison of THP-1 and monocyte responses to LPS

Increasing numbers of (**A**) highly purified human monocytes derived from volunteer donors or (**B**) VD_3 differentiated THP-1 cells were stimulated with LPS (1 ng/ml- 100 ng/ml) for 24 hours. Supernatants were collected and analysed for CXCL8 release by ELISA. Data are expressed as mean ± SEM of n=3. Statistical analysis was carried out by two-way ANOVA with Bonferroni's post-test (*p<0.05, **p<0.01 and ***p<0.001).

3.2 Comparison of direct interaction between monocytic cells and BEAS-2B in an acute model of inflammation

An acute model of inflammation was then created to investigate the ability of $VitD_3$-differentiated THP-1 cells to replace monocytes in the effective cooperative signalling between monocytes and airway epithelial cells. Increasing numbers of monocytes (1,000-30,000 cells/well) or $VitD_3$-differentiated THP-1 cells (3,000-100,000 cells/well) were added to a confluent BEAS-2B monolayer in the presence or absence of LPS (1 ng/ml). LPS-induced CXCL8 release was synergistically enhanced in the presence of monocytes (**Figure 3.3a**), $VitD_3$-differentiated THP-1 cells recapitulated a comparably muted increase in LPS-induced CXCL8 (**Figure 3.3b**). While the addition of 5,000 monocytes results in levels of CXCL8 of over 30 ng/ml, the addition of 100,000 THP-1 cells produces just under 25 ng/ml of CXCL8 (**Figure 3.3**).

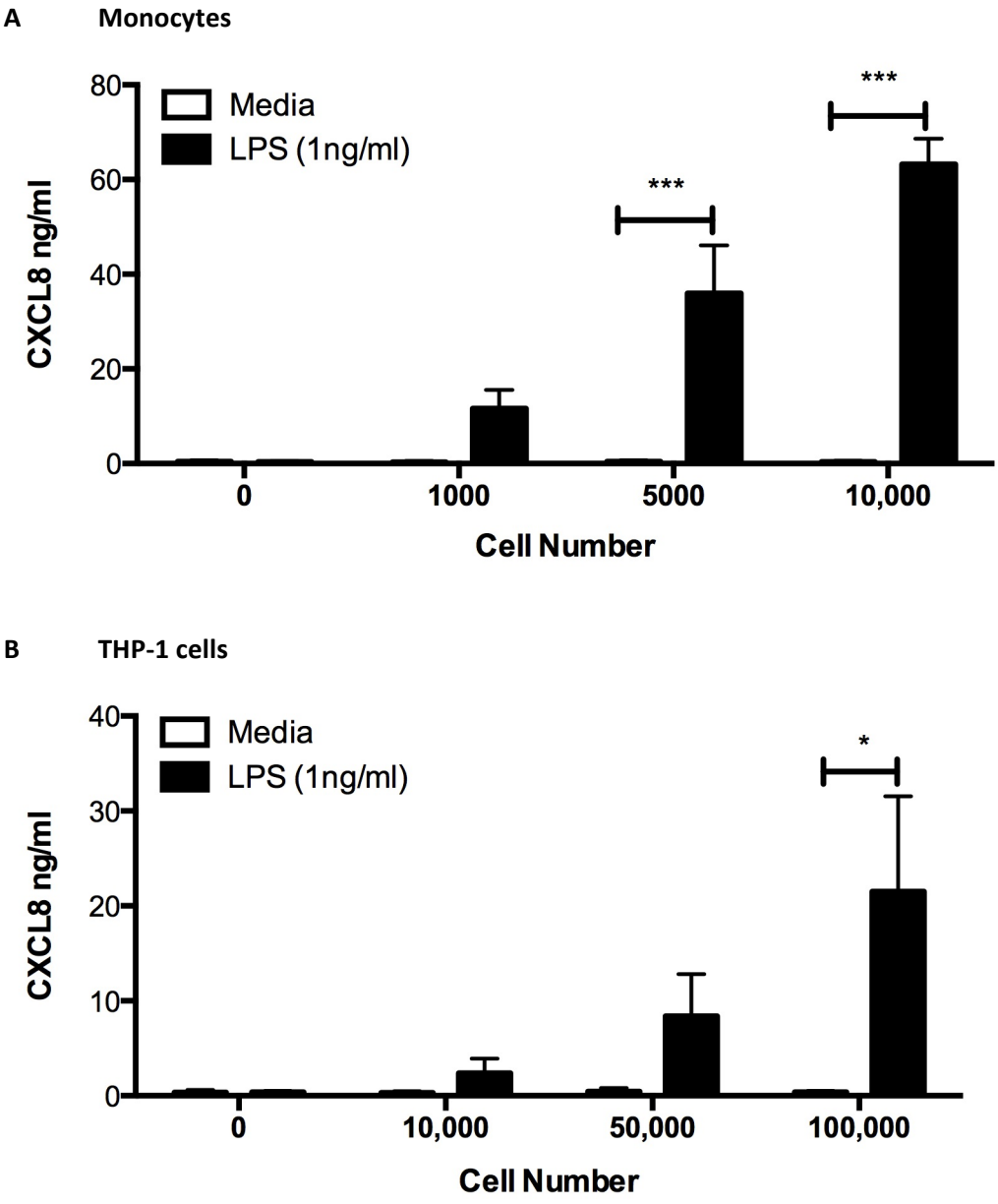

Figure 3.3 Comparison of direct interaction between monocytic cells and BEAS-2B in an acute model of inflammation

BEAS-2B were seeded at 3 x 10^6 cells/24-well plate (125,000 cells/well) for 24 hours followed by the addition of increasing numbers of (**A**) highly purified human monocytes derived from volunteer donors or (**B**) VD_3 differentiated THP-1 cells. These were stimulated with LPS (1 ng/ml) for 24 hours. Supernatants were collected and analysed for CXCL8 release by ELISA. Data are expressed as mean ± SEM of n=3. Statistical analysis was carried out by two-way ANOVA with Bonferroni's post-test (*$p<0.05$ and ***$p<0.001$).

3.3 The effect of cell culture inserts on the interaction between monocytic cells and BEAS-2B in an acute model of inflammation

The importance of cellular communication between immune cells and tissue cells for an effective inflammatory response is well known (Morris et al., 2006; Parker et al., 2008; Standiford et al., 1990). However, examining this communication *in vitro* over an extended period of time required the control of several variables including the change of cell phenotype over time, effects of apoptosis and the ability to maintain a constant cell number across the range of stimulated and unstimulated samples. Therefore to enable the repeated addition of newly differentiated cells to cultures over several days, the use of cell culture inserts with a 0.4 µm pore size was explored. This alteration in protocol allowed for the complete removal of ageing monocytic cells while maintaining the essential released soluble factors necessary for cellular communication.

Increasing numbers of monocytes or $VitD_3$-differentiated THP-1 cells in cell culture inserts were added to a confluent BEAS-2B monolayer in the presence or absence of LPS (1 ng/ml) for 24 hours. The use of cell culture inserts resulted in an approximately 6-fold decrease in CXCL8 release from monocytes (**Figure 3.4a**) when compared to monocytes in direct cell-to-cell contact (**Figure 3.3a**). Similarly, LPS-induced CXCL8 release was dampened by 4-fold in $VitD_3$-differentiated THP-1 cells in cell culture inserts (**Figure 3.4b**) in comparison to the direct cell-to-cell contact model (**Figure 3.3b**). Additionally, in line with previous data, $VitD_3$-differentiated THP-1 cells released less CXCL8 than monocytes.

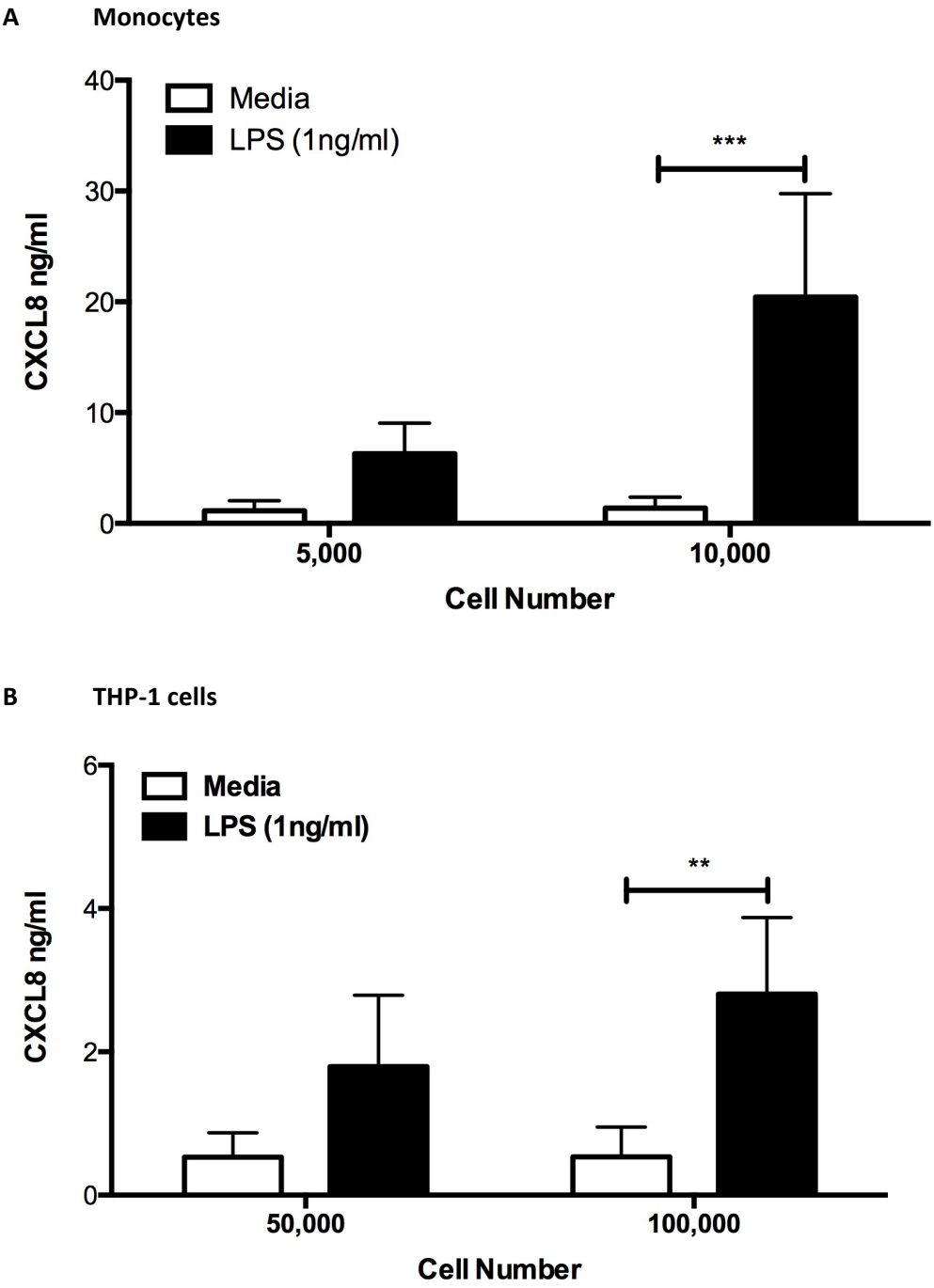

Figure 3.4 Comparison of indirect interaction between monocytic cells and BEAS-2B in an acute model of inflammation

BEAS-2B cells were seeded at 3 x 10^6 cells/24-well plate (125,000 cells/well) for 24 hours followed by the addition of increasing numbers of (A) highly purified human monocytes derived from volunteer donors or (B) VitD3-differentiated THP-1 cells separated by a 0.4 µm cell culture insert. This was followed by stimulation with LPS (1 ng/ml) for 24 hours. Supernatants were collected and analysed for CXCL8 release by ELISA. Data are expressed as

mean ± SEM of n=3. Statistical analysis was carried out by two-way ANOVA with Bonferroni's post-test (**p<0.01 and ***p<0.001).

3.4 Establishing a chronic model of inflammation

3.4.1 Utilising a model system with cell separation via cell culture inserts

A more chronic model of inflammation was developed to further explore how continued exposure of BEAS-2B cells to a proinflammatory environment would affect their responses to stimuli such as pathogens. During the design of the chronic model of inflammation a modest but detectable response to LPS was deemed appropriate to provide a continuous low-grade inflammation. Therefore, based on previous data (**Figure 3.4b**) 100,000 $VitD_3$-differentiated THP-1 cells per sample were determined sufficient to elicit cellular response.

The proposed chronic model of inflammation allowed 24 hours for BEAS-2B cell adherence to culture wells. On day 1 BEAS-2B monolayers were washed with media before the addition of cell culture inserts containing $VitD_3$-differentiated THP-1 cells. These inserts were replaced with freshly differentiated THP-1 cells on days 1, 3 and 5 of the experiment. In addition, the BEAS-2B monolayers and inserts were also stimulated with fresh LPS (1ng/ml) on these days. Finally, on day 7, cell culture inserts were removed and primary monocytes were added directly onto the BEAS-2B monolayer in combination with a fresh dose of LPS (1ng/ml). On day 8 supernatants were collected and measured for CXCL8 release by ELISA (chronic model method depicted in **Figure 3.5d**).

The baseline CXCL8 release (0.5-0.6 ng/ml) from unchallenged BEAS-2Bs served as a control (method depicted in **Figure 3.5a**). The multiple challenges with LPS on days 1, 3, 5 and 7 did not alter the baseline CXCL8 release in these cells (**Figure 3.6a**). The introduction of cell culture inserts containing $VitD_3$-differentiated THP-1 cells (method depicted in **Figure 3.5b**) served as a second control group and revealed no further effect of THP-1 cells on baseline CXCL8 release following continuous LPS stimulation (0.5-0.6 ng/ml) (**Figure 3.6b**).

In the final control group BEAS-2B cells underwent the same continuous stimulation with LPS on days 1, 3, 5 and 7 followed by the direct addition of monocytes with a final LPS stimulation on day 7 for a further 24 hours (method depicted in **Figure 3.5c**). The direct addition of monocytes to the primed BEAS-2B monolayer resulted in a marked CXCL8 production (over 50 ng/ml) (**Figure 3.6c**). Interestingly, no difference in CXCL8 release was observed when compared with the proposed chronic model when BEAS-2B cells were challenged with LPS on

days 1, 3, 5 and 7 in the presence of $VitD_3$-differentiated THP-1 cells in culture inserts followed by the direct addition of monocytes to the primed BEAS-2B monolayer on day 7 (method depicted in **Figure 3.5d** and results in **Figure 3.6d**). In further experiments to determine the relevance of IL-1 to chronic inflammation, BEAS-2B were also stimulated with LPS in the presence of IL-1ra on day 7 and resulted in a significant inhibition of LPS and monocyte-induced CXCL8 release (**Figure 3.6c and Figure 3.6d**).

A BEAS-2B alone

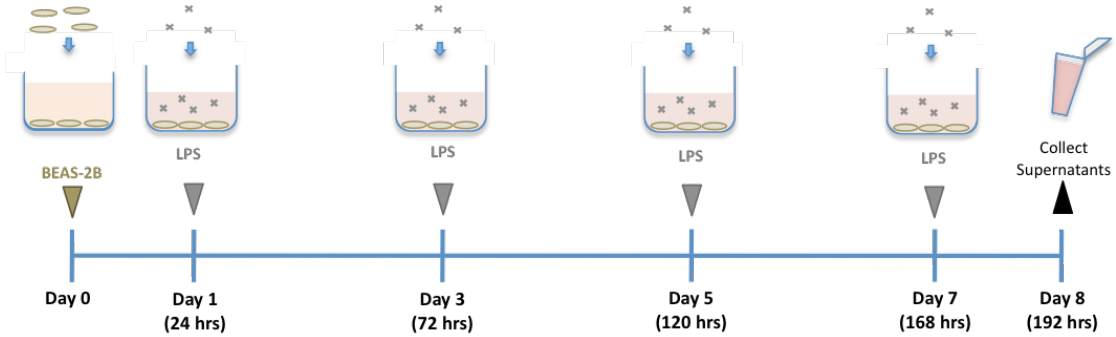

B BEAS-2B and THP-1 cells

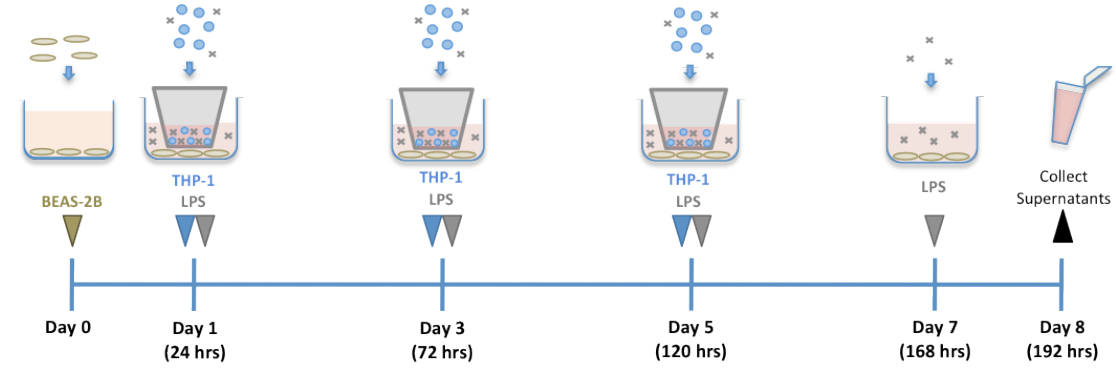

C BEAS-2B and Monocytes

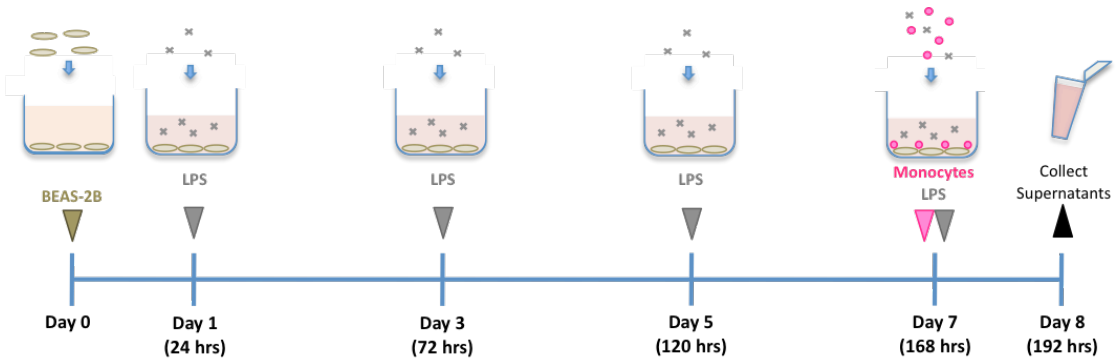

D BEAS-2B, THP-1 cells and Monocytes

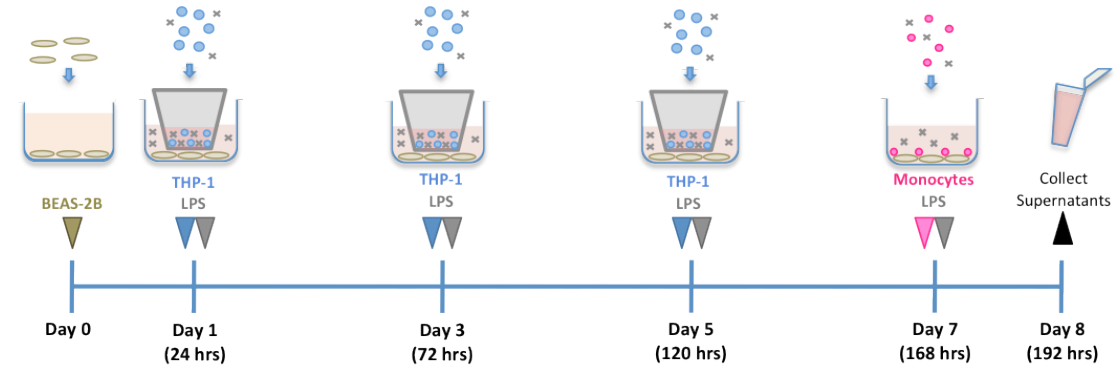

Figure 3.5 Depiction of the chronic model system utilising cell culture inserts and its respective controls

BEAS-2B were seeded at 3 x 10^6 cells/24-well plate (125,000 cells/well) for 24 hours. These were then split into 4 groups titled: A) BEAS-2B alone, B) BEAS-2B and THP-1 cells, C) BEAS-2B and Monocytes and D) BEAS-2B, THP-1 cells and Monocytes. In each group, samples were stimulated with LPS at 1 ng/ml on days 1, 3, 5 and 7. Groups B and D also had the addition of cell culture inserts containing 100,000 $VitD_3$-differentiated THP-1 cells on days 1, 3, and 5. Finally on day 7, all cell culture inserts were discarded and all wells washed with media carefully. Group C and D then underwent the addition of human CD14 positive monocytes. These were isolated from healthy donors and directly added onto the epithelial cell layer to generate co-cultures. All groups also underwent one final treatment with LPS (1 ng/ml) with or without IL-1ra (10 μg/ml) for 24 hours before the collection of supernatants for further analysis.

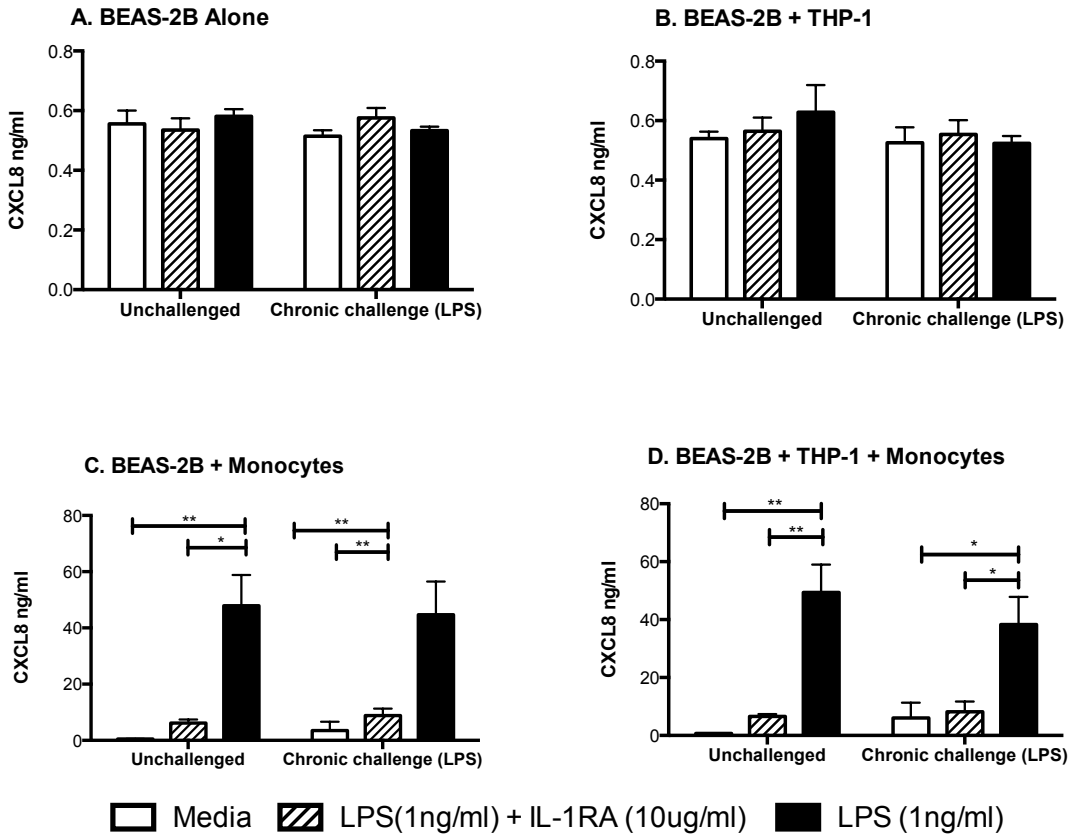

Figure 3.6 Establishing a chronic model system with cell separation via cell culture inserts

BEAS-2B were seeded at 3 x 10^6 cells/24-well plate (125,000 cells/well) for 24 hours and were either unstimulated for 7 days (unchallenged) or underwent chronic stimulation (chronic challenge) as described in **Figure 3.5**. **A**) BEAS-2B alone, **B**) BEAS-2B and THP-1, **C**) BEAS-2B and monocytes and **D**) BEAS-2B, THP-1 and monocytes were stimulated with LPS (1ng/ml) and IL-1ra (10µg/ml) in the indicated wells.

After 24 hours, Cell free supernatants were generated and CXCL8 release measured by ELISA. Data shown are mean ± SEM of n=3 experiments. Significant differences are denoted by ** ($p<0.01$) and *** ($p< 0.001$) as measured by 2-way ANOVA and Bonferroni's post test.

3.4.2 Utilising a model system with direct cell-to-cell contact

The model of chronic inflammation with cell separation via cell culture inserts showed no detectable differences between the BEAS-2B cells that underwent the complete treatment with LPS, THP-1 and monocytes (**Figure 3.6d**) and the control of just LPS and monocytes (**Figure 3.6c**). It was hypothesised that the use of cell culture inserts may have resulted in ineffective cytokine production required for effective inflammatory responses due to cell separation. A model of cell-to-cell contact wherein vitD_3-differentiated THP-1 cells are no longer contained in cell culture inserts for the duration of the experiment was proposed.

Similarly to **section 3.4.1**, BEAS-2B cells alone challenged with LPS on days 1, 3, 5 and 7 were served as a negative control with baseline CXCL8 levels of 0.5-0.6 ng/ml (method depicted in **Figure 3.7a** and results in **Figure 3.8a**). The second control group aimed to determine the effect of THP-1 cell contact on BEAS-2B cells following multiple treatments with LPS (depicted in **Figure 3.7b**) and revealed a negligible effect on baseline CXCL8 release (0.6-0.7 ng/ml) (**Figure 3.8b**). In the third control group (method depicted in **Figure 3.7c**), BEAS-2B cells underwent multiple LPS treatments on days 1, 3 and 5 followed by the addition of purified human monocytes in combination with a final LPS stimulation on day 7 resulting in CXCL8 release of 20-30 ng/ml (**Figure 3.8c**).

Finally, BEAS-2B cells were stimulated with LPS and fresh vitD_3-differentiated THP-1 cells on days 1, 3 and 5 before a final challenge with LPS in the presence of monocytes on day 7. The resulting CXCL8 generation with levels of 12 ng/ml was marginally lower (**Figure 3.8d**) than the BEAS-2B and monocyte control group with levels of 20 ng/ml (**Figure 3.8c**). However it is also important to note that the despite the decrease in CXCL8 levels between the two models, the unchallenged control in BEAS-2B, THP-1 and monocyte model (**Figure 3.8d**) also showed decreased levels of CXCL8 generation (levels of 18 ng/ml) compared with the unchallenged control on the BEAS-2B and monocytes control group (levels of 32 ng/ml) (**Figure 3.8c**).

A BEAS-2B alone

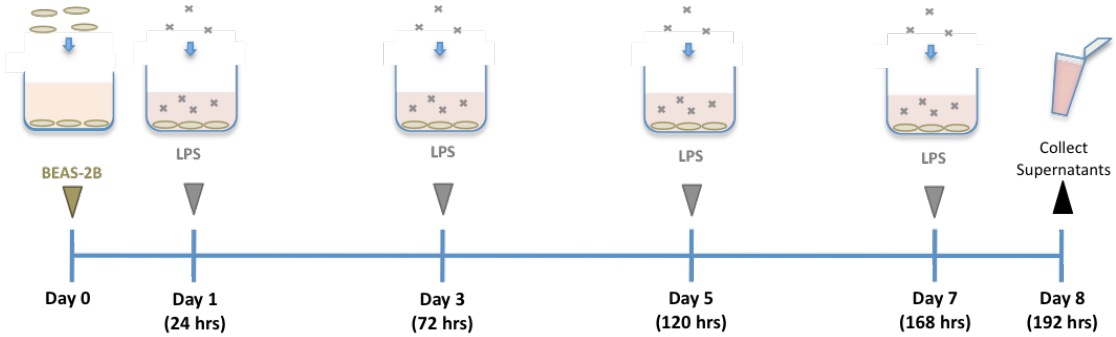

B BEAS-2B and THP-1 cells

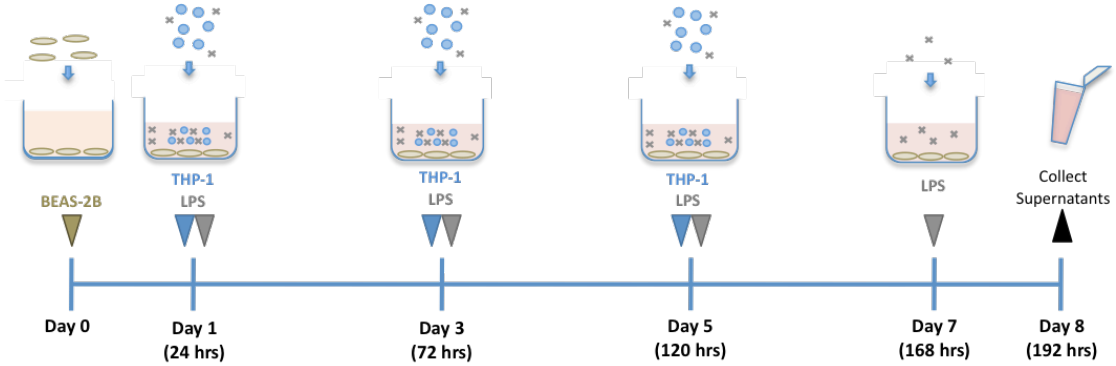

C BEAS-2B and Monocytes

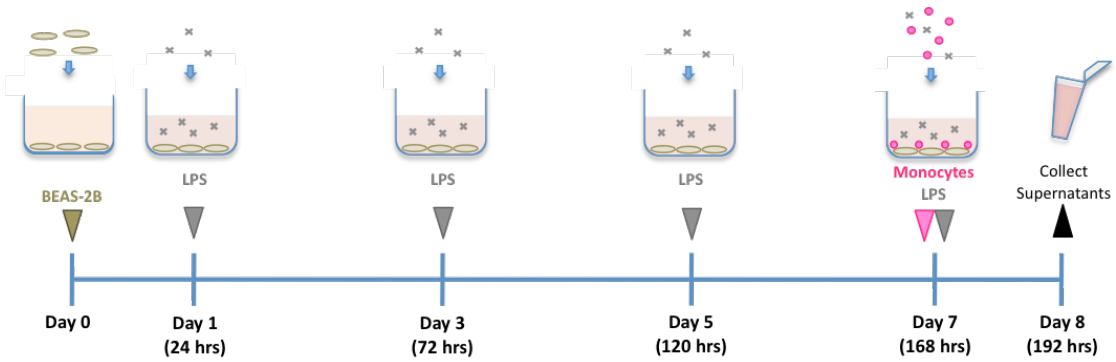

D BEAS-2B, THP-1 cells and Monocytes

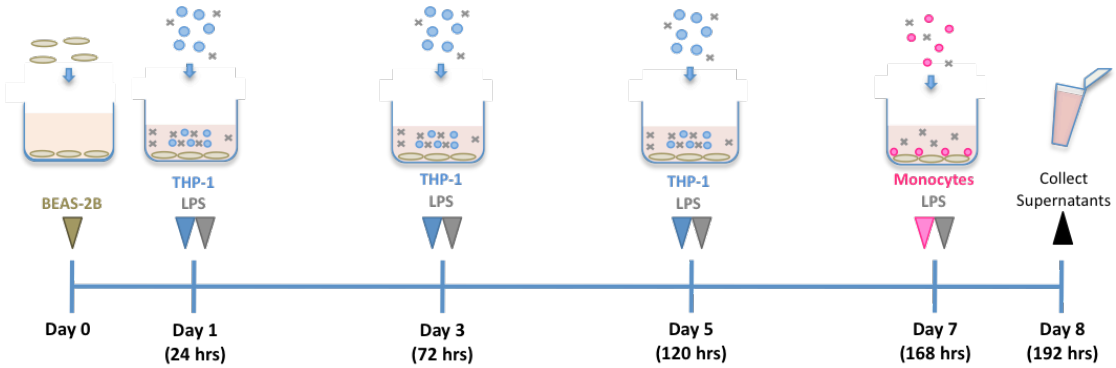

Figure 3.7 Depiction of the direct cell-to-cell chronic model system and its respective controls

BEAS-2B were seeded at 3 x 106 cells/24-well plate (125,000 cells/well) for 24 hours. These were then split into 4 groups titled: **A**) BEAS-2B alone, **B**) BEAS-2B and THP-1 cells, **C**) BEAS-2B and Monocytes and **D**) BEAS-2B, THP-1 cells and Monocytes. In each group, samples were stimulated with LPS at 1 ng/ml on days 1, 3, 5 and 7. Groups B and D also had the addition of 100,000 vitamin D3 differentiated THP-1 cells on days 1, 3, and 5 where all wells were washed with media carefully in between each addition. Group C and D then underwent the addition of human CD14 positive monocytes on day 7. These were isolated from healthy donors and directly added onto the epithelial cell layer to generate co-cultures. All groups also underwent one final treatment with LPS (1 ng/ml) with or without IL-1ra (10 µg/ml) for 24 hours before the collection of supernatants for further analysis.

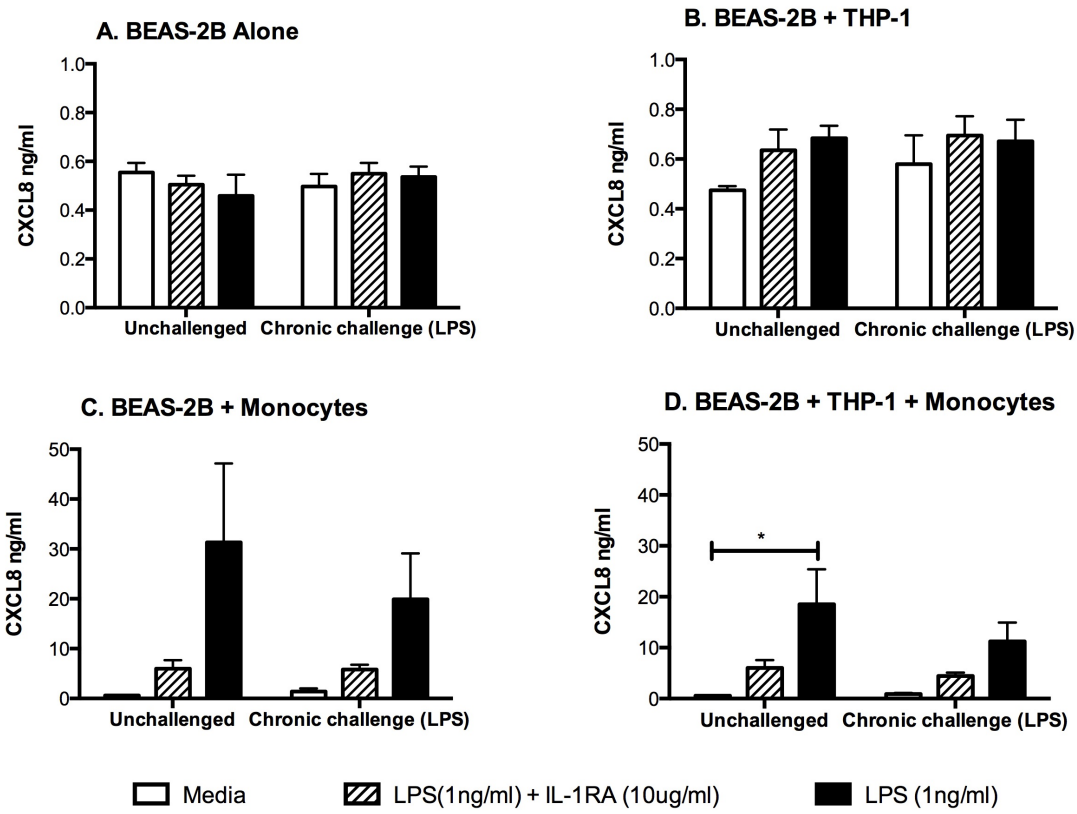

Figure 3.8 Establishing a chronic model system with direct cell contact

BEAS-2B were seeded at 3 x 10^6 cells/24-well plate (125,000 cells/well) for 24 hours and were either unstimulated for 7 days (unchallenged) or underwent chronic stimulation (chronic challenge) as described in **Figure 3.7**. **A**) BEAS-2B alone, **B**) BEAS-2B and THP-1, **C**) BEAS-2B and monocytes and **D**) BEAS-2B, THP-1 and monocytes were stimulated with LPS (1ng/ml) and IL-1ra (10µg/ml) in the indicated wells. Supernatants were collected and analysed for CXCL8 release by ELISA. Data are expressed as mean ± SEM of n=3. Statistical analysis was carried out by two-way ANOVA with Bonferroni's post-test (*p<0.05 and **p<0.01).

3.5 IRFs 1,2,3,6,7 and 9 are expressed in BEAS-2B cells

In parallel with the establishment of the chronic model to study prolonged pathogen handling, techniques for the exploration of cellular signalling and thus downstream cytokine production and cellular communication were also developed.

IRFs are key transcription factors that are involved in cytokine production in the regulation of innate immune responses and are involved predominantly in viral but also in bacterial detection systems (Section 1.2.3.1). Basal expression levels of IRFs 1-9 were measured by RT-PCR as described in Section 2.5. The results in **Figure 3.5** reveal that IRFs 1,2,3,6,7 and 9 are expressed in BEAS-2B whilst IRFs 1,2,3,4,5,7, 8 and 9 are expressed in PBMCs, which were used as a positive control for the primers. The housekeeping gene Glyceraldehyde-3-phosphate dehydrogenase (GAPDH) was a used as a control for loading.

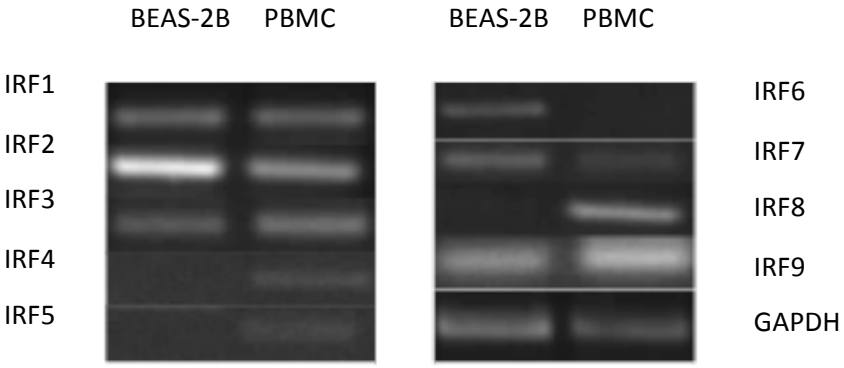

Figure 3.9 IRF expression levels within BEAS-2B cells

IRF expressions levels within BEAS-2B cells and PBMC were measured by RT-PCR as described in section 2.6. IRF 1,2,3,6,7 and 9 were expressed in BEAS-2B cells whilst IRF 1,2,3,4,5,7,8 and 9 were expressed in PBMC. Representative image of 3 gels.

3.6 Establishing a model of inflammation using cigarette smoke

Cigarette smoking is a major risk factor in the development of COPD. The numerous adverse effects of cigarette smoke exposure include increased susceptibility to infections as well as the increased severity and prevalence of respiratory infections (Eddleston et al., 2011; Stampfli and Anderson, 2009).

Cigarette smoke exposure alters the first line of defence within the airway resulting in tissue damage. These damages include disrupted epithelial cell junctions, decreased extracellular matrix remodelling and proliferation of mesenchymal cells leading to fibrogenesis and tissue destruction (Ojo et al., 2014). Indeed enhanced airway epithelial cell permeability and impaired mucociliary clearance increase the burden on immunologic host defences (Eddleston et al., 2011; van der Vaart et al., 2004). This is supported by the elevation in both proinflammatory cell types such as neutrophils, monocytes and macrophages and consequently proinflammatory cytokines such as CXCL8 (Tanino et al., 2002), TNF-α (Churg et al., 2004) and IL-1β (Hellermann et al., 2002; Ryder et al., 2002).

In section 3.4 I demonstrated that an obvious chronic perturbation of cellular phenotype was not achieved with repeated stimulation using endotoxin/monocytes in combination. I therefore proposed an alternative model using the predominant risk factor for the development of COPD as the main chronic stimulus. It is well documented that cigarette smoking can alter airway epithelial cell responses to both bacterial (Pace et al., 2008) and viral infections (Eddleston et al., 2011), and while these studies provide valuable insight into the crucial airway responses to pathogens, the effect of long-term cigarette smoke exposure on inflammation and on the innate immunity of the airway remains poorly understood. Therefore this study aimed to create an *in vitro* chronic model of inflammation to enable the understanding of whether chronic inflammation uses different molecular pathways and presents different targets for treatment of disease.

BEAS-2B cells were cultured for 24 hours with increasing concentrations of cigarette smoke extract (CSE) (ranging from 0-55% CSE) and measured for CXCL8 production (**Figure 3.10**). Cell death was visibly detected under light microscopy from concentrations above 25% CSE (data not shown). Therefore taken in combination with existing literature and keeping in mind the nature of the model to be explored, wherein continuous low-grade exposure to CSE attempts

to mimic frequent cigarette smoke exposure, 10% was deemed sufficient to elicit cellular response without inducing overwhelming toxic effects.

Subsequently BEAS-2B cells were acutely stimulated with 10% CSE alone or in the presence of proinflammatory stimuli for 24 hours then measured for CXCL8 production. 10% CSE alone was sufficient to significantly increase the CXCL8 baseline levels by a third (**Figure 3.11a**). The same levels of CXCL8 production were measured in the LPS stimulated sample suggesting that the measured increase is independent of LPS stimulation (**Figure 3.11b**). In addition, CXCL8 production in response to poly(I:C) was inhibited by the presence of CSE (**Figure 3.11c**). While an increase in CXCL8 production in response to IL-1β was measured (**Figure 3.11d**).

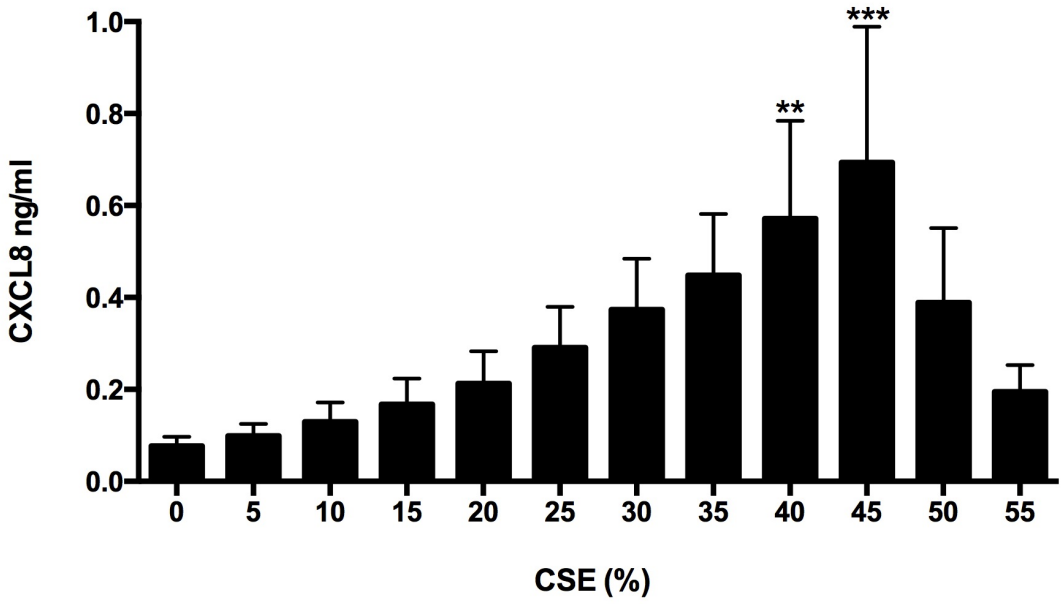

Figure 3.10 Increasing concentrations of CSE results in enhanced CXCL8 production in BEAS-2Bs

BEAS-2B were seeded at 3 x 10^6 cells/24-well plate (125,000 cells/well) for 24 hours followed by a 24 hour stimulation with increasing concentrations of CSE (5-55%). Supernatants were collected and analysed for CXCL8 release by ELISA. Data are expressed as mean ± SEM of n=3. Statistical analysis was carried out by one-way ANOVA with Bonferroni's post-test (**p<0.01 and ***p<0.001).

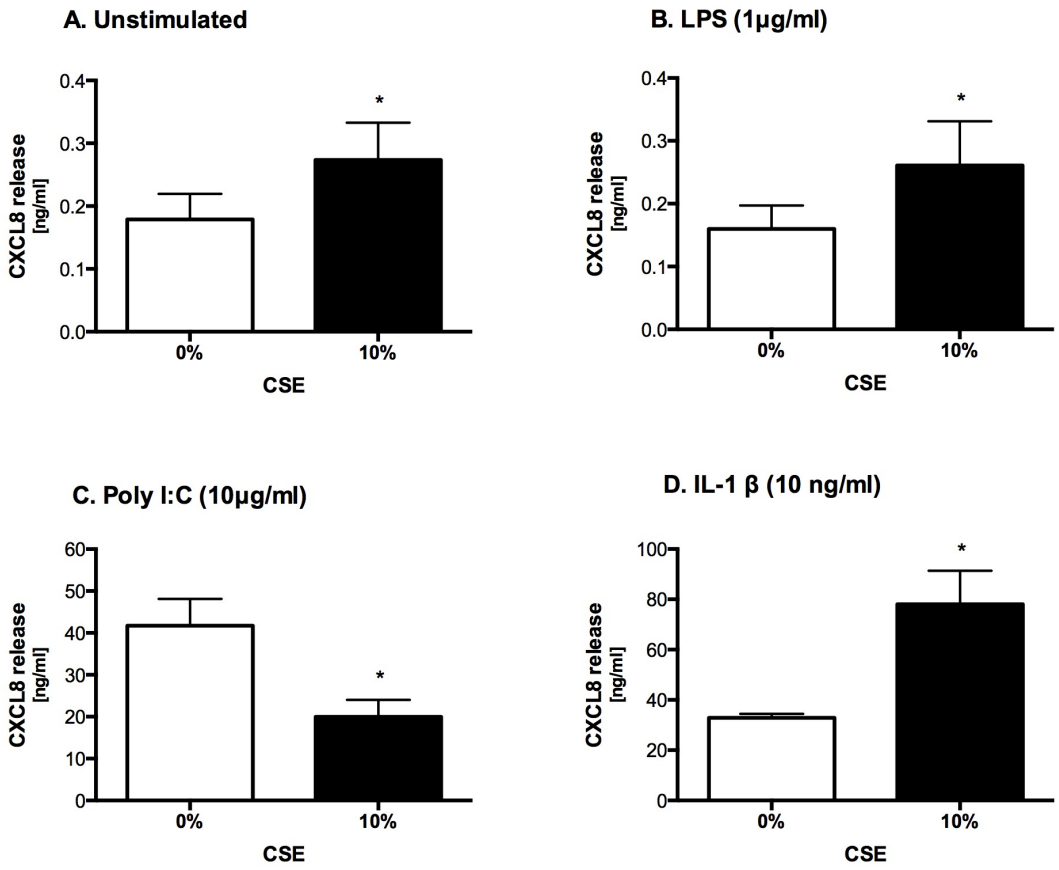

Figure 3.11 BEAS-2B cells exhibit differential regulation to proinflammatory stimuli in the presence of CSE

BEAS-2B cells were seeded at 3 x 10^6 cells/24-well plate (125,000 cells/well) for 24 hours followed by stimulation with (**A**) CSE (10%) alone, or the combination of CSE (10%) and (**B**) LPS (1ug/ml), (**C**) Poly(I:C) (10ug/ml) or (**D**) IL-1β (10ng/ml) for 24 hours. Supernatants were collected and analysed for CXCL8 release by ELISA. Data are expressed as mean ± SEM of n=7. Statistical analysis was carried out by two-way ANOVA with Bonferroni's post-test (**p<0.01 and ***p<0.001).

3.7 CSE potentiates proinflammatory responses to TLR agonists in a chronic model of inflammation

To begin to assess whether chronic exposure to CSE interferes with airway epithelial cells' ability to mount an effective inflammatory response in an ongoing proinflammatory environment, the BEAS-2B cell line was pre-treated with CSE for 6 days wherein fresh CSE (at 2% or 10%) was replaced every 24 hours before the final stimulation with TLR agonists, poly(I:C) and IL-1β, in combination with a fresh dose of CSE (method depicted in **Figure 3.12a**).

As per previous findings in the acute model (**Figure 3.11a**), repeated stimulation with 10% CSE results in an elevated baseline of CXCL8 production (**Figure 3.12b**). Similarly, the stimulation of BEAS-2B cells with IL-1β (10 ng/ml) following six days of repeated stimulation with 10% CSE also resulted in a significant increase in the production of CXCL8 (**Figure 3.12d**). In contrast to previous findings in the acute stimulation model however (**Figure 3.11c**), the repeated stimulation of BEAS-2B cells with 2% and 10% CSE followed by a single stimulation with poly(I:C) (10 ug/ml) resulted in an increase in CXCL8 production (**Figure 3.12c**).

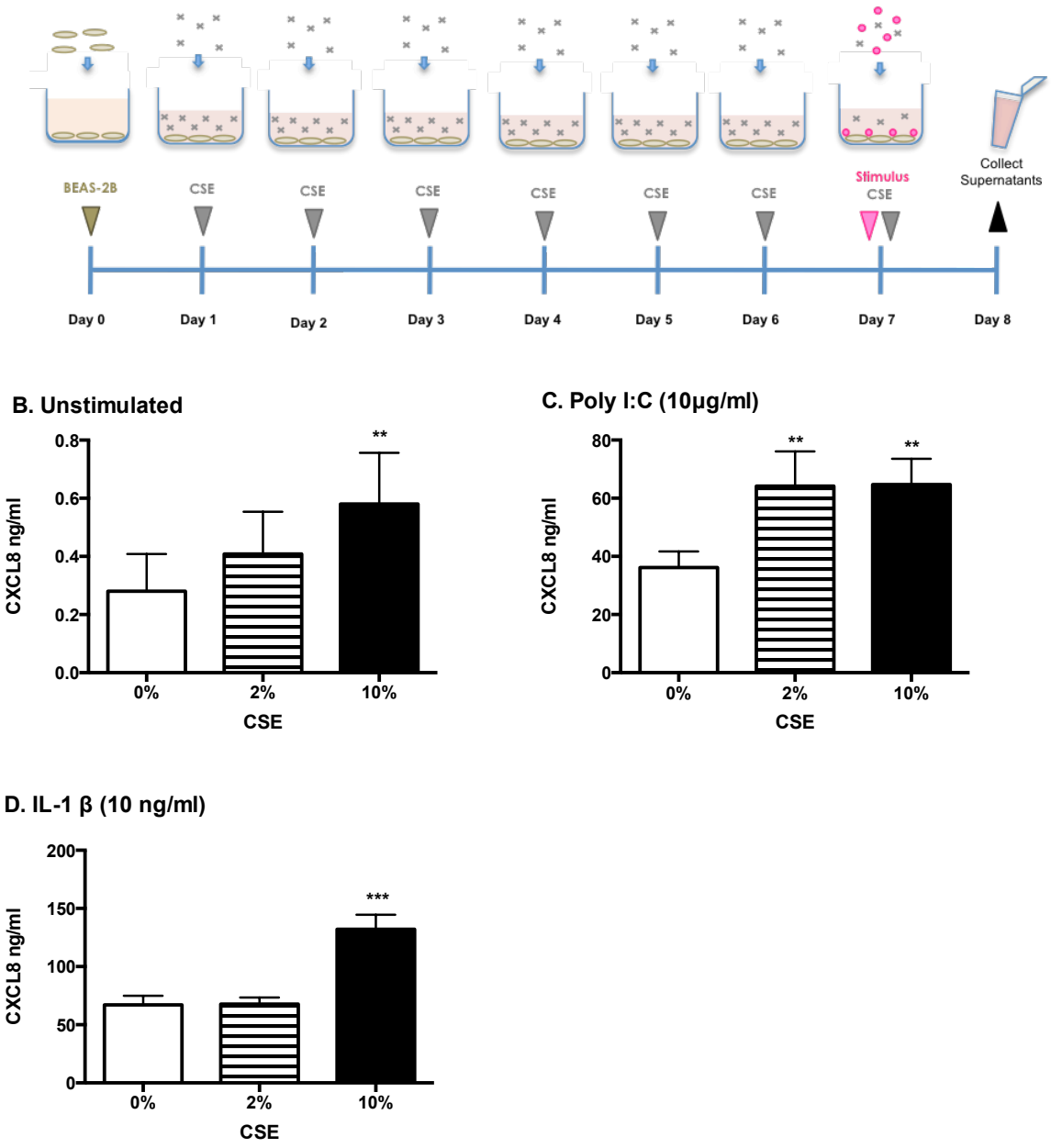

Figure 3.12 Repeated exposure to CSE potentiates the CXCL8 response to TLR agonists in BEAS-2B cells

(**A**) BEAS-2B cells were seeded at 3 x 10^6 cells/24-well plate (125,000 cells/well) for 24 hours followed by stimulation with CSE (2% or 10%) every 24 hours for 6 days followed by a final stimulation of CSE with or without a TLR agonist for a further 24 hours. Supernatants for (**B**) CSE (2% and 10%) alone, or the combination of CSE (2% and 10%) and (**C**) poly(I:C) (10ug/ml) or (**D**) IL-1β (10ng/ml) were collected and analysed for CXCL8 release by ELISA. Data are expressed as mean ± SEM of n=5. Statistical analysis was carried out by one-way ANOVA with Bonferroni's post-test (**p<0.01 and ***p<0.001).

3.8 MyD88 and IRF3 stable knockdown differentially regulate CXCL8 secretion to multiple proinflammatory stimuli in BEAS-2B cells

LPS triggers the TLR4 dependent activation of NF-κB, IRF-3 and MAPK pathways, which are mediated by the adaptors MyD88 and Mal. This early activation results in the expression of a plethora of pro-inflammatory cytokines following the phosphorylation and activation of the IRAK1/IRAK4/TRAF6 activation complex. At late stage activation however, LPS results in the internalisation of TLR4 into endosomes allowing it to associate with TRIF and activate the MyD88-independent pathway (O'Neill et al., 2013). Therefore in order to dissect the effects and roles of IL-1β and IFN signalling on bacterial infection and viral infection in more detail two stable knockdowns were used: MyD88 knockdown (IL-1R1 signalling adaptor) and IRF3 knockdown (IFN signalling transcription factor).

Both stable knockdown cell lines were previously created by a post-doctoral researcher within the group, Dr Clare Stokes, using a lentiviral delivery system containing a shRNA that inserts into the chromosome and results in RNA interference by the long-term degradation of the target mRNA (Stokes et al., 2011).

Both MyD88^{KD} and IRF3^{KD} showed decreasing trends in CXCL8 production when compared with WT even in the absence of any stimulus (**Figure 3.13a**). The exposure to CSE for 24 hours resulted in a significant increase in CXCL8 release in WT cells and an increasing trend in the MyD88^{KD} or IRF3^{KD} cell lines (**Figure 3.13a**). This phenotype was replicated with the addition of LPS, wherein CXCL8 baseline levels were significantly increased in WT cell line only (**Figure 3.13b**).

However, when stimulated with poly(I:C) alone, the CXCL8 levels in the WT cell line were significantly higher than the decreasing trend measured in both MyD88^{KD} and IRF3^{KD} (**Figure 3.13c**). Interestingly, the addition of CSE to poly(I:C) resulted in a decrease in WT CXCL8 release with minimal change measured in MyD88 and IRF3^{KD} CXCL8 levels (**Figure 3.13c**). Finally, the stimulation of WT and IRF3^{KD} cells with the combination of CSE and IL-1β resulted in an increase in levels of CXCL8 while MyD88^{KD} cells remained unchanged (**Figure 3.13d**). It is important to note that MyD88^{KD} and IRF3^{KD} CXCL8 levels produced were consistently lower than WT, even when unstimulated.

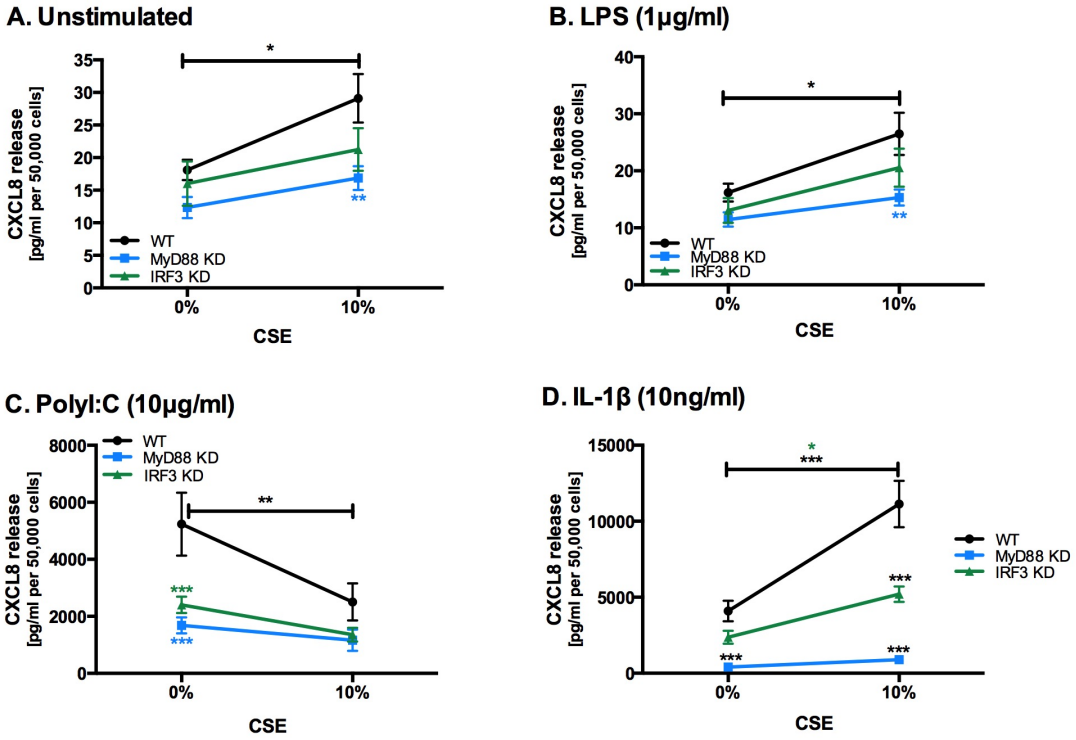

Figure 3.13 MyD88^{KD} and IRF3^{KD} epithelial cell lines exhibit selective defects in responses to proinflammatory stimuli

BEAS-2B, MyD88^{KD} and IRF3^{KD} cells were seeded at 3 x 10^6 cells/24-well plate (125,000 cells/well) for 24 hours followed by stimulation with (**A**) CSE (10%) alone, or the combination of CSE (10%) and (**B**) LPS (1ug/ml), (**C**) Poly(I:C) (10ug/ml) or (**D**) IL-1β (10ng/ml) for 24 hours. Supernatants were collected and analysed for CXCL8 release by ELISA. Data are expressed as mean ± SEM of n=7. Statistical analysis was carried out by two-way ANOVA with Bonferroni's post-test (**p<0.01 and ***p<0.001).

3.9 Altered acute model results in increased CXCL8 production to poly(I:C) stimulation in the presence of CSE

My previous data indicated an altered BEAS-2B CXCL8 response to poly(I:C) stimulation following repeated exposure to CSE over 7 days when compared to an acute 24 hour exposure. While poly(I:C) alone in both models resulted in the increase of CXCL8 production, the addition of poly(I:C) in the presence of CSE for 24 hours lead to a reduction in CXCL8 production acutely (**Figure 3.11c**). Interestingly, the repeated pretreatment of BEAS-2B cells with CSE prior to a 24 hours poly(I:C) stimulation resulted in a potentiated CXCL8 response (**Figure 3.12c**). In order to determine whether this differential was indeed caused by the repetitive CSE pretreatment and not the method itself, a new more comparable control experiment was developed. The new control acute model is maintained for 7 days, the same period of time as the chronic model, and in the same environment however remains unstimulated until the final 24 hours.

BEAS-2Bs were grown to confluence and split into the acute model or the repeated exposure/chronic model. Cells from the acute model were maintained in RPMI 1640 with 5% FCS fresh media changed every 24 hours for 6 days (method depicted in **Figure 3.14**). Whilst cells from the chronic model were exposed to fresh CSE (10%) in RPMI 1640 with 5% FCS every 24 hours for 6 days (method depicted in **Figure 3.14**). On day 7 both groups were washed with PBS and stimulated with poly(I:C) (10 ug/ml) in basal RPMI 1640 for 24 hours before supernatant collection and analysis. As per previous results (**Figure 3.12c**), the repeated exposure model resulted in an increase in CXCL8 production in response to poly(I:C) and CSE in BEAS-2B cells (**Figure 3.14b**). Interestingly, in contrast to previous findings (**Figure 3.11c**), the acute model also resulted in an increase in CXCL8 production to poly(I:C) (**Figure 3.14a**) suggesting the increase in CXCL8 previously observed in the chronic model alone was in fact not due to repeated CSE stimulation, but instead due to the changes in cells over time in culture.

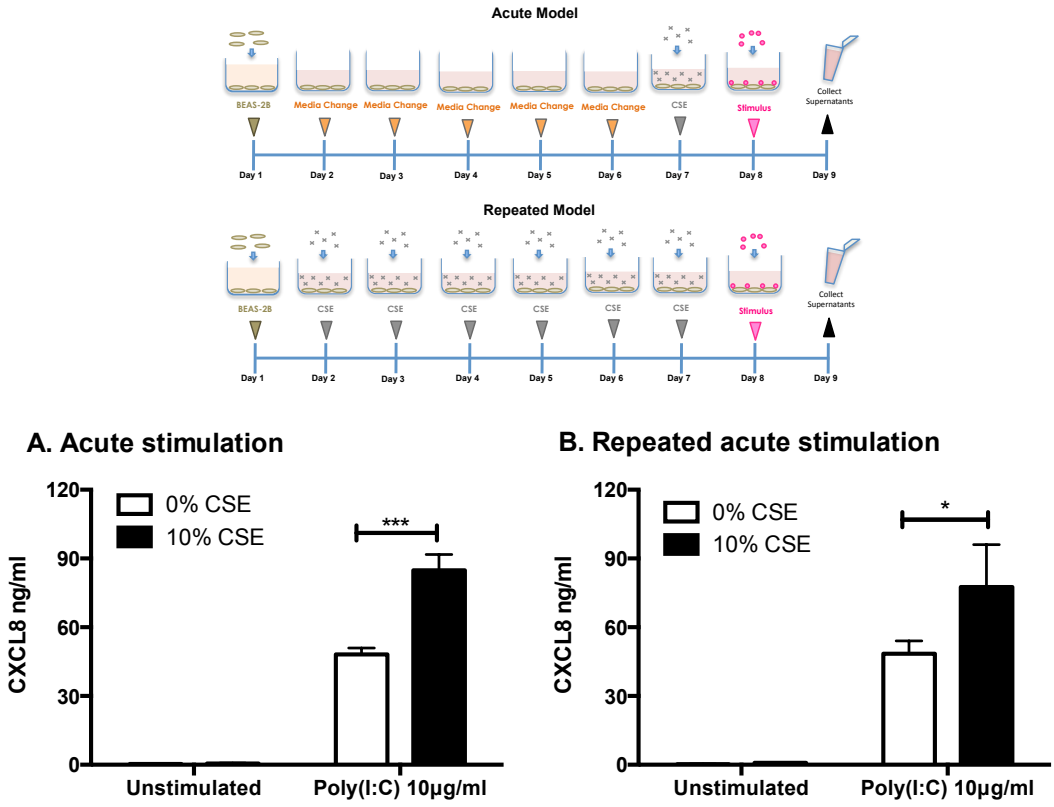

Figure 3.14 Both acute and repeated exposure to CSE potentiates CXCL8 production in response to poly(I:C)

BEAS-2B cells were pretreated with (**A**) fresh media or (**B**) 10% CSE every 24 hours for 6 days before undergoing a final stimulation with poly(I:C) (10 µg/ml). Supernatants were collected and analysed for CXCL8 release by ELISA. Data are expressed as mean ± SEM of n=4. Statistical analysis was carried out by two-way ANOVA with Bonferroni's post-test (*$p<0.05$ and ***$p<0.001$).

3.10 Pretreatment with CSE decreased BEAS-2B cells antiviral response to RV-16

Cigarette smoke exposure is linked with increased occurrence of respiratory viral infections in addition to increased periods of infection and worse prognosis. Epithelial cells are the primary target of human rhinoviral infections and therefore, their response essential to the launch of an effective innate immune response. Evidence supports a role for acute CSE exposure in the inhibition of anti-viral responses (Eddleston et al., 2011). Therefore it was hypothesised that the repeated exposure of BEAS-2B cells to CSE would result in an altered response to RV infection.

CCL5 is among the most highly induced chemokines following rhinoviral infection of airway epithelial cells. To determine whether repeated exposure to CSE alters antiviral responses, BEAS-2B cells were pre-treated with fresh 10% CSE every 24 hours for 6 days and then stimulated with RV-16 at an MOI of 1.3 or control media for a final 24 hours. CCL5 production was then measured by ELISA. Pretreatment with CSE alone did not increase CCL5 production, however, CSE pretreatment did decrease the BEAS-2B cell response to RV-16 in both the control acute model (**Figure 3.15a**) and repeated chronic model (**Figure 3.15b**).

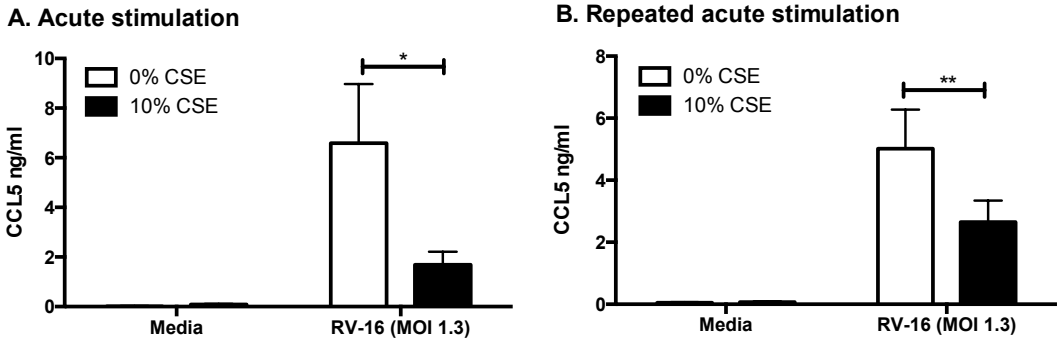

Figure 3.15 CSE inhibits BEAS-2B antiviral response following CSE pretreatment

BEAS-2B cells were pretreated with (**A**) fresh media or (**B**) 10% CSE every 24 hours for 6 days before undergoing a final stimulation with R V-16 at an MOI of 1.3. Supernatants were collected and analysed for CCL5 release by ELISA. Data are expressed as mean ± SEM of n=4. Statistical analysis was carried out by two-way ANOVA with Bonferroni's post-test (*$p<0.05$ and **$p<0.01$).

3.11 CSE enhances BEAS-2B proinflammatory responses to RV-16

Infection of human airway epithelial cells with rhinovirus generates the release of a multitude of pro-inflammatory cytokines and host-defence genes resulting in an enhanced inflammatory environment (Hudy and Proud, 2013; Proud et al., 2008). While there is increasing evidence supporting CSE's ability to alter anti-viral defences in epithelial cells, these are in most cases a down regulation of RV-induced epithelial gene expression (Eddleston et al., 2011; Proud et al., 2012; Wang et al., 2009). Interestingly, the opposite is true for the production of CXCL8 wherein CSE induces CXCL8 mRNA and protein levels (Hudy et al., 2010; Wang et al., 2009). In fact, the combination of CSE and RV results in at least an additive CXCL8 secretion in airway epithelial cells (Hudy and Proud, 2013). The study however focuses on the immediate effects of CSE in an acute environment. Therefore it was hypothesised that repeated exposure to CSE may indeed result in an enhanced CXCL8 response to RV.

BEAS-2B cells were either grown in fresh media or pre-treated with fresh 10% CSE every 24 hours for 6 days and then stimulated with RV-16 at an MOI of 1.3 or control media for a final 24 hours. CXCL8 production was then measured by ELISA. Pretreatment with CSE resulted in an additive CXCL8 production in both the acute and the chronic repeated exposure model (**Figure 3.16a and 3.16b**).

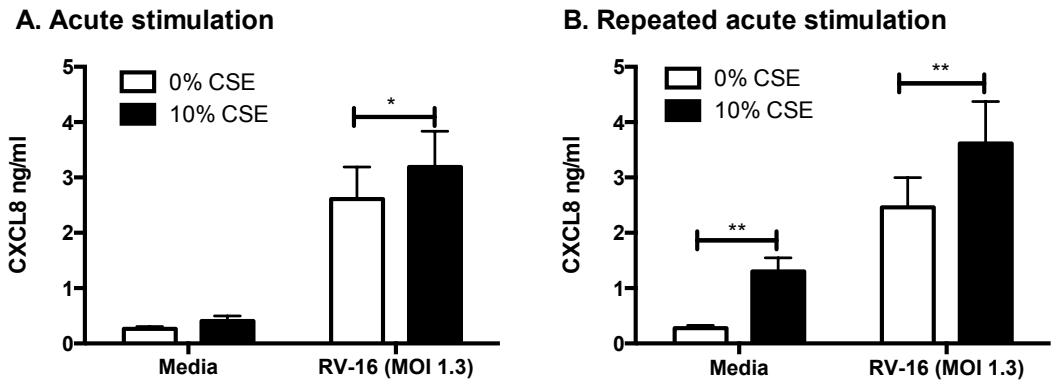

Figure 3.16 CSE increases BEAS-2B proinflammatory response following CSE pretreatment

BEAS-2B cells were pretreated with (**A**) fresh media or (**B**) 10% CSE every 24 hours for 6 days before undergoing a final stimulation with RV-16 at an MOI of 1.3. Supernatants were collected and analysed for CXCL8 release by ELISA. Data are expressed as mean ± SEM of n=4. Statistical analysis was carried out by two-way ANOVA with Bonferroni's post-test (*$p<0.05$ and **$p<0.01$).

3.12 CSE differentially regulates proinflammatory responses to TLR agonists in a chronic model of inflammation in human bronchial epithelial primary cells

BEAS-2B cells are an immortalised cell line which serve only as a representation of airway epithelial cells. Cell signalling pathways in these cell types can be altered or switched on by the immortalisation process making them convenient and reproducible cell type, but not always truly reflective of the physiological functions in the airway. Therefore, it is vital to validate cell line results with primary cells wherever possible.

Human bronchial epithelial primary cells (HBEpCs) were thus also investigated using the acute CSE exposure model and the chronic repeated CSE exposure model (method depicted in **Figure 3.17**). HBEpCs were grown to confluence and split into the acute model or the repeated exposure/chronic model. Cells from the acute model were treated with 50% supplemented Airway Epithelial Cell Growth (AECG) media minus hydrocortisone every 24 hours for 6 days whilst cells from the chronic model were exposed to fresh CSE (10%) in 50% supplemented AECG minus hydrocortisone every 24 hours for 6 days. On day 7 both groups were washed with PBS and stimulated with LPS (1ng/ml), poly(I:C) (10ug/ml) and IL-1β (10ng/ml) in basal AECG media for 24 hours before supernatant collection and analysis. There was no difference in CXCL8 measured in the presence of CSE in both the acute model and the repeated model (**Figure 3.17a**). The presence of CSE also did not significantly alter CXCL8 production in both LPS stimulated (**Figure 3.17b**) and poly(I:C) stimulated models (**Figure 3.17c**). However, the addition of CSE resulted in a significant increase in CXCL8 in response to IL-1β stimulation seen only in the acute model (**Figure 3.17d**).

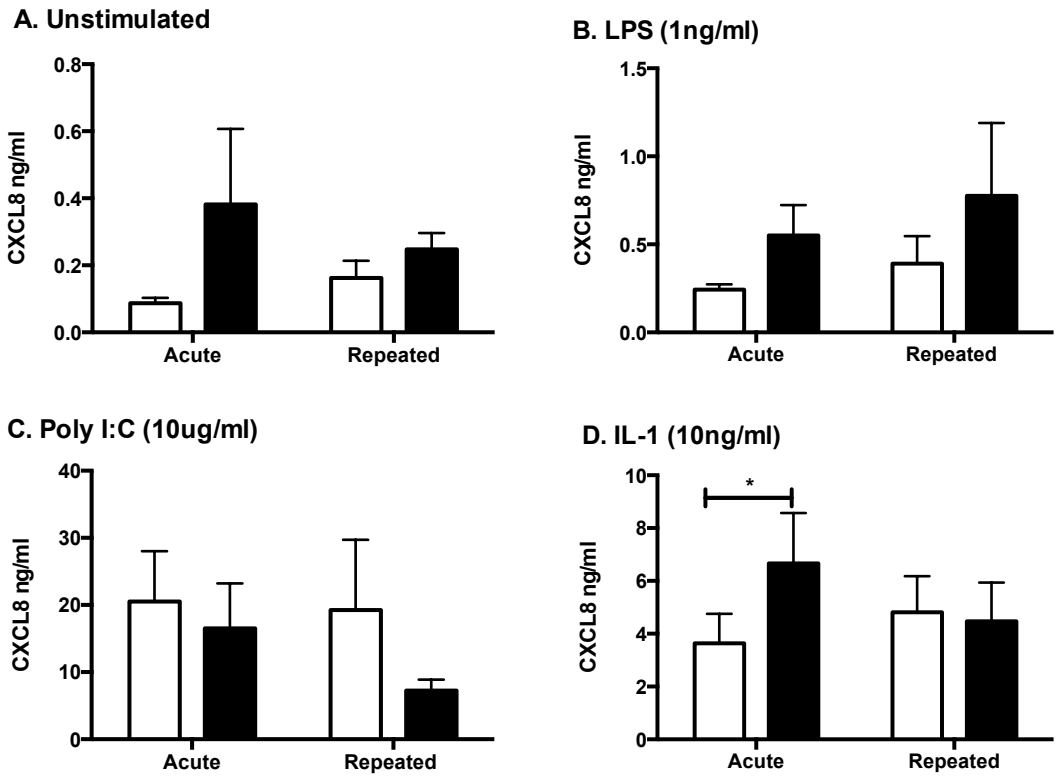

Figure 3.17 HBEpCs cells exhibit differential regulation to proinflammatory stimuli in the presence of CSE

HBEpCs cells were stimulated with fresh media (labelled: acute) or 10% CSE (labelled: repeated) every 24 hours for 6 days before undergoing a final stimulation with TLR agonists for a further 24 hours. The final stimuli were: (**A**) Unstimulated control group, (**B**) LPS (1ug/ml), (**C**) Poly(I:C) (10ug/ml) or (**D**) IL-1β (10ng/ml). Supernatants were collected and analysed for CXCL8 release by ELISA. Data are expressed as mean ± SEM of n=4. Statistical analysis was carried out by two-way ANOVA with Bonferroni's post-test (*$p<0.05$).

3.13 Summary

The aim of this chapter was to generate an *in vitro* chronic model of inflammation to understand the effects of prolonged inflammation on epithelial cell immunity and cellular communication. A homogenous differentiated leukemic monocytic cell line, THP-1, was differentiated with vitamin D_3 to model monocyte function since primary monocytes cannot be readily acquired or maintained for the duration of the proposed model. The monocytic phenotype of these cells was determined by the measure of the monocytic surface marker CD14. In addition, VitD_3-differentiated THP-1 cells are responsive to LPS challenge as measured by CXCL8 production, albeit releasing lower levels of CXCL8 than primary monocytes.

VitD_3-differentiated THP-1 cells also effectively replicated the cooperative signalling between monocytes and BEAS-2B cells in response to LPS, however the levels of the inflammatory marker CXCL8 produced in this model were substantially inferior when VitD_3-differentiated THP-1 cells were used. When monocytic cells were separated from the BEAS-2B monolayer by the use of a cell-culture insert, VitD_3-differentiated THP-1 cells were similarly less sensitive to LPS challenge when compared to monocytes. To compensate, 100,000 VitD_3-differentiated THP-1 cells were used in the proposed chronic model of inflammation. The reason for this decreased sensitivity in THP-1 is most likely due to decreased levels of CD14 expression in THP-1 cells required for effective LPS response.

The chronic model of inflammation involved a continuous low grade LPS challenge of BEAS-2B cells for the duration of 8 days. VitD_3-differentiated THP-1 cells were separated from the BEAS-2B monolayer by cell culture inserts and replaced regularly (on days 1, 3, and 5). This method of cell separation aimed to replicate cellular communication through released soluble factors. On day 7, cell culture inserts were removed, and the BEAS-2B cells directly challenged with a fresh dose of LPS in the presence of primary monocytes. Interestingly, the continuous LPS challenge did not alter BEAS-2B inflammatory responses as measured by CXCL8. The addition of VitD_3-differentiated THP-1 cells also had no impact on the BEAS-2B cells' ability to mount an effective inflammatory response to the final challenge with LPS and monocytes.

This led to the hypothesis that the lack of direct cell-to cell contact between THP-1 cells and BEAS-2B monolayer may have led to ineffective cytokine production required for effective

inflammatory response. Therefore, the same protocol was repeated, only vitD_3-differentiated THP-1 cells were then in direct contact with BEAS-2Bs from day 1-7 of the experiment. Interestingly, while the levels of CXCL8 produced in the direct cell contact model were marginally lower than that of the control model that did not have THP-1 cells throughout, there were still no measurable differences in CXCL8 production between the LPS challenged model and the unchallenged control.

The resistant nature of BEAS-2B cells to multiple low-grade stimulation with LPS led to the development of an alternative model which proposed the use of CSE as a BEAS-2B cell antagonist. Cigarette smoke is one of the predominant causes for the development of COPD and was therefore considered an appropriate stimulus for this study. Acute exposure of BEAS-2B cells to 10% CSE alone significantly increased CXCL8 baseline levels. The addition of LPS did not alter the CSE-induced CXCL8 levels, however stimulation with IL-1β significantly upregulated CSE-induced CXCL8 release. In contrast, CXCL8 production was inhibited by the presence of CSE in response to poly(I:C).

It was then hypothesised that repeated exposure to CSE would result in an altered and primed epithelium to further pathogenic stimulation. The repeated exposure of BEAS-2B cells to CSE followed by a single IL-1β challenge resulted in a significant increase in CXCL8 release as per the acute model. Of interest however, chronic stimulation with CSE resulted in a significant increase in CXCL8 release in response to poly(I:C) in contrast to the acute model. However, when determining whether this differential was caused by the multiple exposures to CSE or the method itself, we found that BEAS-2B cells maintained for 7 days with no CSE pre-treatment prior to a single CSE challenge with poly(I:C) resulted in the increased CXCL8 phenotype as per the chronic model.

CXCL8 and CCL5 release was also quantified in BEAS-2B cells infected with RV-16 following acute and repeated CSE exposure. While CCL5 release was downregulated by CSE exposure, CXCL8 was upregulated in both acute and CSE pre-treated models.

In contrast to BEAS-2B cells, CSE did not result in an elevated CXCL8 release in HBEpCs. In fact, acutely or repeatedly pre-treated HBEpCs with CSE did not significantly alter LPS- or poly(I:C)-induced CXCL8 release. While HBEpCs acutely stimulated with the combination of CSE and IL-1β produced significant levels of CXCL8, the repeated pre-treatment with CSE prevented the

IL-1β induced CXCL8 release. It is however important to note that some of the changes to chemokine production could have been in part as a result of cell death which was unmeasured in these experiments and would need to be further explored in future experiments.

CHAPTER 4 - RESULTS. THE ROLE OF PELLINO-1 IN INFLAMMATORY SIGNALLING

Viral infections, such as rhinoviruses (RVs), account for a majority of exacerbations of COPD (Johnston, 2005) and can subsequently result in pronounced functional impairment of the airway increasing both the severity of the disease and frequency of exacerbations. Therefore the reduction of RV-induced airway inflammation would be of immense clinical value with the reduction in severity and duration of the disease improving patient quality of life and reducing morbidity and mortality. Thus, targeting signalling pathways involved in RV-induced inflammation is an important goal. An optimal anti-inflammatory treatment would reduce RV-induced airway inflammation without impairing host defence.

Pellino-1 was originally identified as a regulator of IL-1 signalling (Jiang et al., 2003), however while knockdown of Pellino-1 in immortalised epithelial cell line BEAS-2B reduces IL-1β-induced expression of pro-inflammatory cytokines, the knockdown of Pellino-1 in HBEpC had no such effect overall suggesting that regulation of IL-1 responses may have solely been a feature of transformed cell lines (Bennett et al., 2012). Strikingly, more recent observations have highlighted a role for Pellino-1 in viral signalling wherein Pellino-1 regulates pro-inflammatory responses to RV infection but does not appear to control production of antiviral IFNs (Bennett et al., 2012; Chang et al., 2009). These data strongly support Pellino-1 as a potential therapeutic drug target. This thesis investigates the regulation of Pellino-1 and its role in viral infection in human bronchial airway epithelial cells.

4.1 Poly(I:C) induced Pellino-1 mRNA expression is inhibited by CSE in primary human bronchial epithelial cells

Since its discovery, increasing evidence suggests a role for Pellino-1 in viral signalling wherein Pellino-1 modulates innate cellular responses to viral infection (Bennett et al., 2012; Chang et al., 2009). To begin investigating the regulation of Pellino-1 in airway epithelial cells in response to viral stimuli, HBEpCs were stimulated with the TLR-3 agonist and viral mimic, poly(I:C) (50 μg/ml). Quantitative RT-PCR (qPCR) was used to determine the changes to Pellino-1 mRNA transcripts following a 24 hour stimulation with poly(I:C) and resulted in a significant

increase in Pellino-1 mRNA expression (**Figure 4.1**).

Cigarette smokers are reported to experience more frequent and severe airway infections than non-smokers (Cohen et al., 1993). Several studies have shown that cigarette smoke exposure can impair innate immune responses in the airway (Bauer et al., 2008; Eddleston et al., 2011; Hudy et al., 2014; Modestou et al., 2010). Whilst the underlying mechanisms are not completely understood, cigarette smoke can result in suppressed anti-viral responses, enhanced pro-inflammatory defences, remodelling of the airway and cellular apoptosis.

To determine the impact of cigarette smoking on Pellino-1 expression during viral infections, HBEpCs were also exposed to CSE (10%) both singularly and in combination with poly(I:C) (50 μg/ml). Stimulation with CSE alone did not alter Pellino-1 mRNA expression. However of interest, the combined stimulation with poly(I:C) and CSE resulted in a suppression of poly(I:C)-induced Pellino-1 expression (**Figure 4.1**).

Similarly, Pellino-1 protein expression, measured by western blotting, was significantly enhanced following a 24 hour poly(I:C) stimulation, and this increase was significantly inhibited when HBEpCs were co-stimulated with poly(I:C) and CSE (**Figure 4.2**).

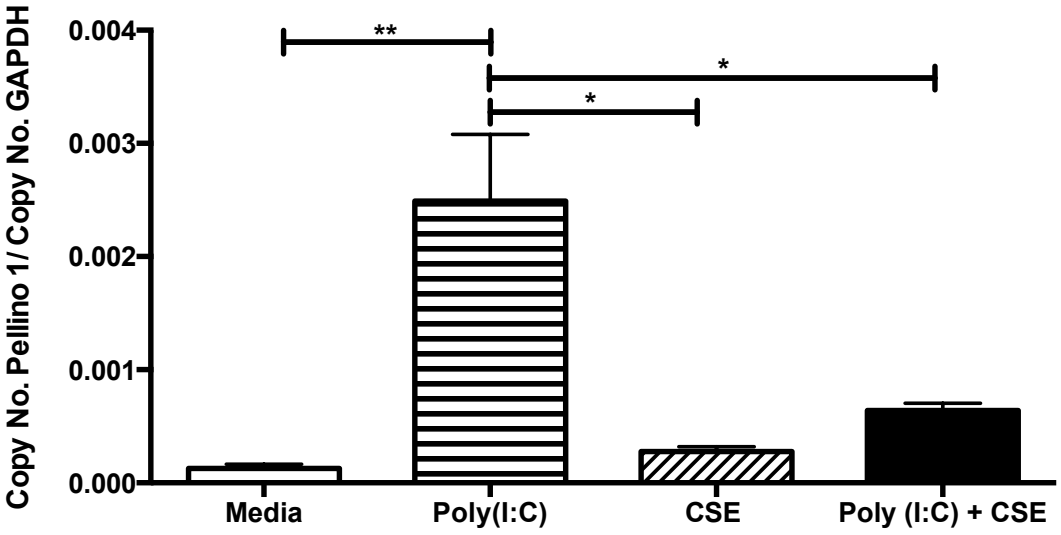

Figure 4.1: Poly(I:C) induced Pellino-1 mRNA expression is inhibited by CSE in primary human bronchial epithelial cells

HBEpCs were stimulated with poly(I:C) (50 µg/ml), CSE (10%) or the combination of both for 24 hours. mRNA expression was determined by quantitative RT-PCR (qPCR). Pellino-1 expression was normalized to GAPDH copy numbers (loading control) and expressed as mean ± SEM of n=3, with each replicate performed on separate donors. Statistical analysis was carried out by one-way ANOVA with Bonferroni's post-test (*$p<0.05$ and **$p<0.01$).

A

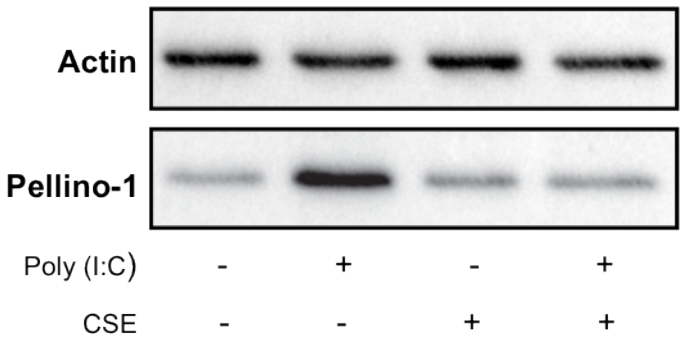

B

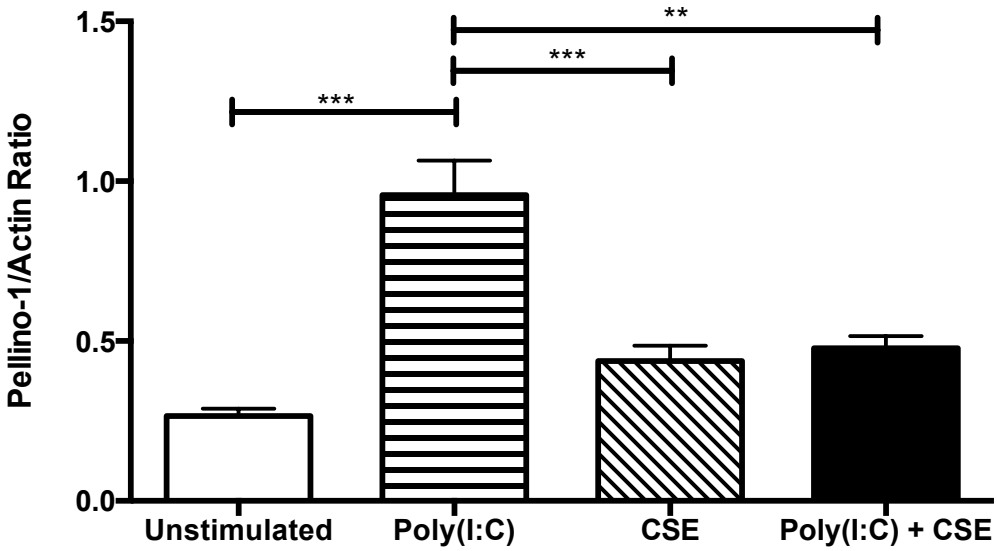

Figure 4.2: Poly(I:C) induced Pellino-1 protein expression is inhibited by CSE in primary human bronchial epithelial cells

HBEpCs were stimulated with poly(I:C) (50 μg/ml), CSE (10%) or the combination of both for 24 hours. Cell lysates were analysed for Pellino-1 or actin expression by western blot. Representative blot is shown in figure (**A**). Quantitative signals were determined by densitometry and expressed as mean ± SEM of n=3, with each replicate performed on separate donors (**B**). Statistical analysis was carried out by one-way ANOVA with Bonferroni's post-test (**p<0.01 and ***p<0.001).

4.2 Pellino-1 transient knockdown reduces poly(I:C) induced CXCL8 expression and secretion in primary human bronchial epithelial cells

Previous work has established a role for Pellino-1 in MyD88-independent NF-κB activation in primary airway epithelial cells in response to poly(I:C) (Chang et al., 2009) (Bennett et al., 2012). Bennett *et al*. demonstrated that CXCL8 release in response to poly(I:C) stimulation was inhibited in Pellino-1 knockdown cells obtained from a single donor. It was therefore hypothesized that Pellino-1 selectively regulates the NF-κB arm of virally induced TLR3 signalling, wherein targeting of Pellino-1 could ultimately reduces inflammation whilst preserving antiviral immunity.

Initial experiments assessed efficiency of transient knockdown showing Pellino-1 transcripts were significantly knocked down by Pellino-1 siRNA transfection for 24 hours (**Figure 4.3**). HBEpCs obtained from 5 different donors were subsequently transfected with Pellino-1 targeted siRNA and non-targeted scrambled siRNA control before undergoing treatment with poly(I:C) for 4, 8, 16 and 24 hours. The generation of CXCL8, a NF-κB stimulated gene, at levels of mRNA expression (**Figure 4.4a**) and protein release (**Figure 4.4b**) were measured using qPCR and ELISA respectively. CXCL8 levels were most pronounced at 16 and 24 hours. Pellino-1 knockdown significantly inhibited both CXCL8 mRNA expression and the resulting CXCL8 cytokine release in response to poly(I:C) at 24 hours post-stimulation (**Figure 4.4**).

A

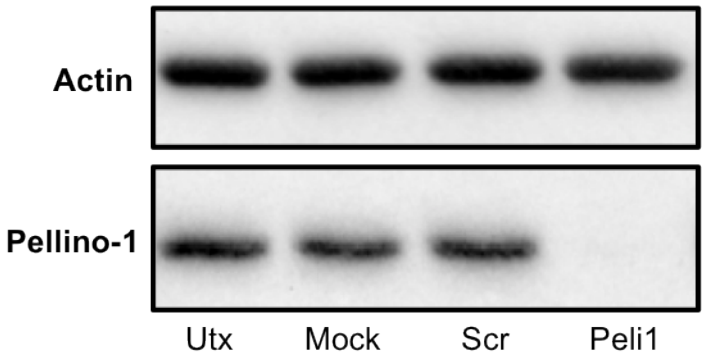

B

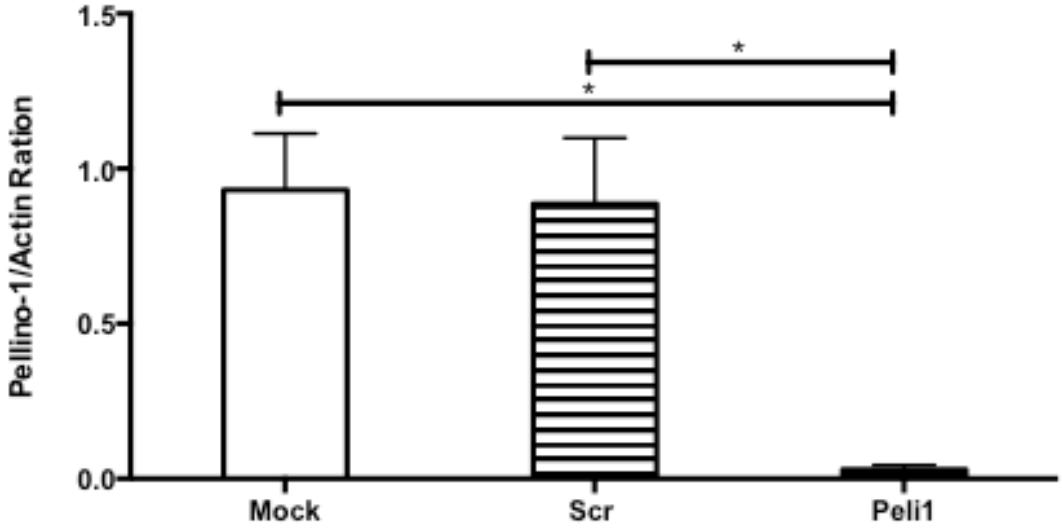

Figure 4.3: Pellino-1 transient knockdown reduces Pellino-1 expression in primary human bronchial epithelial cells

HBEpCs were transiently transfected with Pellino-1 siRNA, non-targeting scrambled siRNA or mock infected (described in **Section 2.9**). Cell lysates were collected 24 hours post-transfection and analysed for Pellino-1 or actin expression by western blot. Representative blot is shown in figure (**A**). Quantitative signals were determined by densitometry and expressed as mean ± SEM of n=4, with each replicate performed on separate donors (**B**). Statistical analysis was carried out by one-way ANOVA with Bonferroni's Post-test (*$p<0.05$).

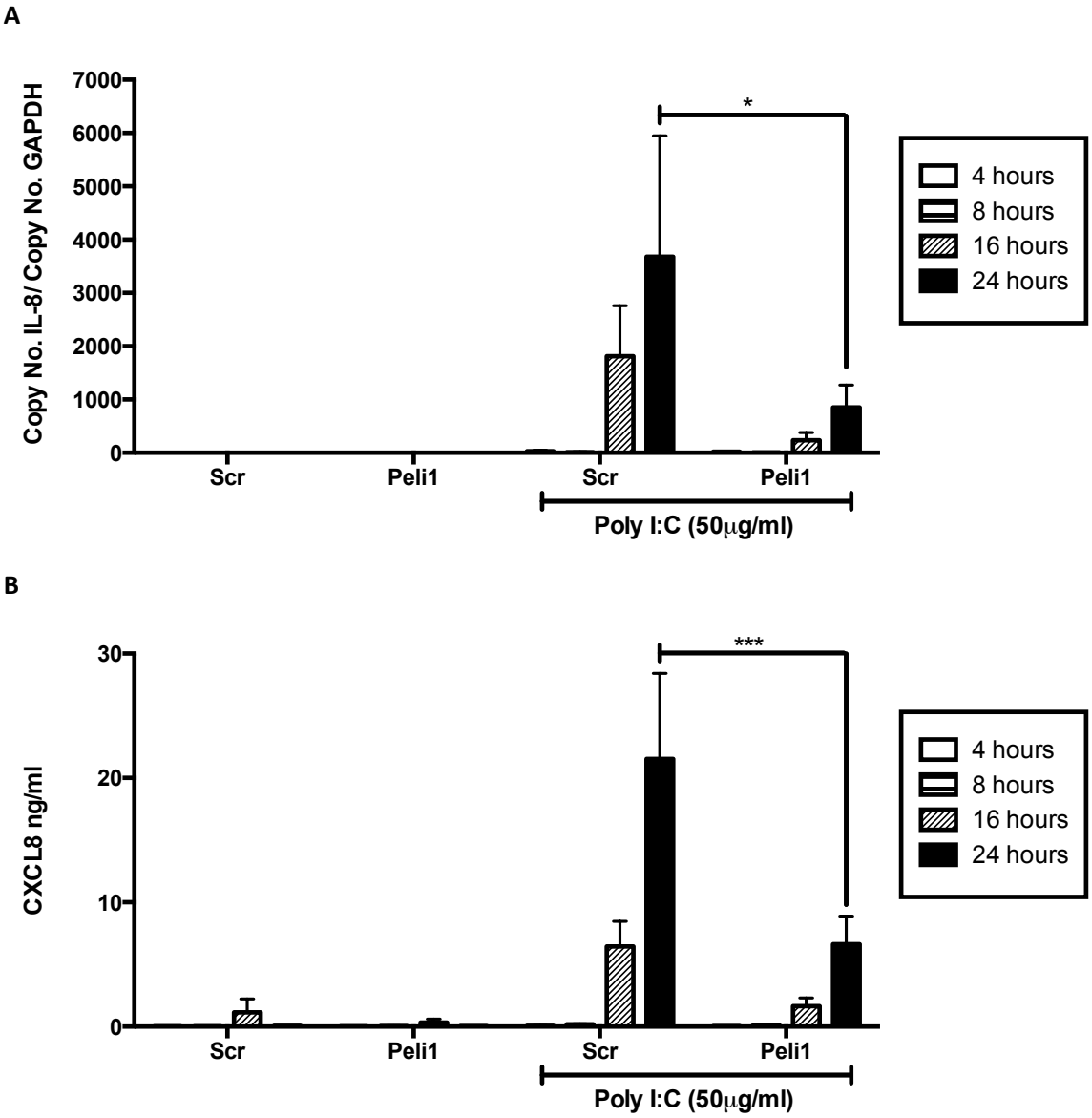

Figure 4.4: Pellino-1 transient knockdown reduces poly(I:C) induced CXCL8 expression and secretion in primary human bronchial epithelial cells

HBEpCs were transiently transfected with Pellino-1 siRNA and non-targeting scrambled siRNA for 24 hours prior to treatment with poly(I:C) (50 μg/ml) for 4, 8, 16 and 24 hours. RNA was extracted and CXCL8 expression levels were analysed by quantitative RT-PCR (**A**). Supernatants were collected and analysed for CXCL8 release by ELISA (**B**). Data are expressed as mean ± SEM of n=5, with each replicate performed on separate donors. Statistical analysis was carried out by two-way ANOVA with Bonferroni's post-test (*$p<0.05$ and ***$p<0.001$).

4.3 Pellino-1 transient knockdown does not alter poly(I:C) induced IFNβ expression in primary human bronchial epithelial cells

The pattern recognition receptor TLR3 recognises dsRNA from replicating viruses and triggers signalling pathways resulting in the production of pro-inflammatory cytokines, chemokines and type I IFNs. The production of type I IFNs is dependent on the activation of IKKε/TBK1 complex and the resulting activation of IRF3.

The only other study on the roles of Pellino-1 in viral infection has shown that Pellino-1 does not alter anti-viral IFN generation and IFN-stimulated gene transcription responses in primary bronchial epithelial cells (Bennett et al., 2012). These data were the result of experiments performed on bronchial epithelial cells from a single donor stimulated with poly(I:C) or RV-1B for 24 hours. In an attempt to support the hypothesis that Pellino-1 selectively regulates the NF-κB arm of virally induced TLR3 signalling by regulating inflammation whilst preserving antiviral immunity, a Pellino-1 transient knockdown was created. The experiments were performed on 5 unique donors to increase robustness and over a time-course of 4-24 hours.

Pellino-1 gene expression in HBEpCs induced with poly(I:C) (50 μg/ml) was transiently inhibited by transfection with Pellino-1 siRNA for 24 hours. The induction of IFNβ transcripts by poly(I:C) peaked at 4 hours and returned to baseline levels by 8 hours (**Figure 4.5**). In addition, the absence of Pellino-1 did not result in any changes to poly(I:C) induced IFNβ expression when compared to scrambled control (**Figure 4.5**).

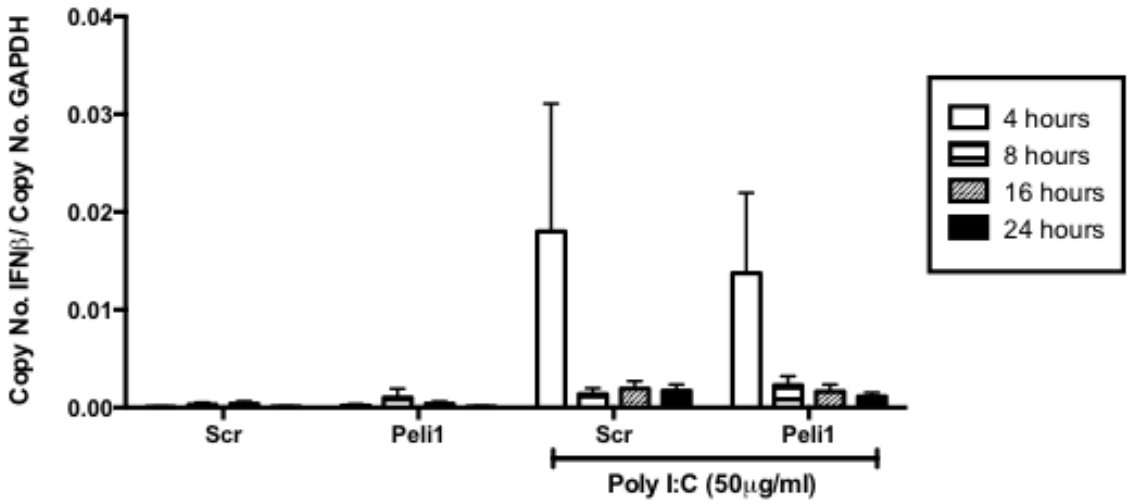

Figure 4.5: Pellino-1 transient knockdown does not alter poly(I:C) induced IFNβ expression in primary human bronchial epithelial cells

HBEpCs were transiently transfected with Pellino-1 siRNA and non-targeting scrambled siRNA for 24 hours prior to treatment with poly(I:C) (50 μg/ml) for 4, 8, 16 and 24 hours. RNA was extracted and IFNβ expression levels were analysed by quantitative RT-PCR. Data are expressed as mean ± SEM of n=5, with each replicate performed on separate donors. Statistical analysis was carried out by two-way ANOVA with Bonferroni's post-test.

4.4 Pellino-1 transient knockdown differentially regulates poly(I:C) induced IL-1 expression in primary human bronchial epithelial cells

Pellino-1 has been implicated in IL-1 signalling through its involvement with the IRAK1/IRAK4/TRAF6 complex. In the human embryonic kidney 293 (HEK293) cell line, the transient knockdown of Pellino-1 by siRNA resulted in the impairment of IL-1-dependent activation of NF-κB (Choi et al., 2006; Jiang et al., 2003). However, in primary human airway epithelial cells, Pellino-1 appears to exert its effects in an IRAK1-independent manner, as Bennett *et al.* clearly showed a role for Pellino-1 in TLR3 activation in response to poly(I:C) and RV-1B (Bennett et al., 2012).

COPD patients have increased baseline levels of IL-1β within their airways, which are increased further in instances of acute exacerbations (Chung, 2001). There is also accumulating evidence suggesting a role for IL-1β in response to RV infections whereby IL-1 is released and acts as an autocrine stimulus to further enhance inflammatory signalling (Grunstein et al., 2000; Hakonarson et al., 1999; Piper et al., 2013; Stokes et al., 2011).

Whilst a role for Pellino-1 in IL-1 signalling has only been established in MyD88-dependent activation, it was hypothesized that Pellino-1 may in fact play a role in virally induced IL-1 production. To investigate this, Pellino-1 was transiently knocked down by siRNA transfection for 24 hours prior to poly(I:C) (50 μg/ml) stimulation for 4, 8, 16 and 24 hours respectively. IL-1 is often described as an early phase cytokine, however the levels of both IL-1α and IL-1β were only increased from 16 hours in response to poly(I:C) (**Figure 4.6a** and **Figure 4.6b**). Interestingly, the knockdown of Pellino-1 also resulted in a significant reduction in IL-1β gene expression to poly(I:C) at 16 and 24 hours (**Figure 4.6b**), whilst IL-1α showed a similar decreasing trend at 16 and 24 hours post-stimulation (**Figure 4.6a**).

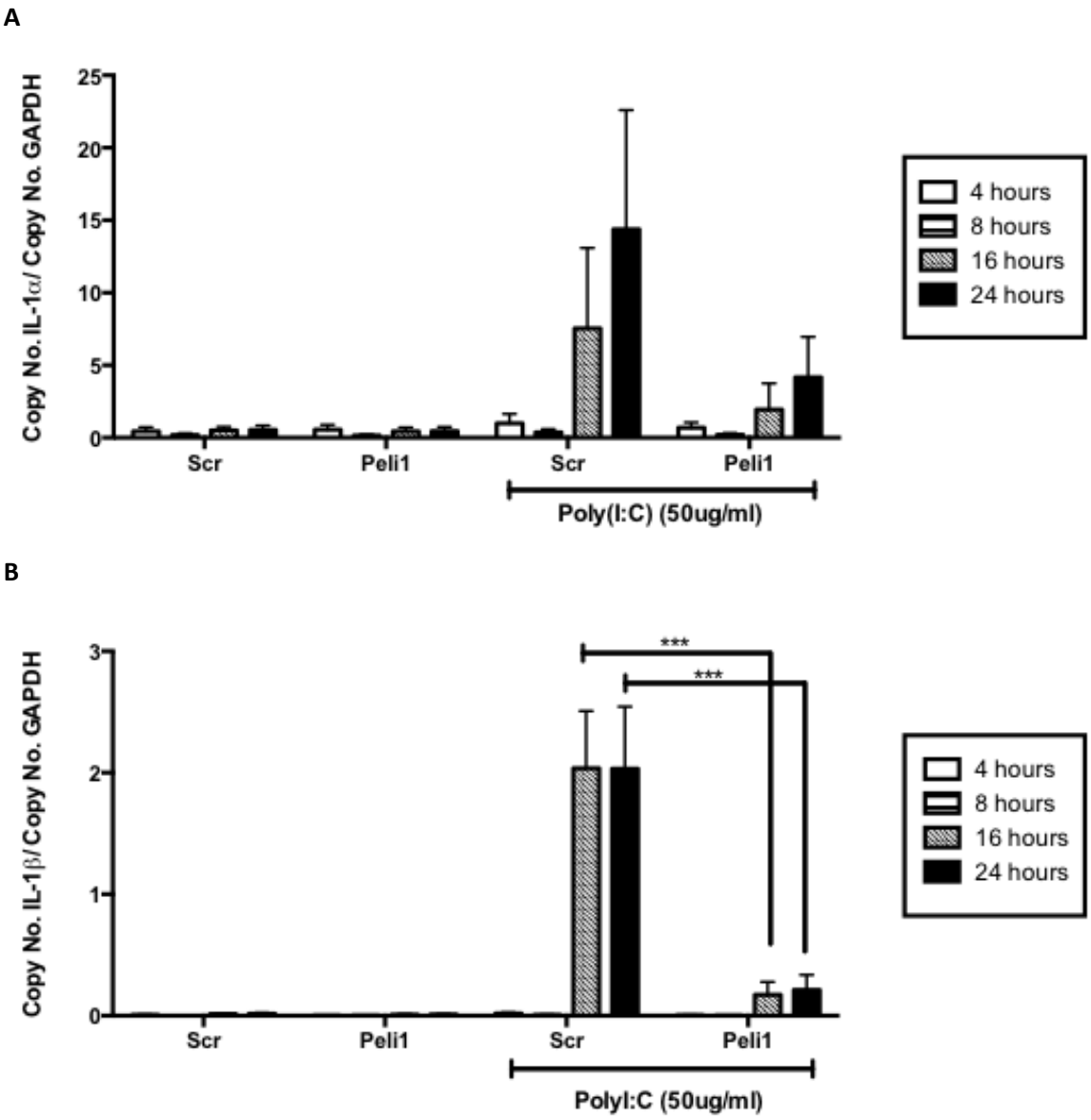

Figure 4.6: Pellino-1 transient knockdown differentially regulates poly(I:C) induced IL-1 expression in primary human bronchial epithelial cells

HBEpCs were transiently transfected with Pellino-1 siRNA and non-targeting scrambled siRNA for 24 hours prior to treatment with poly(I:C) (50 μg/ml) for 4, 8, 16 and 24 hours. RNA was extracted and IL-1α (**A**) and IL-1β (**B**) expression levels were analysed by quantitative RT-PCR. Data are expressed as mean ± SEM of n=4, with each replicate performed on separate donors. Statistical analysis was carried out by two-way ANOVA with Bonferroni's post-test (***p<0.001).

4.5 Pellino-1 transient knockdown reduces poly(I:C) induced IKKα/β but not IκBα phosphorylation in primary human bronchial epithelial cells

The TLR3 signalling pathway culminates in the activation of IRF-3, NF-κB and activating protein-1 (AP-1). Normally, NF-κB resides within the cytoplasm in its inactive form through the association with inhibitors of NF-κB (IκB). However, following TLR3 activation, TRAF6 is recruited and elicits RIP1 activation followed by the degradation of IκBs. IκB degradation is regulated through the activation of the IKK complex consisting of IKKα and IKKβ protein kinases and IKKγ regulatory molecule. This results in the release and translocation of NF-κB into the nucleus for gene transcription (Han et al., 2004; Muzio et al., 2000). Therefore it is possible to establish NF-κB activation by determining the level of both IKK phosphorylation and the resulting IκBα phosphorylation and degradation.

Previous data has shown the ability of transient Pellino-1 knockdown to dampen epithelial cell inflammatory signalling in the form of CXCL8 expression and secretion in response to poly(I:C) (**Figure 4.4**). It was therefore hypothesised that this effect was due to diminishished NF-κB activation via negative regulation of the pathway in the absence of Pellino-1. To assess this, Pellino-1 was transiently transfected with siRNA before undergoing stimulation with poly(I:C) for 4 and 24 hours. The stimulation of HBEpCs with poly(I:C) resulted in a decrease in phosphorylation of IKKα/β (**Figure 4.7**). This decreasing effect appears to be more prominent in the phosphorylation of IKKβ as indicated by the top band seen in the western blot (**Figure 4.7a**). Interestingly, despite the decreased phosphorylation of IKKα/β, the levels of IκBα in Pellino-1 knockdown cells remained unchanged over time (**Figure 4.8**). Due to time constraints and the continued interest in Pellino-1, these experiments were performed jointly with a colleague in our group, Elizabeth Prestwich.

A

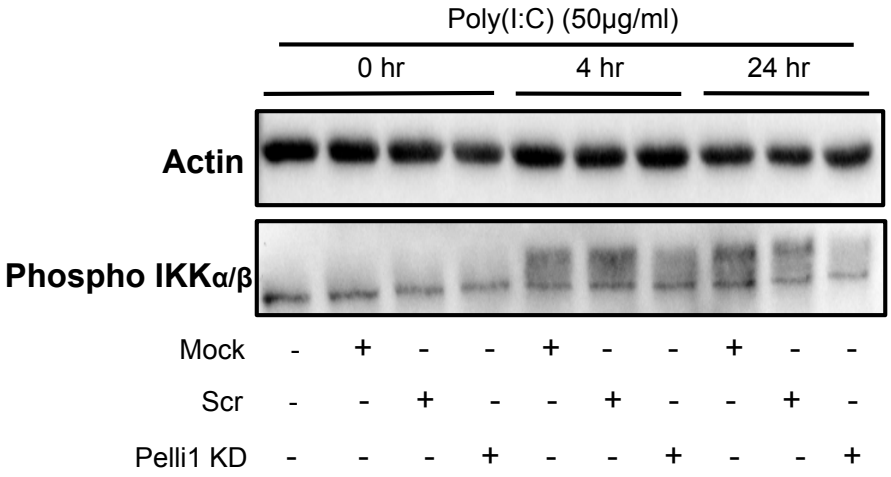

B

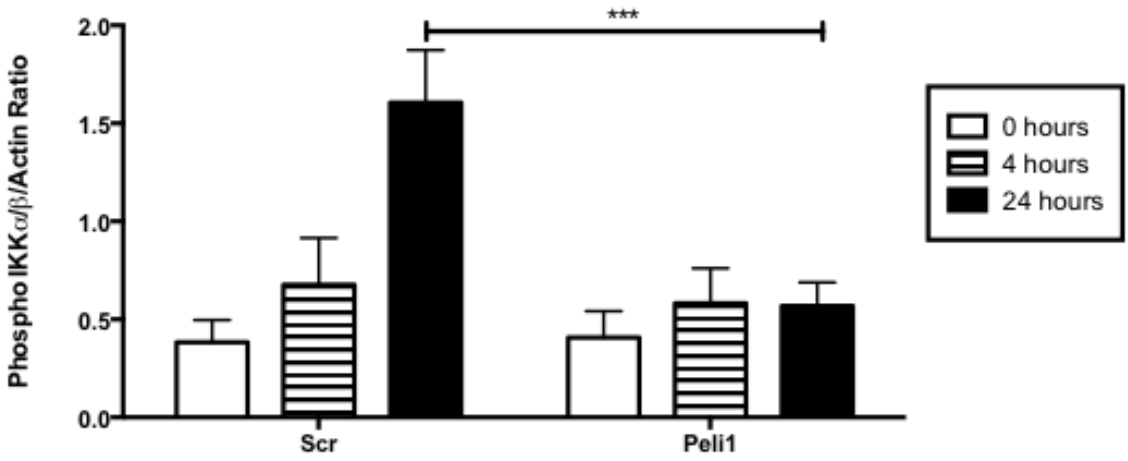

Figure 4.7: Pellino-1 transient knockdown reduces poly(I:C) induced IKKα/β phosphorylation in primary human bronchial epithelial cells

HBEpCs were transiently transfected with Pellino-1 siRNA and non-targeting scrambled siRNA for 24 hours prior to treatment with poly(I:C) (50 µg/ml) for 4 and 24 hour. Cell lysates were analysed for IKKα/β or actin expression by western blot. Representative blot is shown in figure (**A**). Quantitative signals were determined by densitometry and expressed as mean ± SEM of n=9, with replicates performed on 5 separate donors (**B**). Statistical analysis was carried out by two-way ANOVA with Bonferroni's post-test (***p<0.001).

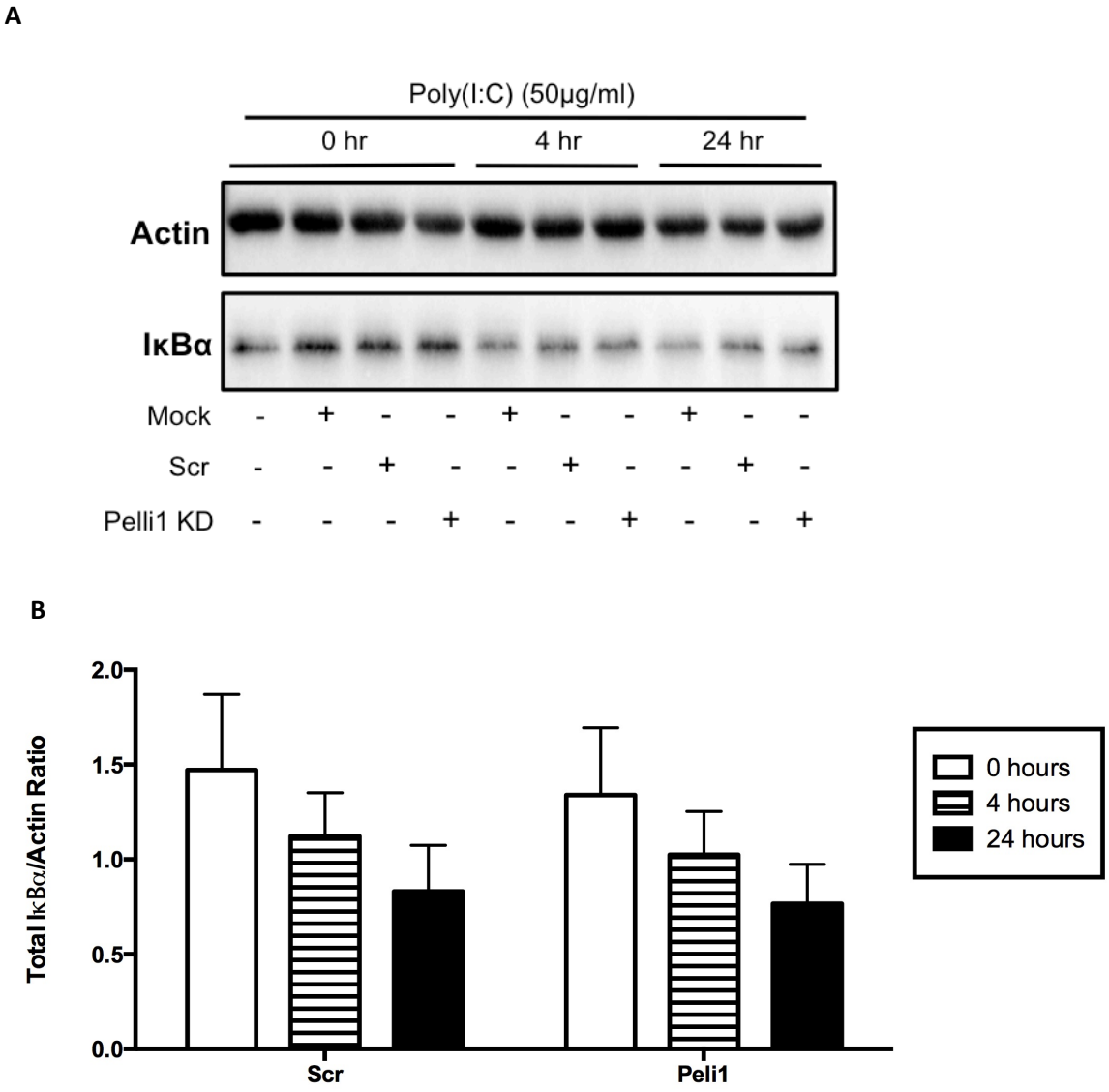

Figure 4.8: Pellino-1 transient knockdown does not alter poly(I:C) induced IκBα degradation in primary human bronchial epithelial cells

HBEpCs were transiently transfected with Pellino-1 siRNA and non-targeting scrambled siRNA for 24 hours prior to treatment with poly(I:C) (50 µg/ml) for 4 and 24 hour. Cell lysates were analysed for IκBα or actin expression by western blot. Representative blot is shown in figure (**A**). Quantitative signals were determined by densitometry and expressed as mean ± SEM of n=8, with each replicate performed on 5 separate donors (**B**). Statistical analysis was carried out by two-way ANOVA with Bonferroni's post-test.

4.6 Pellino-1 transient knockdown reduces poly(I:C) induced p38 MAPK phosphorylation in primary human bronchial epithelial cells

Pro-inflammatory stimuli such as viral dsRNA are capable of inducing CXCL8 gene expression through the activation of a number of protein kinases with the capability to modulate NF-κB or AP-1 activity. Although both of these transcription factors contribute to CXCL8 transcriptional regulation, they do so to varying degrees of importance. NF-κB is essential for CXCL8 induction whilst AP-1 is crucial for maximal gene expression (Hoffmann et al., 2002). Both the activation of NF-κB and AP-1 occurs downstream of TRAF6 and the TAB/TAK1 complex wherein a bifurcation of the signalling pathway occurs. AP-1 is regulated by a three-stage protein kinase cascade that begins with the phosphorylation of MAPKK by MAPKKK resulting in the activation of p38s, ERK and JNK/SAPKs (Karin, 1996).

As Pellino-1 does not appear to elicit its effects through the degradation of IκBα, the rate-limiting step of NF-κB signalling, it was hypothesised that instead Pellino-1 plays a role in the regulation and activation of p38 MAPK as an alternative route to CXCL8 transcription.

Pellino-1 was transiently knocked down with siRNA before undergoing stimulation with poly(I:C) for 4 and 24 hours before protein lysates underwent immunoblotting for phosphorylated p38 MAPK. Stimulation with poly(I:C) for 24 hours resulted in a significant decrease in the phosphorylation of p38 MAPK following transient knockdown of Pellino-1 (**Figure 4.9**).

A

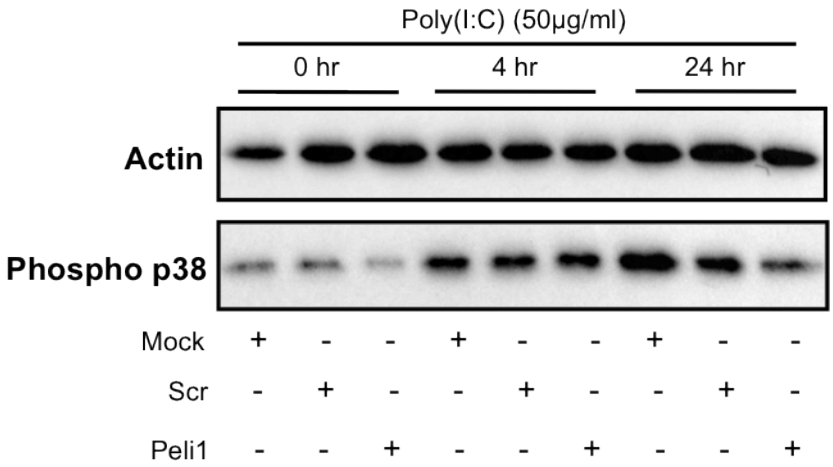

B

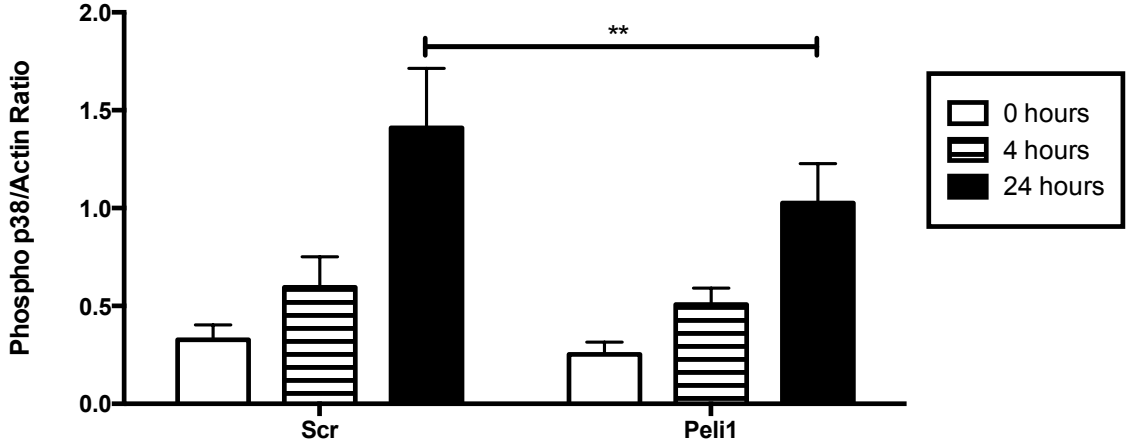

Figure 4.9: Pellino-1 transient knockdown reduces poly(I:C) induced p38 MAPK phosphorylation in primary human bronchial epithelial cells

HBEpCs were transiently transfected with Pellino-1 siRNA and non-targeting scrambled siRNA for 24 hours prior to treatment with poly(I:C) (50 µg/ml) for 4 and 24 hour. Cell lysates were analysed for phosphorylated p38 or actin expression by western blot. Representative blot is shown in figure (**A**). Quantitative signals were determined by densitometry and expressed as mean ± SEM of n=9, with replicates performed on 5 separate donors (**B**). Statistical analysis was carried out by two-way ANOVA with Bonferroni's post-test (**p<0.01).

4.7 Poly(I:C) and CSE stimulation differentially regulate RIP1 expression and cytokine release in primary human bronchial epithelial cells

The TRIF-dependent activation of the transcription factor NF-κB occurs via the recruitment of receptor interacting protein RIP-1 followed by IKK complex activation and IκB degradation (Meylan et al., 2004). Chang *et al.* identified a role for Pellino-1 in regulating IKK activation through interaction and Lys-63 polyubiquitination of RIP-1 in the TRIF-dependent TLR pathway (Chang et al., 2009). Interestingly, Bennett *et al.* challenged these findings through the transient knockdown of RIP1, where instead of mimicking the Pellino-1 knockdown-induced decrease in pro-inflammatory cytokine CXCL8, they instead showed a potentiation of CXCL8 release to poly(I:C) (Bennett et al., 2012). These findings indicated that whilst RIP1 is involved in the regulation of poly(I:C)-activated TLR3 pathway, it does not appear to be regulated by Pellino-1.

In an attempt to determine whether poly(I:C) regulates RIP1 expression, immunoblotting of RIP1 protein was performed and compared with the control housekeeping gene, actin. RIP1 is constitutively expressed in human bronchial epithelial cells (**Figure 4.10**). The stimulation with poly(I:C) (50 μg/ml), CSE (10%) and the combination of both did not regulate RIP1 protein expression (**Figure 4.10**).

The targeted knockdown of Pellino-1 by siRNA transfection resulted in a modest and non-significant decrease (~35%) in RIP1 protein expression in response to a 24 hour stimulation with poly(I:C) (**Figure 4.11**).

The transient knockdown of RIP1 by siRNA transfection in multiple donors stimulated with poly(I:C) for 24 hours resulted in an increasing trend in CXCL8 gene transcripts consistent with Bennett *et al.*'s findings (**Figure 4.12a**). IFNβ mRNA expression levels remained unchanged at 24 hours post stimulation with poly(I:C) (**Figure 4.13a**), whilst CXCL8 (**Figure 4.12b**) and CCL5 (**Figure 4.13b**) release were also unaffected in RIP1 knockdown samples stimulated with poly(I:C), as measured by ELISA. In addition, CSE alone did not induce CXCL8 (**Figure 4.12b**) or CCL5 (**Figure 4.13b**) release from HBEpCs but ablated their induction by poly(I:C).

A

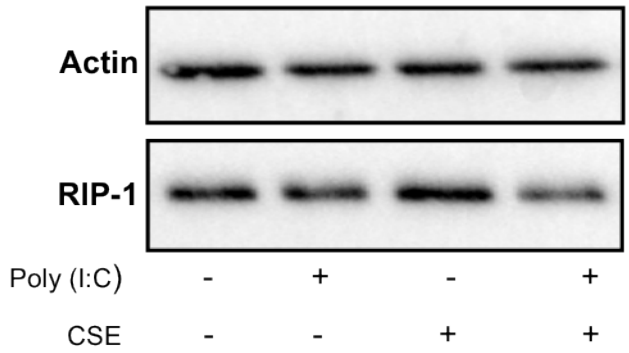

B

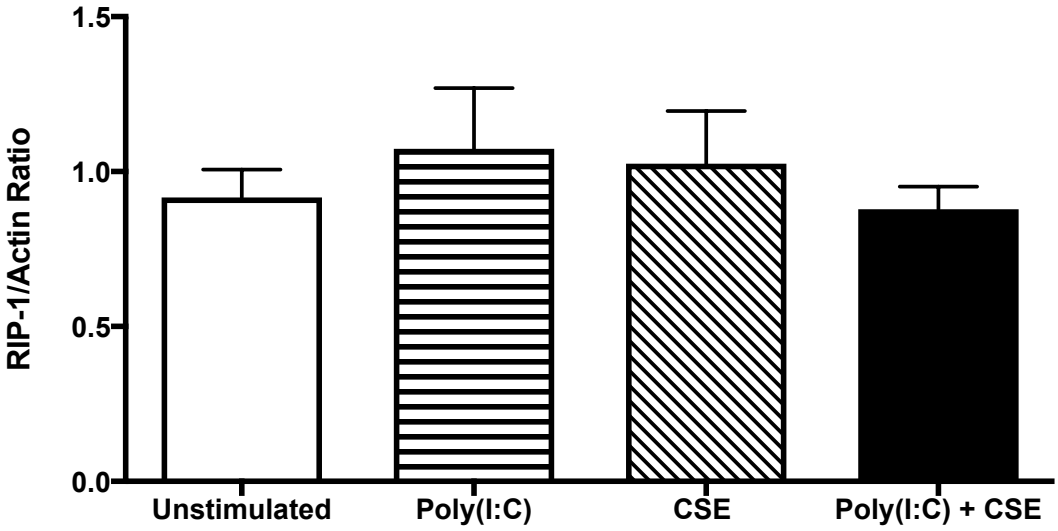

Figure 4.10: Poly(I:C) and CSE stimulation does not alter RIP1 protein expression in primary human bronchial epithelial cells

HBEpCs were stimulated with poly(I:C) (50 μg/ml), CSE (10%) or the combination of both for 24 hours. Cell lysates were analysed for RIP1 or actin expression by western blot. Representative blot is shown in figure (**A**). Quantitative signals were determined by densitometry and expressed as mean ± SEM of n=3, with each replicate performed on separate donors (**B**). Statistical analysis was carried out by one-way ANOVA with Bonferroni's post-test.

A

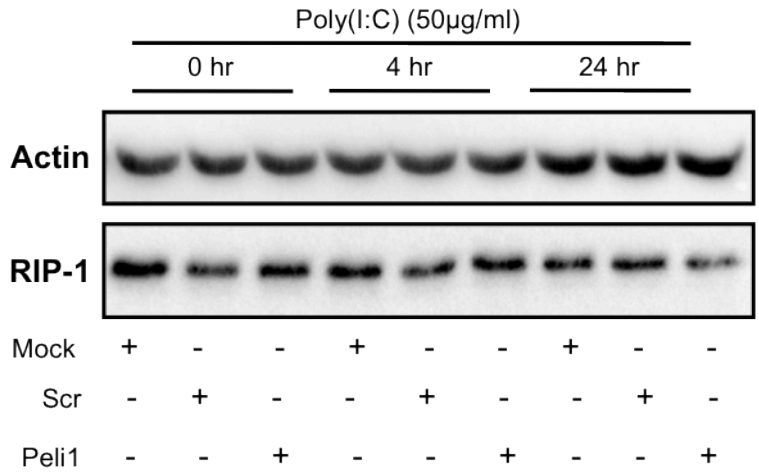

B

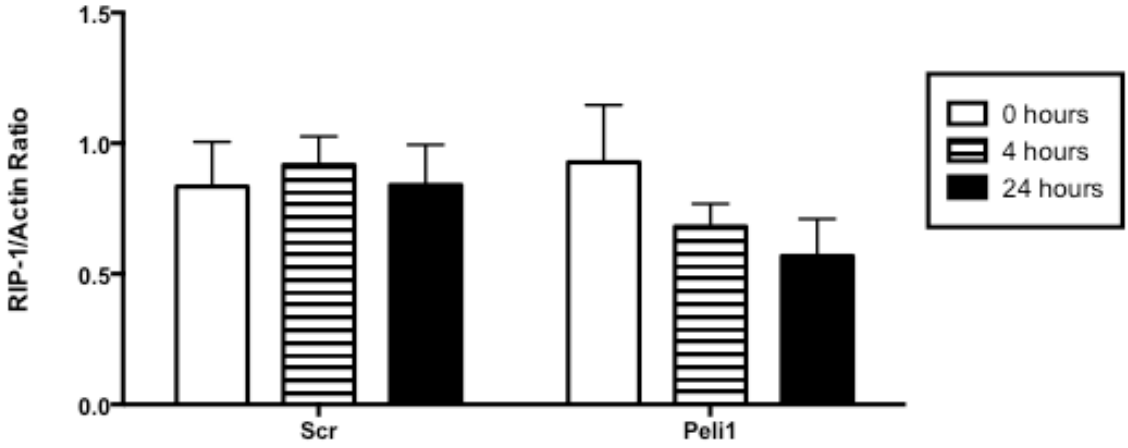

Figure 4.11: Pellino-1 transient knockdown does not regulate RIP1 protein expression in primary human bronchial epithelial cells stimulated with poly(I:C)

HBEpCs were transiently transfected with Pellino-1 siRNA and non-targeting scrambled siRNA for 24 hours prior to treatment with poly(I:C) (50 µg/ml) for 4 and 24 hour. Cell lysates were analysed for RIP1 or actin expression by western blot. Representative blot is shown in figure (**A**). Quantitative signals were determined by densitometry and expressed as mean ± SEM of n=3, with each replicate performed on a separate donors (**B**). Statistical analysis was carried out by two-way ANOVA with Bonferroni's post-test (***p<0.001).

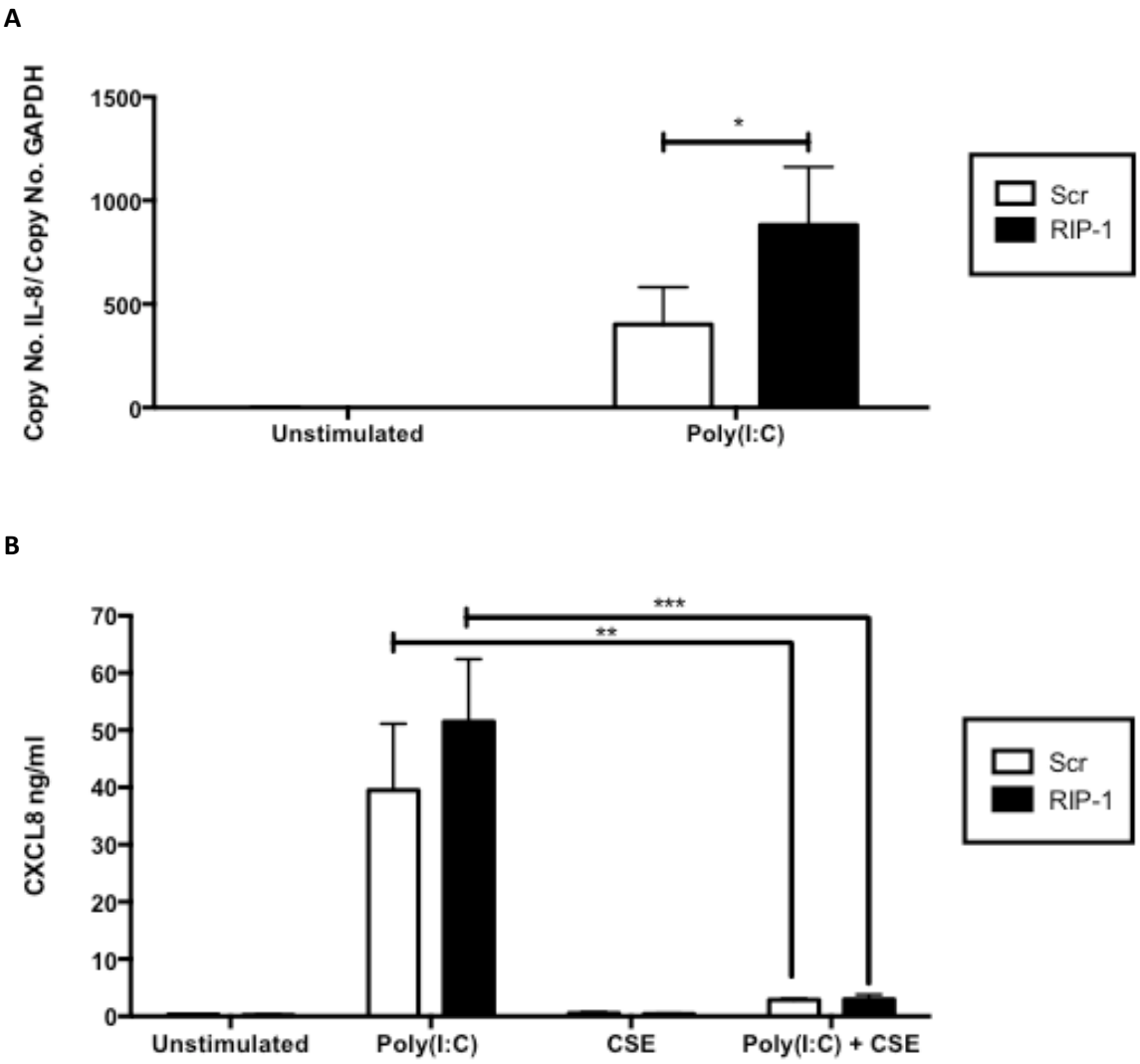

Figure 4.12: RIP1 transient knockdown increases poly(I:C) induced CXCL8 mRNA expression and does not alter CSE induced inhibition of CXCL8 release in primary human bronchial epithelial cells

HBEpCs were transiently transfected with RIP1 siRNA and non-targeting scrambled siRNA for 24 hours prior to treatment with poly(I:C) (50 μg/ml) for 24 hours. RNA was extracted and CXCL8 expression levels were analysed by qPCR (**A**). Supernatants were collected and analysed for CXCL8 release by ELISA (**B**). Data are expressed as mean ± SEM of n=4, with each replicate performed on separate donors. Statistical analysis was carried out by two-way ANOVA with Bonferroni's post-test (*p<0.05, **p<0.01 and ***p<0.001).

A

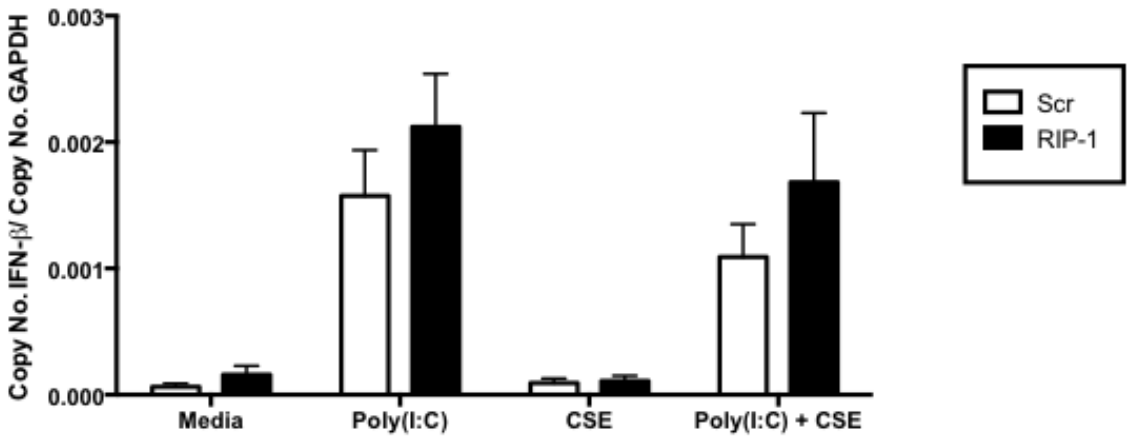

B

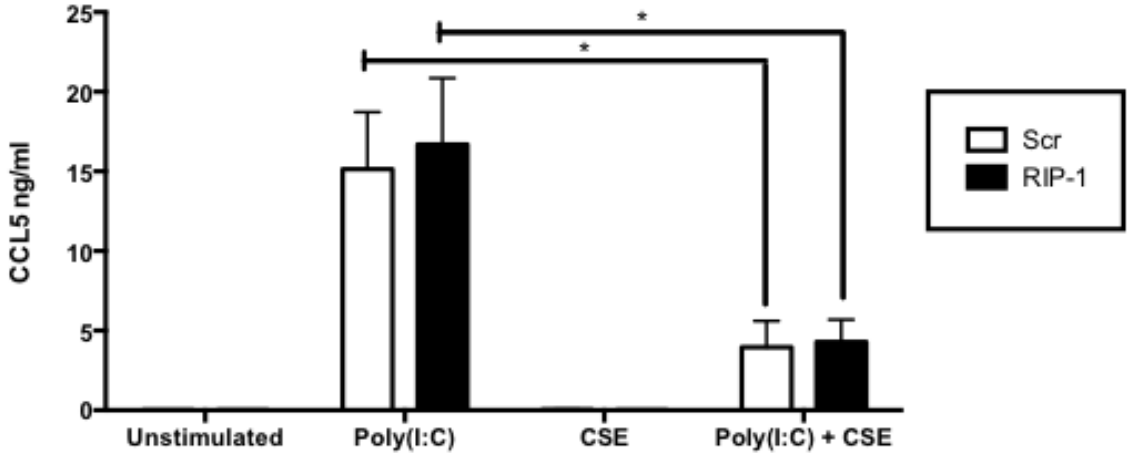

Figure 4.13: RIP1 transient knockdown does not alter CCL5 release in primary human bronchial epithelial cells stimulated with poly(I:C) or CSE

HBEpCs were transiently transfected with RIP1 siRNA and non-targeting scrambled siRNA for 24 hours prior to treatment with poly(I:C) (50 μg/ml) for 24 hours. RNA was extracted and IFNβ expression levels were analysed by qPCR (**A**). Supernatants were collected and analysed for CCL5 release by ELISA (**B**). Data are expressed as mean ± SEM of n=3, with each replicate performed on separate donors. Statistical analysis was carried out by two-way ANOVA with Bonferroni's post-test.

4.8 RIP1 transient knockdown does not alter poly(I:C) and CSE induced Pellino-1 expression in primary human bronchial epithelial cells

Chang et al. identified Pellino-1 as a binding partner and mediator of RIP1 ubiquitination that results in both the recruitment and activation of IKK and subsequent activation of canonical NF-κB signalling (Chang et al., 2009). However, the transient silencing of RIP1 gene expression by siRNA did not recapitulate the phenotype of Pellino-1 knockdown cells, as CXCL8 was significantly increased in RIP1 knockdown and decreased in Pellino-1 knockdown in response to poly(I:C) stimulation (**Figure 4.12** and **Figure 4.4**).

In order to determine the involvement of RIP1 with Pellino-1 and their ability to regulate each other, a transient RIP1 knockdown was performed followed by stimulation with poly(I:C) (50 μg/ml) for 24 hours. The resulting Pellino-1 mRNA expression levels were measured by qPCR. RIP1 knockdown does not alter Pellino-1 expression in response to poly(I:C), CSE nor the combination of both (**Figure 4.14**).

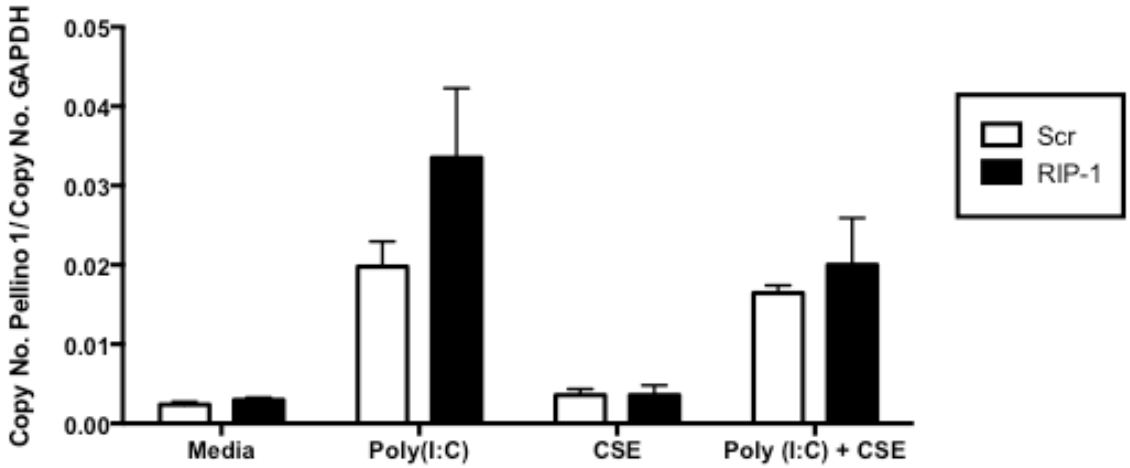

Figure 4.14: RIP1 transient knockdown does not alter poly(I:C) induced Pellino-1 expression in primary human bronchial epithelial cells

HBEpCs were transiently transfected with RIP1 siRNA and non-targeting scrambled siRNA for 24 hours prior to treatment with poly(I:C) (50 µg/ml), CSE (10%) or a combination of both for 24 hours. RNA was extracted and Pellino-1 expression levels were analysed by quantitative RT-PCR. Data are expressed as mean ± SEM of n=3, with each replicate performed on separate donors. Statistical analysis was carried out by two-way ANOVA with Bonferroni's post-test.

4.9 Pellino-1 transient knockdown reduces poly(I:C) induced NFKB1 and NFKB2 protein expression in primary human bronchial epithelial cells

The transcription factor NF-κB consists of five members: RelA (p65), RelB, c-Rel, NFKB1 (p105) and NFKB2 (p100). During the classical activation of NF-κB, also termed canonical-NF-κB, RelA, RelB and c-Rel are sequestered by IκB proteins until IKK-induced degradation of IκB releases them for translocation to the nucleus. However during the alternative activation of NF-κB, also known as non-canonical NF-κB, precursor proteins NFKB1 and NFKB2 are phosphorylated and processed to release their active components p50 and p52 respectively. The freed p50 and p52 active fragments form dimers with other members of the NF-κB family before translocating to the nucleus and initiating gene transcription (Hayden and Ghosh, 2004).

The transient knockdown of Pellino-1 resulted in an anti-inflammatory phenotype in response to poly(I:C) stimulation (**Figure 4.4**) whilst maintaining an intact anti-viral response mediated by IFNβ (**Figure 4.5**). These data suggest that Pellino-1 is eliciting its effects through the NF-κB pathway. However the lack of effective suppression of IκBα degradation by Pellino-1 knockdown (**Figure 4.8**) led to the investigation of possible roles for Pellino-1 on non-canonical NF-κB signalling. Cell lysates of Pellino-1 and scrambled siRNA transfected HBEpCs were collected 4 and 24 hours post-stimulation with poly(I:C) and immunoblotted for NFKB1 and NFKB2 and p52. Pellino-1 knockdown does not alter NFKB1 expression in HBEpC in response to poly(I:C) (**Figure 4.15**). However, NFKB2 protein expression was increased by poly(I:C) stimulation. In turn, Pellino-1 knockdown prevented the poly(I:C) induced expression of NFKB2 (**Figure 4.16**), suggesting a role for Pellino-1 regulation of the non-canonical NF-κB signalling. Due to time constraints and the continued interest in Pellino1, these experiments were performed jointly with a colleague in our group, Elizabeth Prestwich.

A

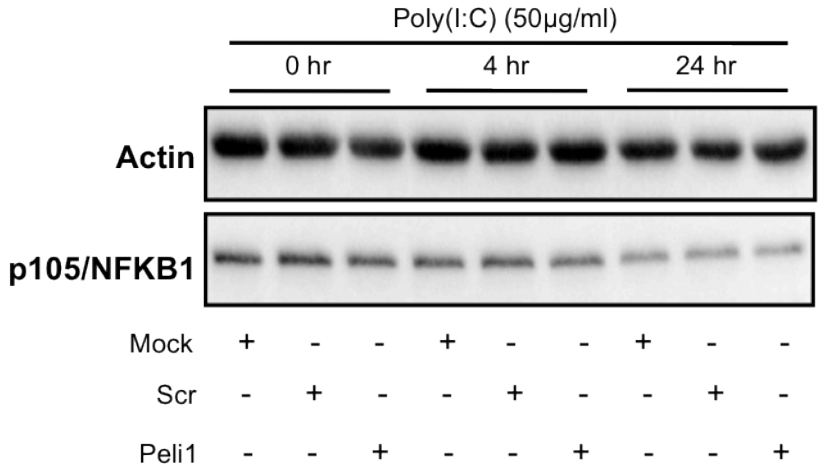

B

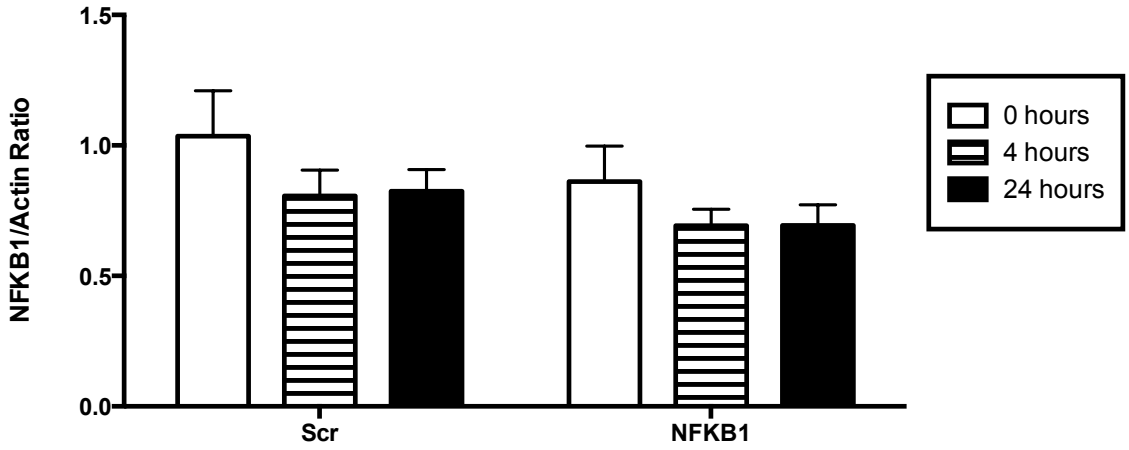

Figure 4.15: Pellino-1 transient knockdown does not regulate NFKB1 protein expression in primary human bronchial epithelial cells stimulated with poly(I:C)

HBEpCs were transiently transfected with Pellino-1 siRNA and non-targeting scrambled siRNA 24 hours prior to treatment with poly(I:C) (50 µg/ml) for 4 and 24 hour. Cell lysates were analysed for NFKB1 or actin expression by western blot. Representative blot is shown in figure (**A**). Quantitative signals were determined by densitometry and expressed as mean ± SEM of n=8, with replicates performed on 5 separate donors (**B**). Statistical analysis was carried out by two-way ANOVA with Bonferroni's post-test.

A

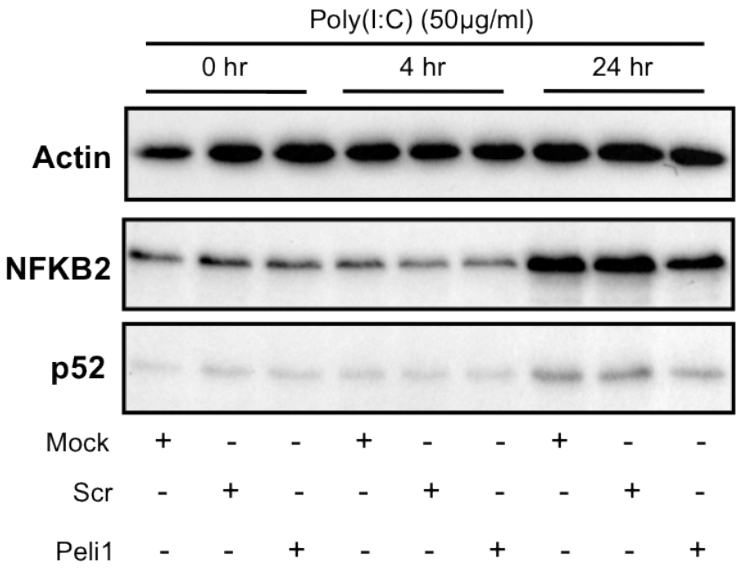

B

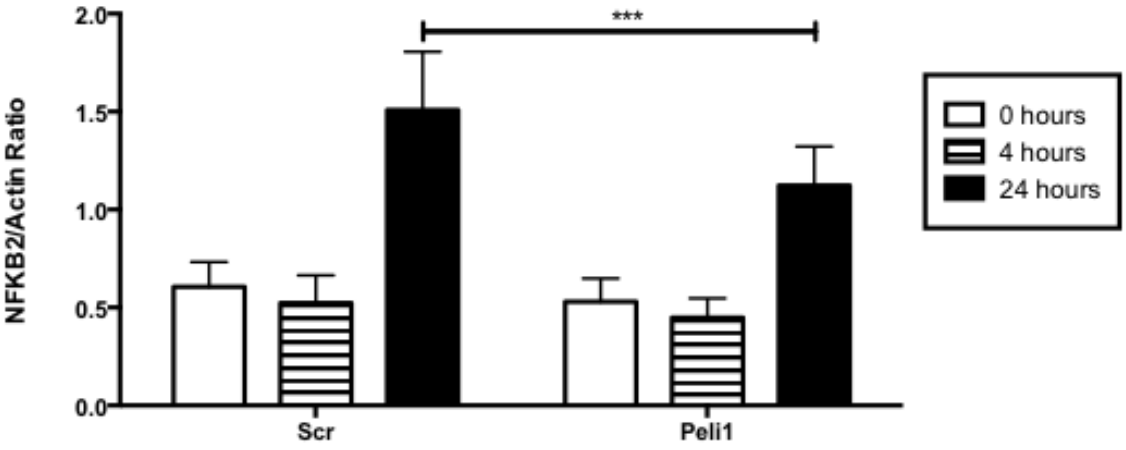

Figure 4.16: Pellino-1 transient knockdown significantly inhibits NFKB2 expression in response to poly(I:C) in primary human bronchial epithelial cells

HBEpCs were transiently transfected with Pellino-1 siRNA and non-targeting scrambled siRNA for 24 hours prior to treatment with poly(I:C) (50 µg/ml) for 4 and 24 hour. Cell lysates were analysed for NFKB2 or actin expression by western blot. Representative blot is shown in figure (**A**). Quantitative signals were determined by densitometry and expressed as mean ± SEM of n=9, with replicates performed on 5 separate donors (**B**). Statistical analysis was carried out by two-way ANOVA with Bonferroni's post-test (***p<0.001).

4.10 NFKB2 transient knockdown increases poly(I:C) induced CXCL8 expression and CCL5 release in primary human bronchial epithelial cells

Previous data showed NFKB2 induction as a result of poly(I:C) stimulation of HBEpCs. Targeted knockdown of Pellino-1 by siRNA in these cells however results in decreased NFKB2 protein expression in response to poly(I:C) (**Figure 4.16**). In addition, the knockdown of Pellino-1 results in a decrease in CXCL8 gene transcription and cytokine release (**Figure 4.4a** and **Figure 4.4b**), whilst IFNβ mRNA expression remains unchanged (**Figure 4.5**). These data combined suggest a specific function for Pellino-1 in non-canonical NF-κB signalling and warrant further investigation.

While the knockdown of Pellino-1 downregulated poly(I:C) induced NFKB2 expression (**Figure 4.16**), the knockdown of NFKB2 in turn did not alter Pellino-1 expression (**Figure 4.17**). Taken in combination these data led to the hypothesis that Pellino-1 may target NFKB2 activation to viral stimuli by acting as a negative regulator; thus the transient knockdown of NFKB2 should recapitulate the phenotype of Pellino-1 knockdown. NFKB2 transcripts were significantly knocked down following a transient transfection with NFKB2 siRNA for 24 hours prior to poly(I:C) stimulation for a further 24 hours to determine efficiency of knockdown (**Figure 4.18**). NFKB2 expression was then transiently inhibited by siRNA transfection prior to stimulation with poly(I:C) (50 μg/ml) for 24 hours to determine the hypothesis. Interestingly, the resulting CXCL8 mRNA expression was significantly increased in the NFKB2 knockdown when compared to the scrambled control in response to poly(I:C) (**Figure 4.19**). Furthermore, the poly(I:C)-induced CCL5 cytokine release was significantly increased in the NFKB2 knockdown HBEpCs (**Figure 4.20**).

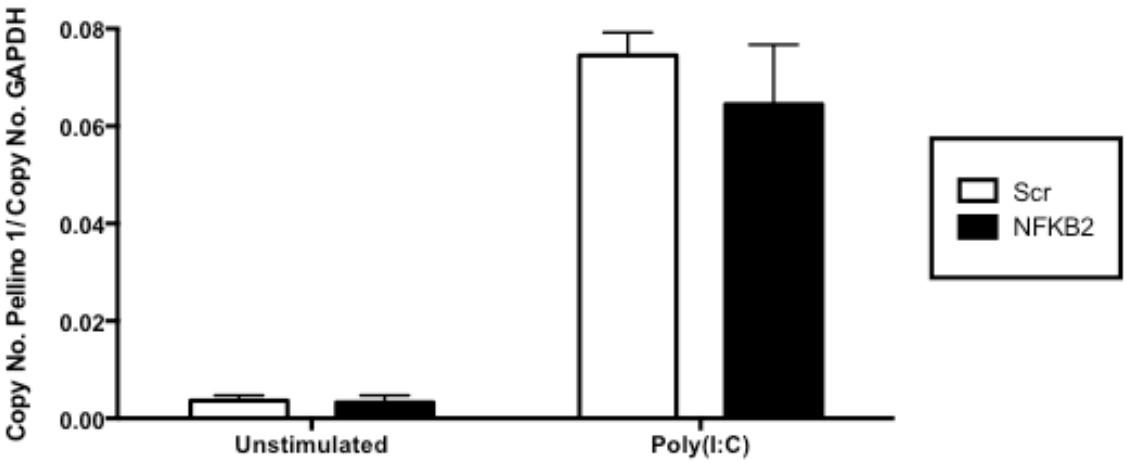

Figure 4.17: NFKB2 transient knockdown does not regulate poly(I:C) induced Pellino-1 expression

HBEpCs were transiently transfected with NFKB2 siRNA and non-targeting scrambled siRNA for 24 hours prior to treatment with poly(I:C) (50 μg/ml) for 24 hours. RNA was extracted and Pellino-1 expression levels were analysed by quantitative RT-PCR. Data are expressed as mean ± SEM of n=3, with each replicate performed on separate donors. Statistical analysis was carried out by two-way ANOVA with Bonferroni's post-test.

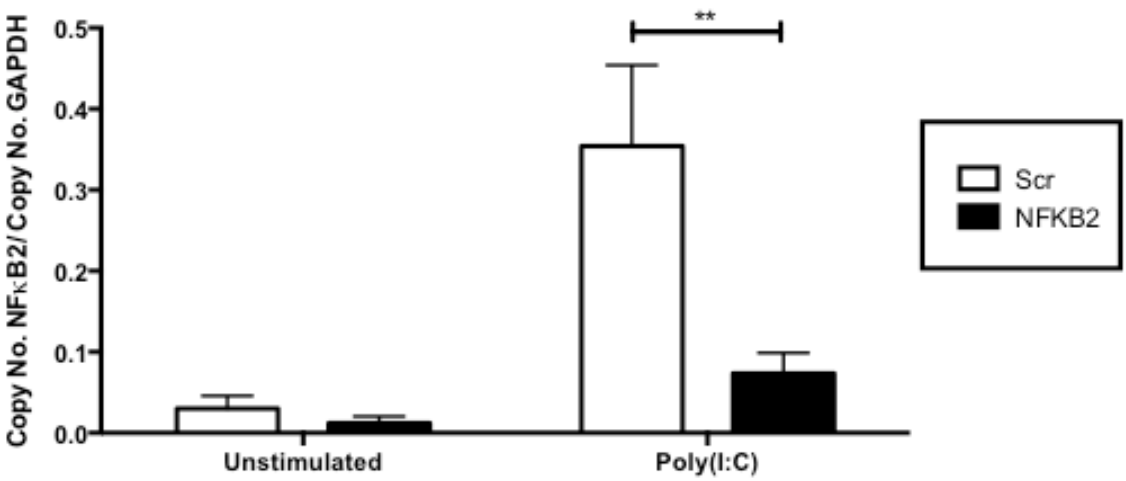

Figure 4.18: NFKB2 transient knockdown inhibits poly(I:C) induced NFKB2 mRNA expression in primary human bronchial epithelial cells

HBEpCs were transiently transfected with NFKB2 siRNA and non-targeting scrambled siRNA for 24 hours prior to treatment with poly(I:C) (50 μg/ml) for 24 hours. RNA was extracted and NFKB2 expression levels were analysed by quantitative RT-PCR. Data are expressed as mean ± SEM of n=3, with each replicate performed on separate donors. Statistical analysis was carried out by two-way ANOVA with Bonferroni's post-test (**p<0.01).

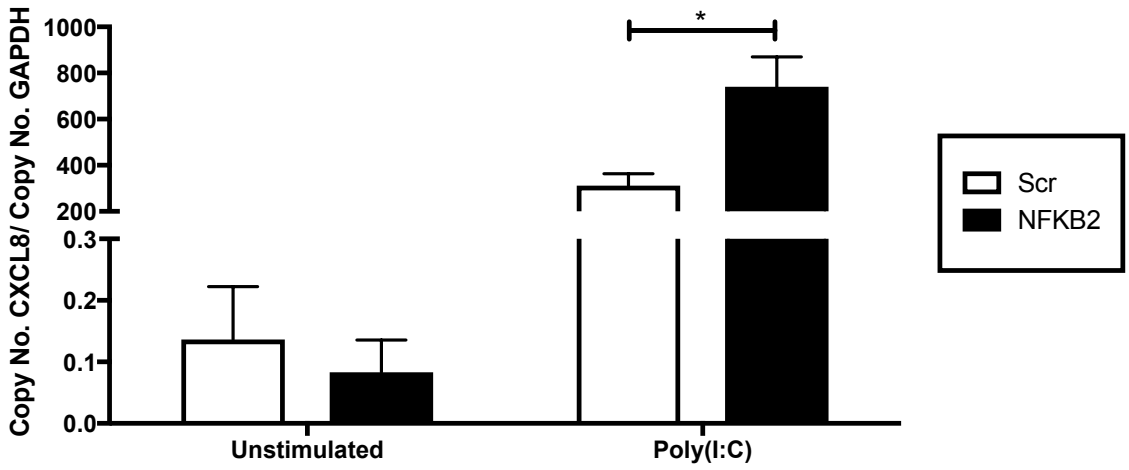

Figure 4.19: NFKB2 transient knockdown increases poly(I:C) induced CXCL8 mRNA expression in primary human bronchial epithelial cells

HBEpCs were transiently transfected with NFKB2 siRNA and non-targeting scrambled siRNA followed by treatment with poly(I:C) (50 µg/ml) for 24 hours. RNA was extracted and CXCL8 expression levels were analysed by quantitative RT-PCR. Statistical analysis was carried out by two-way ANOVA with Bonferroni's post-test (*$p<0.05$).

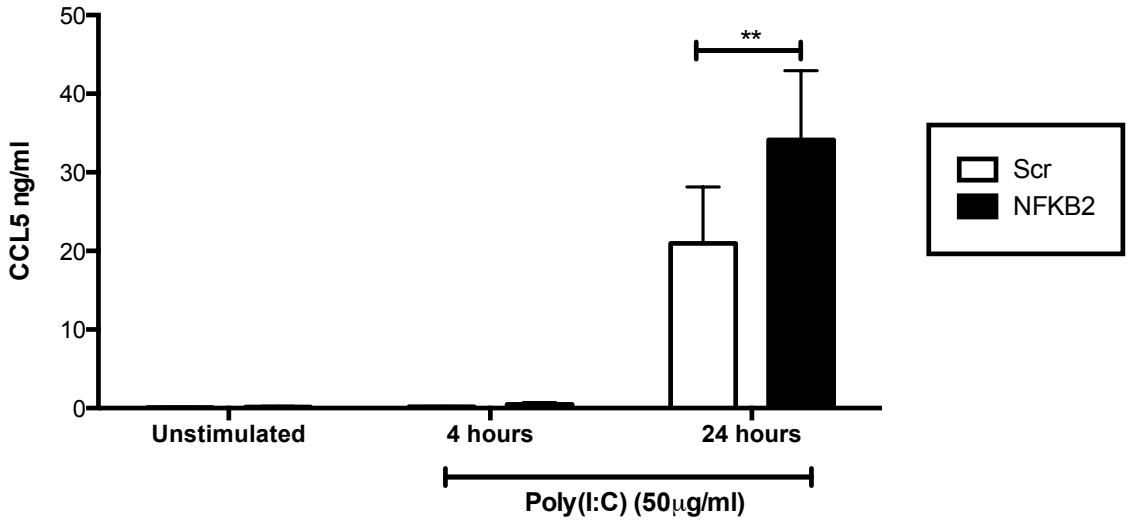

Figure 4.20: NFKB2 transient knockdown increases poly(I:C) induced CCL5 release in primary human bronchial epithelial cells

HBEpCs were transiently transfected with NFKB2 siRNA and non-targeting scrambled siRNA for 24 hours prior to treatment with poly(I:C) (50 μg/ml) for 24 hours. Supernatants were collected and analysed for CCL5 release by ELISA. Data are expressed as mean ± SEM of n=4, with each replicate performed on separate donors. Statistical analysis was carried out by two-way ANOVA with Bonferroni's post-test (**p<0.01).

4.11 Rhinoviral infection increases Pellino-1 mRNA expression in primary human bronchial epithelial cells from COPD patient airways

Chronic obstructive pulmonary disease (COPD) is a complex airway inflammatory disease with poor prognosis and inadequate reversibility. By 2020, COPD is predicted to be the world's third leading cause of death and fifth cause of disability (Lopez and Murray, 1998). Acute exacerbations are a hallmark of COPD and are often associated with exposure to respiratory viruses such as the commonly detected rhinovirus (Mallia et al., 2006).

In order to determine the viability of Pellino-1 as a potential therapeutic drug target for COPD it is essential to investigate the regulation of Pellino-1 and its role in viral infection in human bronchial airway epithelial cells in patients suffering from COPD. Previous data supports a role for Pellino-1 in the TLR3 signalling pathway in primary airway epithelial cells, as Pellino-1 knockdown resulted in a significant reduction in CXCL8 production in response to poly(I:C). However to determine whether the role of Pellino-1 is altered in COPD patient airways, Pellino-1 expression was quantified in epithelial cells isolated from COPD patients then infected with the natural human viral pathogen, rhinovirus.

Irene H Heijink from the University Medical Centre in Groningen supplied the primary airway epithelial cells isolated from brushings of COPD patient airways. Dr. Heijink and her group cultured the harvested airway epithelial cells *in vitro* and infected them with rhinovirus-16 (RV-16) and rhinovirus-1B (RV-1B), supplied by the Ian Sabroe group at the University of Sheffield, at an approximate MOI of 3 for 24 and 48 hours before RNA extraction. The resulting cDNA was then analysed and quantified by qPCR at the University of Sheffield by the group and I. Pellino-1 mRNA transcripts in COPD epithelial cells marginally increase at 24 hours post-infection with RV-16. However, at 48 hours, Pellino-1 is significantly increased in response to RV-16 when compared to baseline (**Figure 4.21a**). Similarly, Pellino-1 appears to be regulated by RV-1B at 48 hours post-infection (**Figure 4.21b**).

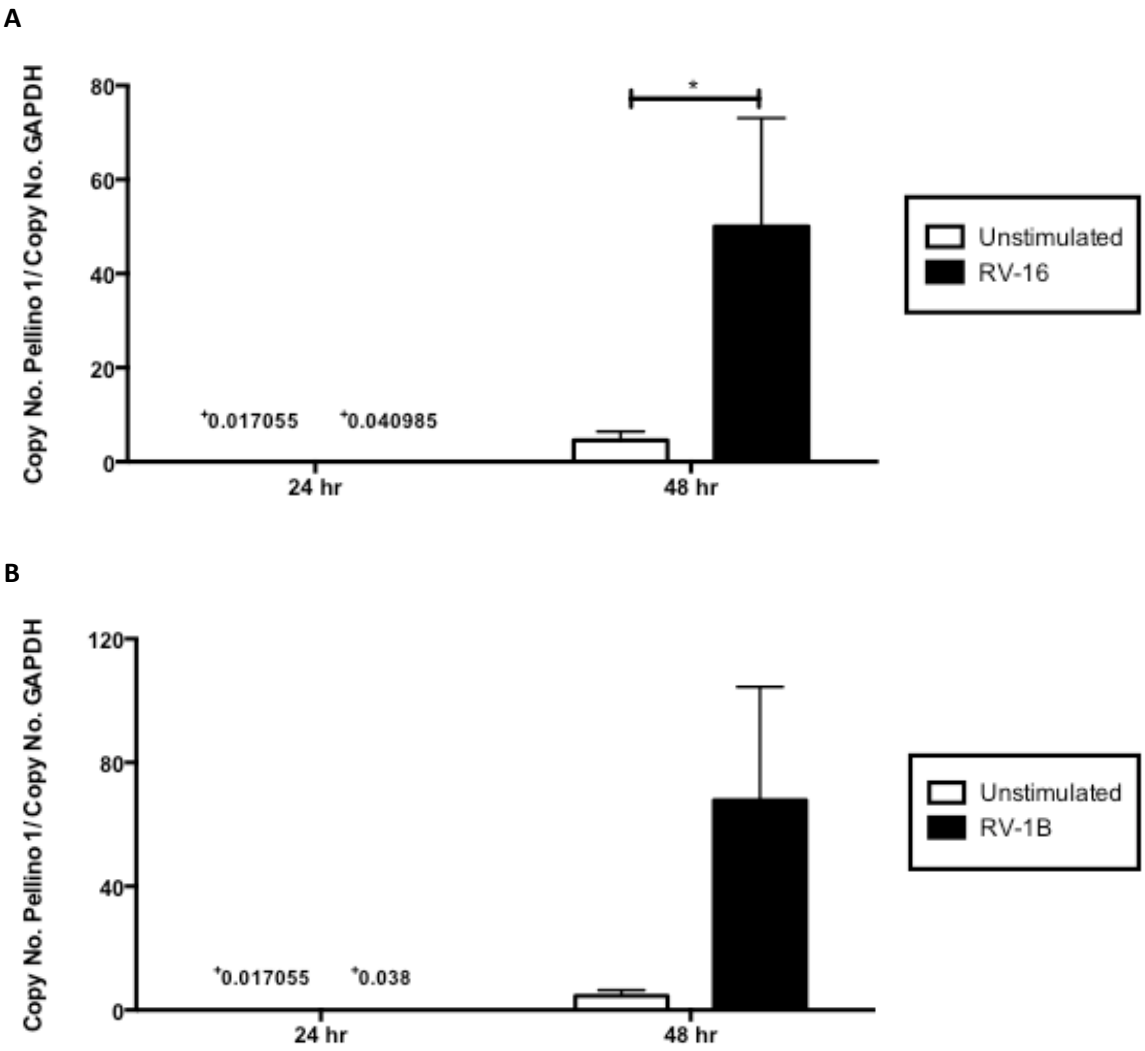

Figure 4.21: Rhinoviral infection increases Pellino-1 mRNA expression in primary human bronchial epithelial cells from COPD patient airways

HBEpC isolated from COPD patient airways were stimulated with RV-16 (**A**) and RV-1B (**B**) for 24 and 48 hours. Pellino-1 mRNA expression was determined by quantitative RT-PCR (qPCR). Pellino-1 expression was normalized to GAPDH copy numbers (loading control) and expressed as mean ± SEM of n=4, with each replicate performed on separate donors. Statistical analysis was carried out by one-way ANOVA with Bonferroni's post-test (*$p<0.05$).

4.12 Rhinoviral infection increases NFKB2 mRNA expression in primary human bronchial epithelial cells from COPD patient airways

Previous data show a role for Pellino-1 in regulating NFKB2 expression in response to viral stimulation wherein transient Pellino-1 knockdown decreases NFKB2 protein expression (**Figure 4.16**). In epithelial cells obtained from COPD patient airways, Pellino-1 expression was significantly increased in response to viral stimulation (**Figure 4.21**). It was therefore hypothesised that NFKB2 expression is regulated by Pellino-1, and is in turn increased in COPD patient airways.

As described in **Section 4.11**, Irene H Heijink from the University Medical Centre in Groningen supplied the primary airway epithelial cells isolated from brushings of COPD patient airways. Dr. Heijink and her group cultured the harvested airway epithelial cells *in vitro* and infected them with rhinovirus-16 (RV-16) and rhinovirus-1B (RV-1B), supplied by the Ian Sabroe group at the University of Sheffield, at an approximate MOI of 3 for 24 and 48 hours before RNA extraction. The resulting cDNA was then analysed and quantified by qPCR at the University of Sheffield by the group and I. The resulting NFKB2 mRNA transcripts were quantified by qPCR. In accordance with Pellino-1 expression (**Figure 4.21a**), NFKB2 expression was unchanged at 24 hours but significantly increased in COPD epithelial cells at 48 hours post-infection with RV-16 (**Figure 4.22a**). Infection of COPD epithelial cells with RV-1B also resulted in a significant induction of NFKB2 gene expression at 48 hours (**Figure 4.22b**).

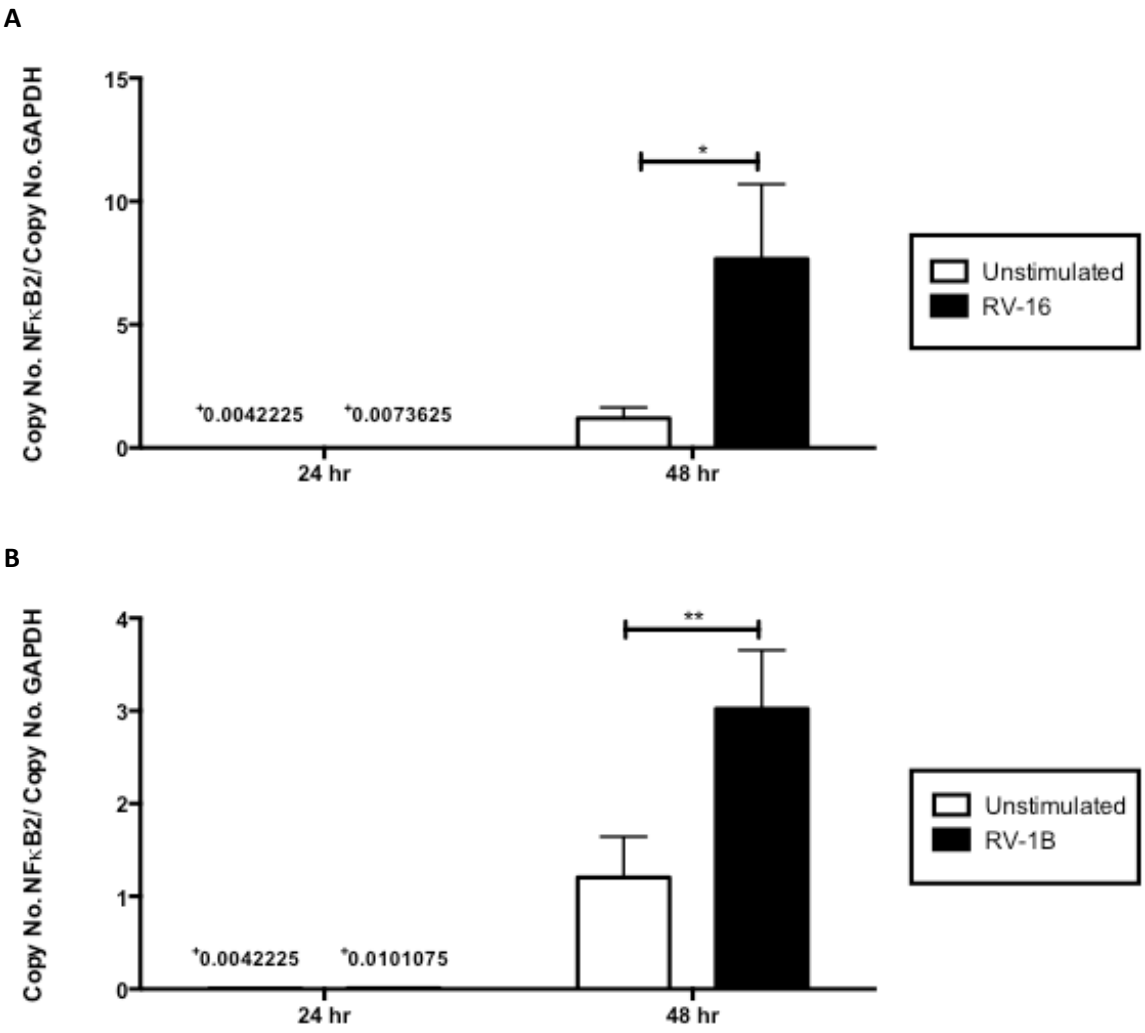

Figure 4.22: Rhinoviral infection increases NFKB2 mRNA expression in primary human bronchial epithelial cells from COPD patient airways

HBEpC isolated from COPD patient airways were stimulated with RV-16 (**A**) and RV-1B (**B**) for 24 and 48 hours. NFKB2 mRNA expression was determined by quantitative RT-PCR (qPCR). Pellino-1 expression was normalized to GAPDH copy numbers (loading control) and expressed as mean ± SEM of n=4, with each replicate performed on separate donors. Statistical analysis was carried out by one-way ANOVA with Bonferroni's post-test (*p<0.05, **p<0.01).

4.13 MEK1 inhibitors regulate Pellino-1 expression in response to poly(I:C) stimulation in primary human bronchial epithelial cells

dsRNA recognition by TLR3 results in the initiation of inflammatory signalling culminating in the activation of NF-κB, IRF-3 and AP-1. Whilst NF-κB activation is regulated by IκB degradation through IKK complex, AP-1 activation is mediated by MAP kinases such as JNK, ERK and p38 (Kawai and Akira, 2007). Preliminary data suggested a role for Pellino-1 in the regulation of AP-1 through p38 MAPK wherein transient knockdown of Pellino-1 decreased phospho p38 activity (**Figure 4.9**).

A pilot experiment aimed to assess the impact of the inhibition of the MAPKs JNK, ERK and p38 on Pellino-1 expression. JNK, ERK and p38 activity was suppressed by their respective inhibitors: SP600125, PD98059 and SB203580. Pellino-1 mRNA expression was then quantified using qPCR. While JNK and p38 inhibition did not alter Pellino-1 expression, the MEK1 inhibitor, PD98059 resulted in a decrease in Pellino-1 expression (**Figure 4.23**). These initial results led to the hypothesis that ERK signalling may regulate Pellino-1 expression.

HBEpCs were pre-incubated with MEK1 inhibitors PD98059 and U0126 respectively for 1 hour prior to stimulation with poly(I:C) for 24 hours. PD98059 and U0126 effectively inhibited the phoshporylation of p44/p42 or ERK1/2 as demonstrated by western blotting (**Figure 4.24a**). Both inhibitors, PD98059 and U0126, also effectively reduced poly(I:C) induced Pellino-1 protein expression (**Figure 4.24b**). In keeping with changes to protein expression, poly(I:C) induced Pellino-1 mRNA expression was also significantly inhibited by both PD98059 and U0126 suggesting a role in the regulation of Pellino-1 by ERK (**Figure 4.25**).

Pellino-1 expression was transiently inhibited by siRNA transfection followed by a stimulation with poly(I:C) for 4 and 24 hours. ERK1/2 protein activity was measured by western blot and showed high levels at baseline at 0 hours (unstimulated samples) across mock, scrambled and Pellino-1 knockdown samples (**Figure 4.26a and Figure 4.26b**). A slight decrease in ERK1/2 levels compared with baseline can be detected at 4 hours post-stimulation with poly(I:C). At 24 hours post-stimulation, both scrambled control and Pellino-1 knockdown show modestly increased levels of ERK1/2 when compared with baseline (**Figure 4.26b**).

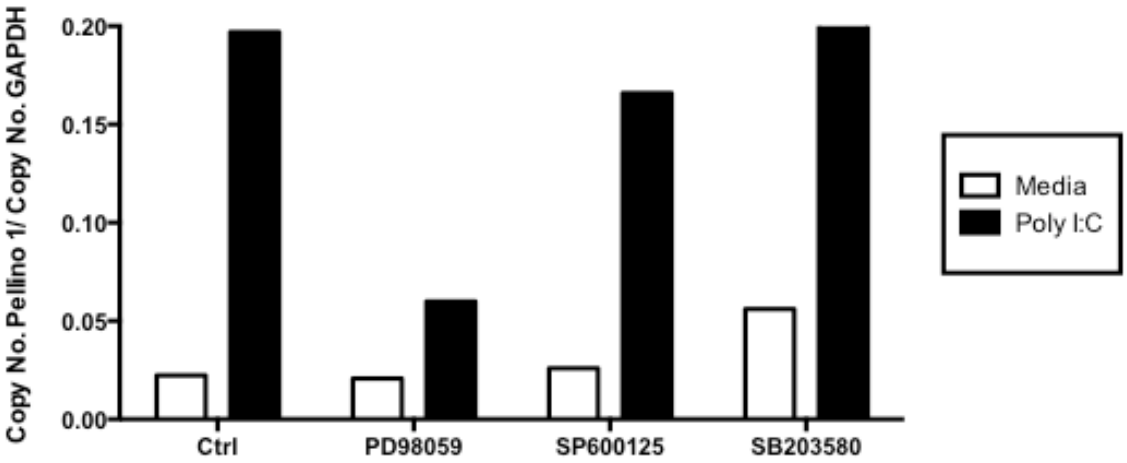

Figure 4.23: MAPK inhibitors alter Pellino-1 protein expression in response to poly(I:C) stimulation in primary human bronchial epithelial cells

HBEpCs were pre-treated with PD98059 (20µM), SP600125 (20µM) and SB203580 (20µM) for 1 hour followed by treatment with poly(I:C) (50 µg/ml) for 24 hours. Quantitative signals for Pellino-1 expression were determined by densitometry from a single experiment.

A

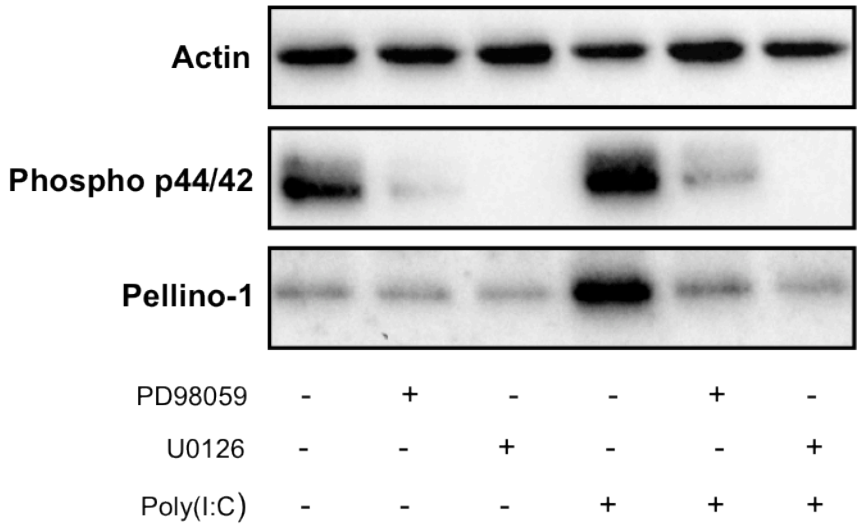

B

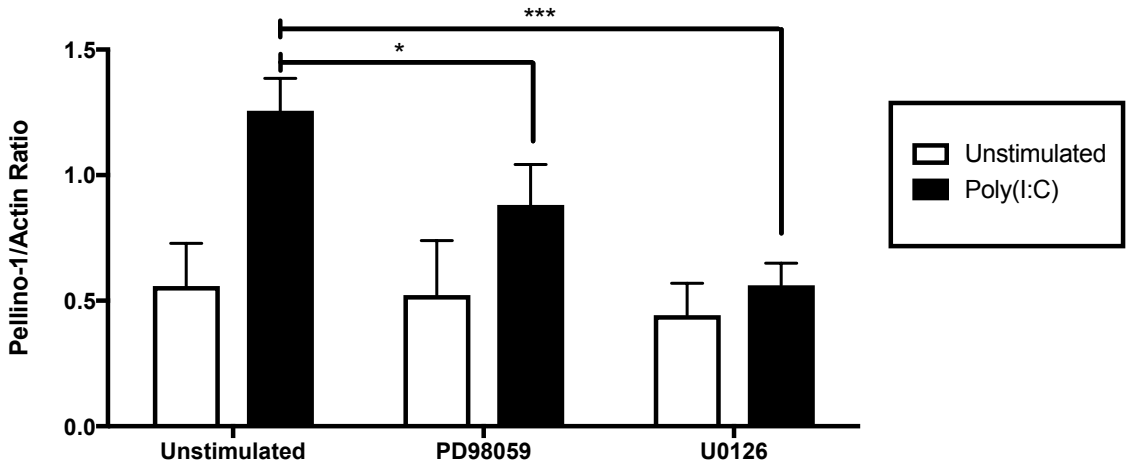

Figure 4.24: MEK1 inhibitors reduce Pellino-1 protein expression in response to poly(I:C) stimulation in primary human bronchial epithelial cells

HBEpCs were pre-treated with PD98059 (20 µM) and U0126 (10 µM) for 1 hour followed by treatment with poly(I:C) (50 µg/ml) for 24 hours. Cell lysates were analysed for phospho p44/p42, Pellino-1 or actin expression by western blot. Representative blot is shown in figure (**A**). Quantitative signals for Pellino-1 expression were determined by densitometry and expressed as mean ± SEM of n=3, with replicates performed on separate donors (**B**). Statistical analysis was carried out by two-way ANOVA with Bonferroni's post-test (*p<0.05, **p<0.01).

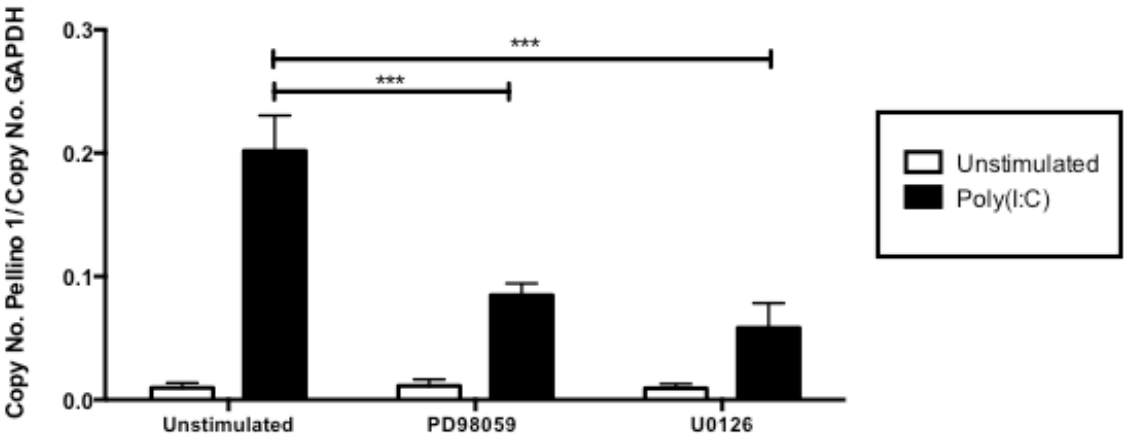

Figure 4.25: MEK1 inhibitors reduce Pellino-1 mRNA expression in response to poly(I:C) stimulation in primary human bronchial epithelial cells

HBEpCs were pre-treated with (20 μM) and U0126 (10 μM) for 1 hour followed by treatment with poly(I:C) (50 μg/ml) for 24 hours. Pellino-1 mRNA expression was determined by quantitative RT-PCR (qPCR). Pellino-1 expression was normalized to GAPDH copy numbers (loading control) and expressed as mean ± SEM of n=4, with each replicate performed on separate donors. Statistical analysis was carried out by two-way ANOVA with Bonferroni's post-test (***p<0.001).

A

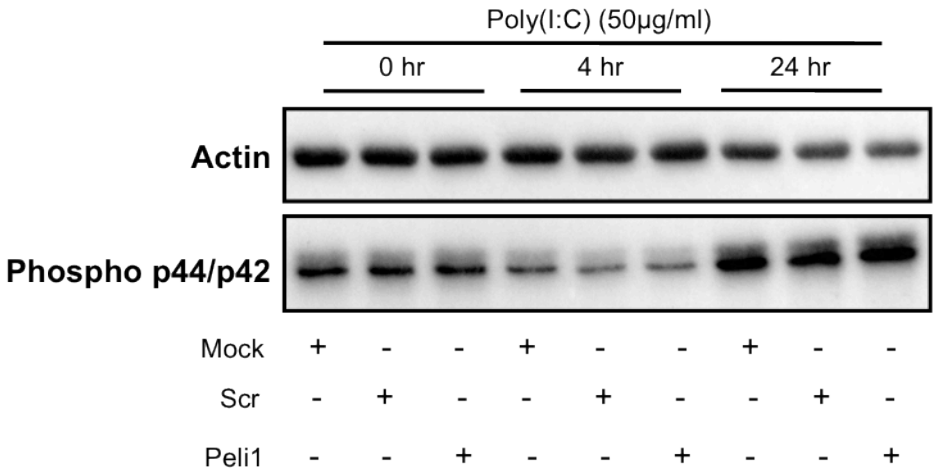

B

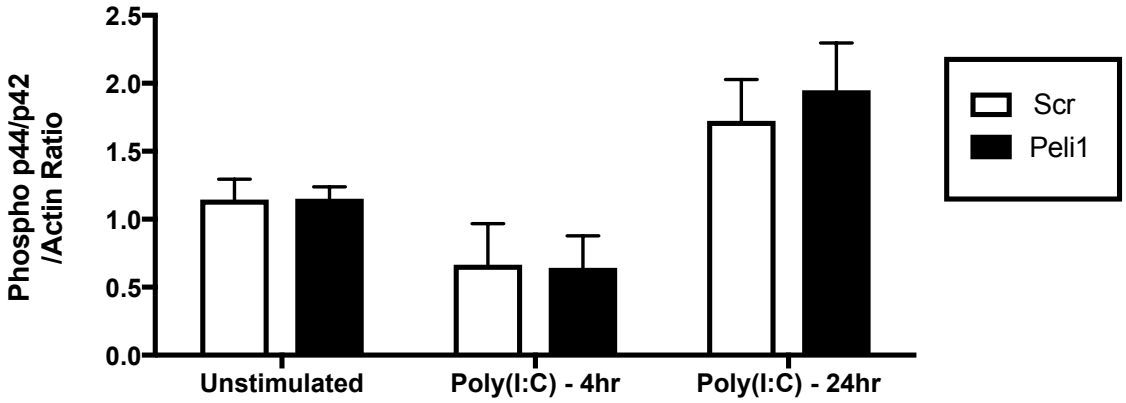

Figure 4.26: Pellino-1 transient knockdown does not regulate poly(I:C) induced p44/p42 phosphorylation in primary human bronchial epithelial cells

HBEpCs were transiently transfected with Pellino-1 siRNA and non-targeting scrambled siRNA followed by treatment with poly(I:C) (50 µg/ml) for 4 and 24 hours. Cell lysates were analysed for phospho p44/p42 or actin expression by western blot. Representative blot is shown in figure (**A**). Quantitative signals were determined by densitometry and expressed as mean ± SEM of n=3, with replicates performed on separate donors (**B**). Statistical analysis was carried out by two-way ANOVA with Bonferroni's post-test (*$p<0.05$).

4.14 IRF-3 transient knockdown decreases Pellino-1 mRNA expression in response to poly(I:C) in primary human bronchial epithelial cells

The pattern recognition receptor TLR3 recognises dsRNA from replicating viruses and triggers signalling pathways resulting in the production of pro-inflammatory cytokines, chemokines and type I IFNs. The production of type I IFNs is dependent on the activation of IKKε/TBK1 complex and the resulting activation of IRF3. Indeed, TBK1/IKKε complex have been identified as mediators of Pellino-1's E3 ligase activity in addition to the induction of the transcription of its gene in a TLR3 dependent manner (Smith et al., 2011).

Previous data indicates that Pellino-1 selectively regulates NF-κB signalling while retaining antiviral immunity in the form of IFN signalling. IFNβ mRNA expression was unaffected by poly(I:C) stimulation following transient Pellino-1 knockdown (**Figure 4.5**). However, data generated through the creation of a Pellino-1 knock-in mouse with a point mutation inhibiting its E3 ligase activity identified a role for Pellino-1 in IFNβ signalling through the interaction with IRF3 (Enesa et al., 2012). While the observations from previous data do not indicate Pellino-1 is essential for IFN signalling, it was hypothesised that Pellino-1 activation may be partially regulated by IRF3 activation.

IRF3 transcripts were significantly knocked down following a transient transfection with IRF3 siRNA for 24 hours prior to poly(I:C) stimulation for a further 24 hours to determine efficiency of knockdown (**Figure 4.27a**). Similarly IFNβ (**Figure 4.27b**) showed a decreasing trend of expression following IRF3 knockdown. IRF3 expression was then inhibited by siRNA transfection prior to stimulation with poly(I:C) (50 μg/ml) for 24 hours to investigate whether IRF-3 regulates Pellino-1 expression. The resulting upregulation of Pellino-1 mRNA expression was inhibited in the IRF3 knockdown HBEpCs when compared to the scrambled control in response to poly(I:C) (**Figure 4.27c**). In addition, while the stimulation with CSE alone did not induce Pellino-1 expression in both IRF3 knockdown HBEpCs and scrambled control HBEpCs, the combination of CSE and poly(I:C) resulted in a decrease in Pellino-1 expression which was further decreased in the IRF3 knockdown cells (**Figure 4.27c**)

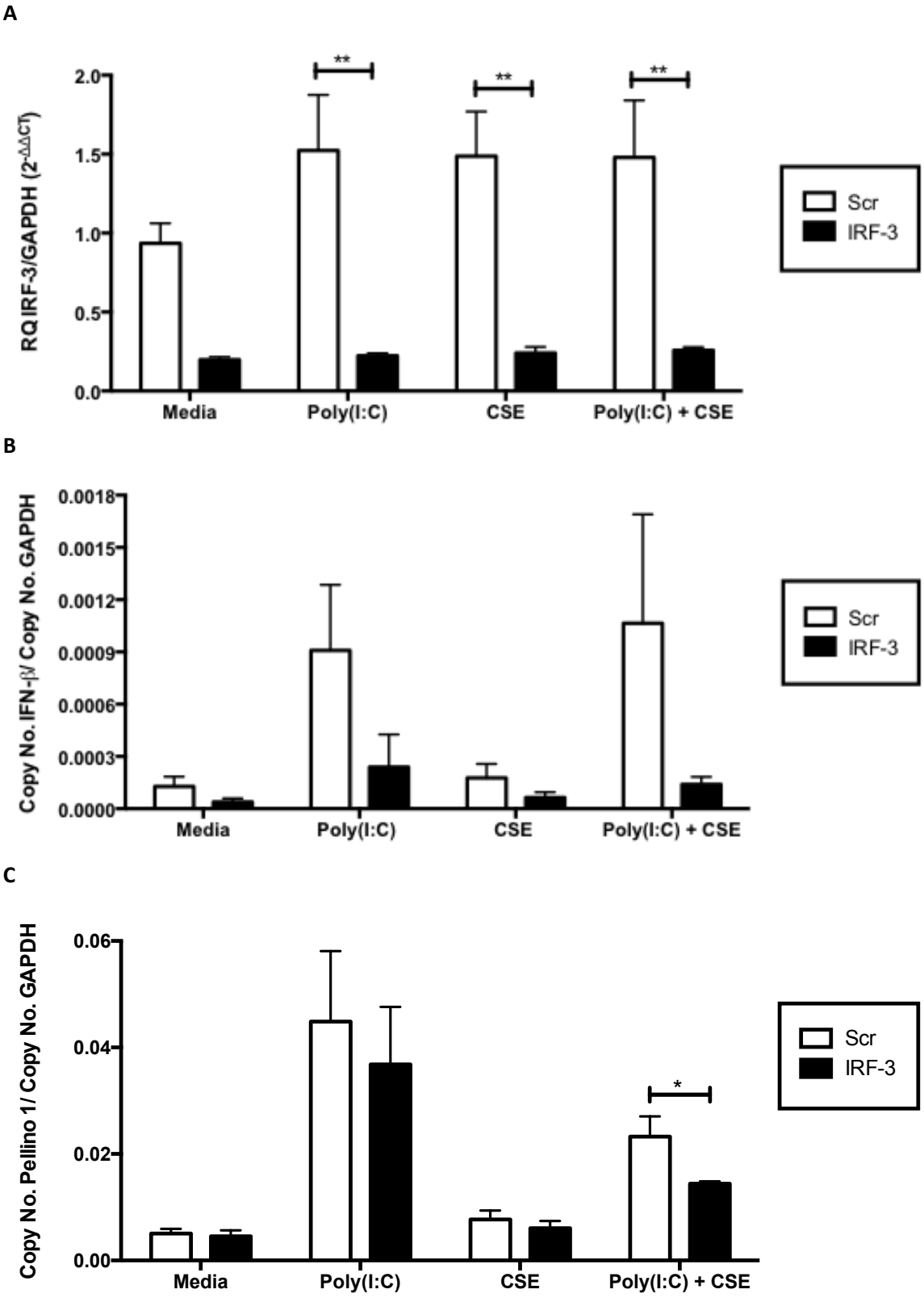

Figure 4.27: IRF-3 transient knockdown decreases Pellino-1 mRNA expression in response to poly(I:C) in primary human bronchial epithelial cells

HBEpCs were transiently transfected with IRF-3 siRNA and non-targeting scrambled siRNA for 24 hours prior to treatment with poly(I:C) (50 μg/ml) for 4, 8, 16 and 24 hours. RNA was extracted and (**A**) IRF-3, (**B**) IFNβ and (**C**) Pellino-1 expression levels were analysed by quantitative RT-PCR. Data are expressed as mean ± SEM of n=3, with each replicate performed on separate donors. Statistical analysis was carried out by two-way ANOVA with Bonferroni's post-test.

4.15 Pellino-1 transient knockdown increases poly(I:C) induced caspase-8 activity in primary human bronchial epithelial cells

The pattern recognition receptor TLR3 recognises dsRNA released during viral infections that triggers the production of pro-inflammatory cytokines and type I IFNs. However in addition to the activation of innate immune responses, TLR3 can induce host cell apoptosis as a means to prevent viral replication, viral dissemination or persistent viral infection (Barber, 2001) (Estornes et al., 2012). Apoptosis is a form of programmed cell death regulated by a family of effector caspases. dsRNA or TLR3-induced apoptosis occurs independently of both IRF3 and NF-κB but is dependent on the c-terminal region of TRIF containing a RIP homotypic interaction motif (RHIM) (Kaiser and Offermann, 2005). In the presence of dsRNA, TRIF complexes with RHIM-containing protein RIP1 resulting in the recruitment and activation of FADD/caspase8 complex.

Poly(I:C) has been shown to induce apoptosis in HBEpCs via a TLR3-mediated caspase-8 dependent pathway (Numata et al., 2011) (Kalai et al., 2002). Therefore it was hypothesised that Pellino-1 may regulate caspase-8 activity through its potential interaction with RIP1. To determine this, targeted knockdown of Pellino-1 by siRNA transfection was performed on HBEpCs followed by stimulation with poly(I:C) for 24 hours. Caspase-8 activity was determined by luminescence with the use of a proluminogenic caspase-8 substrate (Caspase-Glo; Promega) (see **Section 2.12**). The generated luminescence signal corresponds proportionally to the amount of caspase-8 activity present. Pellino-1 knockdown cells showed significantly increased levels of caspase-8 activity to poly(I:C) stimulation when compared to scrambled control (**Figure 4.28**).

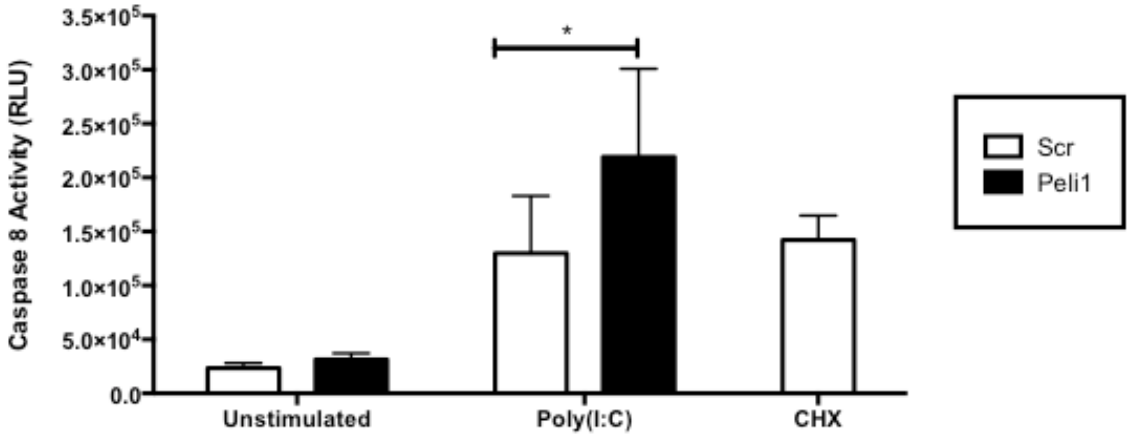

Figure 4.28: Pellino-1 transient knockdown increases poly(I:C) induced caspase-8 activity in primary human bronchial epithelial cells

HBEpCs were transiently transfected with Pellino-1 siRNA and non-targeting scrambled siRNA for 24 hours prior to treatment with Poly(I:C) (50 µg/ml) for 24 hour. Cell lysates were analysed for caspase-8 activity using Caspase-Glo 8 Assay system (described in **Section 2.12**). Quantitative signals were determined by luminescence and expressed as mean ± SEM of n=4, with replicates performed on 4 separate donors. Statistical analysis was carried out by two-way ANOVA with Bonferroni's post-test (*$p<0.05$).

4.16 Identifying Pellino-1 interacting proteins by proteomics & mass spectrometry

With the generation of the Pellino-1 knockout mouse came the discovery of its involvement in the binding and ubiquitination of RIP1, from which RIP1 was suggested to be a potential Pellino-1 intermediary in TLR3 signalling (Chang et al., 2009). While a role for Pellino-1 in regulating IKK activation through the interaction and Lys-63 polyubiquitination of RIP1 in the TRIF-dependent pathway has been identified (Chang et al., 2009), data generated in this thesis do not support this interaction between Pellino-1 and RIP1. In order to determine whether Pellino-1 does in fact interact with RIP1 during anti-viral signalling, a proteomics analysis was commissioned.

Additionally, while a role for ERK and to a lesser extent IRF-3, has been proposed for the regulation of Pellino-1, the targets of Pellino-1 itself remain to be elucidated. To determine potential Pellino-1 targets proteomics analysis was performed and may therefore provide supporting evidence and additional insight to existing data.

HBEpCs were stimulated with poly(I:C) for 4 and 24 hours respectively. Cells were collected, washed and lysed by freeze thawing. The collected samples were then sent to the University of Leeds and analysed by Alexandre Zoughman using the Strap method for bottom-up proteomics, followed by liquid chromatography tandem mass spectrometry, and data processing (Reviewed in (Zougman et al., 2014)). The advantage of bottom-up proteomics is its ability to process membrane proteins which are otherwise not easily digested in aqueous environments due to their hydrophobic properties.

A total 334 proteins were identified (**See Appendix**) providing an extensive list of viable candidates for Pellino-1 binding. However many of these proteins show equally high affinity to Pellino-1 as the control mouse $IgG2_A$ suggesting the possibility of non-specific binding although Pellino-1 was itself was identified suggesting some viability of the data. **Table 4.1** lists all the protein targets and their resulting peptide hits that did show high affinity to Pellino-1. Among these targets, A20 and two of its adaptor proteins TNIP1 and TAX1BP1, have been linked with the negative regulation of NF-κB signalling.

Gene names	Protein names	Peptides Ctrl (4hr)	Peptides Peli1 (4hr)	Peptides Ctrl (24hr)	Peptides Peli1 (24hr)
CACNA1D	Voltage-dependent L-type calcium channel subunit alpha-1D	0	2	0	0
CANX	Calnexin	0	0	0	2
CDKAL1	Threonylcarbamoyladenosine tRNA methylthiotransferase	0	2	0	1
CKAP4	Cytoskeleton-associated protein 4	0	0	0	6
COL1A2	Collagen alpha-2(I) chain	0	3	0	4
COL3A1	Collagen alpha-1(III) chain	0	1	0	1
COPS2		0	1	0	0
CSNK1A1;CSNK1A1L	Casein kinase I isoform alpha;Casein kinase I isoform alpha-like	0	1	0	0
CTNNA1	Catenin alpha-1	0	2	0	1
CTSB	Cathepsin B;Cathepsin B light chain;Cathepsin B heavy chain	0	0	0	2
DBN1	Drebrin	0	1	0	0
ETHE1	Protein ETHE1, mitochondrial	0	0	0	2
FADS2	Fatty acid desaturase 2	0	0	0	1
FTH1	Ferritin heavy chain;Ferritin	0	3	0	0
HIST1H1B	Histone H1.5	0	2	0	1
HNRNPA1	Heterogeneous nuclear ribonucleoprotein A1	0	0	0	1
HNRNPAB		0	0	0	1
HNRNPH1;HNRNPF	Heterogeneous nuclear ribonucleoprotein H;Heterogeneous nuclear ribonucleoprotein H, N-terminally processed;Heterogeneous nuclear ribonucleoprotein F;Heterogeneous nuclear ribonucleoprotein F, N-terminally processed	0	1	0	0
HNRNPL	Heterogeneous nuclear ribonucleoprotein L	0	1	0	0
HSPE1	10 kDa heat shock protein, mitochondrial	0	0	0	2
HYOU1	Hypoxia up-regulated protein 1	0	0	0	4
IARS	Isoleucine--tRNA ligase, cytoplasmic	0	0	0	1
KAT5	Histone acetyltransferase KAT5	0	0	0	1
LGALS3BP	Galectin-3-binding protein	0	0	0	2
LRPPRC	Leucine-rich PPR motif-containing protein, mitochondrial	0	0	0	4
LYZ	Lysozyme C	0	1	0	0
MTMR4	Myotubularin-related protein 4	0	0	0	1
NARS2	Probable asparagine--tRNA ligase, mitochondrial	0	0	0	1
NOP56;NOL5A	Nucleolar protein 56	0	0	0	2
OSBPL10	Oxysterol-binding protein-related protein 10;Oxysterol-binding protein	0	1	0	0
PDHB	Pyruvate dehydrogenase E1 component subunit beta, mitochondrial	0	1	0	3
PELI1	E3 ubiquitin-protein ligase pellino homolog 1	0	1	0	1
PKP3	Plakophilin-3	0	1	0	0
PLEC	Plectin	0	19	0	0
PLOD2	Procollagen-lysine,2-oxoglutarate 5-dioxygenase 2	0	0	0	1
PPA2	Inorganic pyrophosphatase 2, mitochondrial	0	0	0	1
PTBP3;PTBP1	Polypyrimidine tract-binding protein 3;Polypyrimidine tract-binding protein 1	0	0	0	1
RPRD2	Regulation of nuclear pre-mRNA domain-containing protein 2	0	0	0	1
RPS19	40S ribosomal protein S19	0	1	0	0
RPS8	40S ribosomal protein S8	0	1	0	0
SCP2	Non-specific lipid-transfer protein	0	0	0	2
SLC16A1	Monocarboxylate transporter 1	0	0	0	1
SLC35E1	Solute carrier family 35 member E1	0	0	0	1

SQSTM1	Sequestosome-1	0	5	0	0
SRSF4;SRSF 6;SRSF5	Serine/arginine-rich splicing factor 4;Serine/arginine-rich splicing factor 6;Serine/arginine-rich splicing factor 5	0	1	0	0
TAX1BP1	Tax1-binding protein 1	0	1	0	0
TBRG4	Protein TBRG4	0	0	0	1
TENC1	Tensin-like C1 domain-containing phosphatase	0	1	0	1
TICAM1	TIR domain-containing adapter molecule 1	0	1	0	0
TM9SF3	Transmembrane 9 superfamily member 3	0	0	0	1
TMED10	Transmembrane emp24 domain-containing protein 10	0	1	0	0
TNFAIP3	Tumor necrosis factor alpha-induced protein 3	0	17	0	1
TNIP1	TNFAIP3-interacting protein 1	0	10	0	8
VANGL1	Vang-like protein 1	0	1	0	0
YIF1A	Protein YIF1A	0	0	0	1

Table 4.1: Potential Pellino-1 interacting partners generated by mass spectometry

HBEpCs were stimulated with poly(I:C) (50 µg/ml) for 4 and 24 hours. Protein was extracted and analysed by bottom-up proteomics with consequent characterization of the generated peptides by mass spectrometry based on peptide hits. Complete table listed in Appendix.

4.17 Summary

The aim of this chapter was to understand the roles of Pellino-1 in TLR3 signalling and to identify proteins or complexes regulated by Pellino-1 in response to viral stimuli. The results demonstrate that the stimulation of HBEpCs with poly(I:C) resulted in a marked increase of Pellino-1 at both mRNA and protein levels; however experiments exposing these cells to CSE had no effects on Pellino-1 expression. Although, the combination of poly(I:C) and CSE led to a significant reduction in poly(I:C)-induced Pellino-1 expression.

Transient knockdown of Pellino-1 by targeted siRNA transfection showed a profound reduction in Pellino-1 mRNA expression. This Pellino-1 knockdown in HBEpCs led to a decrease in both CXCL8 mRNA expression and CXCL8 cytokine release. However in contrast, Pellino-1 knockdown in HBEpCs did not alter IFNβ mRNA expression in response to poly(I:C). Interestingly, the transient knockdown of IRF-3 in HBEpCs modestly decreases Pellino-1 mRNA expression in response to poly(I:C) suggesting a possible role for IRF3 in Pellino-1 regulation.

Viral dsRNA is capable of inducing CXCL8 gene expression through the activation of a number of protein kinases with the capability of modulating NF-κB. As Pellino-1 knockdown significantly reduced CXCL8 expression and release, it was hypothesized that Pellino-1 elicits its effects through the NF-κB arm of TLR3 signalling. These results show that the stimulation of Pellino-1 knockdown HBEpCs with poly(I:C) resulted in a decrease in phosphorylation of IKKα/β. However, despite this decreased phosphorylation of IKKα/β, the levels of IκBα degradation in Pellino-1 knockdown cells remained unchanged suggesting Pellino-1 is not regulating NF-κB activation. These interesting findings led to the investigation of a role for Pellino-1 in non-canonical NF-κB signalling. While Pellino-1 knockdown does not alter the expression of the non-canonical NF-κB precursor protein, NFKB1, following poly(I:C) stimulation, Pellino-1 knockdown suppressed NFKB2 protein expression in response to poly(I:C) stimulation.

As preliminary data suggested Pellino-1 negatively regulates the non-canonical NF-κB signalling through NFKB2, it was hypothesised that transient knockdown of NFKB2 in HBEpCs would recreate the phenotype of Pellino-1 knockdown. However interestingly, NFKB2 knockdown resulted in significant CXCL8 mRNA and protein expression increase in contrast to Pellino-1 knockdown. Additionally, NFKB2 knockdown does not in turn regulate Pellino-1 mRNA

expression when cells are stimulated with poly(I:C). However, the interferon stimulated gene CCL5 cytokine release was significantly increased in NFKB2 knockdown HBEpCs stimulated with poly(I:C). Pellino-1 and NFKB2 expression was also quantified in epithelial cells isolated from diseased lung airway epithelium of COPD patients then infected with RV-1B and RV-16. Both Pellino-1 and NFKB2 were significantly expressed in these cells at 48 hours post stimulation compared with unstimulated control.

As Pellino-1 seems to have a role in distinct inflammatory pathways, we wanted to investigate whether Pellino-1 regulated other major signalling pathways mediators – the MAPKs. The data in this thesis suggests Pellino-1 may play a role in the regulation and activation of p38 MAPK as an alternative route to CXCL8 transcription. Pellino-1 knockdown dampened the poly(I:C) induced p38 protein expression. p38 regulates the transcription factor AP-1 which is crucial but not essential for maximal CXCL8 gene expression.

Pilot data aiming to assess the impact of the inhibition of the MAPKs on Pellino-1 expression led to the discovery of ERK as a potential Pellino-1 regulator. An ERK-specific MAP kinase, MEK1 inhibitors PD98059 and U0126 effectively reduced poly(I:C) induced Pellino-1 mRNA and protein levels. Moreover, Pellino-1 knockdown does not alter ERK expression.

Pellino-1 was originally implicated in IL-1 signalling however previously published work and data in this thesis suggest Pellino-1 may exert its effects in an IRAK1-independent manner. It was hypothesized that Pellino-1 may in fact play a role in virally induced IL-1 production. Poly(I:C) induced late phase IL-1α and IL-1β mRNA expression, which in turn was dampened by the knockdown of Pellino-1. Specifically, IL-1β gene expression was significantly decreased in Pellino-1 knockdown HBEpCs.

A role for Pellino-1 in regulating TLR3 signalling through the interaction with RIP1 has previously been identified (Chang et al., 2009). However this role for RIP1 as a target of Pellino-1 remains controversial. It was hypothesised that if RIP1 were indeed a target of Pellino-1 then RIP1 knockdown should recapitulate the Pellino-1 knockdown phenotype. In contrast, RIP1 knockdown significantly increased CXCL8 generation in response to poly(I:C). Proteomics analysis of Pellino-1 interacting proteins did not identify RIP1 as a Pellino-1 binding partner at 4 or 24 hours post stimulation with poly(I:C).

RIP1 is also associated with the recruitment and activation of the FADD/caspase-8 complex resulting in cellular apoptosis. Viral infection can result in host cell death as a form of anti-viral defence to prevent further viral replication and dissemination. Therefore it was hypothesised that Pellino-1 may have a regulatory role in caspase-8 apoptosis through the possible interaction with RIP1. Pellino-1 knockdown HBEpCs stimulated with poly(I:C) showed increased levels of caspase-8 activity when compared to scrambled control.

CHAPTER 5- DISCUSSION

Viral infections, such as rhinoviruses (RVs), account for a majority of exacerbations of COPD (Johnston, 2005) and can subsequently result in pronounced functional impairment of the airway increasing both the severity of the disease and frequency of exacerbations. Therefore the reduction of RV-induced airway inflammation would be of immense clinical value with the reduction in severity and duration of the disease improving patient quality of life and reducing morbidity and mortality. Thus, targeting signalling pathways involved in RV-induced inflammation is an important goal. An optimal anti-inflammatory treatment would reduce RV-induced airway inflammation without impairing host defence.

Pellino-1 was originally identified as a regulator of IL-1 signalling (Jiang et al., 2003), however while knockdown of Pellino-1 in immortalised epithelial cell line BEAS-2B reduces IL-1β-induced expression of pro-inflammatory cytokines, the knockdown of Pellino-1 in HBEpC had no such effect overall suggesting that regulation of IL-1 responses may have solely been a feature of transformed cell lines (Bennett et al., 2012). Strikingly, more recent observations have highlighted a role for Pellino-1 in viral signalling wherein Pellino-1 regulates pro-inflammatory responses to RV infection but does not appear to control production of antiviral IFNs (Bennett et al., 2012; Chang et al., 2009). These data strongly support Pellino-1 as a potential therapeutic drug target. This thesis investigates the regulation of Pellino-1 and its role in viral infection in human bronchial airway epithelial cells.

5.1 Chronic Inflammation

COPD is a chronic inflammatory disease that is driven by a multitude of inflammatory mediators derived from activated inflammatory cells, including monocytes and macrophages, as well as structural cells such as epithelial and endothelial cells (**See section 1.2**). COPD patients often exhibit chronic or sustained infiltration of inflammatory cells, including monocytes, macrophages, neutrophils and T lymphocytes, into their airway. The continuous recruitment of monocytes into COPD patient airways (**described in Section 1.2**) causes an initial release of chemotactic factors such as CXCL8 from epithelial cells through their IL-1 driven communication and eventually other subsequent factors leading to further neutrophil

infiltration (Di Stefano et al., 1994; Tanino et al., 2002). Alveolar macrophages, monocytes, neutrophils and epithelial cells themselves are sources of CXCL8 which is present in high quantities in COPD patient sputum (Beeh et al., 2003). This reinforces the importance of cell communication in COPD pathophysiology (Marsh et al., 1995), and can also explain the excessive inflammatory responses witnessed in patients.

Exposure to inhaled pollutants such as cigarette smoke is thought to be a leading cause of the chronic airway inflammation seen in COPD through the activation of structural and inflammatory cells within the lung resulting in a perpetuating state of chronic inflammation through the release of chemotactic factors (Rovina et al., 2013). It was hypothesised that this perpetual state of chronic inflammation leads to a 'hypersensitive state' leaving the airway susceptible to further common viral and bacterial respiratory infections often associated with exacerbations of COPD. Therefore the work in this thesis was designed to investigate the mechanisms that underpin the pathogenesis of the disease by elucidating dysregulation of the immune signalling in these patients.

With particular interest in patients presenting with chronic bacterial and/or viral infections within their airways and the resulting effects on their responses to further stimuli, it was hypothesised that this persistent infection leaves airways primed to further pathogenic invasion presented in the form of acute exacerbations. Chronic inflammation of COPD is underpinned by airway colonization and infection, and activation of both IL-1 and IFN pathways. The model of chronic inflammation proposed in this thesis therefore aimed to better understand the intrinsic changes to patient epithelium caused by prolonged infection in healthy epithelial cells. The chronic model aimed to mimic this prolonged infection through the exposure of epithelial cells to long-term low-grade bacterial stimulation in the presence of monocytic cells (THP-1 cells and purified monocytes) to simulate inflammatory cell infiltration.

Interactions between different cell types are paramount when mounting an effective inflammatory response to varied stimuli. Evidence from *in vitro* studies supports the role of cell-cell communication in driving the inflammation observed in COPD, with co-culturing of inflammatory cells and structural cells (such as epithelial cells, endothelial cells and vascular or airway smooth muscle cells) causing synergistic production of cytokines (Chaudhuri et al., 2010; Morris et al., 2006; Morris et al., 2005; Ward et al., 2009). For instance, the combined culturing of airway smooth muscle cells with low numbers of PBMCs resulted in a cooperative

response to TLR stimuli, and synergistic production of cytokines CXCL8 and IL-6. This stimulation was dependent on IL-1 production from monocytes that activated tissue cells to produce proinflammatory cytokines in response to LPS (Morris et al., 2005). The collective research into co-cultures reinforce the importance of cell networks and cooperative signalling between cells of the immune system and tissue cells in mounting a response to bacterial and viral pathogens. The chronic model of inflammation described in this thesis uses monocytic cells due to their predominant role in COPD.

The chronic model of inflammation was set up with the use of BEAS-2B cells, which are themselves a model of primary epithelial cells. BEAS-2B cells are well described and closely resemble bronchial epithelial cells as demonstrated by electron microscopy, mucin production, formation of tight junctions, and presence of keratin (Noah et al., 1995; Reddel et al., 1988). As BEAS-2Bs are derived from airway epithelium and retain these physiological features, the results of altered signalling to the stimulus tested could potentially signpost to their involvement in disease tissue. These cells also provide initial reproducibility, which is essential in the early stages of establishing the model.

The chronic model of inflammation also uses the monocytic cell line THP-1 due to its many obvious advantages in terms of availability, immortality and standardisation of responses due to lack of donor variability as compared to primary monocytes. The THP-1 state of differentiation has also been previously optimised to best mimic monocytes (Colsky et al., 1991; Daigneault et al., 2010; Murao et al., 1983; Tsuchiya et al., 1980). However, it was observed that THP-1 cells are much less responsive to LPS in both mono- and co-cultures when compared to primary monocytes. In an attempt to address this difference between monocytes and THP-1 cells, the THP-1 cell numbers were normalised against the LPS-induced CXCL8 output of 10ng/ml per 5,000 monocytes as described in previously established acute models of inflammation (Chaudhuri et al., 2010). It was therefore determined that 100,000 $VitD_3$-differentiated THP-1 were required to reproduce this amount and to be used in the model and for future work.

Initial experiments aimed to determine the effect of repeated LPS stimulation on BEAS-2B cells in the presence and absence of monocytic cells in cell culture inserts showed that while an increase in CXCL8 in response to LPS was measured, this was not altered in challenged versus unchallenged models. These data suggest that BEAS-2B cells remained unaffected by the

chronic low-grade bacterial stimulation despite the inflammatory mediators released by the THP-1 cells required for effective LPS response. While BEAS-2B cells and bronchial epithelial cells express TLR4 constitutively, they lack CD14 expression required for LPS recognition and in turn do not release CXCL8 when chronically stimulated with LPS (Frey et al., 1992; Landmann et al., 1996). Instead, BEAS-2B cells respond to LPS indirectly through the presence of other inflammatory mediators such as IL-1, as secreted by monocytes and THP-1 cells, and in turn enhance their own inflammatory response resulting in a synergistic response to LPS (Chaudhuri et al., 2010; Daigneault et al., 2010; Morris et al., 2006; Yang et al., 2001).

A previously established acute model of inflammation highlighted IL-1 as a key communicator leading to the synergistic CXCL8 release by the co-culture (Chaudhuri et al., 2010). To determine the role of IL-1 cytokine release in the response of BEAS-2B cells to LPS in the chronic model, IL-1 receptor antagonist (IL-1Ra) was used to prevent IL-1 signalling. A significant inhibition of LPS-induced CXCL8 release was observed in the presence of IL-1Ra. The results show a role for IL-1 in eliciting CXCL8 release during chronic inflammation. This is particularly important as IL-1 has been described in COPD for its important roles in leukocytosis and the release of other cytokines, including IL-6, CXCL8 and CCL5, from a variety of cells. Patients with COPD show increased levels of IL-1 in both induced sputum and BAL as well as increase in secretion from alveolar macrophages (Chung, 2001). Of note, direct IL-1 release from these chronically challenged BEAS-2B cells could not be measured using standard ELISA (data not shown) due to the low levels of the cytokine. Future work could include high-sensitivity ELISAs. Real-time PCR could also be carried out to measure mRNA changes within the epithelial cells, although IL-1 can be generated post translationally through inflammasome activation (Martinon et al., 2002), therefore initial changes may not be detected.

The lack of detectable IL-1 cytokine release by ELISA but significant reduction in CXCL8 release when co-stimulated with IL-1Ra may be explained by a more focussed release of high concentrations of IL-1 directly on membrane receptors on BEAS-2B, which would induce a more pronounced effect. Lack of cell contact or proximity has been shown to lead to a reduction in chemokine expression (Smith et al., 1997; Zujovic and Taupin, 2003), which is indeed supported by the direct cell-to-cell contact model. Data in this thesis showed that the long-term stimulation of BEAS-2B cells with LPS in direct contact with THP-1 cells led to slightly lower CXCL8 release during the final 24 hour LPS stimulation in the presence of monocytes, compared to the control group of BEAS-2B and monocytes which did not have prior LPS

stimulation. More importantly however, BEAS-2B cells chronically stimulated with LPS show a decrease in CXCL8 release when monocytes and LPS are added on day 8, whether or not THP-1 cells were also present during the induction of chronic inflammation. Again, while these data are not significant and require further exploration and reproduction, this lowering of CXCL8 release after induction of chronic inflammation by LPS may suggest tolerance of BEAS-2B cells to further pathogenic stimulation. The measure of other pro-inflammatory cytokines such as TNF-α and IL-6 and anti-inflammatory cytokine IL-10 would help provide a more complete and informative picture. The DNA binding activity of NF-κB in response to repeated LPS stimulaion would also provide an alternative measure of the intensity of TLR4 signalling.

After induction of inflammation, BEAS-2B cells were stimulated with monocytes and LPS. This final stimulus of monocytes and LPS depends on IL-1 production by the monocytes to activate epithelial cells, but could theoretically be tolerised by pretreatment of the BEAS-2B cells by LPS. LPS tolerance is a protective mechanism to prevent endotoxin shock, where cells exposed to low levels of endotoxins are unaffected by further exposure. Therefore it was postulated that the chronic LPS treatment could induce tolerance of IL-1 signalling.

Tolerance in this context represents a complex diminished pro-inflammatory response due to exposure to low concentrations of endotoxins resulting in the reprogramming of innate immune cells. This state of tolerance is not represented by 'immunoparalysis' but instead the activation of alternative pathways. The mechanisms of endotoxin tolerance are vague, however roles for negative regulators such as suppressor of cytokine signalling 1 (SOCS1), IRAK-M and SHIP have been identified, in addition to the down regulation of TLR-4 on cell surface and gene re-programming.

Induction of tolerance in cells has been shown to affect protein-protein interactions downstream of TLR-receptors such as diminished IRAK-1 activity, MyD88-TLR4 association and interaction of MyD88 with IRAK-1 ultimately resulting in decreased pro-inflammatory cytokines (Medvedev et al., 2006). For example, repeated exposure to bioactive LPS present in cigarette smoke impairs the function of alveolar macrophages (AM). This leads to a restriction of LPS-induced expression of TLR-2 and -4 induced pro-inflammatory cytokine and chemokine release including IL-1β, IL-6 and TNFα. The activation of IRAK-1, p38 and NF-κB was also found to be impeded leading to a subdued expression of proinflammatory mediators (Chen et al., 2007; Hasday et al., 1994).

It is therefore possible that airways of COPD patients have a poorly explored underlying epithelial microbial tolerance that limits the initial production of pro-inflammatory cytokines that results in hypersensitivity to secondary bacterial infections.

5.2 CSE exposure results in an additive CXCL8 release in response to Poly(I:C) or RV-16

Cigarette smoking is a dangerous and addictive habit increasingly spreading throughout the developing world. Smoking has profound consequences on human health and has been linked to the progression of many diseases including respiratory conditions such as asthma and COPD (Arnson et al., 2010). Human RVs are one of the predominant viral pathogens involved in the onset of the common cold and are a major cause of asthma and COPD acute exacerbations (Johnston, 2005). Human rhinoviral infections have been linked to up to 60% of exacerbations of COPD (Del Vecchio et al., 2015). Although many studies have investigated airway epithelial cell responses to RV infection and CSE contact, how repeated or chronic exposure to CSE alters RV-induced responses in airway epithelial cells remains to be comprehensively explored. Therefore, this thesis sought to determine whether host inflammatory responses to viral infections are affected following repeated exposure to CSE.

In accordance with previously published studies (Hudy and Proud, 2013; Pace et al., 2008; Wang et al., 2009), acute exposure to CSE alone resulted in a significant increase in CXCL8 production in airway epithelial cells. Surprisingly, the addition of the viral mimic poly(I:C) in combination with CSE for 24 hours resulted in an inhibition of CXCL8 production in BEAS-2B cells. In contrast, pre-treatment with CSE for 6 days prior to poly(I:C) stimulation resulted in a potentiation in CXCL8 response. At first glance, these data appear to indicate an effect of prolonged treatment of CSE on subsequent responses to viral infection, supporting the hypothesis of altered cellular responses to invading pathogens by CSE. However, following the modification of the protocol, wherein both the acute model and chronic repeated model are maintained in the same environment for the duration of the experiment, these differences in CXCL8 production were lost. In fact, both acute pre-

treatment with CSE and repeated pre-treatment with CSE followed by a single stimulation with poly(I:C) resulted in a similarly exaggerated CXCL8 production in both. These results highlight the importance of the choice of experimental protocol and the detrimental effects the inappropriate model can have in the interpretation of data. *In vitro* experiments are inadvertently limited by the very nature of their simplicity, as it is impossible to accurately replicate *in vivo* conditions in a cell-culture plate. When comparing the results obtained from the 2 day acute model with the 8 day acute model, it is important to consider which model may be a better representative of airway epithelium. While both models were treated using the same quantities of CSE and viral stimulus, the biggest differentiating factor is the density of the BEAS-2B cell monolayer. The 8 day acute model allowed for the epithelial cell layer to grow into a compact and stable monolayer more closely resembling airway epithelium than that of the 2 day acute model.

With the use of the prolonged acute and repeated model, BEAS-2B cells were also infected with RV-16 and CSE. While CSE and RV-16 alone induced CXCL8 production, the combination of both resulted in an additive CXCL8 response. Data published by Wang *et al* did not demonstrate augmented CXCL8 beyond that induced by RV alone in A549 cells, while Hudy *et al* showed enhanced CXCL8 production to the combination of RV-16 and CSE in primary bronchial epithelial cells (Hudy and Proud, 2013; Wang et al., 2009).

Under normal conditions, the infection of epithelial cells with RV induces a wide range of cytokines, primarily CCL5 and CXCL10 at the highest concentrations (Proud, 2008). Therefore the CCL5 induction by RV-16 was also assessed as an indirect measure of effective early innate immune response. Indeed RV-16 infection of BEAS-2B cells resulted in increased CCL5 production. The acute and repeated pre-treatment with CSE however attenuated the CCL5 production to RV-16. In fact, these results are in keeping with existing studies wherein CSE decreases the activation of the IFN-STAT-1 and SAP/JNK pathways resulting in the suppression of CXCL10 and CCL5 production and lead to an increase in viral RNA (Eddleston et al., 2011). CSE has also been shown to decrease the expression of IFN-stimulated gene 15 (ISG15) and IRF-7 transcripts in response to poly(I:C) in BEAS-2B cells and the translocation of NF-κB and IRF3 transcription factors (Bauer et al., 2008).

5.3 CSE differentially regulates epithelial cell response to LPS and IL-1

A chronic experimental model was created to understand the effects of repeated cigarette smoking on epithelial cells' ability to respond to infections. In accordance with previous published works, acute pre-treatment with CSE increased the BEAS-2B cell inflammatory response, measured in the form of CXCL8 production. However when pre-treated cells were stimulated with LPS, no additional CXCL8 was measured. In fact these data are in contrast to that of Pace et al, where they demonstrated that CSE exerts its effects through the increased externalisation and expression of TLR4, and the ability to bind LPS with favoured ERK activation instead of the NF-κB signalling (Pace et al., 2008). Indeed CSE alone does not activate the ERK pathway (Luppi et al., 2005) unless in combination with LPS wherein CSE differentially regulates LPS-induced signalling (Pace et al., 2008). Perhaps these results could be explained by the different cell lines used. As previously discussed, BEAS-2B cells express TLR4 constitutively but lack CD14 expression required for LPS recognition and in turn do not release CXCL8 when chronically stimulated with LPS (Frey et al., 1992; Landmann et al., 1996) unless in the presence of inflammatory mediators such as IL-1. By stimulating CSE treated BEAS-2B cells with IL-1, a potentiation in CXCL8 production was measured. While this amplification of CXCL8 is MyD88 dependent, additional experiments would need to be carried out to determine if this effect is uniquely due to ERK. The measure of ERK by western blot analysis and ELISA would be the first step experimentally to support the presence of ERK expression. This would be followed by the inhibition of ERK using MEK1 inhibitors to confirm effects measured are uniquely due to ERK. Interestingly, in alveolar macrophages while CSE also modulates CXCL8 mRNA and protein expression (Sarir et al., 2009) CSE has been shown to amplify LPS-induced secretion of IL-1βb and TNF-α through NF-κB activation (Xu et al., 2011).

Repeated stimulation with CSE did not alter the CXCL8 production of BEAS-2B cells. Again, this could be due to the insufficient pre-treatment with CSE wherein the chronic model is in fact not 'chronic' enough, or simply the epithelial cells have a superior resistance to low grade infection or stimulation than initially predicted.

5.4 Pellino-1 in NF-κB signalling

Pellino-1 is a ubiquitously expressed protein, however its relative levels of expression are tissue specific. In the mouse, Pellino-1 is highly expressed in peripheral blood leukocytes, moderately expressed in the placenta, lung, liver, kidney, spleen, thymus, skeletal muscle and brain, and is expressed at low levels in the small intestine, colon and heart (Jiang et al., 2003). The data in this thesis demonstrates Pellino-1's expression in primary human airway epithelial cells in accordance with previous published data in the same cell type (Bennett et al., 2012). Furthermore, Pellino-1 expression is upregulated in response to the TLR3 agonist poly(I:C) following 24 hours of stimulation in human airway epithelial cells. These data suggest Pellino-1 is being upregulated in response to poly(I:C) activation of the TRIF-dependent pathway it regulates. These data also reflect findings from the Pellino-1-deficient mouse wherein Pellino-1 has a functional role in TRIF-dependent signalling (Chang et al., 2009). Data from murine bone marrow derived macrophages stimulated with poly(I:C) also shows a striking enhancement of Pellino-1 transcription and protein expression in a TRIF-dependent induction (Smith et al., 2011).

The functionality of Pellino-1 in human airway epithelial cells was further investigated by the transient knockdown of Pellino-1 by targeted siRNA transfection. The targeted knockdown of Pellino-1 stimulated with poly(I:C) at 4, 8, 16 and 24 hours resulted in a decrease in CXCL8 mRNA expression and cytokine secretion in HBEpCs at the 24 hour time point. IFNβ mRNA expression was also determined following transient Pellino-1 knockdown and poly(I:C) stimulation, and resulted in no measurable effect on IFNβ production. These results reflect previously published work wherein pro-inflammatory cytokines CXCL8 and IL-6 were significantly inhibited in response to poly(I:C) in HBEpCs following Pellino-1 knockdown, whilst the interferon-stimulated gene CCL5 remained unaffected (Bennett et al., 2012). Taken together, these data indicate a role for Pellino-1 in selectively mediating the TRIF-dependent NF-κB/MAPK pathway and not TLR3-mediated IRF3 and IFNβ activation. In support, the Pellino-1-deficient mouse showed a decrease in circulating pro-inflammatory cytokines in serum 1 and 4 hours post systemic poly(I:C) challenge (Chang et al., 2009). In the mouse, the group demonstrated that Pellino-1 both interacts with, and ubiquitinates RIP1 leading to IKK phosphorylation and the downstream activation of canonical NF-κB in a TRIF-dependent manner. In addition, IKKε and IFNβ induction in embryonic fibroblasts from Pellino-1-deficient mice remain intact (Chang et al., 2009).

It is well documented that TLR3 signalling pathway culminates in the activation of NF-κB among other transcription factors. Normally, NF-κB resides within the cytoplasm in its inactive form through the association with IκB inhibitors. Following TLR3 activation, the canonical NF-κB proteins p65, RelB and c-Rel are activated through the degradation of IκBs by the IKK complex consisting of IKKα and IKKβ protein kinases and IKKγ regulatory molecule. This results in the release and translocation of NF-κB into the nucleus for gene transcription (**Figure 1.3**) (Han et al., 2004; Muzio et al., 2000). Therefore it is possible to establish the extent of canonical NF-κB activation by determining the level of both IKK phosphorylation and the resulting IκBα phosphorylation and degradation. The transient knockdown of Pellino-1 in cells stimulated with poly(I:C) for 4 and 24 hours resulted in the decrease in IKKα/β phosphorylation at 24 hours post-stimulation. Surprisingly, total IκBα degradation was not compromised in Pellino-1 knockdown samples at 4 or 24 hours post-stimulation, as would have been expected following IKKα/β phosphorylation. It is possible that a lack of IκBα assay sensitivity is to blame and the measure of NF-κB phosphorylation status would be of great additional value to determine if in fact poly(I:C) is acting via the canonical pathway. The measure of NF-κB nuclear translocation by microscopy could be an alternative experiment to further explore this. Alternatively however, when taking this data in combination with that of Bennett *et al.* where no evidence of IκBα degradation can be measured following poly(I:C) stimulation over 15-240 minutes in primary bronchial epithelial cells (Bennett et al., 2012), it is thus possible to postulate that poly(I:C) itself does not utilize the canonical NF-κB signaling pathway and therefore the site at which Pellino-1 regulates NF-κB signaling may also lay outside this pathway. Since NF-κB is essential for CXCL8 induction and Pellino-1 regulates CXCL8 expression in response to poly(I:C), it is possible that Pellino-1 is operating through the non-canonical NF-κB pathway (See **Section 1.6.1.2**).

COPD patients have increased baseline levels of IL-1β within their airways, which are increased further in instances of acute exacerbations (Chung, 2001). There is also accumulating evidence suggesting a role for IL-1β in response to RV infections whereby IL-1 is released and acts as an autocrine stimulus to further enhance inflammatory signalling (Grunstein et al., 2000; Hakonarson et al., 1999; Piper et al., 2013; Stokes et al., 2011). In primary human epithelial cells, both IL-1α and IL-1β are secreted following viral infection resulting in increased pro-inflammatory signalling and recruitment and activation of immune cells (Piper et al., 2013). Through the knockdown of Pellino-1, a significant reduction in IL-1β gene expression to poly(I:C) was measured at 16 and 24 hours, and a similar trend was noted in IL-1α expression.

In keeping with previous data, these findings support the role for Pellino-1 in IL-1 signalling, providing further evidence of its involvement in NF-κB regulation.

5.5 Pellino-1 in non-canonical NF-κB signalling

Originally, the non-canonical NF-κB pathway was mainly associated with the regulation of specific adaptive immune functions such as lymphoid organogenesis, dendritic cell activation and B-cell survival and maturation (Dejardin, 2006). Emerging evidence suggests that the non-canonical NF-κB signalling pathway is also involved in the regulation of innate antiviral immunity. A549 cells showed inhibited RIG-I-mediated non-canonical NF-κB activation and expression of the non-canonical target CCL19 following infection with influenza virus A (Ruckle et al., 2012). More recently, non-canonical NF-κB signalling was found to negatively regulate type I IFN induction in murine BMDM stimulated with Sendai virus and vascular stomatitis virus (Jin et al., 2014). This increasing evidence for a non-canonical NF-κB role in antiviral innate immunity coupled with lack of IκBα degradation in Pellino-1 KD following poly(I:C) stimulation further support a role for Pellino-1 involvement in the non-canonical arm of this pathway.

During non-canonical NF-κB signalling, the precursor proteins NFKB1 (p105) and NFKB2 (p100) undergo proteolytic processing to release their active components, p50 and p52 respectively, followed by dimerisation with RelB, c-Rel or p65 resulting in the nuclear translocation and activation of gene transcription (**Figure 1.3**) (Bonizzi and Karin, 2004; Senftleben et al., 2001). Preliminary data suggests that Pellino-1 plays a role in the processing of NFKB2 as both the measure of NFKB2 protein and its p52 active component in Pellino-1 knockdown HBEpCs showed a reduced upregulation induced by NF-κB in response to poly(I:C) at 24 hours post stimulation. The data in this thesis specifically place Pellino-1 in NFKB2-dependent signalling arm rather than NFKB1 as NFKB1 protein levels remain unchanged in response to poly(I:C) in Pellino-1 knockdown HBEpCs at both 4 and 24 hours while Pellino-1 knockdown prevents upregulation of poly(I:C) induced NFKB2 protein expression in HBEpCs.

In an attempt to determine a role for Pellino-1 in NFKB2 signalling and support the hypothesis of NFKB2 as a Pellino-1 target, NFKB2 was transiently inhibited by siRNA transfection. Interestingly, NFKB2 knockdown resulted in an increase in both CXCL8 expression and release at 24 hours post stimulation, contrasting the Pellino-1 knockdown phenotype wherein CXCL8 is

suppressed in response to poly(I:C). Additionally, the transient knockdown of NFKB2 also increased CCL5 secretion from HBEpCs at 24 hours post stimulation. This finding is perhaps not surprising as NFKB2 has recently been shown to negatively regulate type-1 IFN induction (Jin et al., 2014). A preliminary interpretation of these data could indicate that the up-regulation of NFKB2 could act as a compensatory negative feedback loop, potentially exerting its actions through its ability to act as an IκB-like molecule. The mechanism for this could be the result of the formation of p52 homodimers that function much like IκBs, however lack transactivation domain (TADs) required to activate gene transcription (Zhong et al., 2002). NFKB2 has also been previously described as a negative regulator of NF-κB through the supression of preformed RelA:p50 dimer activity following RSV-infection or during prolonged TLR-mediated IKK signalling (Savinova et al., 2009). It is possible that following viral infection in airway epithelial cells, TLR3 activation culminates in the up-regulation of Pellino-1 leading to an increase in NFKB2 expression, resulting in the suppression of NF-κB specific gene transcription (demonstrated in **Figure 5.1**). Whilst regulation of TLR4 signalling by induction of tolerance is well-described, this is the first clear negative regulatory pathway that may limit ongoing TLR3 signalling in a pathway-specific manner, and suggests that future exploration of non-canonical NF-κB signalling in airways epithelial cells will be important in understanding how chronic inflammation may be regulated in these cells.

The identification of a poxviral homolog of the Pellino family with immunoevasive characteristics through the inhibition of TLR signalling highlights an interesting insight for its role in disease (Griffin et al., 2011). Viral pellino showed functional consequences for pro-inflammatory gene expression wherein transduction of THP-1 cells with lentivirus expressing Pellino caused the inhibition of CXCL8 production in response to LPS. It is possible therefore that viral homologues can deplete pellino functionality in a disease state like that of COPD.

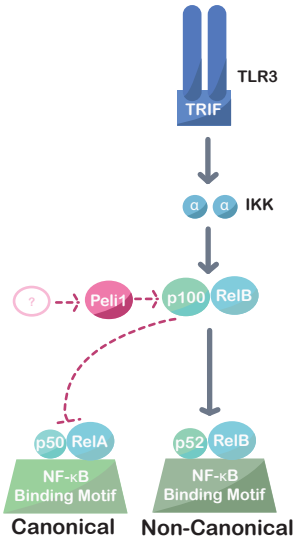

Figure 5.1 Possible mechanism for the negative regulation of NF-κB by Pellino-1 through NFKB2

This figure highlights a possible mechanism for the negative regulation of p100/NFKB2 by Pellino-1 in HBEpCs. Upon TLR3 activation, Pellino-1 is up-regulated by a currently uncharacterised mediator leading to an increase in NFKB2 expression which in turn has a negative regulator role, possibly through suppression of RelA:p50 dimer activity resulting in the suppression of NF-κB specific gene transcription

5.6 Pellino-1 and RIP1

With the generation of the Pellino-1 knockout mouse came the discovery of its involvement in the binding and ubiquitination of RIP1, from which RIP1 was suggested to be a potential Pellino-1 intermediary in TLR3 signalling (Chang et al., 2009). RIP1 has been implicated in TLR3-mediated NF-κB response to dsRNA (Meylan et al., 2004) and shown to directly bind TRIF via the RIP homotypic interaction motif (RHIM) where it then undergoes phosphorylation and polyubiquitination, resulting in IKK activation (Cusson-Hermance et al., 2005). The E3 ubiquitin ligase responsible for the ubiquitination of RIP1 in the TRIF-dependent TLR pathway remains elusive. While a role for Pellino-1 in regulating IKK activation through the interaction and Lys-63 polyubiquitination of RIP1 in the TRIF-dependent pathway has been identified (Chang et al., 2009), contrasting data generated from the Pellino-1 knock-in mouse, expressing a deficient form of the Pellino-1 E3 ubiquitin ligase, showed no deficiency in poly(I:C)-induced

polyubiquitination of RIP1, the downstream activation of canonical IKKs or the activation of MAP kinases in BMDM, altogether eliminating Pellino-1 involvement (Enesa et al., 2012). The differences are likely attributed to the model used for each study. Knock-out mice are created by the insertion of a selection marker or reporter into a target gene locus to either completely remove one or more exons from a gene resulting in a mutated or truncated protein, or the deletion of the protein altogether (Aida et al., 2014). While a knock-in mouse is created by the insertion of a transgene at a specific pre-selected locus resulting in the exogenous expression of the protein of choice (Aida et al., 2014). It is therefore possible that despite the lack of ligase activity in the Pellino-1 knock-in mouse, it may in fact still maintain a scaffolding role, bringing in other signalling molecules that would otherwise not be recruited in the knock-out mouse. It is also plausible that these two different models result in different expression of compensatory pathways, such as other Pellinos. However, it is critical to note that the differences in the execution of both these models may have measurable effects on their results. Chang et al.'s knockout mice were generated using conventional gene targeting strategy in which lacZ-neomycin cassette replaces the coding exons 1 and 2. DNA from both WT mice and knockout mice were genotyped to acertain effective knockout of Pelino-1. Additionally knockout mice showed no signs of birth or growth abnormalities compared to WT.

However for the creation of knock-in mice, Enesa et al. demonstrated low sequence affinity following homology modelling between Pellino-1 RING domain and known RING figure structures (Enesa et al., 2012). They generated their knock-in mouse using partial matches to Pellino-1 RING domain in the zinc-coordinating residues of the E3 ubiquitin ligase c-Cbl. Further structural studies resulted in the identification of contact points between c-Cbl and E2-conjugating enzyme UbcH7 leading to the putative identification of equivalent residues in Pellino-1. Furthermore the success of the knock-in was determined by an artificial in vitro assay wherein bacterial Pellino-1's E3 ligase activity was abolished in a Ub assay. The greatest flaw in the model is the lack of evidence of the loss of Pellino-1 E3 ligase activity *in vivo*. Additionally, the knock-in mice demonstrated slightly lower than expected frequency in birth rates. Most notably however, the expression of Pellino-1 protein in the knock-in is lower than WT protein in all studied tissues. Similarly, protein levels measured from BMDM were consistently lower in knock-in samples either before or after LPS and poly(I:C) stimulation.

In order to determine whether RIP1 is indeed a Pellino-1 target in primary cells, poly(I:C) regulation of RIP1 was first determined, and while RIP1 is constitutively expressed in HBEpCs,

the stimulation of these with poly(I:C) does not regulate RIP1 protein expression. Furthermore, the transient knockdown of RIP1 by siRNA transfection resulted in both a significant increase in CXCL8 gene expression release in response to poly(I:C). These findings do not reflect those of Pellino-1 knockdown wherein CXCL8 was significantly reduced in response to poly(I:C) which would indicate that whilst RIP1 is involved in the regulation of poly(I:C)-activated TLR3 pathway, it does not appear to be regulated by Pellino-1. These data are in keeping with previous work by Bennett *et al.* where the group challenged Pellino-1 as a RIP1 target through the transient knockdown of RIP1, similarly showing a potentiation of CXCL8 to poly(I:C) (Bennett et al., 2012). The study of Bennett et al showed a greater increase in CXCL8 release after RIP1 knockdown in comparison to data presented in this thesis. However, Bennett et al were only able to look at consequences of RIP1 knockdown in a single primary cell donor. The data presented in this thesis was obtained from up to 5 individual donor cells and provide a more robust analysis to establish true phenotype.

The contrasting effect on CXCL8 release of RIP1 knockdown and Pellino-1 knockdown on poly(I:C)-induced CXCL8 release suggests a negative regulatory role for RIP1 in TLR3 signalling. These data contrast published work highlighting RIP1 as an essential mediator in TRIF-dependent NF-κB signalling (Meylan et al., 2004). Nonetheless, there is culminating evidence corroborating a negative regulatory role for RIP1. In support, RIP1 has been shown to negatively regulate TNFα-activated non-canonical NF-κB signalling through TRAF2 degradation, NIK stabilization, IKKα phosphorylation and the processing of p100 to generate p52 (Kim et al., 2011b). In RIG-I signalling, RIP1 also acts as a negative regulator of IRF3 signalling through its cleavage by caspase-8 (Rajput et al., 2011).

Initially it was speculated that Pellino-1's mechanism of action might involve the negative regulation of inhibitory functions of RIP1. Pellino-1 could exert its negative regulatory role through the mediation of Lys-48 induced degradation of RIP1. This proposed hypothesis would explain the spike in pro-inflammatory cytokine CXCL8 following RIP1 knockdown due to the removal of the NF-κB inhibitory function of RIP1, whilst Pellino-1 knockdown would result in the opposite effect due to removal of the regulator of the inhibitory RIP1. However, while this theory explains the presence of constitutively expressed RIP1 seen in unstimulated HBEpCs, it does not explain the lack of RIP1 inhibition following poly(I:C) stimulation, as it would follow that Pellino-1 would induce Lys-48 linked degradation of RIP1. Furthermore, proteomic analysis used to identify proteins with an affinity for Pellino-1 yielded no matches with RIP1 at

4 or 24 hours post-stimulation with poly(I:C) indicating further exploration into the action of RIP1 is required to determine the hypothesis.

In addition to the regulation of canonical NF-κB signalling, RIP1 was originally described as a regulator of apoptotic cell death in RIP1 knockout mice (Kelliher et al., 1998). Viral infections frequently result in apoptosis as part of the host cell's viral defence. The activation of TRIF-dependent apoptosis is mediated at least in part by RIP1, FADD and caspase 8 (Numata et al., 2011) (Estornes et al., 2012; McAllister et al., 2013). Both TLR3 and RIP1 are linked with regulating virally-induced apoptosis, it was therefore hypothesized that Pellino-1 may have a role in apoptosis through the TLR3/Pellino-1/RIP1 interaction.

Preliminary data measuring caspase-8 activity in Pellino-1 knockdown HBEpCs stimulated with poly(I:C) showed increased caspase-8 levels in Pellino-1 knockdown samples when compared to control. These data raise the possibility of a link between Pellino-1 and antiviral defence in the form of cell death. Previously published work shows that the ubiquitination of RIP1 by the E3-ubiquitin ligase called cellular inhibitor of apoptosis protein (cIAP) prevents it from activating caspase-8-dependent extrinsic apoptotic pathway to TNF-induced cell death (Vanlangenakker et al., 2011). It is therefore possible that Pellino-1 may similarly serve as a negative regulator of apoptosis via the polyubiquitination of RIP1 in response to viral stimuli. Further work into the action of Pellino-1 in virally induced apoptotic cell death would be required to investigate the proposed mechanism, including characterization of the apoptotic pathways involved in virally-induced cell death. RV and poly(I:C)-induced cell death could be quantified by the use of Cell Titer-glo luminescence assay. In addition, cell viability could be determined by cell membrane integrity, and apoptosis by DNA fragmentation and TUNEL staining. Survival can then be correlated with the activation of caspase-3 and caspase-8.
Following the identification of occurring death pathways, key experiments can be repeated with Pellino-1 knockdown to determine its involvement in the cell death and the consequences on viral replication rates as measured by qPCR.

5.7 Pellino-1 in IFN signalling

Data presented in this thesis indicates that Pellino-1 selectively regulates NF-κB signalling instead of IFN signalling. IFNβ mRNA expression was unaffected by poly(I:C) stimulation following transient Pellino-1 knockdown. These results are supported by the unaltered CCL5

secretion, an interferon-stimulated gene, in primary epithelial cells from healthy controls and patients with asthma in response to dsRNA (Bennett et al., 2012). Interestingly, IRF3 knockdown in HBEpCs result in a small reduction in Pellino-1 expression following poly(I:C) stimulation. While these observations do not indicate IFN signalling is essential for Pellino-1 expression, they do support a potential involvement, wherein IRF3 activation may partially regulate Pellino-1 activation. Indeed, the TBK1/IKKε complex have been identified as mediators of Pellino-1's E3 ligase activity in addition to the induction of the transcription of its gene in a TLR3 dependent manner (Smith et al., 2011). However, in contrast to data presented in this thesis, IRF3 knockout murine BMDMs resulted in the complete abolishment of Pellino-1 upregulation by poly(I:C) (Smith et al., 2011). Again, these observations highlight differences between mouse and humans in the regulation of Pellino-1 and its potential functional roles.

Further contradicting findings came with the creation of the Pellino-1 knock-in mouse with a point mutation inhibiting its E3 ubiquitin ligase activity (Enesa et al., 2012). Myeloid cells and embryonic fibroblasts from these knock-in mice showed a reduction in IFNβ expression and secretion in response to poly(I:C). This reduction is due to the impaired interaction of IRF3 with the IFNβ promoter; to a lesser extent Pellino-1 also regulates the IFNβ positive feedback loop wherein small amounts of IFNβ expressed following activation further amplify IFNβ production through the JAK-STAT pathway (Enesa et al., 2012). Recently findings also identified deformed epidermal autoregulatory factor 1 homologue (DEAF1) as a Pellino-1-interacting protein required for IFNβ transcription (Ordureau et al., 2013).

The varied functional data for Pellino-1 in TRIF-dependent signalling places Pellino-1 in distinct arms of the pathway. While the use of Pellino-1 knockout mice indicate an essential role for RIP1 ubiquitination and resultant NF-κB activation (Chang et al., 2009), the inhibition of Pellino-1's E3 ubiqutin ligase activity in knock-in mice indicate a role in the recruitment of IRF3 to the IFNβ promoter (Enesa et al., 2012). It may be that variations reported on Pellino'1 role in IFNβ signalling is due to functional compensation by other members of the Pellino family in Pellino-1 knockout mice (Moynagh, 2014). However, as discussed in **section 5.6** it is very likely that the creation of the knock-in model itself has had implications on the functionality of the protein. Further evidence is required to support the depletion of the E3 ligase activity in the knock-in model. Data in this thesis, supports the placement of Pellino-1 in the TRIF dependent arm NF-κB signalling. These data also potentially show substantial differences between human

and mouse models, and reinforces the need to study primary cells from specific human organs such as the lungs in order to understand roles in specific diseases in humans.

5.8 Pellino-1 potential binding partners: A20, TNIP1 and TAX1BP1

Data presented in this thesis highlights substantial differences between human and mouse models. Additionally, the role of Pellino-1 in regulating TLR3 signalling through the interaction with RIP1 remains controversial. Proteomics analysis was therefore explored with the aim of Identifying binding partners that would help clarify signalling.

Proteomic analysis identified multiple proteins that may have an affinity to Pellino-1. A total of 334 proteins were identified across both 4 hours and 24 hours stimulation with poly(I:C) providing an extensive list of viable candidates for Pellino-1 binding. It is however important to note that many of these proteins identified by mass-spectrometry show equally high affinity to our protein of interest Pellino-1 as the control mouse $IgG2_A$ suggesting non-specific binding. These data must therefore be interpreted with caution and serve only as a guide to possible Pellino-1 targets requiring further confirmation with techniques such as protein complex-immunoprecipitation (Co-IP), ligand binding assays, transient knockdowns or over-expression.

Of the identified proteins, A20 [also known as tumour necrosis factor, alpha-induced protein 3 (TNFAIP3)], TNFAIP3 interacting protein (TNIP1) (also known as ABIN1) and Tax1-binding protein 1 (TAX1BP1) were of particular interest due to their involvement with NF-κB signalling.

A20 is a potent negative regulator of NF-κB signalling wherein its knockdown results in chronic multi-organ inflammation and cell death in mice (Lee et al., 2012). A20 displays a protective role against both bacterial and viral infections (Reviewed in (Kelly et al., 2011)). A20 has been shown to attenuate NF-κB activation in bronchial airway epithelial cells following infection with H3N2 and H1N1 influenza virus (Onose et al., 2006). A20 contains two ubiquitin-editing domains giving it both a deubiquitinating (DUB) and an E3 ubiquitin ligase activity. A20 downregulates NF-κB activity in the TNFR pathway through the cleavage of lysine 63 (K63)–linked polyubiquitin chains on RIP1 followed by the conjugation of lysine 48 (K48)–linked polyubiquitin chains that target RIP1 for degradation by the proteasome (Wertz et al., 2004). A20 also exerts its negative regulatory effects on TLR dependent NF-κB signalling through the deubiquitination of TRAF6 (Boone et al., 2004). Furthermore, A20 also uses multiple adaptors to deubiquitinate specific signalling molecules.

One of these many adaptors and interacting partners is TNIP1. While both A20 and TNIP1 overexpression inhibits TNF, LPS and IL-1 induced NF-κB activation in HEK293 cells (Heyninck et al., 1999), the inhibitory effect of TNIP1 overexpression can be impaired by the RNA interference of A20 suggesting that TNIP1 regulates NF-κB activation through A20. Specifically, TNIP1 has been found to physically link A20 to ubiquitinated IKKγ rendering it inactive through A20-mediated deubiquitination of IKKγ and leading to NF-κB inhibition (Mauro et al., 2006). Tandem affinity purification also revealed NFKB1 and NFKB2 as TNIP1 interacting proteins, but not their active components p52 and p50 (Bouwmeester et al., 2004). Additionally, the interaction with NFKB2 was dependent on NIK activation, however no functional significance has yet been attributed to these interactions (Bouwmeester et al., 2004).

The overexpression of TNIP1 also led to the discovery of its anti-apoptotic activities, wherein TNIP1 prevents TNF-induced apoptosis in cultured hepatocytes and *in vivo* (Wullaert et al., 2005). While A20 also displays anti-apoptotic features, A20 deficient cells still retain TNIP1-induced anti-apoptotic effects suggesting these are A20-independent functions. Moreover, TNIP1 inhibits caspase-8 recruitment to FADD, thus preventing caspase-8 cleavage and apoptosis in response to TNF (Oshima et al., 2009).

Another A20 adaptor displaying similar functions is ubiquitin-binding-domain-containing TAX1BP1. TAX1BP1 similarly inhibits RIP1 and TRAF6 polyubiquitination via the recruitment of ubiquitin-editing A20 (Iha et al., 2008). In addition, A20 regulates antiviral immunity through TAX1BP1, by disrupting Lys63-ubiquitination of TBK1/IKKε in mouse embryonic fibroblasts (Parvatiyar et al., 2010).

These data indicate a potentially novel mechanism of action for Pellino-1, wherein it regulates NF-κB signalling through the negative regulator A20 or its adaptor proteins TNIP1 or TAX1BP1. With epithelial cells from COPD patient airways showing increased levels of Pellino-1 expression following viral stimulation, it is possible that Pellino-1 inhibits A20's negative regulatory functions and that through the manipulation of Pellino-1 expression could result in decreased hallmark inflammatory response of COPD. These preliminary proteomics will require confirmation with protein co-immunoprecipitation (Co-IP) and ligand binding assays to determine their significance. If any of these targets are confirmed as Pellino-1 binding partners, further investigations into the signalling molecules regulated by these in Pellino-1 knockdown cells could help determine Pellino-1's regulation profile. The transient knockdown of A20, TNIP1 or TAX1BP1 in Pellino-1 knockdown cells compared with control cells would also help determine if the effects of A20 knockdown are mediated by the targeting of Pellino-1.

Finally, the use of ubiquitin-linkage specific antibodies will provide insight into the type ubiquitin chains tagged by Pellino-1.

5.9 Pellino-1 in MAPK signalling

TLR3 signalling following viral induction bifurcates downstream of TRIF (**Figure 1.1**). While the initiation of inflammatory signalling can lead to the phosphorylation of IRF3 and the resulting IFNβ, it can also lead to the activation of IKKs and MAP kinases and in turn the activation of NF-κB and AP-1 respectively (see **section 1.6.3**). Coordinated activation of MAPKs has been shown to regulate CXCL8 expression in response to TNFα in airway epithelial cell line (Li et al., 2002). Stabilization of CXCL8 mRNA can also be controlled by p38 (Hoffmann et al., 2002). As Pellino-1 does not appear to elicit its effects through the degradation of IκBα, the rate-limiting step of canonical NF-κB signalling, it was hypothesised that instead Pellino-1 may play a role in the regulation and activation of MAPK as an alternative route to CXCL8 transcription.

AP-1 activation is mediated by MAP kinases such as JNK, ERK and p38 (Kawai and Akira, 2007). Preliminary data suggested a role for Pellino-1 in the regulation of AP-1 in HBEpCs through p38 MAPK due to a measurable decrease in phospho p38 activity in Pellino-1 knockdown samples. These data contrast that from the Pellino-1 knock-in mouse showing no deficiency in poly(I:C)-induced activation of MAP kinases in BMDM (Enesa et al., 2012).

Further assessment of Pellino-1 involvement in AP-1 signalling was measured by the inhibition of JNK, ERK and p38 through their respective inhibitors SP600125, PD98059 and SB203580. Surprisingly, while JNK and p38 inhibitors did not alter Pellino-1 expression in response to poly(I:C), Pellino-1 mRNA and protein were inhibited by MEK1 inhibitor PD98059 and U0126 suggesting that Pellino-1 is regulated by ERK (demonstrated in **Figure 5.2**). In addition, Pellino-1 knockdown did not alter phospho ERK expression in HBEpCs at 4 or 24 hour post stimulation with poly(I:C), in keeping with data from Jenson et al. whereby overexpression of Pellino-2, but not Pellino-1, activated the ERK and JNK MAPK pathways (Jensen and Whitehead, 2003a). To add further insight into the role of MEK1 in Pellino-1 regulation, it would be advisable to continue determine the phosphorylation and/or activation of Pellino-1 E3 ligase activity of Pellino-1 following stimulation with poly(I:C) or RV. The phosphorylation of Pellino-1 by MEK1

could be measured by mass spectrometry, and while the E3 ligase activity will be determined by a ubiquitination assay.

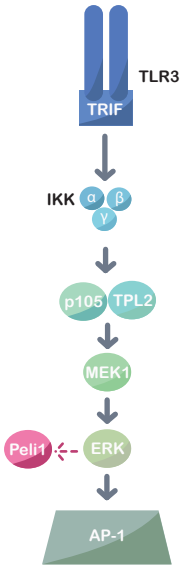

Figure 5.2 Possible mechanism for the regulation of Pellino-1 by ERK

This figure highlights a possible mechanism for the regulation of Pellino-1 by ERK in HBEpCs. Upon TLR3 activation, transcription factors such as NF-κB and MAPKs are activated. MAPKs form part of a protein kinase cascade consisting of at least three sequentially activated enzymes resulting in the activation of ERK, p38s, and JNK/SAPKs. ERK is regulated by the upstream MAPKK ligand MEK1.

5.10 Summary

This thesis has investigated the regulation of Pellino-1 and its role in viral infection in human bronchial airway epithelial cells. Data presented in this thesis showed that Pellino-1 expression is upregulated in response to the TLR3 agonist poly(I:C) in a TRIF-dependent pathway in human airway epithelial cells. These data resulted in the hypothesis that Pellino-1 may be selectively mediating the TRIF-dependent NF-κB/MAPK pathway and not TLR3-mediated IRF3 and IFNβ activation.

In support of the hypothesis, the transient knockdown of Pellino-1 in airway epithelial cells stimulated with poly(I:C) resulted in the decrease in IKKα/β phosphorylation. However, total

IκBα degradation was not compromised which suggested that Pellino-1 may instead be operating through the non-canonical NF-κB pathway. Preliminary data suggested Pellino-1 negatively regulates the non-canonical NF-κB signalling through NFKB2. Additionally, the transient knockdown of NFKB2 in HBEpCs contrasted the phenotype of Pellino-1 knockdown and in turn did not regulate Pellino-1 mRNA expression. It is therefore possible that following viral infection in airway epithelial cells, TLR3 activation culminates in the up-regulation of Pellino-1 leading to an increase in NFKB2 expression, resulting in the suppression of NF-κB specific gene transcription.

NFKB2 expression was also quantified in epithelial cells isolated from diseased lung airway epithelium of COPD patients then virally infected. Both Pellino-1 and NFKB2 were significantly expressed in these cells versus unstimulated control. Existing evidence supports NFKB2 as the first clear negative regulatory pathway that may limit ongoing TLR3 signalling in a pathway-specific manner, and suggests that future exploration of non-canonical NF-κB signalling in airways epithelial cells will be important in understanding how chronic inflammation may be regulated in these cells.

Proteomics analysis further identified a potentially novel mechanism of action for Pellino-1, wherein it regulates NF-κB signalling through the negative regulator A20 or its adaptor proteins TNIP1 or TAX1BP1. With epithelial cells from COPD patient airways showing increased levels of Pellino-1 expression following viral stimulation, it is possible that Pellino-1 inhibits A20's negative regulatory functions and that through the manipulation of Pellino-1 expression could result in decreased hallmark inflammatory response of COPD.

In addition to the roles in non-canonical NF-κB signalling, the role of Pellino-1 in the regulation and activation of MAPK as an alternative route to inflammatory regulation was also explored. Preliminary data suggested a role for Pellino-1 in the regulation of AP-1 in HBEpCs through p38 MAPK. While assessment of the impact of the inhibition of the MAPKs on Pellino-1 expression led to the novel discovery of ERK as a potential Pellino-1 regulator.

A role for Pellino-1 in regulating TLR3 signalling through the interaction with RIP1 has previously been identified but remains controversial. It was therefore hypothesised that if RIP1 were indeed a target of Pellino-1 then RIP1 knockdown should recapitulate the Pellino-1 knockdown phenotype. In contrast, RIP1 knockdown significantly increased the inflammatory

response in HBEpCs. Furthermore, proteomics analysis of Pellino-1 interacting proteins did not identify RIP1 as a Pellino-1 binding partner. However, Pellino-1 seems to have a regulatory role in caspase-8 apoptosis, a RIP1 dependent cell death mechanism. It is therefore possible that Pellino-1 may similarly serve as a negative regulator of apoptosis via the polyubiquitination of RIP1 in response to viral stimuli.

Data in this thesis clearly indicates that the ablation of Pellino-1 in human airway epithelial cells results in a significant reduction in the TLR3-induced activation of the NF-κB induction of cytokines such as CXCL8. This data has been aligned with existing findings adding value and insight into the potential roles and mechanisms of Pellino-1 function in COPD and highlighted as a molecule with potential therapeutic value.

APPENDIX

1. ELISA buffers composition

Wash Buffer (pH 7.2-7.4)

	Final Concentration	Mass/ Volume
NaCl	0.5 M	292.2 g
NaH_2PO_4	2.5 mM	3 g
Na_2HPO_4	7.5 mM	10.7 g
Tween®-20	0.1 %	10 ml
Water		To 10 litres

Coating Buffer (pH 7.2-7.4)

	Final Concentration	Mass/ Volume
NaCl	0.14 M	8.18 g
KCl	2.7 mM	0.2 g
Na_2HPO_4	8.1 mM	1.15 g
KH_2PO_4.	1.5 mM	0.2 g
Water		To 1 litre

2. PCR buffers composition

50 x TAE

	Final Concentration	Mass /Volume
Tris Base	1.67 M	242 g
EDTA	50 mM	37.2 g
Glacial Acetic Acid		57.1 ml
Water		To 1 litre

3. Quantitative PCR primer-probe sequences

Target	Type	Sequence (5'-3')
RV1B	Forward	GTGAAGAGCCSCRTGTGCT
	Reverse	GCTSCAGGGTTAAGGTTAGCC
	Probe	TGAGTCCTCCGGCCCCTGAATG
IFNβ	Forward	CGCCGCATTGACCATCTA
	Reverse	CGCCGCATTGACCATCTA
	Probe	CGCCGCATTGACCATCTA

4. Western Blotting

Phosphatase Lysis Buffer

Reagent	Concentration	Mass/Volume
Tris Base	50mM	0.3 g
Sodium Fluoride	50 mM	0.1 g
β-glycerophosphate	50 mM	0.54 g
Sodium Orthovanadate	10 mM	0.09 g
Triton X-100	1%	500 µl
Water	Up to 50 ml	
PMSF	1 mM *Only add prior to use	
Protease inhibitor cocktail III	1:100 *Only add prior to use	

Resolving Gel

Reagent	10% (40-120 kDa)	12% (15-50 kDa)
Distilled water	5.9 ml	4.9 ml
30% Acrylamide	5 ml	6 ml
1.5 M Tris (pH 8.8)	3.8 ml	3.8 ml
20% SDS	75 µl	75 µl
20% APS	150 µl	150 µl
TEMED	6 µl	6 µl

Stacking Gel

Reagent	5%
Distilled water	2.8 ml
30% Acrylamide	830 µl
1 M Tris (pH 6.8)	1.26 ml
20% SDS	25 µl
20% APS	50 µl
TEMED	5 µl

10 x SDS Running Buffer

Reagent	Concentration	Mass/Volume
Tris	0.2 M	30.3 g
Glycine	1.92 M	144 g
SDS	20%	10 g
Water		Make up to 1 L

10 X Transfer Buffer

Reagent	Concentration	Mass/Volume
Tris	0.25 M	36.3 g
Glycine	2.4 M	181.25 g
Water		Make up to 1 L

5. Full list of potential Pellino-1 interacting partners generated by mass spectometry

Gene names	Protein names	Timepoint
A2M	Alpha-2-macroglobulin	4 and 24 hour
ACAT1	Acetyl-CoA acetyltransferase, mitochondrial	24 hour
ACO2	Aconitate hydratase, mitochondrial	24 hour
ACOT9	Acyl-coenzyme A thioesterase 9, mitochondrial	24 hour
ACSL3	Long-chain-fatty-acid--CoA ligase 3	4 and 24 hour
ACTB	Actin, cytoplasmic 1;Actin, cytoplasmic 1, N-terminally processed	24 hour
ACTB;ACTG1	Actin, cytoplasmic 1, N-terminally processed; Actin, cytoplasmic 2, N-terminally processed	4 hour
ACTBL2	Beta-actin-like protein 2	4 and 24 hour
ACTC1;ACTA1;ACTA2;ACTG2	Actin, alpha cardiac muscle 1;Actin, alpha skeletal muscle;Actin, aortic smooth muscle;Actin, gamma-enteric smooth muscle	4 and 24 hour
AFP	Alpha-fetoprotein	4 and 24 hour
AGPS	Alkyldihydroxyacetonephosphate synthase, peroxisomal	24 hour
AHCY	Adenosylhomocysteinase	4 and 24 hour
AHNAK	Neuroblast differentiation-associated protein AHNAK	4 and 24 hour
AHSG	Alpha-2-HS-glycoprotein;Alpha-2-HS-glycoprotein chain A;Alpha-2-HS-glycoprotein chain B	4 and 24 hour
AIFM1	Apoptosis-inducing factor 1, mitochondrial	24 hour
ALB	Serum albumin	4 and 24 hour
ALDH1B1	Aldehyde dehydrogenase X, mitochondrial	24 hour
ALDH2	Aldehyde dehydrogenase, mitochondrial	24 hour
ALDH4A1	Delta-1-pyrroline-5-carboxylate dehydrogenase, mitochondrial	4 and 24 hour
ALDH7A1	Alpha-aminoadipic semialdehyde dehydrogenase	24 hour
ALDOA	Fructose-bisphosphate aldolase A;Fructose-bisphosphate aldolase	4 and 24 hour
ANXA1	Annexin A1	4 hour
ANXA2;ANXA2P2	Annexin A2;Annexin;Putative annexin A2-like protein	4 and 24 hour
APOA1	Apolipoprotein A-I;Truncated apolipoprotein A-I	4 hour
APOB	Apolipoprotein B-100;Apolipoprotein B-48	4 and 24 hour
APOC3	Apolipoprotein C-III	4 and 24 hour
APOE	Apolipoprotein E	4 and 24 hour
ARG1	Arginase-1	4 hour
ARGLU1	Arginine and glutamate-rich protein 1	4 hour
ARL8A;ARL8B	ADP-ribosylation factor-like protein 8A;ADP-ribosylation factor-like protein 8B	24 hour
ARPC4;ARPC4-TTLL3	Actin-related protein 2/3 complex subunit 4	24 hour
ARID1B	AT-rich interactive domain-containing protein 1B	4 hour
ATAD3A	ATPase family AAA domain-containing protein 3A	24 hour
ATP1A1;ATP4A;ATP1A2;ATP1A3	Sodium/potassium-transporting ATPase subunit alpha-1;Potassium-transporting ATPase alpha chain 1;Sodium/potassium-transporting ATPase subunit alpha-2;Sodium/potassium-transporting ATPase subunit alpha-3	4 and 24 hour
ATP2A2	Sarcoplasmic/endoplasmic reticulum calcium ATPase 2	4 and 24 hour
ATP5A1	ATP synthase subunit alpha, mitochondrial	4 and 24 hour
ATP5B	ATP synthase subunit beta, mitochondrial;ATP synthase subunit beta	4 and 24 hour
ATP5C1	ATP synthase subunit gamma, mitochondrial;ATP synthase gamma chain	4 and 24 hour
ATP5F1	ATP synthase subunit b, mitochondrial	4 and 24 hour
ATP5J2;PTCD1	ATP synthase subunit f, mitochondrial	24 hour
ATP5L	ATP synthase subunit g, mitochondrial	4 and 24 hour
ATP5O	ATP synthase subunit O, mitochondrial	4 and 24 hour
ATP6V1A	V-type proton ATPase catalytic subunit A	24 hour
BASP1	Brain acid soluble protein 1	24 hour
BCAP31	B-cell receptor-associated protein 31	24 hour
BCKDK	[3-methyl-2-oxobutanoate dehydrogenase [lipoamide]] kinase, mitochondrial	24 hour
BCL9L	B-cell CLL/lymphoma 9-like protein	4 hour
C3	Complement C3	4 and 24 hour
C4A;C4B	Complement C4-A;Complement C4-B	4 hour
C5	Complement C5	4 hour
C9	Complement component C9;Complement component C9a;Complement	4 hour

	component C9b	
CACNA1D	Voltage-dependent L-type calcium channel subunit alpha-1D	4 hour
CALR	Calreticulin	24 hour
CALML5	Calmodulin-like protein 5	4 hour
CANX	Calnexin	24 hour
CAPN2	Calpain-2 catalytic subunit	4 hour
CAPZA2;CAPZA1	F-actin-capping protein subunit alpha-2;F-actin-capping protein subunit alpha-1	24 hour
CASP14	Caspase-14;Caspase-14 subunit p19;Caspase-14 subunit p10	4 hour
CAT	Catalase	4 and 24 hour
CBR4	Carbonyl reductase family member 4	24 hour
CCT3	T-complex protein 1 subunit gamma	24 hour
CCT8	T-complex protein 1 subunit theta	24 hour
CD63	CD63 antigen	24 hour
CDK11B;CDK11A;CDC2L2	Cyclin-dependent kinase 11B;Cyclin-dependent kinase 11A	4 hour
CDKAL1	Threonylcarbamoyladenosine tRNA methylthiotransferase	4 and 24 hour
CDRT15L2	CMT1A duplicated region transcript 15 protein-like protein	24 hour
CDSN	Corneodesmosin	4 and 24 hour
CHTOP	Chromatin target of PRMT1 protein	4 and 24 hour
CKAP4	Cytoskeleton-associated protein 4	24 hour
CLTC	Clathrin heavy chain 1	24 hour
COL1A1	Collagen alpha-1(I) chain	4 and 24 hour
COL1A2	Collagen alpha-2(I) chain	4 and 24 hour
COL3A1	Collagen alpha-1(III) chain	4 and 24 hour
COL8A1	Collagen alpha-1(VIII) chain;Vastatin	24 hour
COPS2		4 hour
CRNN	Cornulin	4 hour
CSDA	DNA-binding protein A	24 hour
CSNK1A1;CSNK1A1L	Casein kinase I isoform alpha;Casein kinase I isoform alpha-like	4 hour
CSTA	Cystatin-A	4 and 24 hour
CSTB	Cystatin-B	4 hour
CTNNA1	Catenin alpha-1	24 hour
CTNND1	Catenin delta-1	4 hour
CTSB	Cathepsin B;Cathepsin B light chain;Cathepsin B heavy chain	24 hour
CYB5R3	NADH-cytochrome b5 reductase 3;NADH-cytochrome b5 reductase 3 membrane-bound form;NADH-cytochrome b5 reductase 3 soluble form	24 hour
CTSD	Cathepsin D;Cathepsin D light chain;Cathepsin D heavy chain	4 hour
DBN1	Drebrin	4 hour
DCD	Dermcidin;Survival-promoting peptide;DCD-1	4 and 24 hour
DDB1	DNA damage-binding protein 1	24 hour
DDOST	Dolichyl-diphosphooligosaccharide--protein glycosyltransferase 48 kDa subunit	4 and 24 hour
DDX17;DDX5	Probable ATP-dependent RNA helicase DDX17;Probable ATP-dependent RNA helicase DDX5	4 and 24 hour
DDX47	Probable ATP-dependent RNA helicase DDX47	24 hour
DDX5;DDX17	Probable ATP-dependent RNA helicase DDX5;Probable ATP-dependent RNA helicase DDX17	24 hour
DECR1	2,4-dienoyl-CoA reductase, mitochondrial	24 hour
DHCR7	7-dehydrocholesterol reductase	
DHRS1	Dehydrogenase/reductase SDR family member 1	24 hour
DHRS4L1;DHRS4	Putative dehydrogenase/reductase SDR family member 4-like 2;Dehydrogenase/reductase SDR family member 4	24 hour
DHX15	Putative pre-mRNA-splicing factor ATP-dependent RNA helicase DHX15	4 and 24 hour
DHX9	ATP-dependent RNA helicase A	24 hour
DLG5	Disks large homolog 5	24 hour
DLST	Dihydrolipoyllysine-residue succinyltransferase component of 2-oxoglutarate dehydrogenase complex, mitochondrial	24 hour
DSC1	Desmocollin-1	4 and 24 hour
DSC3	Desmocollin-3	4 hour
DSG1	Desmoglein-1	4 and 24 hour
DSP	Desmoplakin	4 and 24 hour
EBP	3-beta-hydroxysteroid-Delta(8),Delta(7)-isomerase	4 hour
ECM1	Extracellular matrix protein 1	4 hour

EEF1A1;EEF1A1P5;EEF1A2	Elongation factor 1-alpha 1;Putative elongation factor 1-alpha-like 3;Elongation factor 1-alpha 2	4 and 24 hour
EEF1G	Elongation factor 1-gamma	4 and 24 hour
EEF2	Elongation factor 2	24 hour
EIF4A2;EIF4A1	Eukaryotic initiation factor 4A-II;Eukaryotic initiation factor 4A-I	24 hour
EIF4A3	Eukaryotic initiation factor 4A-III	24 hour
ELAVL1	ELAV-like protein 1	24 hour
ENO1	Alpha-enolase	4 and 24 hour
ENO2	Gamma-enolase;Enolase	4 hour
EPHB2;EPHA6;EPHB3;EPHA7; EPHB4;EPHA4;EPHB1;EPHA2	Ephrin type-B receptor 2;Ephrin type-A receptor 6;Ephrin type-B receptor 3;Ephrin type-A receptor 7;Ephrin type-B receptor 4;Ephrin type-A receptor 4;Ephrin type-B receptor 1;Ephrin type-A receptor 2	24 hour
ERAP1	Endoplasmic reticulum aminopeptidase 1	24 hour
ERG	Transcriptional regulator ERG	4 hour
ERH	Enhancer of rudimentary homolog	24 hour
ERLIN1;ERLIN2	Erlin-1;Erlin-2	4 and 24 hour
ERO1L	ERO1-like protein alpha	24 hour
ESYT1	Extended synaptotagmin-1	24 hour
ETFA	Electron transfer flavoprotein subunit alpha, mitochondrial	24 hour
ETFB	Electron transfer flavoprotein subunit beta	24 hour
ETHE1	Protein ETHE1, mitochondrial	24 hour
F2	Prothrombin;Activation peptide fragment 1;Activation peptide fragment 2;Thrombin light chain;Thrombin heavy chain	4 and 24 hour
F5	Coagulation factor V;Coagulation factor V heavy chain;Coagulation factor V light chain	24 hour
FABP5	Fatty acid-binding protein, epidermal	4 and 24 hour
FADS2	Fatty acid desaturase 2	24 hour
FAF2	FAS-associated factor 2	24 hour
FBL	rRNA 2-O-methyltransferase fibrillarin	4 and 24 hour
FBLN1	Fibulin-1	24 hour
FBLN1		24 hour
FDFT1	Squalene synthase	24 hour
FLG	Filaggrin	4 and 24 hour
FLG2	Filaggrin-2	4 and 24 hour
FLNA	Filamin-A	4 and 24 hour
FLNB	Filamin-B	4 and 24 hour
FN1	Fibronectin;Anastellin;Ugl-Y1;Ugl-Y2;Ugl-Y3	4 and 24 hour
FTH1	Ferritin heavy chain;Ferritin	4 hour
FYTTD1	UAP56-interacting factor	24 hour
GAPDH	Glyceraldehyde-3-phosphate dehydrogenase	4 and 24 hour
GBP1	Interferon-induced guanylate-binding protein 1	4 and 24 hour
GC	Vitamin D-binding protein	4 hour
GGCT	Gamma-glutamylcyclotransferase	24 hour
GLS	Glutaminase kidney isoform, mitochondrial	24 hour
GNAI3;GNAI2;GNAO1;GNAI1	Guanine nucleotide-binding protein G(k) subunit alpha;Guanine nucleotide-binding protein G(i) subunit alpha-2;Guanine nucleotide-binding protein G(o) subunit alpha;Guanine nucleotide-binding protein G(i) subunit alpha-1	24 hour
GNB1;GNB2;GNB4;GNB3	Guanine nucleotide-binding protein G(I)/G(S)/G(T) subunit beta-1;Guanine nucleotide-binding protein G(I)/G(S)/G(T) subunit beta-2;Guanine nucleotide-binding protein subunit beta-4;Guanine nucleotide-binding protein G(I)/G(S)/G(T) subunit beta-3	24 hour
GNB2L1	Guanine nucleotide-binding protein subunit beta-2-like 1	4 hour
GOT2	Aspartate aminotransferase, mitochondrial;Aspartate aminotransferase	24 hour
GPD2	Glycerol-3-phosphate dehydrogenase, mitochondrial	24 hour
GRN	Granulins;Acrogranin;Paragranulin;Granulin-1;Granulin-2;Granulin-3;Granulin-4;Granulin-5;Granulin-6;Granulin-7	4 and 24 hour
GSDMA	Gasdermin-A	4 hour
GSN	Gelsolin	24 hour
GSTK1	Glutathione S-transferase kappa 1	24 hour
GTF2I	General transcription factor II-I	24 hour

H2AFX;HIST1H2AA;HIST1H2AB;HIST1H2AG;HIST1H2AD;HIST2H2AA3;HIST3H2A;HIST1H2AC;HIST2H2AB;HIST2H2AC;H2AFJ;HIST1H2AH;HIST1H2AJ	Histone H2A.x;Histone H2A type 1-A;Histone H2A type 1-B/E;Histone H2A type 1;Histone H2A type 1-D;Histone H2A type 2-A;Histone H2A type 3;Histone H2A type 1-C;Histone H2A type 2-B;Histone H2A type 2-C;Histone H2A.J;Histone H2A type 1-H;Histone H2A type 1-J;Histone H2A	4 hour
H2AFZ;H2AFV;H2AFX;HIST1H2AA;HIST1H2AB;HIST1H2AG;HIST1H2AD;HIST2H2AA3;HIST3H2A;HIST2H2AB;HIST1H2AC;HIST2H2AC;H2AFJ;HIST1H2AH;HIST1H2AJ	Histone H2A.Z;Histone H2A.V;Histone H2A;Histone H2A.x;Histone H2A type 1-A;Histone H2A type 1-B/E;Histone H2A type 1;Histone H2A type 1-D;Histone H2A type 2-A;Histone H2A type 3;Histone H2A type 2-B;Histone H2A type 1-C;Histone H2A type 2-C;Histone H2A.J;Histone H2A type 1-H;Histone H2A type 1-J	24 hour
HADHA	Trifunctional enzyme subunit alpha, mitochondrial;Long-chain enoyl-CoA hydratase;Long chain 3-hydroxyacyl-CoA dehydrogenase	4 and 24 hour
HADHB	Trifunctional enzyme subunit beta, mitochondrial;3-ketoacyl-CoA thiolase	24 hour
HBA1;HBA2	Hemoglobin subunit alpha	4 and 24 hour
HBB;HBD	Hemoglobin subunit beta;LVV-hemorphin-7;Hemoglobin subunit delta	4 and 24 hour
HIST1H1B	Histone H1.5	4 and 24 hour
HIST1H1C;HIST1H1D;HIST1H1E	Histone H1.2;Histone H1.3;Histone H1.4	4 and 24 hour
HIST1H4A	Histone H4	4 and 24 hour
HIST2H2BF;HIST1H2BK;H2BFS;HIST1H2BD;HIST1H2BC;HIST1H2BH;HIST1H2BN;HIST1H2BM;HIST1H2BL;HIST1H2BJ;HIST1H2BO;HIST1H2BB;HIST2H2BE;HIST3H2BB;HIST1H2BA	Histone H2B;Histone H2B type 1-K;Histone H2B type F-S;Histone H2B type 1-D;Histone H2B type 1-C/E/F/G/I;Histone H2B type 2-F;Histone H2B type 1-H;Histone H2B type 1-N;Histone H2B type 1-M;Histone H2B type 1-L;Histone H2B type 1-J;Histone H2B type 1-O;Histone H2B type 1-B;Histone H2B type 2-E;Histone H2B type 3-B;Histone H2B type 1-A	4 and 24 hour
HK1	Hexokinase-1	24 hour
HLA-A;HLA-C;HLA-H	HLA class I histocompatibility antigen, A-68 alpha chain;HLA class I histocompatibility antigen, A-2 alpha chain;HLA class I histocompatibility antigen, A-3 alpha chain;HLA class I histocompatibility antigen, A-24 alpha chain;HLA class I histocompatibility antigen, A-32 alpha chain;HLA class I histocompatibility antigen, A-69 alpha chain;HLA class I histocompatibility antigen, A-11 alpha chain;HLA class I histocompatibility antigen, A-30 alpha chain;HLA class I histocompatibility antigen, A-31 alpha chain;HLA class I histocompatibility antigen, A-33 alpha chain;HLA class I histocompatibility antigen, A-25 alpha chain;HLA class I histocompatibility antigen, A-23 alpha chain;HLA class I histocompatibility antigen, A-26 alpha chain;HLA class I histocompatibility antigen, A-34 alpha chain;HLA class I histocompatibility antigen, A-43 alpha chain;HLA class I histocompatibility antigen, A-66 alpha chain;HLA class I histocompatibility antigen, A-74 alpha chain;HLA class I histocompatibility antigen, A-29 alpha chain;HLA class I histocompatibility antigen, A-80 alpha chain;HLA class I histocompatibility antigen, Cw-17 alpha chain;HLA class I histocompatibility antigen, Cw-16 alpha chain;HLA class I histocompatibility antigen, Cw-5 alpha chain;HLA class I histocompatibility antigen, A-1 alpha chain;HLA class I histocompatibility antigen, A-36 alpha chain;Putative HLA class I histocompatibility antigen, alpha chain H	24 hour

HLA-B	HLA class I histocompatibility antigen, B-7 alpha chain;HLA class I histocompatibility antigen, B-8 alpha chain;HLA class I histocompatibility antigen, B-41 alpha chain;HLA class I histocompatibility antigen, B-42 alpha chain;HLA class I histocompatibility antigen, B-40 alpha chain;HLA class I histocompatibility antigen, B-27 alpha chain;HLA class I histocompatibility antigen, B-58 alpha chain;HLA class I histocompatibility antigen, B-37 alpha chain;HLA class I histocompatibility antigen, B-51 alpha chain;HLA class I histocompatibility antigen, B-57 alpha chain;HLA class I histocompatibility antigen, B-14 alpha chain;HLA class I histocompatibility antigen, B-15 alpha chain;HLA class I histocompatibility antigen, B-18 alpha chain;HLA class I histocompatibility antigen, B-39 alpha chain;HLA class I histocompatibility antigen, B-44 alpha chain;HLA class I histocompatibility antigen, B-45 alpha chain;HLA class I histocompatibility antigen, B-46 alpha chain;HLA class I histocompatibility antigen, B-47 alpha chain;HLA class I histocompatibility antigen, B-49 alpha chain;HLA class I histocompatibility antigen, B-50 alpha chain;HLA class I histocompatibility antigen, B-52 alpha chain;HLA class I histocompatibility antigen, B-53 alpha chain;HLA class I histocompatibility antigen, B-54 alpha chain;HLA class I histocompatibility antigen, B-55 alpha chain;HLA class I histocompatibility antigen, B-56 alpha chain;HLA class I histocompatibility antigen, B-78 alpha chain;HLA class I histocompatibility antigen, B-35 alpha chain;HLA class I histocompatibility antigen, B-82 alpha chain;HLA class I histocompatibility antigen, B-67 alpha chain;HLA class I histocompatibility antigen, B-59 alpha chain;HLA class I histocompatibility antigen, B-38 alpha chain;HLA class I histocompatibility antigen, B-13 alpha chain;HLA class I histocompatibility antigen, B-48 alpha chain;HLA class I histocompatibility antigen, B-81 alpha chain	
HNRNPA0	Heterogeneous nuclear ribonucleoprotein A0	4 and 24 hour
HNRNPA1	Heterogeneous nuclear ribonucleoprotein A1	24 hour
HNRNPA2B1	Heterogeneous nuclear ribonucleoproteins A2/B1	4 and 24 hour
HNRNPAB		24 hour
HNRNPC;HNRNPCL1	Heterogeneous nuclear ribonucleoproteins C1/C2;Heterogeneous nuclear ribonucleoprotein C-like 1	4 and 24 hour
HNRNPH1;HNRNPF	Heterogeneous nuclear ribonucleoprotein H;Heterogeneous nuclear ribonucleoprotein H, N-terminally processed;Heterogeneous nuclear ribonucleoprotein F;Heterogeneous nuclear ribonucleoprotein F, N-terminally processed	4 hour
HNRNPK	Heterogeneous nuclear ribonucleoprotein K	24 hour
HNRNPL	Heterogeneous nuclear ribonucleoprotein L	
HNRNPM	Heterogeneous nuclear ribonucleoprotein M	4 and 24 hour
HNRNPU	Heterogeneous nuclear ribonucleoprotein U	4 and 24 hour
HNRNPUL2;hCG_2044799	Heterogeneous nuclear ribonucleoprotein U-like protein 2	24 hour
HRNR	Hornerin	4 and 24 hour
HSD17B10	3-hydroxyacyl-CoA dehydrogenase type-2	24 hour
HSD17B12	Estradiol 17-beta-dehydrogenase 12	
HSD17B4	Peroxisomal multifunctional enzyme type 2;(3R)-hydroxyacyl-CoA dehydrogenase;Enoyl-CoA hydratase 2	24 hour
HSP90AA1;HSP90AA2	Heat shock protein HSP 90-alpha;Putative heat shock protein HSP 90-alpha A2	4 hour
HSP90AB1;HSP90AB3P	Heat shock protein HSP 90-beta;Putative heat shock protein HSP 90-beta-3	4 and 24 hour
HSP90AB2P	Putative heat shock protein HSP 90-beta 2	4 hour
HSP90B1	Endoplasmin	4 and 24 hour
HSPA1A	Heat shock 70 kDa protein 1A/1B	24 hour
HSPA5	78 kDa glucose-regulated protein	4 and 24 hour
HSPA6;HSPA7;HSPA1A;HSPA1L;HSPA8	Heat shock 70 kDa protein 6;Putative heat shock 70 kDa protein 7;Heat shock 70 kDa protein 1A/1B;Heat shock 70 kDa protein 1-like	4 and 24 hour
HSPA8;HSPA2	Heat shock cognate 71 kDa protein;Heat shock-related 70 kDa protein 2	4 and 24 hour
HSPA9	Stress-70 protein, mitochondrial	4 and 24 hour
HSPB1	Heat shock protein beta-1	4 and 24 hour
HSPD1	60 kDa heat shock protein, mitochondrial	4 and 24 hour
HSPE1	10 kDa heat shock protein, mitochondrial	24 hour
HYOU1	Hypoxia up-regulated protein 1	24 hour
IARS	Isoleucine--tRNA ligase, cytoplasmic	24 hour
IDH2	Isocitrate dehydrogenase [NADP], mitochondrial;Isocitrate dehydrogenase [NADP]	4 hour

IGHG1	Ig gamma-1 chain C region	4 and 24 hour
IGHG4;IGHG3	Ig gamma-4 chain C region;Ig gamma-3 chain C region	4 and 24 hour
IGKC	Ig kappa chain C region	4 and 24 hour
IGLC2;IGLC3;IGLC6;IGLC1	Ig lambda-2 chain C regions;Ig lambda-3 chain C regions;Ig lambda-6 chain C region;Ig lambda-1 chain C regions	4 and 24 hour
IGLL5	Immunoglobulin lambda-like polypeptide 5	4 and 24 hour
IL1R1	Interleukin-1 receptor type 1;Interleukin-1 receptor type 1, membrane form;Interleukin-1 receptor type 1, soluble form	24 hour
IMMT	Mitochondrial inner membrane protein	24 hour
ITIH2	Inter-alpha-trypsin inhibitor heavy chain H2	4 and 24 hour
ITIH3	Inter-alpha-trypsin inhibitor heavy chain H3	24 hour
ITIH4	Inter-alpha-trypsin inhibitor heavy chain H4;70 kDa inter-alpha-trypsin inhibitor heavy chain H4;35 kDa inter-alpha-trypsin inhibitor heavy chain H4	4 and 24 hour
JUP	Junction plakoglobin	4 and 24 hour
KAT5	Histone acetyltransferase KAT5	24 hour
KIF14	Kinesin-like protein KIF14	4 hour
KPRP	Keratinocyte proline-rich protein	24 hour
LAD1	Ladinin-1	24 hour
LAMA3	Laminin subunit alpha-3	24 hour
LAMB3	Laminin subunit beta-3	4 and 24 hour
LAMC2	Laminin subunit gamma-2	4 and 24 hour
LAMP1	Lysosome-associated membrane glycoprotein 1	4 hour
LDHA	L-lactate dehydrogenase A chain	4 and 24 hour
LDHB	L-lactate dehydrogenase B chain;L-lactate dehydrogenase	4 hour
LGALS3BP	Galectin-3-binding protein	24 hour
LGALS7	Galectin-7	
LGALS9	Galectin-9	24 hour
LMNA	Prelamin-A/C;Lamin-A/C	4 and 24 hour
LRRC73	Leucine-rich repeat-containing protein 73	4 hour
LRPPRC	Leucine-rich PPR motif-containing protein, mitochondrial	24 hour
LTF	Lactotransferrin;Kaliocin-1;Lactoferroxin-A;Lactoferroxin-B;Lactoferroxin-C	4 and 24 hour
LUC7L2;LUC7L	Putative RNA-binding protein Luc7-like 2;Putative RNA-binding protein Luc7-like 1	4 hour
LUC7L3	Luc7-like protein 3	4 and 24 hour
LYZ	Lysozyme C	4 hour
MBOAT7	Lysophospholipid acyltransferase 7	24 hour
MDH1	Malate dehydrogenase, cytoplasmic;Malate dehydrogenase	24 hour
MDH2	Malate dehydrogenase, mitochondrial;Malate dehydrogenase	4 and 24 hour
MGST1	Microsomal glutathione S-transferase 1	4 and 24 hour
MGST3	Microsomal glutathione S-transferase 3	4 hour
MMTAG2	Multiple myeloma tumor-associated protein 2	4 hour
MON1A	Vacuolar fusion protein MON1 homolog A	24 hour
MRPL14	39S ribosomal protein L14, mitochondrial	4 and 24 hour
MRPL2	39S ribosomal protein L2, mitochondrial	24 hour
MRPL22	39S ribosomal protein L22, mitochondrial	24 hour
MRPL37	39S ribosomal protein L37, mitochondrial	24 hour
MRPL9	39S ribosomal protein L9, mitochondrial	4 and 24 hour
MRPS11	28S ribosomal protein S11, mitochondrial	24 hour
MRPS18A	28S ribosomal protein S18a, mitochondrial	24 hour
MRPS21	28S ribosomal protein S21, mitochondrial	24 hour
MSMO1	Methylsterol monooxygenase 1	24 hour
MTMR4	Myotubularin-related protein 4	24 hour
MYH9	Myosin-9	4 and 24 hour
MYL12B;MYL12A	Myosin regulatory light chain 12B;Myosin regulatory light chain 12A	24 hour
MYO1B	Unconventional myosin-Ib	4 and 24 hour
MYOF	Myoferlin	24 hour
NARS2	Probable asparagine--tRNA ligase, mitochondrial	24 hour
NCL	Nucleolin	4 and 24 hour
NCLN	Nicalin	24 hour
NHP2L1	NHP2-like protein 1	24 hour
NNT	NAD(P) transhydrogenase, mitochondrial	24 hour
NOP56;NOL5A	Nucleolar protein 56	24 hour

OAT	Ornithine aminotransferase, mitochondrial;Ornithine aminotransferase, hepatic form;Ornithine aminotransferase, renal form	4 and 24 hour
OCIAD2	OCIA domain-containing protein 2	4 hour
OSBPL10	Oxysterol-binding protein-related protein 10;Oxysterol-binding protein	4 hour
OXA1L	Mitochondrial inner membrane protein OXA1L	24 hour
P4HB	Protein disulfide-isomerase	4 and 24 hour
PCBP3;PCBP2;PCBP1	Poly(rC)-binding protein 3;Poly(rC)-binding protein 2;Poly(rC)-binding protein 1	4 and 24 hour
PCK2	Phosphoenolpyruvate carboxykinase [GTP], mitochondrial	4 and 24 hour
PDHA1	Pyruvate dehydrogenase E1 component subunit alpha, somatic form, mitochondrial	24 hour
PDHB	Pyruvate dehydrogenase E1 component subunit beta, mitochondrial	4 and 24 hour
PDIA3	Protein disulfide-isomerase A3;Thioredoxin	4 and 24 hour
PDIA4	Protein disulfide-isomerase A4	24 hour
PDIA6	Protein disulfide-isomerase A6	4 and 24 hour
PELI1	**E3 ubiquitin-protein ligase pellino homolog 1**	4 and 24 hour
PGK1	Phosphoglycerate kinase 1;Phosphoglycerate kinase	4 and 24 hour
PHB	Prohibitin	4 and 24 hour
PHB2	Prohibitin-2	24 hour
PKM2	Pyruvate kinase isozymes M1/M2;Pyruvate kinase	4 and 24 hour
PKP1	Plakophilin-1	4 and 24 hour
PKP3	Plakophilin-3	4 hour
PLAA	Phospholipase A-2-activating protein	4 hour
PLEC	Plectin	4 hour
PLG	Plasminogen;Plasmin heavy chain A;Activation peptide;Angiostatin;Plasmin heavy chain A, short form;Plasmin light chain B	24 hour
PLOD2	Procollagen-lysine,2-oxoglutarate 5-dioxygenase 2	24 hour
POF1B	Protein POF1B	4 and 24 hour
PPA2	Inorganic pyrophosphatase 2, mitochondrial	24 hour
PPIB	Peptidyl-prolyl cis-trans isomerase B	4 and 24 hour
PRDX1;PRDX4	Peroxiredoxin-1;Peroxiredoxin-4	4 and 24 hour
PRDX2	Peroxiredoxin-2	4 hour
PRDX3	Thioredoxin-dependent peroxide reductase, mitochondrial	24 hour
PRDX4	Peroxiredoxin-4	24 hour
PRKDC	DNA-dependent protein kinase catalytic subunit	24 hour
PRPF40A	Pre-mRNA-processing factor 40 homolog A	24 hour
PRSS3	Trypsin-3	4 and 24 hour
PSMB5	Proteasome subunit beta type-5	24 hour
PSMC1	26S protease regulatory subunit 4	24 hour
PTBP3;PTBP1	Polypyrimidine tract-binding protein 3;Polypyrimidine tract-binding protein 1	24 hour
PTCD1;ATP5J2	ATP synthase subunit f, mitochondrial	4 hour
PUF60	Poly(U)-binding-splicing factor PUF60	4 and 24 hour
PYGL	Glycogen phosphorylase, liver form	4 hour
PZP	Pregnancy zone protein	4 and 24 hour
RAB10	Ras-related protein Rab-10	4 and 24 hour
RAB11B;RAB11A	Ras-related protein Rab-11B;Ras-related protein Rab-11A	4 and 24 hour
RAB14	Ras-related protein Rab-14	4 and 24 hour
RAB1A;RAB1C;RAB1B	Ras-related protein Rab-1A;Putative Ras-related protein Rab-1C;Ras-related protein Rab-1B	4 and 24 hour
RAB21	Ras-related protein Rab-21	4 and 24 hour
RAB2A;RAB2B	Ras-related protein Rab-2A;Ras-related protein Rab-2B	4 and 24 hour
RAB5B;RAB5A	Ras-related protein Rab-5B;Ras-related protein Rab-5A	24 hour
RAB5C	Ras-related protein Rab-5C	4 and 24 hour
RAB6A	Ras-related protein Rab-6A	24 hour
RAB7A	Ras-related protein Rab-7a	4 and 24 hour
RAB8A	Ras-related protein Rab-8A	24 hour
RAC2;RAC3;RAC1	Ras-related C3 botulinum toxin substrate 2;Ras-related C3 botulinum toxin substrate 3;Ras-related C3 botulinum toxin substrate 1	24 hour
RALY	RNA-binding protein Raly	4 hour
RAP1B;RAP1A	Ras-related protein Rap-1b;Ras-related protein Rap-1A	24 hour
RAP2C;RAP2A;RAP2B	Ras-related protein Rap-2c;Ras-related protein Rap-2a;Ras-related protein Rap-2b	24 hour
RBM14	RNA-binding protein 14	4 and 24 hour

RBM25	RNA-binding protein 25	4 hour
RBM39	RNA-binding protein 39	4 and 24 hour
RDH11	Retinol dehydrogenase 11	24 hour
RER1	Protein RER1	24 hour
RG9MTD1	Mitochondrial ribonuclease P protein 1	24 hour
RHOA;RHOC	Transforming protein RhoA;Rho-related GTP-binding protein RhoC	24 hour
RHOC;RHOA	Rho-related GTP-binding protein RhoC;Transforming protein RhoA	4 hour
RPL11	60S ribosomal protein L11	4 and 24 hour
RPL12	60S ribosomal protein L12	4 and 24 hour
RPL13	60S ribosomal protein L13	4 and 24 hour
RPL14	60S ribosomal protein L14	4 and 24 hour
RPL18	60S ribosomal protein L18	24 hour
RPL18A	60S ribosomal protein L18a	4 and 24 hour
RPL21	60S ribosomal protein L21	4 and 24 hour
RPL23	60S ribosomal protein L23	4 hour
RPL24	60S ribosomal protein L24	4 hour
RPL26;RPL26L1	60S ribosomal protein L26;60S ribosomal protein L26-like 1	4 and 24 hour
RPL27	60S ribosomal protein L27	4 hour
RPL27A	60S ribosomal protein L27a	4 and 24 hour
RPL28	60S ribosomal protein L28	4 and 24 hour
RPL29	60S ribosomal protein L29	4 and 24 hour
RPL3	60S ribosomal protein L3	4 and 24 hour
RPL30	60S ribosomal protein L30	4 hour
RPL34	60S ribosomal protein L34	4 hour
RPL35	60S ribosomal protein L35	4 and 24 hour
RPL35A	60S ribosomal protein L35a	4 and 24 hour
RPL36AL;RPL36A	60S ribosomal protein L36a-like;60S ribosomal protein L36a	4 hour
RPL37A;RPL37L	60S ribosomal protein L37a;Putative 60S ribosomal protein L37a-like	4 hour
RPL38	60S ribosomal protein L38	4 and 24 hour
RPL4	60S ribosomal protein L4	4 and 24 hour
RPL7	60S ribosomal protein L7	4 and 24 hour
RPL8	60S ribosomal protein L8	4 hour
RPL9	60S ribosomal protein L9	4 and 24 hour
RPLP0;RPLP0P6	60S acidic ribosomal protein P0;60S acidic ribosomal protein P0-like	4 and 24 hour
RPN1	Dolichyl-diphosphooligosaccharide--protein glycosyltransferase subunit 1	4 and 24 hour
RPN2	Dolichyl-diphosphooligosaccharide--protein glycosyltransferase subunit 2	4 and 24 hour
RPRD2	Regulation of nuclear pre-mRNA domain-containing protein 2	24 hour
RPS13	40S ribosomal protein S13	4 and 24 hour
RPS14	40S ribosomal protein S14	4 and 24 hour
RPS16	40S ribosomal protein S16	4 and 24 hour
RPS18	40S ribosomal protein S18	4 and 24 hour
RPS19	40S ribosomal protein S19	4 hour
RPS19BP1	Active regulator of SIRT1	24 hour
RPS20	40S ribosomal protein S20	4 and 24 hour
RPS23	40S ribosomal protein S23	4 and 24 hour
RPS25	40S ribosomal protein S25	24 hour
RPS3	40S ribosomal protein S3	24 hour
RPS4X;RPS4Y1	40S ribosomal protein S4, X isoform;40S ribosomal protein S4, Y isoform 1	4 and 24 hour
RPS8	40S ribosomal protein S8	4 hour
RPS9	40S ribosomal protein S9	4 and 24 hour
RPSAP58;RPSA	40S ribosomal protein SA	24 hour
RRP1B	Ribosomal RNA processing protein 1 homolog B	24 hour
RTN4	Reticulon-4	4 and 24 hour
RYK	Tyrosine-protein kinase RYK	24 hour
S100A14	Protein S100-A14	24 hour
S100A16	Protein S100-A16	24 hour
S100A7	Protein S100-A7	4 hour
S100A9	Protein S100-A9	4 hour
SBSN	Suprabasin	4 and 24 hour
SCAMP3	Secretory carrier-associated membrane protein 3	24 hour
SCP2	Non-specific lipid-transfer protein	24 hour
SEC61B	Protein transport protein Sec61 subunit beta	24 hour
SEMG2;SEMG1	Semenogelin-2;Semenogelin-1;Alpha-inhibin-92;Alpha-inhibin-31;Seminal	4 hour

	basic protein	
SERPINA7	Thyroxine-binding globulin	4 and 24 hour
SERPINB12	Serpin B12	4 and 24 hour
SERPINB3;SERPINB4	Serpin B3;Serpin B4	4 and 24 hour
SERPINC1	Antithrombin-III	4 hour
SERPINF1	Pigment epithelium-derived factor	4 and 24 hour
SERPINF2	Alpha-2-antiplasmin	4 hour
SERPINH1	Serpin H1	4 and 24 hour
SF3B3	Splicing factor 3B subunit 3	
SFPQ	Splicing factor, proline- and glutamine-rich	4 and 24 hour
SFXN1	Sideroflexin-1	4 and 24 hour
SHMT2	Serine hydroxymethyltransferase, mitochondrial;Serine hydroxymethyltransferase	24 hour
SLC16A1	Monocarboxylate transporter 1	24 hour
SLC16A3	Monocarboxylate transporter 4	24 hour
SLC25A1	Tricarboxylate transport protein, mitochondrial	4 and 24 hour
SLC25A11	Mitochondrial 2-oxoglutarate/malate carrier protein	4 and 24 hour
SLC25A13;SLC25A12	Calcium-binding mitochondrial carrier protein Aralar2;Calcium-binding mitochondrial carrier protein Aralar1	24 hour
SLC25A24	Calcium-binding mitochondrial carrier protein SCaMC-1	24 hour
SLC25A3	Phosphate carrier protein, mitochondrial	4 and 24 hour
SLC25A5	ADP/ATP translocase 2	4 and 24 hour
SLC25A6;SLC25A4	ADP/ATP translocase 3;ADP/ATP translocase 1	4 and 24 hour
SLC2A1	Solute carrier family 2, facilitated glucose transporter member 1	4 and 24 hour
SLC35E1	Solute carrier family 35 member E1	24 hour
SLC3A2	4F2 cell-surface antigen heavy chain	4 and 24 hour
SLC7A5	Large neutral amino acids transporter small subunit 1	4 and 24 hour
SNRPD1	Small nuclear ribonucleoprotein Sm D1	4 hour
SNRPD2	Small nuclear ribonucleoprotein Sm D2	24 hour
SOD2	Superoxide dismutase [Mn], mitochondrial;Superoxide dismutase	24 hour
SPAG17	Sperm-associated antigen 17	4 hour
SPRR3	Small proline-rich protein 3	4 hour
SQRDL	Sulfide:quinone oxidoreductase, mitochondrial	4 and 24 hour
SQSTM1	Sequestosome-1	4 hour
SRRM1	Serine/arginine repetitive matrix protein 1	4 hour
SSR4	Translocon-associated protein subunit delta	24 hour
SRSF4;SRSF6;SRSF5	Serine/arginine-rich splicing factor 4;Serine/arginine-rich splicing factor 6;Serine/arginine-rich splicing factor 5	4 hour
STOM	Erythrocyte band 7 integral membrane protein	4 and 24 hour
SUCLA2	Succinyl-CoA ligase [ADP-forming] subunit beta, mitochondrial	24 hour
SUCLG1	Succinyl-CoA ligase [ADP/GDP-forming] subunit alpha, mitochondrial	24 hour
TAP1	Antigen peptide transporter 1	24 hour
TAP2	Antigen peptide transporter 2	24 hour
TARDBP	TAR DNA-binding protein 43	24 hour
TAX1BP1	**Tax1-binding protein 1**	4 hour
TBRG4	Protein TBRG4	24 hour
TCOF1	Treacle protein	4 hour
TENC1	Tensin-like C1 domain-containing phosphatase	4 and 24 hour
TF	Serotransferrin	
TGM1	Protein-glutamine gamma-glutamyltransferase K	24 hour
TGM3	Protein-glutamine gamma-glutamyltransferase E;Protein-glutamine gamma-glutamyltransferase E 50 kDa catalytic chain;Protein-glutamine gamma-glutamyltransferase E 27 kDa non-catalytic chain	4 and 24 hour
THBS1	Thrombospondin-1	4 and 24 hour
THRAP3	Thyroid hormone receptor-associated protein 3	24 hour
TICAM1	***TIR domain-containing adapter molecule 1***	4 hour
TIMM50	Mitochondrial import inner membrane translocase subunit TIM50	24 hour
TM9SF1;CHMP4A	Charged multivesicular body protein 4a	4 hour
TM9SF3	Transmembrane 9 superfamily member 3	24 hour
TMED10	Transmembrane emp24 domain-containing protein 10	4 hour
TMED2	Transmembrane emp24 domain-containing protein 2	24 hour
TMEM165	Transmembrane protein 165	24 hour

TMEM33	Transmembrane protein 33	24 hour
TMF1	TATA element modulatory factor	24 hour
TNFAIP3	**Tumor necrosis factor alpha-induced protein 3**	4 and 24 hour
TNIP1	**TNFAIP3-interacting protein 1**	4 and 24 hour
TOMM40	Mitochondrial import receptor subunit TOM40 homolog	24 hour
TOR1AIP1	Torsin-1A-interacting protein 1	24 hour
TPI1	Triosephosphate isomerase	4 and 24 hour
TRAP1	Heat shock protein 75 kDa, mitochondrial	24 hour
TREX1	Three prime repair exonuclease 1	24 hour
TRIM21	E3 ubiquitin-protein ligase TRIM21	24 hour
TRIM39;TRIM39R	Tripartite motif-containing protein 39	24 hour
TRIM65	Tripartite motif-containing protein 65	4 hour
TRY6;PRSS1;PRSS2	Putative trypsin-6;Trypsin-1;Alpha-trypsin chain 1;Alpha-trypsin chain 2;Trypsin-2	4 hour
TUBA1B;TUBA4A	Tubulin alpha-1B chain;Tubulin alpha-4A chain	4 and 24 hour
TUBB;TUBB4B;TUBB2A;TUBB 2B;TUBB3	Tubulin beta chain;Tubulin beta-4B chain;Tubulin beta-2A chain;Tubulin beta-2B chain;Tubulin beta-3 chain	4 and 24 hour
TUFM	Elongation factor Tu, mitochondrial	4 and 24 hour
U2AF1	Splicing factor U2AF 35 kDa subunit	4 and 24 hour
U2AF2	Splicing factor U2AF 65 kDa subunit	4 hour
UBA52	Ubiquitin-60S ribosomal protein L40;Ubiquitin;60S ribosomal protein L40	4 hour
UBC;UBB;RPS27A;UBA52	Polyubiquitin-C;Ubiquitin;Polyubiquitin-B;Ubiquitin;Ubiquitin-40S ribosomal protein S27a;Ubiquitin;40S ribosomal protein S27a;Ubiquitin-60S ribosomal protein L40;Ubiquitin;60S ribosomal protein L40	24 hour
UBE3B	Ubiquitin-protein ligase E3B	24 hour
UQCRC1	Cytochrome b-c1 complex subunit 1, mitochondrial	24 hour
UQCRC2	Cytochrome b-c1 complex subunit 2, mitochondrial	4 and 24 hour
VANGL1	Vang-like protein 1	4 hour
VDAC1	Voltage-dependent anion-selective channel protein 1	4 and 24 hour
VDAC2	Voltage-dependent anion-selective channel protein 2	4 and 24 hour
VDAC3	Voltage-dependent anion-selective channel protein 3	4 and 24 hour
VIM	Vimentin	4 hour
VTN	Vitronectin;Vitronectin V65 subunit;Vitronectin V10 subunit;Somatomedin-B	4 and 24 hour
XP32	Skin-specific protein 32	4 hour
YBX1	Nuclease-sensitive element-binding protein 1	24 hour
YIF1A	Protein YIF1A	24 hour
YWHAZ;YWHAE;SFN;YWHAG; YWHAB;YWHAH;YWHAQ	14-3-3 protein zeta/delta;14-3-3 protein epsilon;14-3-3 protein sigma;14-3-3 protein gamma;14-3-3 protein gamma, N-terminally processed;14-3-3 protein beta/alpha;14-3-3 protein beta/alpha, N-terminally processed;14-3-3 protein eta;14-3-3 protein theta	4 and 24 hour
ZNF280A	Zinc finger protein 280A	4 hour
ZNF355P	Putative zinc finger protein 355P	4 hour
	Ig kappa chain V-III region HAH;Ig kappa chain V-III region HIC;Ig kappa chain V-III region SIE;Ig kappa chain V-III region Ti;Ig kappa chain V-III region WOL;Ig kappa chain V-III region GOL	24 hour
	Ig heavy chain V-II region OU	4 and 24 hour
	Ig kappa chain V-II region RPMI 6410;Ig kappa chain V-II region GM607;Ig kappa chain V-II region Cum;Ig kappa chain V-II region TEW	4 hour
	Ig kappa chain V-III region HAH;Ig kappa chain V-III region WOL;Ig kappa chain V-I region AG;Ig kappa chain V-I region Ka	4 hour
	Ig kappa chain V-III region NG9	4 and 24 hour
	Ig kappa chain V-II region RPMI 6410;Ig kappa chain V-II region GM607;Ig kappa chain V-II region Cum;Ig kappa chain V-II region TEW	24 hour

REFERENCES

Aida, T., Imahashi, R., and Tanaka, K. (2014). Translating human genetics into mouse: the impact of ultra-rapid in vivo genome editing. Dev Growth Differ *56*, 34-45.

Akdis, M., Burgler, S., Crameri, R., Eiwegger, T., Fujita, H., Gomez, E., Klunker, S., Meyer, N., O'Mahony, L., Palomares, O.*, et al.* (2011). Interleukins, from 1 to 37, and interferon-gamma: receptors, functions, and roles in diseases. J Allergy Clin Immunol *127*, 701-721 e701-770.

Akira, S., Uematsu, S., and Takeuchi, O. (2006). Pathogen recognition and innate immunity. Cell *124*, 783-801.

Alexopoulou, L., Holt, A.C., Medzhitov, R., and Flavell, R.A. (2001). Recognition of double-stranded RNA and activation of NF-kappaB by Toll-like receptor 3. Nature *413*, 732-738.

Ank, N., West, H., Bartholdy, C., Eriksson, K., Thomsen, A.R., and Paludan, S.R. (2006). Lambda interferon (IFN-lambda), a type III IFN, is induced by viruses and IFNs and displays potent antiviral activity against select virus infections in vivo. J Virol *80*, 4501-4509.

Araya, J., and Nishimura, S.L. (2010). Fibrogenic reactions in lung disease. Annu Rev Pathol *5*, 77-98.

Arend, W.P. (1993). Interleukin-1 receptor antagonist. Adv Immunol *54*, 167-227.

Arend, W.P., and Guthridge, C.J. (2000). Biological role of interleukin 1 receptor antagonist isoforms. Ann Rheum Dis *59 Suppl 1*, i60-64.

Arenzana-Seisdedos, F., Turpin, P., Rodriguez, M., Thomas, D., Hay, R.T., Virelizier, J.L., and Dargemont, C. (1997). Nuclear localization of I kappa B alpha promotes active transport of NF-kappa B from the nucleus to the cytoplasm. J Cell Sci *110 (Pt 3)*, 369-378.

Arnson, Y., Shoenfeld, Y., and Amital, H. (2010). Effects of tobacco smoke on immunity, inflammation and autoimmunity. J Autoimmun *34*, J258-265.

Arthur, J.S., and Ley, S.C. (2013). Mitogen-activated protein kinases in innate immunity. Nat Rev Immunol *13*, 679-692.

Baeuerle, P.A., and Baltimore, D. (1996). NF-kappa B: ten years after. Cell *87*, 13-20.

Bafadhel, M., McKenna, S., Terry, S., Mistry, V., Reid, C., Haldar, P., McCormick, M., Haldar, K., Kebadze, T., Duvoix, A.*, et al.* (2011). Acute exacerbations of chronic obstructive pulmonary disease: identification of biologic clusters and their biomarkers. Am J Respir Crit Care Med *184*, 662-671.

Bainton, D.F., Ullyot, J.L., and Farquhar, M.G. (1971). The development of neutrophilic polymorphonuclear leukocytes in human bone marrow. J Exp Med *134*, 907-934.

Barber, G.N. (2001). Host defense, viruses and apoptosis. Cell Death Differ *8*, 113-126.

Barnes, P.J. (2004). Mediators of chronic obstructive pulmonary disease. Pharmacol Rev *56*, 515-548.

Barnes, P.J. (2008a). The cytokine network in asthma and chronic obstructive pulmonary disease. J Clin Invest *118*, 3546-3556.

Barnes, P.J. (2008b). Immunology of asthma and chronic obstructive pulmonary disease. Nat Rev Immunol *8*, 183-192.

Bauer, C.M., Dewitte-Orr, S.J., Hornby, K.R., Zavitz, C.C., Lichty, B.D., Stampfli, M.R., and Mossman, K.L. (2008). Cigarette smoke suppresses type I interferon-mediated antiviral immunity in lung fibroblast and epithelial cells. J Interferon Cytokine Res *28*, 167-179.

Beckham, J.D., Cadena, A., Lin, J., Piedra, P.A., Glezen, W.P., Greenberg, S.B., and Atmar, R.L. (2005). Respiratory viral infections in patients with chronic, obstructive pulmonary disease. J Infect *50*, 322-330.

Beeh, K.M., Kornmann, O., Buhl, R., Culpitt, S.V., Giembycz, M.A., and Barnes, P.J. (2003). Neutrophil chemotactic activity of sputum from patients with COPD: role of interleukin 8 and leukotriene B4. Chest *123*, 1240-1247.
Belge, K.U., Dayyani, F., Horelt, A., Siedlar, M., Frankenberger, M., Frankenberger, B., Espevik, T., and Ziegler-Heitbrock, L. (2002). The proinflammatory CD14+CD16+DR++ monocytes are a major source of TNF. J Immunol *168*, 3536-3542.
Belsham, G.J., and Sonenberg, N. (1996). RNA-protein interactions in regulation of picornavirus RNA translation. Microbiol Rev *60*, 499-511.
Bennett, J.A., Prince, L.R., Parker, L.C., Stokes, C.A., de Bruin, H.G., van den Berge, M., Heijink, I.H., Whyte, M.K., and Sabroe, I. (2012). Pellino-1 selectively regulates epithelial cell responses to rhinovirus. J Virol *86*, 6595-6604.
Berke, I.C., Li, Y., and Modis, Y. (2013). Structural basis of innate immune recognition of viral RNA. Cell Microbiol *15*, 386-394.
Betts, J.C., and Nabel, G.J. (1996). Differential regulation of NF-kappaB2(p100) processing and control by amino-terminal sequences. Mol Cell Biol *16*, 6363-6371.
Blenis, J. (1993). Signal transduction via the MAP kinases: proceed at your own RSK. Proc Natl Acad Sci U S A *90*, 5889-5892.
Bode, A.M., and Dong, Z. (2007). The functional contrariety of JNK. Mol Carcinog *46*, 591-598.
Bonizzi, G., and Karin, M. (2004). The two NF-kappaB activation pathways and their role in innate and adaptive immunity. Trends Immunol *25*, 280-288.
Boone, D.L., Turer, E.E., Lee, E.G., Ahmad, R.C., Wheeler, M.T., Tsui, C., Hurley, P., Chien, M., Chai, S., Hitotsumatsu, O.*, et al.* (2004). The ubiquitin-modifying enzyme A20 is required for termination of Toll-like receptor responses. Nat Immunol *5*, 1052-1060.
Borgerding, M., and Klus, H. (2005). Analysis of complex mixtures--cigarette smoke. Exp Toxicol Pathol *57 Suppl 1*, 43-73.
Borregaard, N., Sorensen, O.E., and Theilgaard-Monch, K. (2007). Neutrophil granules: a library of innate immunity proteins. Trends Immunol *28*, 340-345.
Boulton, T.G., Nye, S.H., Robbins, D.J., Ip, N.Y., Radziejewska, E., Morgenbesser, S.D., DePinho, R.A., Panayotatos, N., Cobb, M.H., and Yancopoulos, G.D. (1991). ERKs: a family of protein-serine/threonine kinases that are activated and tyrosine phosphorylated in response to insulin and NGF. Cell *65*, 663-675.
Boulton, T.G., Yancopoulos, G.D., Gregory, J.S., Slaughter, C., Moomaw, C., Hsu, J., and Cobb, M.H. (1990). An insulin-stimulated protein kinase similar to yeast kinases involved in cell cycle control. Science *249*, 64-67.
Bouwmeester, T., Bauch, A., Ruffner, H., Angrand, P.O., Bergamini, G., Croughton, K., Cruciat, C., Eberhard, D., Gagneur, J., Ghidelli, S.*, et al.* (2004). A physical and functional map of the human TNF-alpha/NF-kappa B signal transduction pathway. Nat Cell Biol *6*, 97-105.
Bowie, A., and O'Neill, L.A. (2000). The interleukin-1 receptor/Toll-like receptor superfamily: signal generators for pro-inflammatory interleukins and microbial products. J Leukoc Biol *67*, 508-514.
Braiman, A., and Priel, Z. (2008). Efficient mucociliary transport relies on efficient regulation of ciliary beating. Respir Physiol Neurobiol *163*, 202-207.
Brown, J., Wang, H., Hajishengallis, G.N., and Martin, M. (2010). TLR-signaling Networks: An Integration of Adaptor Molecules, Kinases, and Cross-talk. J Dent Res.
Brusselle, G.G., Joos, G.F., and Bracke, K.R. (2011). New insights into the immunology of chronic obstructive pulmonary disease. Lancet *378*, 1015-1026.
Buckley, C.D., Pilling, D., Lord, J.M., Akbar, A.N., Scheel-Toellner, D., and Salmon, M. (2001). Fibroblasts regulate the switch from acute resolving to chronic persistent inflammation. Trends Immunol *22*, 199-204.

Budulac, S.E., Boezen, H.M., Hiemstra, P.S., Lapperre, T.S., Vonk, J.M., Timens, W., and Postma, D.S. (2012). Toll-like receptor (TLR2 and TLR4) polymorphisms and chronic obstructive pulmonary disease. PLoS One *7*, e43124.
Butler, M.P., Hanly, J.A., and Moynagh, P.N. (2005). Pellino3 is a novel upstream regulator of p38 MAPK and activates CREB in a p38-dependent manner. J Biol Chem *280*, 27759-27768.
Butler, M.P., Hanly, J.A., and Moynagh, P.N. (2007). Kinase-active interleukin-1 receptor-associated kinases promote polyubiquitination and degradation of the Pellino family: direct evidence for PELLINO proteins being ubiquitin-protein isopeptide ligases. J Biol Chem *282*, 29729-29737.
Cannon, J.G. (2000). Inflammatory Cytokines in Nonpathological States. News Physiol Sci *15*, 298-303.
Cao, Z., Xiong, J., Takeuchi, M., Kurama, T., and Goeddel, D.V. (1996). TRAF6 is a signal transducer for interleukin-1. Nature *383*, 443-446.
Caramori, G., Ito, K., Contoli, M., Di Stefano, A., Johnston, S.L., Adcock, I.M., and Papi, A. (2006). Molecular mechanisms of respiratory virus-induced asthma and COPD exacerbations and pneumonia. Curr Med Chem *13*, 2267-2290.
Caramori, G., Romagnoli, M., Casolari, P., Bellettato, C., Casoni, G., Boschetto, P., Chung, K.F., Barnes, P.J., Adcock, I.M., Ciaccia, A.*, et al.* (2003). Nuclear localisation of p65 in sputum macrophages but not in sputum neutrophils during COPD exacerbations. Thorax *58*, 348-351.
Celli, B.R., and Barnes, P.J. (2007). Exacerbations of chronic obstructive pulmonary disease. Eur Respir J *29*, 1224-1238.
Chang, M., Jin, W., and Sun, S.C. (2009). Peli1 facilitates TRIF-dependent Toll-like receptor signaling and proinflammatory cytokine production. Nat Immunol *10*, 1089-1095.
Chaudhuri, N., Paiva, C., Donaldson, K., Duffin, R., Parker, L.C., and Sabroe, I. (2010). Diesel exhaust particles override natural injury-limiting pathways in the lung. Am J Physiol Lung Cell Mol Physiol *299*, L263-271.
Chen, G., Shaw, M.H., Kim, Y.G., and Nunez, G. (2009). NOD-like receptors: role in innate immunity and inflammatory disease. Annu Rev Pathol *4*, 365-398.
Chen, H., Cowan, M.J., Hasday, J.D., Vogel, S.N., and Medvedev, A.E. (2007). Tobacco smoking inhibits expression of proinflammatory cytokines and activation of IL-1R-associated kinase, p38, and NF-kappaB in alveolar macrophages stimulated with TLR2 and TLR4 agonists. J Immunol *179*, 6097-6106.
Choi, K.C., Lee, Y.S., Lim, S., Choi, H.K., Lee, C.H., Lee, E.K., Hong, S., Kim, I.H., Kim, S.J., and Park, S.H. (2006). Smad6 negatively regulates interleukin 1-receptor-Toll-like receptor signaling through direct interaction with the adaptor Pellino-1. Nat Immunol *7*, 1057-1065.
Chuang, T.H., Lee, J., Kline, L., Mathison, J.C., and Ulevitch, R.J. (2002). Toll-like receptor 9 mediates CpG-DNA signaling. J Leukoc Biol *71*, 538-544.
Chung, K.F. (2001). Cytokines in chronic obstructive pulmonary disease. Eur Respir J Suppl *34*, 50s-59s.
Churg, A., Wang, R.D., Tai, H., Wang, X., Xie, C., and Wright, J.L. (2004). Tumor necrosis factor-alpha drives 70% of cigarette smoke-induced emphysema in the mouse. Am J Respir Crit Care Med *170*, 492-498.
Cohen, S., Tyrrell, D.A., Russell, M.A., Jarvis, M.J., and Smith, A.P. (1993). Smoking, alcohol consumption, and susceptibility to the common cold. Am J Public Health *83*, 1277-1283.
Colsky, A.S., Mendez, L.E., and Peacock, J.S. (1991). FcR-independent antibody-mediated cellular cytotoxicity. J Leukoc Biol *49*, 548-555.
Combadiere, C., Ahuja, S.K., Tiffany, H.L., and Murphy, P.M. (1996). Cloning and functional expression of CC CKR5, a human monocyte CC chemokine receptor selective for MIP-1(alpha), MIP-1(beta), and RANTES. J Leukoc Biol *60*, 147-152.

Coope, H.J., Atkinson, P.G., Huhse, B., Belich, M., Janzen, J., Holman, M.J., Klaus, G.G., Johnston, L.H., and Ley, S.C. (2002). CD40 regulates the processing of NF-kappaB2 p100 to p52. EMBO J *21*, 5375-5385.
Cosio, M.G., Hale, K.A., and Niewoehner, D.E. (1980). Morphologic and morphometric effects of prolonged cigarette smoking on the small airways. Am Rev Respir Dis *122*, 265-221.
Cox, D.W., and Le Souef, P.N. (2014). Rhinovirus and the developing lung. Paediatr Respir Rev.
Cromwell, O., Hamid, Q., Corrigan, C.J., Barkans, J., Meng, Q., Collins, P.D., and Kay, A.B. (1992). Expression and generation of interleukin-8, IL-6 and granulocyte-macrophage colony-stimulating factor by bronchial epithelial cells and enhancement by IL-1 beta and tumour necrosis factor-alpha. Immunology *77*, 330-337.
Cuadrado, A., and Nebreda, A.R. (2010). Mechanisms and functions of p38 MAPK signalling. Biochem J *429*, 403-417.
Cusson-Hermance, N., Khurana, S., Lee, T.H., Fitzgerald, K.A., and Kelliher, M.A. (2005). Rip1 mediates the Trif-dependent toll-like receptor 3- and 4-induced NF-{kappa}B activation but does not contribute to interferon regulatory factor 3 activation. J Biol Chem *280*, 36560-36566.
d'Azzo, A., Bongiovanni, A., and Nastasi, T. (2005). E3 ubiquitin ligases as regulators of membrane protein trafficking and degradation. Traffic *6*, 429-441.
Daigneault, M., Preston, J.A., Marriott, H.M., Whyte, M.K., and Dockrell, D.H. (2010). The identification of markers of macrophage differentiation in PMA-stimulated THP-1 cells and monocyte-derived macrophages. PLoS One *5*, e8668.
Darnell, J.E., Jr., Kerr, I.M., and Stark, G.R. (1994). Jak-STAT pathways and transcriptional activation in response to IFNs and other extracellular signaling proteins. Science *264*, 1415-1421.
Daugherty, B.L., Siciliano, S.J., DeMartino, J.A., Malkowitz, L., Sirotina, A., and Springer, M.S. (1996). Cloning, expression, and characterization of the human eosinophil eotaxin receptor. J Exp Med *183*, 2349-2354.
de Boer, W.I., Sont, J.K., van Schadewijk, A., Stolk, J., van Krieken, J.H., and Hiemstra, P.S. (2000). Monocyte chemoattractant protein 1, interleukin 8, and chronic airways inflammation in COPD. J Pathol *190*, 619-626.
Dejardin, E. (2006). The alternative NF-kappaB pathway from biochemistry to biology: pitfalls and promises for future drug development. Biochem Pharmacol *72*, 1161-1179.
Dejardin, E., Droin, N.M., Delhase, M., Haas, E., Cao, Y., Makris, C., Li, Z.W., Karin, M., Ware, C.F., and Green, D.R. (2002). The lymphotoxin-beta receptor induces different patterns of gene expression via two NF-kappaB pathways. Immunity *17*, 525-535.
Del Vecchio, A.M., Branigan, P.J., Barnathan, E.S., Flavin, S.K., Silkoff, P.E., and Turner, R.B. (2015). Utility of animal and in vivo experimental infection of humans with rhinoviruses in the development of therapeutic agents for viral exacerbations of asthma and chronic obstructive pulmonary disease. Pulm Pharmacol Ther *30*, 32-43.
Demoly, P., Simony-Lafontaine, J., Chanez, P., Pujol, J.L., Lequeux, N., Michel, F.B., and Bousquet, J. (1994). Cell proliferation in the bronchial mucosa of asthmatics and chronic bronchitics. Am J Respir Crit Care Med *150*, 214-217.
Deng, L., Wang, C., Spencer, E., Yang, L., Braun, A., You, J., Slaughter, C., Pickart, C., and Chen, Z.J. (2000). Activation of the IkappaB kinase complex by TRAF6 requires a dimeric ubiquitin-conjugating enzyme complex and a unique polyubiquitin chain. Cell *103*, 351-361.
Di Paolo, N.C., and Shayakhmetov, D.M. (2013). Interleukin-1 receptor 2 keeps the lid on interleukin-1alpha. Immunity *38*, 203-205.
Di Stefano, A., Capelli, A., Lusuardi, M., Balbo, P., Vecchio, C., Maestrelli, P., Mapp, C.E., Fabbri, L.M., Donner, C.F., and Saetta, M. (1998). Severity of airflow limitation is associated with severity of airway inflammation in smokers. Am J Respir Crit Care Med *158*, 1277-1285.
Di Stefano, A., Maestrelli, P., Roggeri, A., Turato, G., Calabro, S., Potena, A., Mapp, C.E., Ciaccia, A., Covacev, L., Fabbri, L.M*., et al.* (1994). Upregulation of adhesion molecules in the bronchial

mucosa of subjects with chronic obstructive bronchitis. Am J Respir Crit Care Med *149*, 803-810.
Diamond, G., Legarda, D., and Ryan, L.K. (2000). The innate immune response of the respiratory epithelium. Immunol Rev *173*, 27-38.
Dimopoulos, G., Lerikou, M., Tsiodras, S., Chranioti, A., Perros, E., Anagnostopoulou, U., Armaganidis, A., and Karakitsos, P. (2012). Viral epidemiology of acute exacerbations of chronic obstructive pulmonary disease. Pulm Pharmacol Ther *25*, 12-18.
Dinarello, C.A. (1996). Biologic basis for interleukin-1 in disease. Blood *87*, 2095-2147.
Dinarello, C.A. (2007). Historical insights into cytokines. Eur J Immunol *37 Suppl 1*, S34-45.
Dinarello, C.A. (2009). Immunological and inflammatory functions of the interleukin-1 family. Annu Rev Immunol *27*, 519-550.
Dinarello, C.A. (2011). Interleukin-1 in the pathogenesis and treatment of inflammatory diseases. Blood *117*, 3720-3732.
Dinarello, C.A., Ikejima, T., Warner, S.J., Orencole, S.F., Lonnemann, G., Cannon, J.G., and Libby, P. (1987). Interleukin 1 induces interleukin 1. I. Induction of circulating interleukin 1 in rabbits in vivo and in human mononuclear cells in vitro. J Immunol *139*, 1902-1910.
Drake, J.W. (1999). The distribution of rates of spontaneous mutation over viruses, prokaryotes, and eukaryotes. Ann N Y Acad Sci *870*, 100-107.
Eddleston, J., Lee, R.U., Doerner, A.M., Herschbach, J., and Zuraw, B.L. (2011). Cigarette smoke decreases innate responses of epithelial cells to rhinovirus infection. Am J Respir Cell Mol Biol *44*, 118-126.
Enesa, K., Ordureau, A., Smith, H., Barford, D., Cheung, P.C., Patterson-Kane, J., Arthur, J.S., and Cohen, P. (2012). Pellino1 is required for interferon production by viral double-stranded RNA. J Biol Chem *287*, 34825-34835.
Estornes, Y., Toscano, F., Virard, F., Jacquemin, G., Pierrot, A., Vanbervliet, B., Bonnin, M., Lalaoui, N., Mercier-Gouy, P., Pacheco, Y.*, et al.* (2012). dsRNA induces apoptosis through an atypical death complex associating TLR3 to caspase-8. Cell Death Differ *19*, 1482-1494.
Fan, C.M., and Maniatis, T. (1991). Generation of p50 subunit of NF-kappa B by processing of p105 through an ATP-dependent pathway. Nature *354*, 395-398.
Ferhani, N., Letuve, S., Kozhich, A., Thibaudeau, O., Grandsaigne, M., Maret, M., Dombret, M.C., Sims, G.P., Kolbeck, R., Coyle, A.J.*, et al.* (2010). Expression of high-mobility group box 1 and of receptor for advanced glycation end products in chronic obstructive pulmonary disease. Am J Respir Crit Care Med *181*, 917-927.
Fitzgerald, K.A., Palsson-McDermott, E.M., Bowie, A.G., Jefferies, C.A., Mansell, A.S., Brady, G., Brint, E., Dunne, A., Gray, P., Harte, M.T.*, et al.* (2001). Mal (MyD88-adapter-like) is required for Toll-like receptor-4 signal transduction. Nature *413*, 78-83.
Fong, A., and Sun, S.C. (2002). Genetic evidence for the essential role of beta-transducin repeat-containing protein in the inducible processing of NF-kappa B2/p100. J Biol Chem *277*, 22111-22114.
Fredericksen, B.L., Keller, B.C., Fornek, J., Katze, M.G., and Gale, M., Jr. (2008). Establishment and maintenance of the innate antiviral response to West Nile Virus involves both RIG-I and MDA5 signaling through IPS-1. J Virol *82*, 609-616.
Frey, E.A., Miller, D.S., Jahr, T.G., Sundan, A., Bazil, V., Espevik, T., Finlay, B.B., and Wright, S.D. (1992). Soluble CD14 participates in the response of cells to lipopolysaccharide. J Exp Med *176*, 1665-1671.
Gao, J.L., Kuhns, D.B., Tiffany, H.L., McDermott, D., Li, X., Francke, U., and Murphy, P.M. (1993). Structure and functional expression of the human macrophage inflammatory protein 1 alpha/RANTES receptor. J Exp Med *177*, 1421-1427.
Gay, N.J., and Keith, F.J. (1991). Drosophila Toll and IL-1 receptor. Nature *351*, 355-356.
Geissmann, F., Jung, S., and Littman, D.R. (2003). Blood monocytes consist of two principal subsets with distinct migratory properties. Immunity *19*, 71-82.

Gordon, S., and Taylor, P.R. (2005). Monocyte and macrophage heterogeneity. Nat Rev Immunol *5*, 953-964.
Grage-Griebenow, E., Flad, H.D., and Ernst, M. (2001). Heterogeneity of human peripheral blood monocyte subsets. J Leukoc Biol *69*, 11-20.
Gray, C.M., Remouchamps, C., McCorkell, K.A., Solt, L.A., Dejardin, E., Orange, J.S., and May, M.J. (2014). Noncanonical NF-kappaB signaling is limited by classical NF-kappaB activity. Sci Signal *7*, ra13.
Greve, J.M., Davis, G., Meyer, A.M., Forte, C.P., Yost, S.C., Marlor, C.W., Kamarck, M.E., and McClelland, A. (1989). The major human rhinovirus receptor is ICAM-1. Cell *56*, 839-847.
Griffin, B.D., Mellett, M., Campos-Torres, A., Kinsella, G.K., Wang, B., and Moynagh, P.N. (2011). A poxviral homolog of the Pellino protein inhibits Toll and Toll-like receptor signalling. Eur J Immunol *41*, 798-812.
Grosshans, J., Schnorrer, F., and Nusslein-Volhard, C. (1999). Oligomerisation of Tube and Pelle leads to nuclear localisation of dorsal. Mech Dev *81*, 127-138.
Grunstein, M.M., Hakonarson, H., Maskeri, N., and Chuang, S. (2000). Autocrine cytokine signaling mediates effects of rhinovirus on airway responsiveness. Am J Physiol Lung Cell Mol Physiol *278*, L1146-1153.
Haghayeghi, A., Sarac, A., Czerniecki, S., Grosshans, J., and Schock, F. (2010). Pellino enhances innate immunity in Drosophila. Mech Dev *127*, 301-307.
Hakonarson, H., Carter, C., Maskeri, N., Hodinka, R., and Grunstein, M.M. (1999). Rhinovirus-mediated changes in airway smooth muscle responsiveness: induced autocrine role of interleukin-1beta. Am J Physiol *277*, L13-21.
Hallgren, O., Nihlberg, K., Dahlback, M., Bjermer, L., Eriksson, L.T., Erjefalt, J.S., Lofdahl, C.G., and Westergren-Thorsson, G. (2010). Altered fibroblast proteoglycan production in COPD. Respir Res *11*, 55.
Hammond, M.E., Lapointe, G.R., Feucht, P.H., Hilt, S., Gallegos, C.A., Gordon, C.A., Giedlin, M.A., Mullenbach, G., and Tekamp-Olson, P. (1995). IL-8 induces neutrophil chemotaxis predominantly via type I IL-8 receptors. J Immunol *155*, 1428-1433.
Han, J., Jiang, Y., Li, Z., Kravchenko, V.V., and Ulevitch, R.J. (1997). Activation of the transcription factor MEF2C by the MAP kinase p38 in inflammation. Nature *386*, 296-299.
Han, J., Lee, J.D., Bibbs, L., and Ulevitch, R.J. (1994). A MAP kinase targeted by endotoxin and hyperosmolarity in mammalian cells. Science *265*, 808-811.
Han, K.J., Su, X., Xu, L.G., Bin, L.H., Zhang, J., and Shu, H.B. (2004). Mechanisms of the TRIF-induced interferon-stimulated response element and NF-kappaB activation and apoptosis pathways. J Biol Chem *279*, 15652-15661.
Hasan, U., Chaffois, C., Gaillard, C., Saulnier, V., Merck, E., Tancredi, S., Guiet, C., Briere, F., Vlach, J., Lebecque, S*., et al.* (2005). Human TLR10 is a functional receptor, expressed by B cells and plasmacytoid dendritic cells, which activates gene transcription through MyD88. J Immunol *174*, 2942-2950.
Hasday, J.D., McCrea, K.A., Meltzer, S.S., and Bleeker, E.R. (1994). Dysregulation of airway cytokine expression in chronic obstructive pulmonary disease and asthma. Am J Respir Crit Care Med *150*, S54-58.
Hashimoto, C., Hudson, K.L., and Anderson, K.V. (1988). The Toll gene of Drosophila, required for dorsal-ventral embryonic polarity, appears to encode a transmembrane protein. Cell *52*, 269-279.
Hatada, E.N., Nieters, A., Wulczyn, F.G., Naumann, M., Meyer, R., Nucifora, G., McKeithan, T.W., and Scheidereit, C. (1992). The ankyrin repeat domains of the NF-kappa B precursor p105 and the protooncogene bcl-3 act as specific inhibitors of NF-kappa B DNA binding. Proc Natl Acad Sci U S A *89*, 2489-2493.
Hatakeyama, S., and Nakayama, K.I. (2003). U-box proteins as a new family of ubiquitin ligases. Biochem Biophys Res Commun *302*, 635-645.

Hayden, M.S., and Ghosh, S. (2004). Signaling to NF-kappaB. Genes Dev *18*, 2195-2224.
Hayden, M.S., and Ghosh, S. (2008). Shared principles in NF-kappaB signaling. Cell *132*, 344-362.
Hazuda, D.J., Strickler, J., Kueppers, F., Simon, P.L., and Young, P.R. (1990). Processing of precursor interleukin 1 beta and inflammatory disease. J Biol Chem *265*, 6318-6322.
Heikkinen, T., and Jarvinen, A. (2003). The common cold. Lancet *361*, 51-59.
Hellermann, G.R., Nagy, S.B., Kong, X., Lockey, R.F., and Mohapatra, S.S. (2002). Mechanism of cigarette smoke condensate-induced acute inflammatory response in human bronchial epithelial cells. Respir Res *3*, 22.
Heusch, M., Lin, L., Geleziunas, R., and Greene, W.C. (1999). The generation of nfkb2 p52: mechanism and efficiency. Oncogene *18*, 6201-6208.
Heyninck, K., De Valck, D., Vanden Berghe, W., Van Criekinge, W., Contreras, R., Fiers, W., Haegeman, G., and Beyaert, R. (1999). The zinc finger protein A20 inhibits TNF-induced NF-kappaB-dependent gene expression by interfering with an RIP- or TRAF2-mediated transactivation signal and directly binds to a novel NF-kappaB-inhibiting protein ABIN. J Cell Biol *145*, 1471-1482.
Hoebe, K., Du, X., Georgel, P., Janssen, E., Tabeta, K., Kim, S.O., Goode, J., Lin, P., Mann, N., Mudd, S.*, et al.* (2003). Identification of Lps2 as a key transducer of MyD88-independent TIR signalling. Nature *424*, 743-748.
Hoffmann, E., Dittrich-Breiholz, O., Holtmann, H., and Kracht, M. (2002). Multiple control of interleukin-8 gene expression. J Leukoc Biol *72*, 847-855.
Hogg, J.C., Chu, F., Utokaparch, S., Woods, R., Elliott, W.M., Buzatu, L., Cherniack, R.M., Rogers, R.M., Sciurba, F.C., Coxson, H.O.*, et al.* (2004). The nature of small-airway obstruction in chronic obstructive pulmonary disease. N Engl J Med *350*, 2645-2653.
Holmes, W.E., Lee, J., Kuang, W.J., Rice, G.C., and Wood, W.I. (1991). Structure and functional expression of a human interleukin-8 receptor. Science *253*, 1278-1280.
Honda, K., Takaoka, A., and Taniguchi, T. (2006). Type I interferon [corrected] gene induction by the interferon regulatory factor family of transcription factors. Immunity *25*, 349-360.
Honda, K., and Taniguchi, T. (2006). IRFs: master regulators of signalling by Toll-like receptors and cytosolic pattern-recognition receptors. Nat Rev Immunol *6*, 644-658.
Honda, K., Yanai, H., Negishi, H., Asagiri, M., Sato, M., Mizutani, T., Shimada, N., Ohba, Y., Takaoka, A., Yoshida, N.*, et al.* (2005). IRF-7 is the master regulator of type-I interferon-dependent immune responses. Nature *434*, 772-777.
Horng, T., Barton, G.M., Flavell, R.A., and Medzhitov, R. (2002). The adaptor molecule TIRAP provides signalling specificity for Toll-like receptors. Nature *420*, 329-333.
Hoshino, K., Takeuchi, O., Kawai, T., Sanjo, H., Ogawa, T., Takeda, Y., Takeda, K., and Akira, S. (1999). Cutting edge: Toll-like receptor 4 (TLR4)-deficient mice are hyporesponsive to lipopolysaccharide: evidence for TLR4 as the Lps gene product. J Immunol *162*, 3749-3752.
Huang, T., Wang, W., Bessaud, M., Ren, P., Sheng, J., Yan, H., Zhang, J., Lin, X., Wang, Y., Delpeyroux, F.*, et al.* (2009). Evidence of recombination and genetic diversity in human rhinoviruses in children with acute respiratory infection. PLoS One *4*, e6355.
Huber, A.R., Kunkel, S.L., Todd, R.F., 3rd, and Weiss, S.J. (1991). Regulation of transendothelial neutrophil migration by endogenous interleukin-8. Science *254*, 99-102.
Hudy, M.H., and Proud, D. (2013). Cigarette smoke enhances human rhinovirus-induced CXCL8 production via HuR-mediated mRNA stabilization in human airway epithelial cells. Respir Res *14*, 88.
Hudy, M.H., Traves, S.L., and Proud, D. (2014). Transcriptional and epigenetic modulation of human rhinovirus-induced CXCL10 production by cigarette smoke. Am J Respir Cell Mol Biol *50*, 571-582.
Hudy, M.H., Traves, S.L., Wiehler, S., and Proud, D. (2010). Cigarette smoke modulates rhinovirus-induced airway epithelial cell chemokine production. Eur Respir J *35*, 1256-1263.

Hultmark, D. (1994). Macrophage differentiation marker MyD88 is a member of the Toll/IL-1 receptor family. Biochem Biophys Res Commun *199*, 144-146.
Hurst, J.R., Perera, W.R., Wilkinson, T.M., Donaldson, G.C., and Wedzicha, J.A. (2006). Systemic and upper and lower airway inflammation at exacerbation of chronic obstructive pulmonary disease. Am J Respir Crit Care Med *173*, 71-78.
Hutchinson, A.F., Ghimire, A.K., Thompson, M.A., Black, J.F., Brand, C.A., Lowe, A.J., Smallwood, D.M., Vlahos, R., Bozinovski, S., Brown, G.V.*, et al.* (2007). A community-based, time-matched, case-control study of respiratory viruses and exacerbations of COPD. Respir Med *101*, 2472-2481.
Hwang, S.Y., Hertzog, P.J., Holland, K.A., Sumarsono, S.H., Tymms, M.J., Hamilton, J.A., Whitty, G., Bertoncello, I., and Kola, I. (1995). A null mutation in the gene encoding a type I interferon receptor component eliminates antiproliferative and antiviral responses to interferons alpha and beta and alters macrophage responses. Proc Natl Acad Sci U S A *92*, 11284-11288.
Iha, H., Peloponese, J.M., Verstrepen, L., Zapart, G., Ikeda, F., Smith, C.D., Starost, M.F., Yedavalli, V., Heyninck, K., Dikic, I.*, et al.* (2008). Inflammatory cardiac valvulitis in TAX1BP1-deficient mice through selective NF-kappaB activation. EMBO J *27*, 629-641.
Irmler, M., Hertig, S., MacDonald, H.R., Sadoul, R., Becherer, J.D., Proudfoot, A., Solari, R., and Tschopp, J. (1995). Granzyme A is an interleukin 1 beta-converting enzyme. J Exp Med *181*, 1917-1922.
Jacobs, B.L., and Langland, J.O. (1996). When two strands are better than one: the mediators and modulators of the cellular responses to double-stranded RNA. Virology *219*, 339-349.
Janeway, C.A., Jr., and Medzhitov, R. (2002). Innate immune recognition. Annu Rev Immunol *20*, 197-216.
Jeffery, P.K. (1998). Structural and inflammatory changes in COPD: a comparison with asthma. Thorax *53*, 129-136.
Jensen, L.E., and Whitehead, A.S. (2003a). Pellino2 activates the mitogen activated protein kinase pathway. FEBS Lett *545*, 199-202.
Jensen, L.E., and Whitehead, A.S. (2003b). Pellino3, a novel member of the Pellino protein family, promotes activation of c-Jun and Elk-1 and may act as a scaffolding protein. J Immunol *171*, 1500-1506.
Jiang, D., Liang, J., Fan, J., Yu, S., Chen, S., Luo, Y., Prestwich, G.D., Mascarenhas, M.M., Garg, H.G., Quinn, D.A.*, et al.* (2005). Regulation of lung injury and repair by Toll-like receptors and hyaluronan. Nat Med *11*, 1173-1179.
Jiang, Z., Johnson, H.J., Nie, H., Qin, J., Bird, T.A., and Li, X. (2003). Pellino 1 is required for interleukin-1 (IL-1)-mediated signaling through its interaction with the IL-1 receptor-associated kinase 4 (IRAK4)-IRAK-tumor necrosis factor receptor-associated factor 6 (TRAF6) complex. J Biol Chem *278*, 10952-10956.
Jin, J., Hu, H., Li, H.S., Yu, J., Xiao, Y., Brittain, G.C., Zou, Q., Cheng, X., Mallette, F.A., Watowich, S.S.*, et al.* (2014). Noncanonical NF-kappaB pathway controls the production of type I interferons in antiviral innate immunity. Immunity *40*, 342-354.
Johnston, S.L. (2005). Overview of virus-induced airway disease. Proc Am Thorac Soc *2*, 150-156.
Johnston, S.L., Bardin, P.G., and Pattemore, P.K. (1993). Viruses as precipitants of asthma symptoms. III. Rhinoviruses: molecular biology and prospects for future intervention. Clin Exp Allergy *23*, 237-246.
Kaiser, W.J., and Offermann, M.K. (2005). Apoptosis induced by the toll-like receptor adaptor TRIF is dependent on its receptor interacting protein homotypic interaction motif. J Immunol *174*, 4942-4952.
Kalai, M., Van Loo, G., Vanden Berghe, T., Meeus, A., Burm, W., Saelens, X., and Vandenabeele, P. (2002). Tipping the balance between necrosis and apoptosis in human and murine cells treated with interferon and dsRNA. Cell Death Differ *9*, 981-994.

Kariko, K., Ni, H., Capodici, J., Lamphier, M., and Weissman, D. (2004). mRNA is an endogenous ligand for Toll-like receptor 3. J Biol Chem *279*, 12542-12550.
Karin, M. (1996). The regulation of AP-1 activity by mitogen-activated protein kinases. Philos Trans R Soc Lond B Biol Sci *351*, 127-134.
Karin, M., and Ben-Neriah, Y. (2000). Phosphorylation meets ubiquitination: the control of NF-[kappa]B activity. Annu Rev Immunol *18*, 621-663.
Karin, M., Liu, Z., and Zandi, E. (1997). AP-1 function and regulation. Curr Opin Cell Biol *9*, 240-246.
Kato, H., Takahasi, K., and Fujita, T. (2011). RIG-I-like receptors: cytoplasmic sensors for non-self RNA. Immunol Rev *243*, 91-98.
Kato, H., Takeuchi, O., Sato, S., Yoneyama, M., Yamamoto, M., Matsui, K., Uematsu, S., Jung, A., Kawai, T., Ishii, K.J.*, et al.* (2006). Differential roles of MDA5 and RIG-I helicases in the recognition of RNA viruses. Nature *441*, 101-105.
Kawagoe, T., Sato, S., Matsushita, K., Kato, H., Matsui, K., Kumagai, Y., Saitoh, T., Kawai, T., Takeuchi, O., and Akira, S. (2008). Sequential control of Toll-like receptor-dependent responses by IRAK1 and IRAK2. Nat Immunol *9*, 684-691.
Kawai, T., Adachi, O., Ogawa, T., Takeda, K., and Akira, S. (1999). Unresponsiveness of MyD88-deficient mice to endotoxin. Immunity *11*, 115-122.
Kawai, T., and Akira, S. (2007). TLR signaling. Semin Immunol *19*, 24-32.
Kawai, T., Takahashi, K., Sato, S., Coban, C., Kumar, H., Kato, H., Ishii, K.J., Takeuchi, O., and Akira, S. (2005). IPS-1, an adaptor triggering RIG-I- and Mda5-mediated type I interferon induction. Nat Immunol *6*, 981-988.
Kawai, T., Takeuchi, O., Fujita, T., Inoue, J., Muhlradt, P.F., Sato, S., Hoshino, K., and Akira, S. (2001). Lipopolysaccharide stimulates the MyD88-independent pathway and results in activation of IFN-regulatory factor 3 and the expression of a subset of lipopolysaccharide-inducible genes. J Immunol *167*, 5887-5894.
Kayagaki, N., Yan, M., Seshasayee, D., Wang, H., Lee, W., French, D.M., Grewal, I.S., Cochran, A.G., Gordon, N.C., Yin, J.*, et al.* (2002). BAFF/BLyS receptor 3 binds the B cell survival factor BAFF ligand through a discrete surface loop and promotes processing of NF-kappaB2. Immunity *17*, 515-524.
Keating, S.E., Baran, M., and Bowie, A.G. (2011). Cytosolic DNA sensors regulating type I interferon induction. Trends Immunol *32*, 574-581.
Kelliher, M.A., Grimm, S., Ishida, Y., Kuo, F., Stanger, B.Z., and Leder, P. (1998). The death domain kinase RIP mediates the TNF-induced NF-kappaB signal. Immunity *8*, 297-303.
Kelly, C., Shields, M.D., Elborn, J.S., and Schock, B.C. (2011). A20 regulation of nuclear factor-kappaB: perspectives for inflammatory lung disease. Am J Respir Cell Mol Biol *44*, 743-748.
Kenny, E.F., and O'Neill, L.A. (2008). Signalling adaptors used by Toll-like receptors: an update. Cytokine *43*, 342-349.
Kherad, O., and Rutschmann, O.T. (2010). [Viral infections as a cause of chronic obstructive pulmonary disease (COPD) exacerbation]. Praxis (Bern 1994) *99*, 235-240.
Kim, J.H., Sung, K.S., Jung, S.M., Lee, Y.S., Kwon, J.Y., Choi, C.Y., and Park, S.H. (2011a). Pellino-1, an adaptor protein of interleukin-1 receptor/toll-like receptor signaling, is sumoylated by Ubc9. Mol Cells *31*, 85-89.
Kim, J.Y., Morgan, M., Kim, D.G., Lee, J.Y., Bai, L., Lin, Y., Liu, Z.G., and Kim, Y.S. (2011b). TNFalpha induced noncanonical NF-kappaB activation is attenuated by RIP1 through stabilization of TRAF2. J Cell Sci *124*, 647-656.
Kim, T.W., Yu, M., Zhou, H., Cui, W., Wang, J., DiCorleto, P., Fox, P., Xiao, H., and Li, X. (2012). Pellino 2 is critical for Toll-like receptor/interleukin-1 receptor (TLR/IL-1R)-mediated post-transcriptional control. J Biol Chem *287*, 25686-25695.
Kirchberger, S., Majdic, O., and Stockl, J. (2007). Modulation of the immune system by human rhinoviruses. Int Arch Allergy Immunol *142*, 1-10.

Knapp, S., Wieland, C.W., van 't Veer, C., Takeuchi, O., Akira, S., Florquin, S., and van der Poll, T. (2004). Toll-like receptor 2 plays a role in the early inflammatory response to murine pneumococcal pneumonia but does not contribute to antibacterial defense. J Immunol *172*, 3132-3138.
Ko, F.W., Tam, W., Wong, T.W., Chan, D.P., Tung, A.H., Lai, C.K., and Hui, D.S. (2007). Temporal relationship between air pollutants and hospital admissions for chronic obstructive pulmonary disease in Hong Kong. Thorax *62*, 780-785.
Kobe, B., and Deisenhofer, J. (1994). The leucine-rich repeat: a versatile binding motif. Trends Biochem Sci *19*, 415-421.
Komander, D. (2009). The emerging complexity of protein ubiquitination. Biochem Soc Trans *37*, 937-953.
Komuro, A., and Horvath, C.M. (2006). RNA- and virus-independent inhibition of antiviral signaling by RNA helicase LGP2. J Virol *80*, 12332-12342.
Kulkarni, R., Rampersaud, R., Aguilar, J.L., Randis, T.M., Kreindler, J.L., and Ratner, A.J. (2010). Cigarette smoke inhibits airway epithelial cell innate immune responses to bacteria. Infect Immun *78*, 2146-2152.
Kurai, D., Saraya, T., Ishii, H., and Takizawa, H. (2013). Virus-induced exacerbations in asthma and COPD. Front Microbiol *4*, 293.
Lacoste, J.Y., Bousquet, J., Chanez, P., Van Vyve, T., Simony-Lafontaine, J., Lequeu, N., Vic, P., Enander, I., Godard, P., and Michel, F.B. (1993). Eosinophilic and neutrophilic inflammation in asthma, chronic bronchitis, and chronic obstructive pulmonary disease. J Allergy Clin Immunol *92*, 537-548.
Landmann, R., Knopf, H.P., Link, S., Sansano, S., Schumann, R., and Zimmerli, W. (1996). Human monocyte CD14 is upregulated by lipopolysaccharide. Infect Immun *64*, 1762-1769.
Lawrence, T., Bebien, M., Liu, G.Y., Nizet, V., and Karin, M. (2005). IKKalpha limits macrophage NF-kappaB activation and contributes to the resolution of inflammation. Nature *434*, 1138-1143.
Ledford, R.M., Patel, N.R., Demenczuk, T.M., Watanyar, A., Herbertz, T., Collett, M.S., and Pevear, D.C. (2004). VP1 sequencing of all human rhinovirus serotypes: insights into genus phylogeny and susceptibility to antiviral capsid-binding compounds. J Virol *78*, 3663-3674.
Lee, C.C., Avalos, A.M., and Ploegh, H.L. (2012). Accessory molecules for Toll-like receptors and their function. Nat Rev Immunol.
Lee, F.S., Hagler, J., Chen, Z.J., and Maniatis, T. (1997). Activation of the IkappaB alpha kinase complex by MEKK1, a kinase of the JNK pathway. Cell *88*, 213-222.
Lee, Y.S., Kim, J.H., Kim, S.T., Kwon, J.Y., Hong, S., Kim, S.J., and Park, S.H. (2010). Smad7 and Smad6 bind to discrete regions of Pellino-1 via their MH2 domains to mediate TGF-beta1-induced negative regulation of IL-1R/TLR signaling. Biochem Biophys Res Commun *393*, 836-843.
Lemaitre, B., Nicolas, E., Michaut, L., Reichhart, J.M., and Hoffmann, J.A. (1996). The dorsoventral regulatory gene cassette spatzle/Toll/cactus controls the potent antifungal response in Drosophila adults. Cell *86*, 973-983.
Leto, T.L., and Geiszt, M. (2006). Role of Nox family NADPH oxidases in host defense. Antioxid Redox Signal *8*, 1549-1561.
Li, J., Kartha, S., Iasvovskaia, S., Tan, A., Bhat, R.K., Manaligod, J.M., Page, K., Brasier, A.R., and Hershenson, M.B. (2002). Regulation of human airway epithelial cell IL-8 expression by MAP kinases. Am J Physiol Lung Cell Mol Physiol *283*, L690-699.
Li, Z., Zhang, J., Chen, D., and Shu, H.B. (2003). Casper/c-FLIP is physically and functionally associated with NF-kappaB1 p105. Biochem Biophys Res Commun *309*, 980-985.
Lin, R., Heylbroeck, C., Pitha, P.M., and Hiscott, J. (1998). Virus-dependent phosphorylation of the IRF-3 transcription factor regulates nuclear translocation, transactivation potential, and proteasome-mediated degradation. Mol Cell Biol *18*, 2986-2996.

Liu, Y.C., Penninger, J., and Karin, M. (2005). Immunity by ubiquitylation: a reversible process of modification. Nat Rev Immunol *5*, 941-952.
Loo, Y.M., Fornek, J., Crochet, N., Bajwa, G., Perwitasari, O., Martinez-Sobrido, L., Akira, S., Gill, M.A., Garcia-Sastre, A., Katze, M.G*., et al.* (2008). Distinct RIG-I and MDA5 signaling by RNA viruses in innate immunity. J Virol *82*, 335-345.
Loo, Y.M., and Gale, M., Jr. (2011). Immune signaling by RIG-I-like receptors. Immunity *34*, 680-692.
Lopez, A.D., and Murray, C.C. (1998). The global burden of disease, 1990-2020. Nat Med *4*, 1241-1243.
Lund, J.M., Alexopoulou, L., Sato, A., Karow, M., Adams, N.C., Gale, N.W., Iwasaki, A., and Flavell, R.A. (2004). Recognition of single-stranded RNA viruses by Toll-like receptor 7. Proc Natl Acad Sci U S A *101*, 5598-5603.
Luppi, F., Aarbiou, J., van Wetering, S., Rahman, I., de Boer, W.I., Rabe, K.F., and Hiemstra, P.S. (2005). Effects of cigarette smoke condensate on proliferation and wound closure of bronchial epithelial cells in vitro: role of glutathione. Respir Res *6*, 140.
Maelfait, J., Vercammen, E., Janssens, S., Schotte, P., Haegman, M., Magez, S., and Beyaert, R. (2008). Stimulation of Toll-like receptor 3 and 4 induces interleukin-1beta maturation by caspase-8. J Exp Med *205*, 1967-1973.
Mallia, P., Footitt, J., Sotero, R., Jepson, A., Contoli, M., Trujillo-Torralbo, M.B., Kebadze, T., Aniscenko, J., Oleszkiewicz, G., Gray, K*., et al.* (2012). Rhinovirus infection induces degradation of antimicrobial peptides and secondary bacterial infection in chronic obstructive pulmonary disease. Am J Respir Crit Care Med *186*, 1117-1124.
Mallia, P., Message, S.D., Gielen, V., Contoli, M., Gray, K., Kebadze, T., Aniscenko, J., Laza-Stanca, V., Edwards, M.R., Slater, L*., et al.* (2011). Experimental rhinovirus infection as a human model of chronic obstructive pulmonary disease exacerbation. Am J Respir Crit Care Med *183*, 734-742.
Mallia, P., Message, S.D., Kebadze, T., Parker, H.L., Kon, O.M., and Johnston, S.L. (2006). An experimental model of rhinovirus induced chronic obstructive pulmonary disease exacerbations: a pilot study. Respir Res *7*, 116.
Malynn, B.A., and Ma, A. (2010). Ubiquitin makes its mark on immune regulation. Immunity *33*, 843-852.
Mamane, Y., Heylbroeck, C., Genin, P., Algarte, M., Servant, M.J., LePage, C., DeLuca, C., Kwon, H., Lin, R., and Hiscott, J. (1999). Interferon regulatory factors: the next generation. Gene *237*, 1-14.
Maniatis, T., Falvo, J.V., Kim, T.H., Kim, T.K., Lin, C.H., Parekh, B.S., and Wathelet, M.G. (1998). Structure and function of the interferon-beta enhanceosome. Cold Spring Harb Symp Quant Biol *63*, 609-620.
Mantovani, A., Cassatella, M.A., Costantini, C., and Jaillon, S. (2011). Neutrophils in the activation and regulation of innate and adaptive immunity. Nat Rev Immunol *11*, 519-531.
Marie, I., Durbin, J.E., and Levy, D.E. (1998). Differential viral induction of distinct interferon-alpha genes by positive feedback through interferon regulatory factor-7. EMBO J *17*, 6660-6669.
Marlovits, T.C., Zechmeister, T., Gruenberger, M., Ronacher, B., Schwihla, H., and Blaas, D. (1998). Recombinant soluble low density lipoprotein receptor fragment inhibits minor group rhinovirus infection in vitro. FASEB J *12*, 695-703.
Marquez, R.T., Wendlandt, E., Galle, C.S., Keck, K., and McCaffrey, A.P. (2010). MicroRNA-21 is upregulated during the proliferative phase of liver regeneration, targets Pellino-1, and inhibits NF-kappaB signaling. Am J Physiol Gastrointest Liver Physiol *298*, G535-541.
Marsh, C.B., Gadek, J.E., Kindt, G.C., Moore, S.A., and Wewers, M.D. (1995). Monocyte Fc gamma receptor cross-linking induces IL-8 production. J Immunol *155*, 3161-3167.

Martinon, F., Burns, K., and Tschopp, J. (2002). The inflammasome: a molecular platform triggering activation of inflammatory caspases and processing of proIL-beta. Mol Cell *10*, 417-426.
Mathers, C.D., and Loncar, D. (2006). Projections of global mortality and burden of disease from 2002 to 2030. PLoS Med *3*, e442.
Matsushima, K., Morishita, K., Yoshimura, T., Lavu, S., Kobayashi, Y., Lew, W., Appella, E., Kung, H.F., Leonard, E.J., and Oppenheim, J.J. (1988). Molecular cloning of a human monocyte-derived neutrophil chemotactic factor (MDNCF) and the induction of MDNCF mRNA by interleukin 1 and tumor necrosis factor. J Exp Med *167*, 1883-1893.
Mauro, C., Pacifico, F., Lavorgna, A., Mellone, S., Iannetti, A., Acquaviva, R., Formisano, S., Vito, P., and Leonardi, A. (2006). ABIN-1 binds to NEMO/IKKgamma and co-operates with A20 in inhibiting NF-kappaB. J Biol Chem *281*, 18482-18488.
Maus, U.A., Janzen, S., Wall, G., Srivastava, M., Blackwell, T.S., Christman, J.W., Seeger, W., Welte, T., and Lohmeyer, J. (2006). Resident alveolar macrophages are replaced by recruited monocytes in response to endotoxin-induced lung inflammation. Am J Respir Cell Mol Biol *35*, 227-235.
McAllister, C.S., Lakhdari, O., Pineton de Chambrun, G., Gareau, M.G., Broquet, A., Lee, G.H., Shenouda, S., Eckmann, L., and Kagnoff, M.F. (2013). TLR3, TRIF, and caspase 8 determine double-stranded RNA-induced epithelial cell death and survival in vivo. J Immunol *190*, 418-427.
McManus, T.E., Marley, A.M., Baxter, N., Christie, S.N., O'Neill, H.J., Elborn, J.S., Coyle, P.V., and Kidney, J.C. (2008). Respiratory viral infection in exacerbations of COPD. Respir Med *102*, 1575-1580.
Medvedev, A.E., Sabroe, I., Hasday, J.D., and Vogel, S.N. (2006). Tolerance to microbial TLR ligands: molecular mechanisms and relevance to disease. J Endotoxin Res *12*, 133-150.
Medzhitov, R., Preston-Hurlburt, P., and Janeway, C.A., Jr. (1997). A human homologue of the Drosophila Toll protein signals activation of adaptive immunity. Nature *388*, 394-397.
Mercurio, F., Zhu, H., Murray, B.W., Shevchenko, A., Bennett, B.L., Li, J., Young, D.B., Barbosa, M., Mann, M., Manning, A.*, et al.* (1997). IKK-1 and IKK-2: cytokine-activated IkappaB kinases essential for NF-kappaB activation. Science *278*, 860-866.
Message, S.D., Laza-Stanca, V., Mallia, P., Parker, H.L., Zhu, J., Kebadze, T., Contoli, M., Sanderson, G., Kon, O.M., Papi, A.*, et al.* (2008). Rhinovirus-induced lower respiratory illness is increased in asthma and related to virus load and Th1/2 cytokine and IL-10 production. Proc Natl Acad Sci U S A *105*, 13562-13567.
Meylan, E., Burns, K., Hofmann, K., Blancheteau, V., Martinon, F., Kelliher, M., and Tschopp, J. (2004). RIP1 is an essential mediator of Toll-like receptor 3-induced NF-kappa B activation. Nat Immunol *5*, 503-507.
Meylan, E., Curran, J., Hofmann, K., Moradpour, D., Binder, M., Bartenschlager, R., and Tschopp, J. (2005). Cardif is an adaptor protein in the RIG-I antiviral pathway and is targeted by hepatitis C virus. Nature *437*, 1167-1172.
Mizutani, H., Schechter, N., Lazarus, G., Black, R.A., and Kupper, T.S. (1991). Rapid and specific conversion of precursor interleukin 1 beta (IL-1 beta) to an active IL-1 species by human mast cell chymase. J Exp Med *174*, 821-825.
Modestou, M.A., Manzel, L.J., El-Mahdy, S., and Look, D.C. (2010). Inhibition of IFN-gamma-dependent antiviral airway epithelial defense by cigarette smoke. Respir Res *11*, 64.
Mordmuller, B., Krappmann, D., Esen, M., Wegener, E., and Scheidereit, C. (2003). Lymphotoxin and lipopolysaccharide induce NF-kappaB-p52 generation by a co-translational mechanism. EMBO Rep *4*, 82-87.
Morris, G.E., Parker, L.C., Ward, J.R., Jones, E.C., Whyte, M.K., Brightling, C.E., Bradding, P., Dower, S.K., and Sabroe, I. (2006). Cooperative molecular and cellular networks regulate Toll-like receptor-dependent inflammatory responses. FASEB J *20*, 2153-2155.

Morris, G.E., Whyte, M.K., Martin, G.F., Jose, P.J., Dower, S.K., and Sabroe, I. (2005). Agonists of toll-like receptors 2 and 4 activate airway smooth muscle via mononuclear leukocytes. Am J Respir Crit Care Med *171*, 814-822.
Moynagh, P.N. (2009). The Pellino family: IRAK E3 ligases with emerging roles in innate immune signalling. Trends Immunol *30*, 33-42.
Moynagh, P.N. (2014). The roles of Pellino E3 ubiquitin ligases in immunity. Nat Rev Immunol *14*, 122-131.
Mukaida, N. (2003). Pathophysiological roles of interleukin-8/CXCL8 in pulmonary diseases. Am J Physiol Lung Cell Mol Physiol *284*, L566-577.
Murakami, N., Sakata, Y., and Watanabe, T. (1990). Central action sites of interleukin-1 beta for inducing fever in rabbits. J Physiol *428*, 299-312.
Murao, S., Gemmell, M.A., Callaham, M.F., Anderson, N.L., and Huberman, E. (1983). Control of macrophage cell differentiation in human promyelocytic HL-60 leukemia cells by 1,25-dihydroxyvitamin D3 and phorbol-12-myristate-13-acetate. Cancer Res *43*, 4989-4996.
Murphy, P.M., and Tiffany, H.L. (1991). Cloning of complementary DNA encoding a functional human interleukin-8 receptor. Science *253*, 1280-1283.
Muzio, M., Polentarutti, N., Bosisio, D., Manoj Kumar, P.P., and Mantovani, A. (2000). Toll-like receptor family and signalling pathway. Biochem Soc Trans *28*, 563-566.
Nadel, J.A. (2000). Role of neutrophil elastase in hypersecretion during COPD exacerbations, and proposed therapies. Chest *117*, 386S-389S.
Napetschnig, J., and Wu, H. (2013). Molecular basis of NF-kappaB signaling. Annu Rev Biophys *42*, 443-468.
Netea, M.G., Nold-Petry, C.A., Nold, M.F., Joosten, L.A., Opitz, B., van der Meer, J.H., van de Veerdonk, F.L., Ferwerda, G., Heinhuis, B., Devesa, I.*, et al.* (2009). Differential requirement for the activation of the inflammasome for processing and release of IL-1beta in monocytes and macrophages. Blood *113*, 2324-2335.
Noah, T.L., Yankaskas, J.R., Carson, J.L., Gambling, T.M., Cazares, L.H., McKinnon, K.P., and Devlin, R.B. (1995). Tight junctions and mucin mRNA in BEAS-2B cells. In Vitro Cell Dev Biol Anim *31*, 738-740.
Noordhoek, J.A., Postma, D.S., Chong, L.L., Menkema, L., Kauffman, H.F., Timens, W., van Straaten, J.F., and van der Geld, Y.M. (2005). Different modulation of decorin production by lung fibroblasts from patients with mild and severe emphysema. COPD *2*, 17-25.
Numata, T., Araya, J., Fujii, S., Hara, H., Takasaka, N., Kojima, J., Minagawa, S., Yumino, Y., Kawaishi, M., Hirano, J.*, et al.* (2011). Insulin-dependent phosphatidylinositol 3-kinase/Akt and ERK signaling pathways inhibit TLR3-mediated human bronchial epithelial cell apoptosis. J Immunol *187*, 510-519.
Nurani, G., Lindqvist, B., and Casasnovas, J.M. (2003). Receptor priming of major group human rhinoviruses for uncoating and entry at mild low-pH environments. J Virol *77*, 11985-11991.
O'Neill, L.A., Golenbock, D., and Bowie, A.G. (2013). The history of Toll-like receptors - redefining innate immunity. Nat Rev Immunol *13*, 453-460.
Ohnishi, K., Takagi, M., Kurokawa, Y., Satomi, S., and Konttinen, Y.T. (1998). Matrix metalloproteinase-mediated extracellular matrix protein degradation in human pulmonary emphysema. Lab Invest *78*, 1077-1087.
Ojo, O., Lagan, A.L., Rajendran, V., Spanjer, A., Chen, L., Sohal, S.S., Heijink, I., Jones, R., Maarsingh, H., and Hackett, T.L. (2014). Pathological changes in the COPD lung mesenchyme - Novel lessons learned from in vitro and in vivo studies. Pulm Pharmacol Ther *29*, 121-128.
Onoguchi, K., Yoneyama, M., Takemura, A., Akira, S., Taniguchi, T., Namiki, H., and Fujita, T. (2007). Viral infections activate types I and III interferon genes through a common mechanism. J Biol Chem *282*, 7576-7581.

Onose, A., Hashimoto, S., Hayashi, S., Maruoka, S., Kumasawa, F., Mizumura, K., Jibiki, I., Matsumoto, K., Gon, Y., Kobayashi, T*., et al.* (2006). An inhibitory effect of A20 on NF-kappaB activation in airway epithelium upon influenza virus infection. Eur J Pharmacol *541*, 198-204.
Ordureau, A., Enesa, K., Nanda, S., Le Francois, B., Peggie, M., Prescott, A., Albert, P.R., and Cohen, P. (2013). DEAF1 Is a Pellino1-interacting Protein Required for Interferon Production by Sendai Virus and Double-stranded RNA. J Biol Chem *288*, 24569-24580.
Ordureau, A., Smith, H., Windheim, M., Peggie, M., Carrick, E., Morrice, N., and Cohen, P. (2008). The IRAK-catalysed activation of the E3 ligase function of Pellino isoforms induces the Lys63-linked polyubiquitination of IRAK1. Biochem J *409*, 43-52.
Oshima, S., Turer, E.E., Callahan, J.A., Chai, S., Advincula, R., Barrera, J., Shifrin, N., Lee, B., Benedict Yen, T.S., Woo, T*., et al.* (2009). ABIN-1 is a ubiquitin sensor that restricts cell death and sustains embryonic development. Nature *457*, 906-909.
Pace, E., Ferraro, M., Siena, L., Melis, M., Montalbano, A.M., Johnson, M., Bonsignore, M.R., Bonsignore, G., and Gjomarkaj, M. (2008). Cigarette smoke increases Toll-like receptor 4 and modifies lipopolysaccharide-mediated responses in airway epithelial cells. Immunology *124*, 401-411.
Paludan, S.R., and Bowie, A.G. (2013). Immune sensing of DNA. Immunity *38*, 870-880.
Papi, A., Bellettato, C.M., Braccioni, F., Romagnoli, M., Casolari, P., Caramori, G., Fabbri, L.M., and Johnston, S.L. (2006). Infections and airway inflammation in chronic obstructive pulmonary disease severe exacerbations. Am J Respir Crit Care Med *173*, 1114-1121.
Parker, L.C., Prestwich, E.C., Ward, J.R., Smythe, E., Berry, A., Triantafilou, M., Triantafilou, K., and Sabroe, I. (2008). A phosphatidylserine species inhibits a range of TLR- but not IL-1beta-induced inflammatory responses by disruption of membrane microdomains. J Immunol *181*, 5606-5617.
Parker, L.C., Prince, L.R., and Sabroe, I. (2007). Translational mini-review series on Toll-like receptors: networks regulated by Toll-like receptors mediate innate and adaptive immunity. Clin Exp Immunol *147*, 199-207.
Parker, L.C., Whyte, M.K., Dower, S.K., and Sabroe, I. (2005). The expression and roles of Toll-like receptors in the biology of the human neutrophil. J Leukoc Biol *77*, 886-892.
Parker, L.C., Whyte, M.K., Vogel, S.N., Dower, S.K., and Sabroe, I. (2004). Toll-like receptor (TLR)2 and TLR4 agonists regulate CCR expression in human monocytic cells. J Immunol *172*, 4977-4986.
Parvatiyar, K., Barber, G.N., and Harhaj, E.W. (2010). TAX1BP1 and A20 inhibit antiviral signaling by targeting TBK1-IKKi kinases. J Biol Chem *285*, 14999-15009.
Patel, I.S., Seemungal, T.A., Wilks, M., Lloyd-Owen, S.J., Donaldson, G.C., and Wedzicha, J.A. (2002). Relationship between bacterial colonisation and the frequency, character, and severity of COPD exacerbations. Thorax *57*, 759-764.
Pauwels, R.A., Buist, A.S., Ma, P., Jenkins, C.R., and Hurd, S.S. (2001). Global strategy for the diagnosis, management, and prevention of chronic obstructive pulmonary disease: National Heart, Lung, and Blood Institute and World Health Organization Global Initiative for Chronic Obstructive Lung Disease (GOLD): executive summary. Respir Care *46*, 798-825.
Pearson, G., Robinson, F., Beers Gibson, T., Xu, B.E., Karandikar, M., Berman, K., and Cobb, M.H. (2001). Mitogen-activated protein (MAP) kinase pathways: regulation and physiological functions. Endocr Rev *22*, 153-183.
Pereira, S.G., and Oakley, F. (2008). Nuclear factor-kappaB1: regulation and function. Int J Biochem Cell Biol *40*, 1425-1430.
Perotin, J.M., Dury, S., Renois, F., Deslee, G., Wolak, A., Duval, V., De Champs, C., Lebargy, F., and Andreoletti, L. (2013). Detection of multiple viral and bacterial infections in acute exacerbation of chronic obstructive pulmonary disease: a pilot prospective study. J Med Virol *85*, 866-873.
Pickart, C.M. (2001). Mechanisms underlying ubiquitination. Annu Rev Biochem *70*, 503-533.

Piper, S.C., Ferguson, J., Kay, L., Parker, L.C., Sabroe, I., Sleeman, M.A., Briend, E., and Finch, D.K. (2013). The role of interleukin-1 and interleukin-18 in pro-inflammatory and anti-viral responses to rhinovirus in primary bronchial epithelial cells. PLoS One *8*, e63365.
Posada, J., Yew, N., Ahn, N.G., Vande Woude, G.F., and Cooper, J.A. (1993). Mos stimulates MAP kinase in Xenopus oocytes and activates a MAP kinase kinase in vitro. Mol Cell Biol *13*, 2546-2553.
Proud, D. (2008). Upper airway viral infections. Pulm Pharmacol Ther *21*, 468-473.
Proud, D., Hudy, M.H., Wiehler, S., Zaheer, R.S., Amin, M.A., Pelikan, J.B., Tacon, C.E., Tonsaker, T.O., Walker, B.L., Kooi, C.*, et al.* (2012). Cigarette smoke modulates expression of human rhinovirus-induced airway epithelial host defense genes. PLoS One *7*, e40762.
Proud, D., Turner, R.B., Winther, B., Wiehler, S., Tiesman, J.P., Reichling, T.D., Juhlin, K.D., Fulmer, A.W., Ho, B.Y., Walanski, A.A.*, et al.* (2008). Gene expression profiles during in vivo human rhinovirus infection: insights into the host response. Am J Respir Crit Care Med *178*, 962-968.
Rajput, A., Kovalenko, A., Bogdanov, K., Yang, S.H., Kang, T.B., Kim, J.C., Du, J., and Wallach, D. (2011). RIG-I RNA helicase activation of IRF3 transcription factor is negatively regulated by caspase-8-mediated cleavage of the RIP1 protein. Immunity *34*, 340-351.
Randall, R.E., and Goodbourn, S. (2008). Interferons and viruses: an interplay between induction, signalling, antiviral responses and virus countermeasures. J Gen Virol *89*, 1-47.
Read, M.A., Whitley, M.Z., Gupta, S., Pierce, J.W., Best, J., Davis, R.J., and Collins, T. (1997). Tumor necrosis factor alpha-induced E-selectin expression is activated by the nuclear factor-kappaB and c-JUN N-terminal kinase/p38 mitogen-activated protein kinase pathways. J Biol Chem *272*, 2753-2761.
Reddel, R.R., Ke, Y., Gerwin, B.I., McMenamin, M.G., Lechner, J.F., Su, R.T., Brash, D.E., Park, J.B., Rhim, J.S., and Harris, C.C. (1988). Transformation of human bronchial epithelial cells by infection with SV40 or adenovirus-12 SV40 hybrid virus, or transfection via strontium phosphate coprecipitation with a plasmid containing SV40 early region genes. Cancer Res *48*, 1904-1909.
Resch, K., Jockusch, H., and Schmitt-John, T. (2001). Assignment of homologous genes, Peli1/PELI1 and Peli2/PELI2, for the Pelle adaptor protein Pellino to mouse chromosomes 11 and 14 and human chromosomes 2p13.3 and 14q21, respectively, by physical and radiation hybrid mapping. Cytogenet Cell Genet *92*, 172-174.
Retamales, I., Elliott, W.M., Meshi, B., Coxson, H.O., Pare, P.D., Sciurba, F.C., Rogers, R.M., Hayashi, S., and Hogg, J.C. (2001). Amplification of inflammation in emphysema and its association with latent adenoviral infection. Am J Respir Crit Care Med *164*, 469-473.
Rich, T., Allen, R.L., Lucas, A.M., Stewart, A., and Trowsdale, J. (2000). Pellino-related sequences from Caenorhabditis elegans and Homo sapiens. Immunogenetics *52*, 145-149.
Ropert, C., Almeida, I.C., Closel, M., Travassos, L.R., Ferguson, M.A., Cohen, P., and Gazzinelli, R.T. (2001). Requirement of mitogen-activated protein kinases and I kappa B phosphorylation for induction of proinflammatory cytokines synthesis by macrophages indicates functional similarity of receptors triggered by glycosylphosphatidylinositol anchors from parasitic protozoa and bacterial lipopolysaccharide. J Immunol *166*, 3423-3431.
Rossmann, M.G., and Palmenberg, A.C. (1988). Conservation of the putative receptor attachment site in picornaviruses. Virology *164*, 373-382.
Rot, A., Krieger, M., Brunner, T., Bischoff, S.C., Schall, T.J., and Dahinden, C.A. (1992). RANTES and macrophage inflammatory protein 1 alpha induce the migration and activation of normal human eosinophil granulocytes. J Exp Med *176*, 1489-1495.
Roth, S.J., Carr, M.W., and Springer, T.A. (1995). C-C chemokines, but not the C-X-C chemokines interleukin-8 and interferon-gamma inducible protein-10, stimulate transendothelial chemotaxis of T lymphocytes. Eur J Immunol *25*, 3482-3488.

Rovina, N., Koutsoukou, A., and Koulouris, N.G. (2013). Inflammation and immune response in COPD: where do we stand? Mediators Inflamm *2013*, 413735.
Ruckle, A., Haasbach, E., Julkunen, I., Planz, O., Ehrhardt, C., and Ludwig, S. (2012). The NS1 protein of influenza A virus blocks RIG-I-mediated activation of the noncanonical NF-kappaB pathway and p52/RelB-dependent gene expression in lung epithelial cells. J Virol *86*, 10211-10217.
Rupp, J., Kothe, H., Mueller, A., Maass, M., and Dalhoff, K. (2003). Imbalanced secretion of IL-1beta and IL-1RA in Chlamydia pneumoniae-infected mononuclear cells from COPD patients. Eur Respir J *22*, 274-279.
Ryder, M.I., Saghizadeh, M., Ding, Y., Nguyen, N., and Soskolne, A. (2002). Effects of tobacco smoke on the secretion of interleukin-1beta, tumor necrosis factor-alpha, and transforming growth factor-beta from peripheral blood mononuclear cells. Oral Microbiol Immunol *17*, 331-336.
Saito, T., Hirai, R., Loo, Y.M., Owen, D., Johnson, C.L., Sinha, S.C., Akira, S., Fujita, T., and Gale, M., Jr. (2007). Regulation of innate antiviral defenses through a shared repressor domain in RIG-I and LGP2. Proc Natl Acad Sci U S A *104*, 582-587.
Saitoh, T., Nakayama, M., Nakano, H., Yagita, H., Yamamoto, N., and Yamaoka, S. (2003). TWEAK induces NF-kappaB2 p100 processing and long lasting NF-kappaB activation. J Biol Chem *278*, 36005-36012.
Sajjan, U., Wang, Q., Zhao, Y., Gruenert, D.C., and Hershenson, M.B. (2008). Rhinovirus disrupts the barrier function of polarized airway epithelial cells. Am J Respir Crit Care Med *178*, 1271-1281.
Sapey, E., and Stockley, R.A. (2006). COPD exacerbations . 2: aetiology. Thorax *61*, 250-258.
Sarir, H., Mortaz, E., Karimi, K., Kraneveld, A.D., Rahman, I., Caldenhoven, E., Nijkamp, F.P., and Folkerts, G. (2009). Cigarette smoke regulates the expression of TLR4 and IL-8 production by human macrophages. J Inflamm (Lond) *6*, 12.
Sato, M., Tanaka, N., Hata, N., Oda, E., and Taniguchi, T. (1998). Involvement of the IRF family transcription factor IRF-3 in virus-induced activation of the IFN-beta gene. FEBS Lett *425*, 112-116.
Sato, M., Taniguchi, T., and Tanaka, N. (2001). The interferon system and interferon regulatory factor transcription factors -- studies from gene knockout mice. Cytokine Growth Factor Rev *12*, 133-142.
Savinova, O.V., Hoffmann, A., and Ghosh, G. (2009). The Nfkb1 and Nfkb2 proteins p105 and p100 function as the core of high-molecular-weight heterogeneous complexes. Mol Cell *34*, 591-602.
Schall, T.J., Bacon, K., Toy, K.J., and Goeddel, D.V. (1990). Selective attraction of monocytes and T lymphocytes of the memory phenotype by cytokine RANTES. Nature *347*, 669-671.
Schauvliege, R., Janssens, S., and Beyaert, R. (2006). Pellino proteins are more than scaffold proteins in TLR/IL-1R signalling: a role as novel RING E3-ubiquitin-ligases. FEBS Lett *580*, 4697-4702.
Schauvliege, R., Janssens, S., and Beyaert, R. (2007). Pellino proteins: novel players in TLR and IL-1R signalling. J Cell Mol Med *11*, 453-461.
Schneider, D., Ganesan, S., Comstock, A.T., Meldrum, C.A., Mahidhara, R., Goldsmith, A.M., Curtis, J.L., Martinez, F.J., Hershenson, M.B., and Sajjan, U. (2010). Increased cytokine response of rhinovirus-infected airway epithelial cells in chronic obstructive pulmonary disease. Am J Respir Crit Care Med *182*, 332-340.
Schreiber, R.D., and Farrar, M.A. (1993). The biology and biochemistry of interferon-gamma and its receptor. Gastroenterol Jpn *28 Suppl 4*, 88-94; discussion 95-86.
Seemungal, T., Harper-Owen, R., Bhowmik, A., Moric, I., Sanderson, G., Message, S., Maccallum, P., Meade, T.W., Jeffries, D.J., Johnston, S.L*., et al.* (2001). Respiratory viruses,

symptoms, and inflammatory markers in acute exacerbations and stable chronic obstructive pulmonary disease. Am J Respir Crit Care Med *164*, 1618-1623.
Seemungal, T.A., Donaldson, G.C., Paul, E.A., Bestall, J.C., Jeffries, D.J., and Wedzicha, J.A. (1998). Effect of exacerbation on quality of life in patients with chronic obstructive pulmonary disease. Am J Respir Crit Care Med *157*, 1418-1422.
Sen, G.C. (2001). Viruses and interferons. Annu Rev Microbiol *55*, 255-281.
Senftleben, U., Cao, Y., Xiao, G., Greten, F.R., Krahn, G., Bonizzi, G., Chen, Y., Hu, Y., Fong, A., Sun, S.C*., et al.* (2001). Activation by IKKalpha of a second, evolutionary conserved, NF-kappa B signaling pathway. Science *293*, 1495-1499.
Seth, R.B., Sun, L., Ea, C.K., and Chen, Z.J. (2005). Identification and characterization of MAVS, a mitochondrial antiviral signaling protein that activates NF-kappaB and IRF 3. Cell *122*, 669-682.
Sethi, J.M., and Rochester, C.L. (2000). Smoking and chronic obstructive pulmonary disease. Clin Chest Med *21*, 67-86, viii.
Sethi, S., and Murphy, T.F. (2008). Infection in the pathogenesis and course of chronic obstructive pulmonary disease. N Engl J Med *359*, 2355-2365.
Shapiro, S.D. (1999). The macrophage in chronic obstructive pulmonary disease. Am J Respir Crit Care Med *160*, S29-32.
Silvers, A.L., Bachelor, M.A., and Bowden, G.T. (2003). The role of JNK and p38 MAPK activities in UVA-induced signaling pathways leading to AP-1 activation and c-Fos expression. Neoplasia *5*, 319-329.
Slack, J.L., Schooley, K., Bonnert, T.P., Mitcham, J.L., Qwarnstrom, E.E., Sims, J.E., and Dower, S.K. (2000). Identification of two major sites in the type I interleukin-1 receptor cytoplasmic region responsible for coupling to pro-inflammatory signaling pathways. J Biol Chem *275*, 4670-4678.
Smith, H., Liu, X.Y., Dai, L., Goh, E.T., Chan, A.T., Xi, J., Seh, C.C., Qureshi, I.A., Lescar, J., Ruedl, C*., et al.* (2011). The role of TBK1 and IKKepsilon in the expression and activation of Pellino 1. Biochem J *434*, 537-548.
Smith, H., Peggie, M., Campbell, D.G., Vandermoere, F., Carrick, E., and Cohen, P. (2009). Identification of the phosphorylation sites on the E3 ubiquitin ligase Pellino that are critical for activation by IRAK1 and IRAK4. Proc Natl Acad Sci U S A *106*, 4584-4590.
Smith, R.E., Hogaboam, C.M., Strieter, R.M., Lukacs, N.W., and Kunkel, S.L. (1997). Cell-to-cell and cell-to-matrix interactions mediate chemokine expression: an important component of the inflammatory lesion. J Leukoc Biol *62*, 612-619.
Solan, N.J., Miyoshi, H., Carmona, E.M., Bren, G.D., and Paya, C.V. (2002). RelB cellular regulation and transcriptional activity are regulated by p100. J Biol Chem *277*, 1405-1418.
Stampfli, M.R., and Anderson, G.P. (2009). How cigarette smoke skews immune responses to promote infection, lung disease and cancer. Nat Rev Immunol *9*, 377-384.
Standiford, T.J., Kunkel, S.L., Basha, M.A., Chensue, S.W., Lynch, J.P., 3rd, Toews, G.B., Westwick, J., and Strieter, R.M. (1990). Interleukin-8 gene expression by a pulmonary epithelial cell line. A model for cytokine networks in the lung. J Clin Invest *86*, 1945-1953.
Stanescu, D., Sanna, A., Veriter, C., Kostianev, S., Calcagni, P.G., Fabbri, L.M., and Maestrelli, P. (1996). Airways obstruction, chronic expectoration, and rapid decline of FEV1 in smokers are associated with increased levels of sputum neutrophils. Thorax *51*, 267-271.
Stillie, R., Farooq, S.M., Gordon, J.R., and Stadnyk, A.W. (2009). The functional significance behind expressing two IL-8 receptor types on PMN. J Leukoc Biol *86*, 529-543.
Stokes, C.A., Ismail, S., Dick, E.P., Bennett, J.A., Johnston, S.L., Edwards, M.R., Sabroe, I., and Parker, L.C. (2011). Role of Interleukin-1 and MyD88-Dependent Signaling in Rhinovirus Infection. J Virol *85*, 7912-7921.
Sun, S.C. (2010). Controlling the fate of NIK: a central stage in noncanonical NF-kappaB signaling. Sci Signal *3*, pe18.
Sun, S.C. (2011). Non-canonical NF-kappaB signaling pathway. Cell Res *21*, 71-85.

Takeda, K., and Akira, S. (2004). TLR signaling pathways. Semin Immunol *16*, 3-9.
Takeuchi, O., and Akira, S. (2001). Toll-like receptors; their physiological role and signal transduction system. Int Immunopharmacol *1*, 625-635.
Takeuchi, O., and Akira, S. (2009). Innate immunity to virus infection. Immunol Rev *227*, 75-86.
Takeuchi, O., and Akira, S. (2010). Pattern recognition receptors and inflammation. Cell *140*, 805-820.
Tan, W.C., Xiang, X., Qiu, D., Ng, T.P., Lam, S.F., and Hegele, R.G. (2003). Epidemiology of respiratory viruses in patients hospitalized with near-fatal asthma, acute exacerbations of asthma, or chronic obstructive pulmonary disease. Am J Med *115*, 272-277.
Taniguchi, T., Mantei, N., Schwarzstein, M., Nagata, S., Muramatsu, M., and Weissmann, C. (1980). Human leukocyte and fibroblast interferons are structurally related. Nature *285*, 547-549.
Taniguchi, T., Ogasawara, K., Takaoka, A., and Tanaka, N. (2001). IRF family of transcription factors as regulators of host defense. Annu Rev Immunol *19*, 623-655.
Tanimura, N., Saitoh, S., Matsumoto, F., Akashi-Takamura, S., and Miyake, K. (2008). Roles for LPS-dependent interaction and relocation of TLR4 and TRAM in TRIF-signaling. Biochem Biophys Res Commun *368*, 94-99.
Tanino, M., Betsuyaku, T., Takeyabu, K., Tanino, Y., Yamaguchi, E., Miyamoto, K., and Nishimura, M. (2002). Increased levels of interleukin-8 in BAL fluid from smokers susceptible to pulmonary emphysema. Thorax *57*, 405-411.
Tanner, N.K., and Linder, P. (2001). DExD/H box RNA helicases: from generic motors to specific dissociation functions. Mol Cell *8*, 251-262.
Taub, D.D., Sayers, T.J., Carter, C.R., and Ortaldo, J.R. (1995). Alpha and beta chemokines induce NK cell migration and enhance NK-mediated cytolysis. J Immunol *155*, 3877-3888.
Tetley, T.D. (2002). Macrophages and the pathogenesis of COPD. Chest *121*, 156S-159S.
Thorley, A.J., and Tetley, T.D. (2007). Pulmonary epithelium, cigarette smoke, and chronic obstructive pulmonary disease. Int J Chron Obstruct Pulmon Dis *2*, 409-428.
Triantafilou, K., Orthopoulos, G., Vakakis, E., Ahmed, M.A., Golenbock, D.T., Lepper, P.M., and Triantafilou, M. (2005). Human cardiac inflammatory responses triggered by Coxsackie B viruses are mainly Toll-like receptor (TLR) 8-dependent. Cell Microbiol *7*, 1117-1126.
Tsuchiya, S., Yamabe, M., Yamaguchi, Y., Kobayashi, Y., Konno, T., and Tada, K. (1980). Establishment and characterization of a human acute monocytic leukemia cell line (THP-1). Int J Cancer *26*, 171-176.
Turner, R.B., Weingand, K.W., Yeh, C.H., and Leedy, D.W. (1998). Association between interleukin-8 concentration in nasal secretions and severity of symptoms of experimental rhinovirus colds. Clin Infect Dis *26*, 840-846.
van Boxel-Dezaire, A.H., Rani, M.R., and Stark, G.R. (2006). Complex modulation of cell type-specific signaling in response to type I interferons. Immunity *25*, 361-372.
van der Vaart, H., Postma, D.S., Timens, W., and ten Hacken, N.H. (2004). Acute effects of cigarette smoke on inflammation and oxidative stress: a review. Thorax *59*, 713-721.
Vanlangenakker, N., Vanden Berghe, T., Bogaert, P., Laukens, B., Zobel, K., Deshayes, K., Vucic, D., Fulda, S., Vandenabeele, P., and Bertrand, M.J. (2011). cIAP1 and TAK1 protect cells from TNF-induced necrosis by preventing RIP1/RIP3-dependent reactive oxygen species production. Cell Death Differ *18*, 656-665.
Vestbo, J., Anderson, J., Brook, R.D., Calverley, P.M., Celli, B.R., Crim, C., Haumann, B., Martinez, F.J., Yates, J., and Newby, D.E. (2013). The Study to Understand Mortality and Morbidity in COPD (SUMMIT) study protocol. Eur Respir J *41*, 1017-1022.
Vestbo, J., and Hogg, J.C. (2006). Convergence of the epidemiology and pathology of COPD. Thorax *61*, 86-88.
Vlasak, M., Goesler, I., and Blaas, D. (2005). Human rhinovirus type 89 variants use heparan sulfate proteoglycan for cell attachment. J Virol *79*, 5963-5970.

Wang, J.H., Kim, H., and Jang, Y.J. (2009). Cigarette smoke extract enhances rhinovirus-induced toll-like receptor 3 expression and interleukin-8 secretion in A549 cells. Am J Rhinol Allergy *23*, e5-9.
Ward, J.R., Francis, S.E., Marsden, L., Suddason, T., Lord, G.M., Dower, S.K., Crossman, D.C., and Sabroe, I. (2009). A central role for monocytes in Toll-like receptor-mediated activation of the vasculature. Immunology *128*, 58-68.
Waterfield, M.R., Zhang, M., Norman, L.P., and Sun, S.C. (2003). NF-kappaB1/p105 regulates lipopolysaccharide-stimulated MAP kinase signaling by governing the stability and function of the Tpl2 kinase. Mol Cell *11*, 685-694.
Wedzicha, J.A., Brill, S.E., Allinson, J.P., and Donaldson, G.C. (2013). Mechanisms and impact of the frequent exacerbator phenotype in chronic obstructive pulmonary disease. BMC Med *11*, 181.
Weissmann, C., and Weber, H. (1986). The interferon genes. Prog Nucleic Acid Res Mol Biol *33*, 251-300.
Wertz, I.E., O'Rourke, K.M., Zhou, H., Eby, M., Aravind, L., Seshagiri, S., Wu, P., Wiesmann, C., Baker, R., Boone, D.L*., et al.* (2004). De-ubiquitination and ubiquitin ligase domains of A20 downregulate NF-kappaB signalling. Nature *430*, 694-699.
Wilkinson, T.M., Hurst, J.R., Perera, W.R., Wilks, M., Donaldson, G.C., and Wedzicha, J.A. (2006). Effect of interactions between lower airway bacterial and rhinoviral infection in exacerbations of COPD. Chest *129*, 317-324.
Wullaert, A., Wielockx, B., Van Huffel, S., Bogaert, V., De Geest, B., Papeleu, P., Schotte, P., El Bakkouri, K., Heyninck, K., Libert, C*., et al.* (2005). Adenoviral gene transfer of ABIN-1 protects mice from TNF/galactosamine-induced acute liver failure and lethality. Hepatology *42*, 381-389.
Xia, Z.P., Sun, L., Chen, X., Pineda, G., Jiang, X., Adhikari, A., Zeng, W., and Chen, Z.J. (2009). Direct activation of protein kinases by unanchored polyubiquitin chains. Nature *461*, 114-119.
Xiao, G., Fong, A., and Sun, S.C. (2004). Induction of p100 processing by NF-kappaB-inducing kinase involves docking IkappaB kinase alpha (IKKalpha) to p100 and IKKalpha-mediated phosphorylation. J Biol Chem *279*, 30099-30105.
Xiao, G., Harhaj, E.W., and Sun, S.C. (2001). NF-kappaB-inducing kinase regulates the processing of NF-kappaB2 p100. Mol Cell *7*, 401-409.
Xiao, H., Qian, W., Staschke, K., Qian, Y., Cui, G., Deng, L., Ehsani, M., Wang, X., Qian, Y.W., Chen, Z.J*., et al.* (2008). Pellino 3b negatively regulates interleukin-1-induced TAK1-dependent NF kappaB activation. J Biol Chem *283*, 14654-14664.
Xu, J., Xu, F., and Lin, Y. (2011). Cigarette smoke synergizes lipopolysaccharide-induced interleukin-1beta and tumor necrosis factor-alpha secretion from macrophages via substance P-mediated nuclear factor-kappaB activation. Am J Respir Cell Mol Biol *44*, 302-308.
Xu, L.G., Wang, Y.Y., Han, K.J., Li, L.Y., Zhai, Z., and Shu, H.B. (2005). VISA is an adapter protein required for virus-triggered IFN-beta signaling. Mol Cell *19*, 727-740.
Yamamoto, M., Sato, S., Hemmi, H., Uematsu, S., Hoshino, K., Kaisho, T., Takeuchi, O., Takeda, K., and Akira, S. (2003). TRAM is specifically involved in the Toll-like receptor 4-mediated MyD88-independent signaling pathway. Nat Immunol *4*, 1144-1150.
Yang, S., Tamai, R., Akashi, S., Takeuchi, O., Akira, S., Sugawara, S., and Takada, H. (2001). Synergistic effect of muramyldipeptide with lipopolysaccharide or lipoteichoic acid to induce inflammatory cytokines in human monocytic cells in culture. Infect Immun *69*, 2045-2053.
Yerkovich, S.T., Hales, B.J., Carroll, M.L., Burel, J.G., Towers, M.A., Smith, D.J., Thomas, W.R., and Upham, J.W. (2012). Reduced rhinovirus-specific antibodies are associated with acute exacerbations of chronic obstructive pulmonary disease requiring hospitalisation. BMC Pulm Med *12*, 37.
Yoneyama, M., and Fujita, T. (2007). Function of RIG-I-like receptors in antiviral innate immunity. J Biol Chem *282*, 15315-15318.

Yoneyama, M., and Fujita, T. (2008). Structural mechanism of RNA recognition by the RIG-I-like receptors. Immunity *29*, 178-181.
Yoneyama, M., and Fujita, T. (2010). Recognition of viral nucleic acids in innate immunity. Rev Med Virol *20*, 4-22.
Yoneyama, M., Kikuchi, M., Natsukawa, T., Shinobu, N., Imaizumi, T., Miyagishi, M., Taira, K., Akira, S., and Fujita, T. (2004). The RNA helicase RIG-I has an essential function in double-stranded RNA-induced innate antiviral responses. Nat Immunol *5*, 730-737.
Yu, K.Y., Kwon, H.J., Norman, D.A., Vig, E., Goebl, M.G., and Harrington, M.A. (2002). Cutting edge: mouse pellino-2 modulates IL-1 and lipopolysaccharide signaling. J Immunol *169*, 4075-4078.
Zalacain, R., Sobradillo, V., Amilibia, J., Barron, J., Achotegui, V., Pijoan, J.I., and Llorente, J.L. (1999). Predisposing factors to bacterial colonization in chronic obstructive pulmonary disease. Eur Respir J *13*, 343-348.
Zhang, Z., Louboutin, J.P., Weiner, D.J., Goldberg, J.B., and Wilson, J.M. (2005). Human airway epithelial cells sense Pseudomonas aeruginosa infection via recognition of flagellin by Toll-like receptor 5. Infect Immun *73*, 7151-7160.
Zheng, Y., Humphry, M., Maguire, J.J., Bennett, M.R., and Clarke, M.C. (2013). Intracellular interleukin-1 receptor 2 binding prevents cleavage and activity of interleukin-1alpha, controlling necrosis-induced sterile inflammation. Immunity *38*, 285-295.
Zhong, H., May, M.J., Jimi, E., and Ghosh, S. (2002). The phosphorylation status of nuclear NF-kappa B determines its association with CBP/p300 or HDAC-1. Mol Cell *9*, 625-636.
Zhu, Z., Tang, W., Ray, A., Wu, Y., Einarsson, O., Landry, M.L., Gwaltney, J., Jr., and Elias, J.A. (1996). Rhinovirus stimulation of interleukin-6 in vivo and in vitro. Evidence for nuclear factor kappa B-dependent transcriptional activation. J Clin Invest *97*, 421-430.
Ziegler-Heitbrock, L. (2007). The CD14+ CD16+ blood monocytes: their role in infection and inflammation. J Leukoc Biol *81*, 584-592.
Ziegler-Heitbrock, L., Ancuta, P., Crowe, S., Dalod, M., Grau, V., Hart, D.N., Leenen, P.J., Liu, Y.J., MacPherson, G., Randolph, G.J*., et al.* (2010). Nomenclature of monocytes and dendritic cells in blood. Blood *116*, e74-80.
Zougman, A., Selby, P.J., and Banks, R.E. (2014). Suspension trapping (STrap) sample preparation method for bottom-up proteomics analysis. Proteomics *14*, 1006-1000.
Zujovic, V., and Taupin, V. (2003). Use of cocultured cell systems to elucidate chemokine-dependent neuronal/microglial interactions: control of microglial activation. Methods *29*, 345-350.